JPL PUBLICATION 85-57

Dynamic Modeling and Adaptive Control for Space Stations

Che-Hang Charles Ih
Shyh Jong Wang

July 15, 1985

NASA
National Aeronautics and
Space Administration

Jet Propulsion Laboratory
California Institute of Technology
Pasadena, California

JPL PUBLICATION 85-57

Dynamic Modeling and Adaptive Control for Space Stations

Che-Hang Charles Ih
Shyh Jong Wang

July 15, 1985

NASA

National Aeronautics and
Space Administration

Jet Propulsion Laboratory
California Institute of Technology
Pasadena, California

The research described in this publication was carried out by the Jet Propulsion Laboratory, California Institute of Technology, under a contract with the National Aeronautics and Space Administration.

ABSTRACT

Of all large space structural systems, space stations present a unique challenge and requirement to advanced control technology. Their operations require control system stability over an extremely broad range of parameter changes and high level of disturbances. During shuttle docking the system mass may suddenly increase by more than 100% and during station assembly the mass may vary even more drastically. These coupled with the inherent dynamic model uncertainties associated with large space structural systems require highly sophisticated control systems that can grow as the stations evolve and cope with the uncertainties and time-varying elements to maintain the stability and pointing of the space stations.

This report first deals with the aspects of space station operational properties including configurations, dynamic models, shuttle docking contact dynamics, solar panel interaction and load reduction to yield a set of system models and conditions. A model reference adaptive control algorithm along with the inner-loop plant augmentation design for controlling the space stations under severe operational conditions of shuttle docking, excessive model parameter errors, and model truncation are then investigated. The instability problem caused by the zero-frequency rigid body modes and a proposed solution using plant augmentation are addressed. Two sets of sufficient conditions which guarantee the globally asymptotic stability for the space station systems are obtained.

The performance of this adaptive control system on space stations is analyzed through extensive simulations. Asymptotic stability, high

rate of convergence, and robustness of the system are observed under the above-mentioned severe conditions and constraints induced by control hardware saturation. It is also found that further actuation level reductions can be achieved by using model switching and disturbance modeling techniques.

TABLE OF CONTENTS

LIST OF TABLES

LIST OF FIGURES

CHAPTER I

INTRODUCTION

1.1 Adaptive Control and Large Space Structures

Most of the well-developed control theory, either in the frequency domain or in the time domain, deals with systems whose mathematical representations are completely known. However, in many practical situations, the parameters of the systems are either poorly known or time-varying. In such situations the usual fixed-gain controller will be inadequate to achieve satisfactory performance in the entire range over which the characteristics of the system may vary. Hence, some type of monitoring of the system's behavior, followed by the adjustment of the control input, is needed and is referred to as adaptive control. In other words, while a conventional control system is oriented toward the elimination of the effects of state perturbations, the adaptive control system is oriented toward the elimination of the effects of structural perturbations upon the performance of the control system.

Model Reference Adaptive Control (MRAC) and Self Tuning Regulators (STR) are two principal approaches to the adaptive control problems. In MRAC, the objective is to make the output of an unknown plant asymptotically approach that of a given reference model which specifies the desired performance of the plant. With STR, a controller for a plant with assumed parameters is first chosen and the control gains are then updated with the recursively estimated parameters of the unknown plant.

MRAC can be classified into the following two types based on the adaptation method used:

(i) Indirect Control, in which the plant parameters are estimated and these in turn are used to adjust the controller parameters to meet the performance requirement dictated by the reference model.

(ii) Direct Control, in which no effort is made to identify the plant parameters, the control parameters are adjusted directly so that the error between the plant outputs and the model outputs approaches zero asymptotically.

Since the adaptive control systems are highly nonlinear closed-loop feedback systems, there is a distinct possibility that such systems can become unstable. In fact, the proof of global stability of adaptive control schemes had been a long standing problem for two decades and was not resolved until around 1979-1980. One ideal application area for adaptive control is in large space structures (LSS). The purposes of applying adaptive control to LSS are to reduce the structural and parameter sensitivities of the controller. This is due to the fundamental difficulties of obtaining an accurate model for a distributed parameter system. One often has to deal with linearized reduced-order models; hence, a great deal of uncertainties in the mathematical model describing the dynamics of LSS exist. In addition, time variation in the parameter values are quite common in LSS environments. Slow time-varying effects may be caused by structural settling, thermal distortions, or reorientations of system or subsystems. Spontaneous changes can also happen, especially for space stations.

1.2 Objectives and Motivations

After the space shuttle, the next major space endeavor will be a permanent manned space station. The launching of an initial space station is planned for the early 1990's. By virtue of its mission and function, the space station is a large space structure with a very unique operational environment. As such, it suffers the same drawbacks as other large space structures. These are related to its large size, flexibility, and the way it is built and deployed. The size and flexibility prevent it from comprehensive ground measurement and test, which implies that pre-flight knwoledge of the spacecraft dynamics will be far from precise. In-flight system identification will enhance out knowledge on flight dynamics but it cannot totally eliminate the model parameter uncertainites. Structural flexibility implies infinite dimensionality; hence, model truncation is inevitable. With current technology, only a relatively small number of states can be handled in control design and state estimation. Previous studies of control of large space antennas, for instance, have concluded that destabilization can occur when the parameters of a design model deviate from those of the actual plant by a significant amount [1,2]. In addition to model errors, dynamic disturbances of many orders of magnitude greater than those of the conventional spacecraft will be routine for space stations. Shuttle docking can cause an instantaneous change of mass of more than 100% accompanied by a high intensity shock load. Station assembly, payload articulation, crew motion, launching and retrieving of satellites, etc., will all contribute to disturbance and model parameter variations. The adaptive control problems for space stations are summarized in Fig. 1. Although fixed-gain robust control designs can desensitize the system performance, it is only effective to a limited extent, i.e., for cases where parameter values deviate slightly from their nominal values [3]. All these have motivated us to investigate the feasibility of applying adaptive control techniques to space stations to maintain the stability and pointing.

1.3 Literature Review

Indirect adaptive control was first proposed by Kalman [4] in 1958. The control task may be divided into two parts: a prestructured controller and a recursive plant identification scheme. The parameter estimates are used by the controller to compute appropriate control actions. Feldbaum [5] called this dual control because of the two steps involved in finding the control. In Ref. 6 Iserman et al. compared six on-line identification and parameter estimation methods that can be used for indirect control. Ljung [7,8] has proposed a general technique for analyzing the convergence of discrete-time stochastic adaptive algorithms, yet the problem of boundedness has not been resolved. More recently, Landau [9] and Martin-Sanchez [10] have proven the stability of certain

POINTING/STABILITY

- SYSTEM POINTING $1^\circ \sim 2^\circ$
- SYSTEM JITTER $0.1^\circ \sim 0.2^\circ$
- PAYLOAD STABILITY $0.1 \sim 1$ sec
- ACTIVE VIBRATION DAMPING
- MODULAR/DISTRIBUTED CONTROL TECHNIQUES

DISTURBANCES

- SHUTTLE DOCKING 0.02–0.20 g (PANEL BUCKLE)
- MAN-PUSH OFF 4–10 mg
- REBOOST
- SOFT DOCKING TECHNOLOGY
- DISTURBANCE ESTIMATION AND ISOLATION

GROWTH AND CONFIGURATION CHANGE ACCOMMODATION CONTROL

- MODULAR RECONFIGURABLE CONTROL
- ADAPTIVE CONTROL/GAIN SWITCHING
- FAILURE DETERMINATION AND CONTROL
- AUTONOMOUS MASS PROPERTY MANAGEMENT

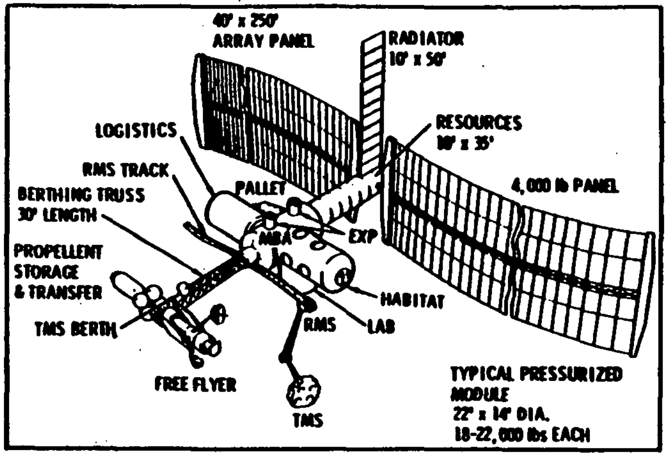

USER/PAYLOAD ACCOMMODATION AND CONTROL

- MULTI-DOF CONTROLLED DISTURBANCE DECOUPLING
- CLOSE FORMATION FLIGHT TECHNIQUES
- BASE MOTION COMPENSATION
- JITTER SUPPRESSION CONTROL

SYSTEM IDENTIFICATION AND DYNAMIC PARAMETER ESTIMATION

- IDENTIFICATION OF
  - MASS PROPERTIES
  - DISTURBANCES
  - DYNAMICS
  - C.P. AND C.M. OF MAJOR COMPONENTS

RENDEZVOUS/DOCKING/TRAFFIC CONTROL

- OPERATIONAL SAFETY/CONTAMINATION
- DOCKING SENSOR TECHNOLOGY
- AUTOMATIC DOCKING METHODOLOGY AND CONTROL LAWS

Figure 1 Adaptive Control Problems for Space Stations types of indirect adaptive controllers. These results had been extended by Johnstone [11] in 1979. Narendra and Valavani [12] derived, in 1979, some indirect adaptive control laws by employing a specific controller structure and the concept of positive realness and showed that these laws are identical to those obtained in the case of direct control. Goodwin [13] has utilized a projection algorithm to obtain a class of globally convergent adaptive algorithms in 1980 and established global convergence of a stochastic adaptive control algorithm for discrete-time linear systems [14] in 1981.

Direct adaptive control was first designed using the performance index minimization method proposed by Whitaker [15] of the MIT Instrumentation Laboratory in 1961 and has since then been referred to as the MIT design rule. The performance index used is the integral square of the response error. An improved design rule with respect to the speed of response had been proposed in 1963 by Donalson et al. [16], who used a more general performance index than that of Whitaker. Winsor [17] had also modified the MIT rule in 1968 to reduce the response sensitivity to the loop gain, at the expense of additional instrumentation. Although some progress was made then, none of the design rules mentioned so far are globally stable. From then on, stability has become a major concern for subsequent studies.

The most common application of stability theory to direct MRAC had been Lyapunov's second method. The adaptive rule is obtained by selecting the design equations to satisfy conditions derived from Lyapunov's second method. Butchart and Shackcloth [18] first suggested the use of a quadratic Lyapunov function, which was employed later in 1966 by Parks [19] to redesign a system formerly designed by the MIT rule. The use of a different Lyapunov function by Phillipson [20] and Gilbart et al. [21] has resulted in the introduction of feedforward loops that would improve the damping of adaptive response. Unfortunately, all these algorithms are difficult to realize in practice because of the requirement of measuring the entire state vector, which is often impossible.

Landau [22] was the first one to apply Popov's hyperstability criterion [23] to multi-input multi-output continuous MRAC systems subject to perfect model following conditions. He also used the same technique to treat the discrete-time MRAC problems [24,25], as did Bethoux et al. [26]. Anderson has given a lucid proof of Popov's hyperstability criterion in Ref. 27. An important contribution was made by Monopoli [28] (1974), who proposed an ingenious control scheme for continuous single-input single-output systems involving an auxiliary signal fed into the reference model and a corresponding augmented error between the model and the plant outputs, so that the use of pure differentiators in the algorithm can be avoided. However, as pointed out in Ref. 29 (1978), the arguments given in Ref. 28 concerning stability are incomplete. Following the augmented error signal concept, Narendra [30] (1978) and [31] (1980) and Morse [32] (1978) and [33] (1980) succeeded in designing globally stable, asymptotic output tracking algorithms for continuous single-input single-output systems. Both Narendra and Morse have assumed that the relative degrees of the plant transfer function are known. Besides, Morse's algorithm is much too complex for use in practical applications. The application of augmented error technique to discrete-time single-input single-output systems was made by Ionescu [34], Narendra [35] and Suzuki [36]. Johnstone et al. [37] have extended Suzuki's technique to solve some simple non-minimum phase problems by optimizing an augmented optimization criterion. Goodwin [13] took a different approach. Instead of relying upon the use of augmented errors or auxiliary inputs, he used the projection theorem to establish the global convergence of a class of adaptive control algorithms for discrete-time deterministic linear multi-input multi-output systems.

Narendra and Valavani have proved that the direct and indirect control would arrive at the same result [38]. Using a typical error model, they also found that when all the signals in the plant are uniformly bounded, hyperstability and asymptotic hyperstability are achieved under exactly the same conditions as stability and asymptotic stability in the sense of Lyapunov [39].

Most stability proofs for direct model reference adaptive control systems have been restricted to single-input single-output or at best, multi-input single-output systems [40] (1975). Results pertaining to direct MRAC for multi-input multi-output continuous systems which do not satisfy the perfect model following conditions are limited. Also, the assumption made by the above algorithms that the relative degrees (difference between the number of poles and zeros) of the plant are known is too restrictive from the engineering point of view.

One particular adaptive control algorithm applied to multi-input multi-output (MIMO) systems was proposed by Sobel et al. [41] (1979) and [42] (1982). Using the Command Generator Tracker (CGT) law developed by Broussard [43] and a direct Lyapunov stability approach, they designed a direct MRAC algorithm that, without the need for parameter identification, forced the error between the outputs of plant and model (which need not be of the same order as the plant) to approach zero. Like all other MIMO adaptive control algorithms, this one also requires that the number of controls equals the number of outputs and the plant input-output transfer function matrix is strictly positive real for some feedback gain matrix.

As far as applications of adaptive control to large space structures is concerned, direct control is superior to indirect control. Since large space structures are infinite dimensional, the identification of all or a large number of parameters of the plant is clearly impossible or unfeasible. As described in Ref. 44, the adaptive controller must then be based on a reduced-order model (ROM) whose order is substantially lower than that of the plant. However, when the adaptive controller operates in closed-loop with the plant, it interacts with the unmodeled residual subsystems, this may cause great difficulties or disastrous problems [45].

The literature which deals with the application of adaptive control to large space structures is very limited. This is due to the difficulties associated with LSS in both the model truncations and parameter uncertainties.

Rohrs et al. [46] (1982) developed a method of analyzing stability and robustness properties of a wide class of adaptive control algorithms for systems that have unmodeled dynamics and output disturbances. According to their investigation, none of the algorithms they tested including those of the widely recognized researchers are stable under these conditions.

Bar-Kana et al. [47] (1983) applied and extended the algorithm proposed by Sobel et al. [42] to the control of large space structural systems, in which they have treated the problems of unmodeled dynamics and other model uncertainties. This work also suffers from some drawbacks, e.g., it cannot handle rigid body modes which always play an important role in large space sructural systems; the design and analysis are specific to the control of a simply supported beam while LSS are usually much more complex; the sufficient conditions for stability are too restrictive, etc. All these necessitate further investigation for the application of adaptive control to large space structures in general, and to space stations in particular.

1.4 Outline of This Report

In Chapter II, two space station configurations and their mass properties are described. Finite-element dynamic models for both the two-panel and four-panel station configurations are developed in Chapter III. In Chapter IV, the adaptive control problem is formulated. The control structure is addressed in Chapter V. In Chapter VI, a direct model reference adaptive control algorithm together with the plant augmentation design is presented and two sets of sufficient conditions for asymptotic stability of the system are derived. In Chapter VII, extensive performance analyses through simulation are discussed, and conclusions are summarized in Chapter VIII.

CHAPTER II

CONFIGURATIONS AND MASS PROPERTIES OF SPACE STATIONS

During the last few years, many space station configurations have been proposed and studied. The configuration development is indeed an evolutionary process, since there are so many factors that need to be considered and assessed against various configuration concepts [48,49].

Two configurations have drawn particular attention -- the NASA Space Station Task Force Initial Operation Center (IOC) Baseline Configuration and the Concept Development Group (CDG) Split-Module Planar Configuration [49]. They are also referred to as the two-panel baseline configuration (or 6 degree-of-freedom model) and four-panel planar configuration (or 19 degree-of-freedom model), respectively, hereafter.

2.1 Two-Panel Baseline Configuration

Figure 2 shows the Task Force IOC Baseline Configuration which was developed by the Space Station Task Force with the Jet Propulsion Laboratory. The system dynamics of this configuration is dominated by the two very large solar panels measuring 250 ft x 40 ft and weighing 4000 lbs each on the ground. It also has a 50 ft x 10 ft radiator panel, a central bus structure consisting of a resource module, habitat module, logistics module, laboratory module, berthing truss, payloads, etc. The entire station weighs 134,000 lbs. Note that the lighter weight of this configuration compared with that of the four-panel configuration is due to the fact that fewer modules

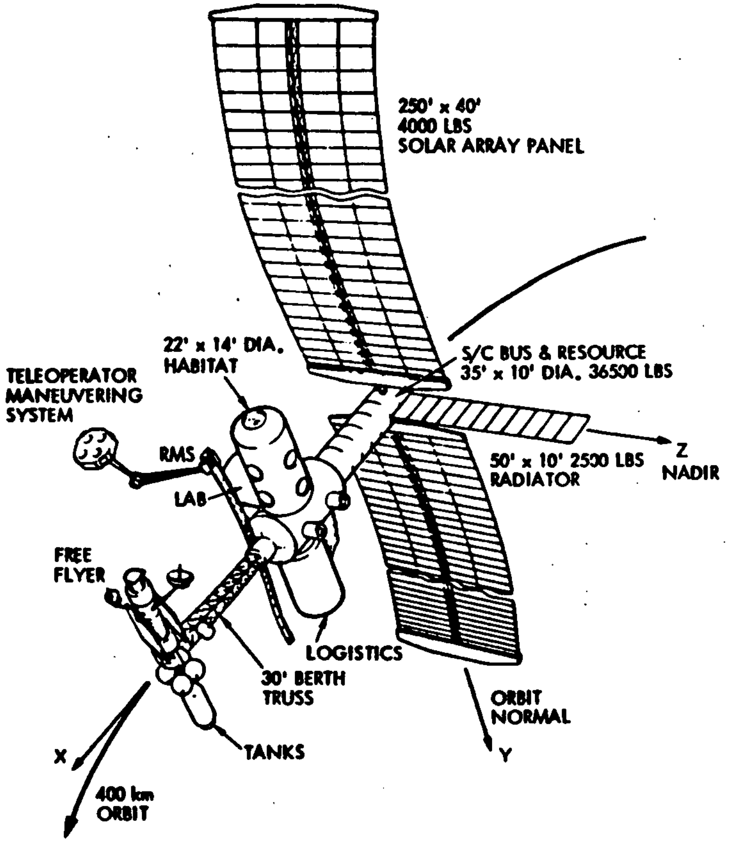

WEIGHT ON GROUND

134000 LBS

CENTER OF MASS

X = 27 FT

Y = -2.3 FT

Z = 5.0 FT

MOMENT OF INERTIA

$I_{XX} = 8.75 \times 10^6$ SLUG-FT^2

$I_{YY} = 1.58 \times 10^6$ SLUG-FT^2

$I_{ZZ} = 8.60 \times 10^6$ SLUG-FT^2

$I_{XY} = -9.57 \times 10^4$ SLUG-FT^2

$I_{YZ} = -4.89 \times 10^4$ SLUG-FT^2

$I_{XZ} = 5.18 \times 10^4$ SLUG-FT^2

Figure 2 Two-Panel IOC Baseline Configuration were considered for this configuration rather than the structural differences between the two concepts.

The moments of inertia for this configuration are $I_{xx} = 8.75\times10^6$ slug-ft^2, $I_{yy} = 1.58\times10^6$ slug-ft^2, and $I_{zz} = 8.60\times10^6$ slug-ft^2. Due to the asymmetric design, the products of inertia are quite high, $I_{xy} = -9.57\times10^4$ slug-ft^2, $I_{yz} = -4.89\times10^4$ slug-ft^2, and $I_{xz} = 5.18\times10^4$ slug-ft^2. With the selection of the reference coordinates as shown in Fig. 2, the center of mass has a high bias of $X = 27$ ft, $Y = -2.3$ ft, and $Z = 5$ ft.

Figure 3 shows a similar configuration with additional modules and payloads attached. The 6 degree-of-freedom (DOF) dynamic model that is developed in Chapter III and used extensively for feasibility analysis is based on the mass properties of the configuration shown in Fig. 2. As far as dynamic properties are concerned, the 6-DOF model is closer to that illustrated in Fig. 4.

2.2 Four-Panel Planar Configuration [48,49]

Figure 5 shows a version of the CDG Split-Module Planar Configuration. The basic difference between this configuration and that of Fig. 2 is that this configuration consists of 4 smaller solar panels (100 ft x 50 ft) and 4 larger radiator panels (70 ft x 20 ft) and, in addition, this configuration is a dynamically balanced design with structural symmetry. Since the solar panels are of much smaller size and a more reasonable aspect ratio, the structural strength improves and the fundamental modal frequencies increase.

The main structure of this configuration measures 280 ft in length and it supports two resource modules, several pressurized

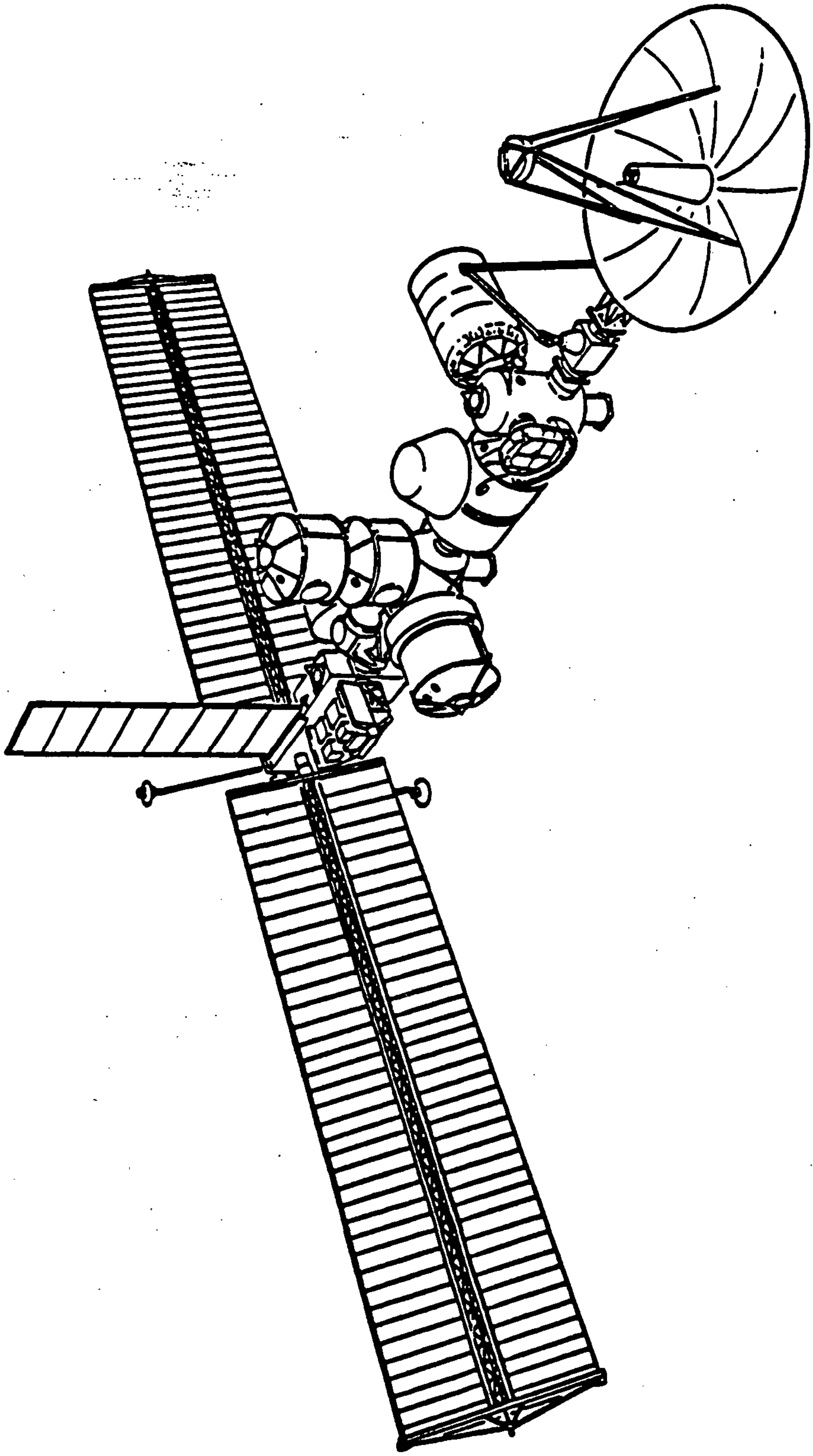

Figure 3 IOC Baseline Configuration with Payloads

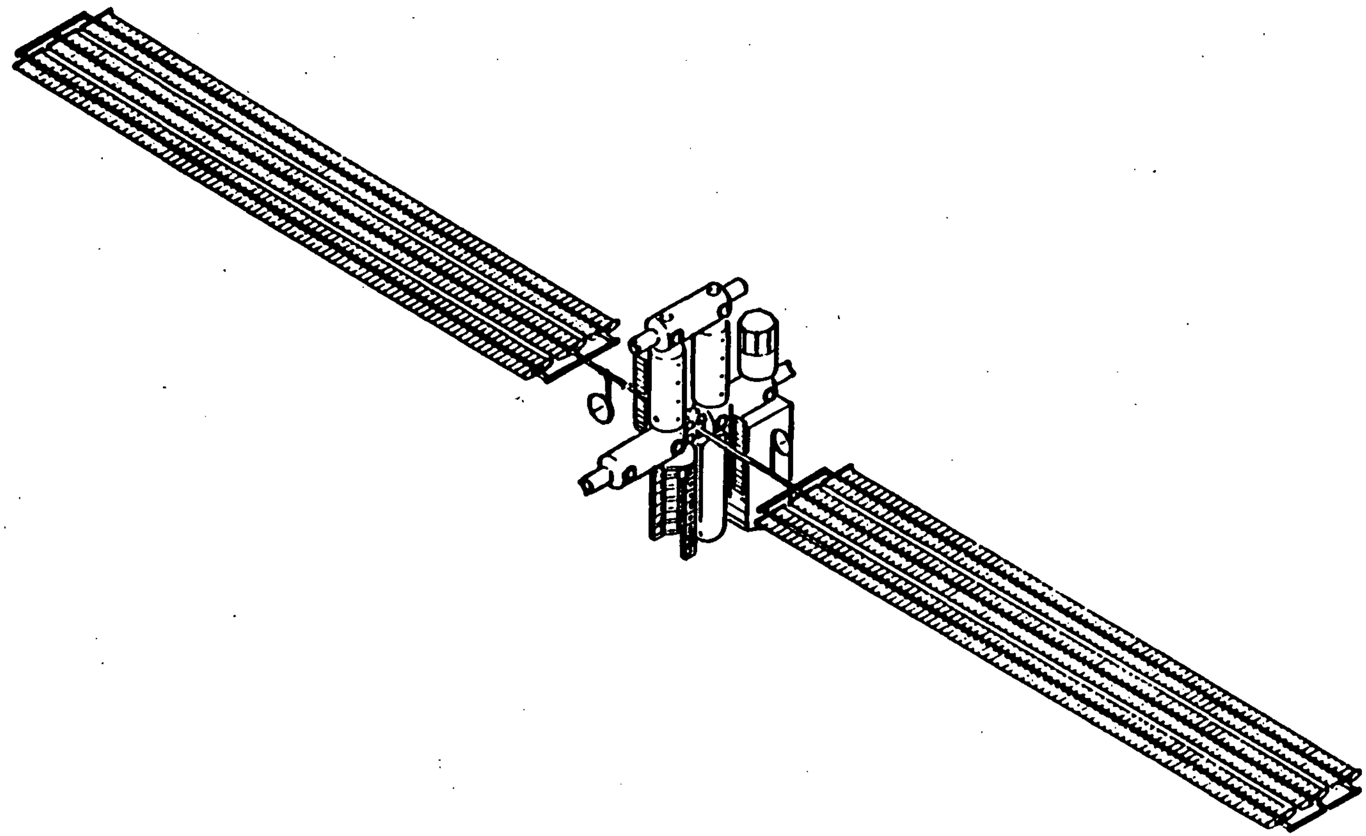

Figure 4 IOC Baseline Configuration Closest to the 6-DOF Dynamic Model

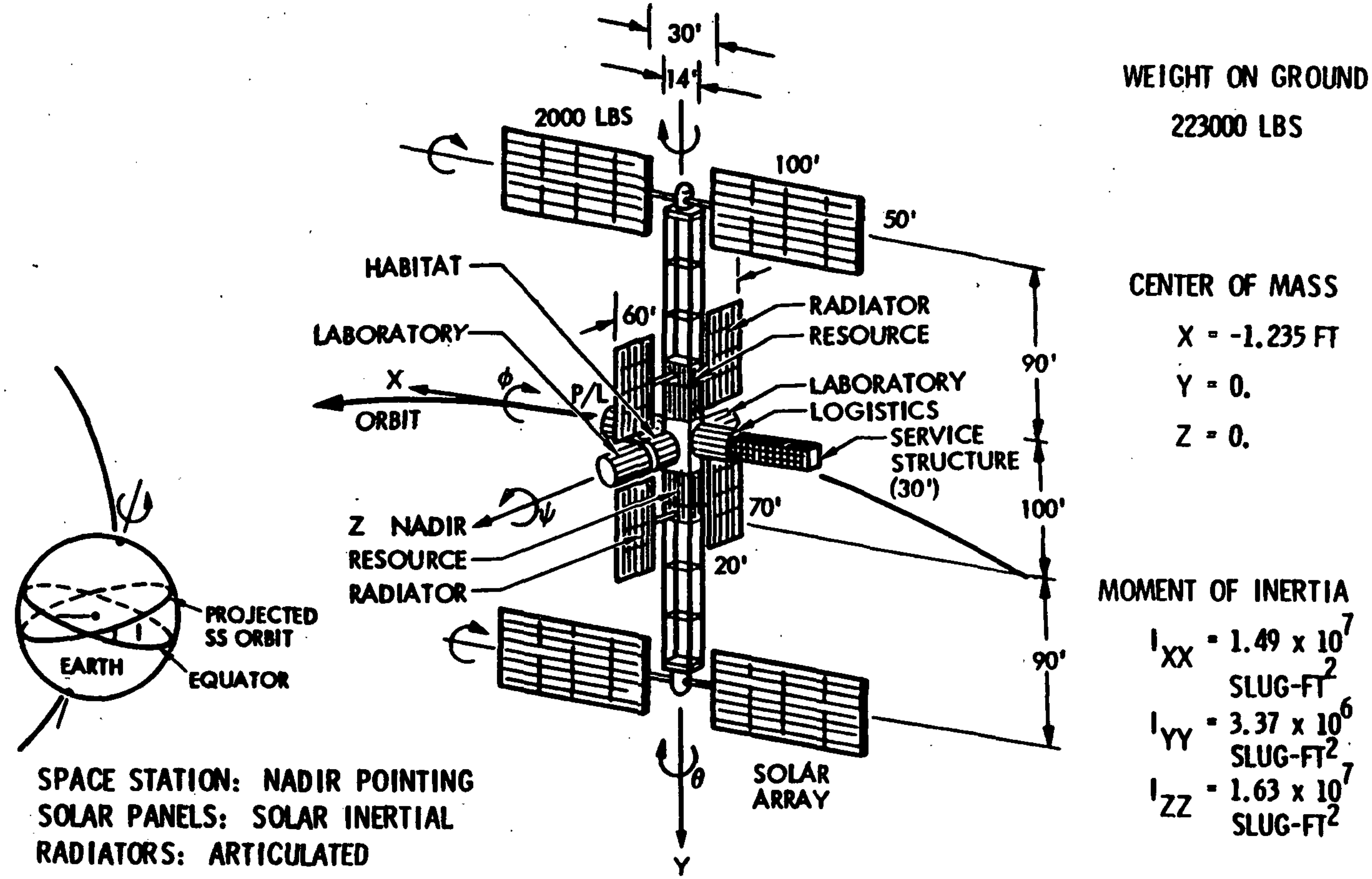

Figure 5 Four-Panel CDG Split-Module Planar Configuration

modules, a 30-ft service truss, and payloads. The pressurized modules are sized 22 ft x 14 ft diameter determined by the space shuttle payload bay size. The solar panels are hinged to rotate about the axes parallel to roll (X) and pitch (Y) axes, respectively, for solar inertial pointing. The radiators are also hinged for articulation, and the core or the bus of the station is pointed to the nadir direction. Again due to its large size and flexibility, the solar panels are the dominant factor for the flexible body dynamics.

Referring to Fig. 5, Table 1 lists the dimensions and masses of the major components. Using the body coordinates with origin placed at the geometric center of the station, the center of mass is,

$$X_{cm} = \frac{\sum_i M_i X_i}{\sum_i M_i} = -1.235 \text{ ft}$$

$$Y_{cm} = \frac{\sum_i M_i Y_i}{\sum_i M_i} = 0$$

$$Z_{cm} = \frac{\sum_i M_i Z_i}{\sum_i M_i} = 0$$

The self moments of inertia of each component are computed using the mass and dimension data shown in Table 1. Each of the components falls in one of the three basic structures — a rectangular plate, a rectangular cube, or a right cylinder. For simplicity, all the component masses are assumed uniformly distributed throughout the respective component structure. Table 2 shows the self moments of inertia for each component and Table 3 shows the component moments of inertia with respect to the center of the reference frame which is also the center of mass if we ignore the small offset along the X-axis.

Table 1

Component Dimension and Mass for Four-Panel Configuration

Component	Dimension Feet	Unit Weight Lbs	Weight Lbs
Solar Panels (4)*	100 x 50	2,000	8,000
Radiators (4)*	70 x 20	1,875	7,500
Resource Modules (2)	22 x 14 Dia	30,000	60,000
Laboratory Modules (2)	22 x 14 Dia	26,000	52,000
Habitat Module	22 x 14 Dia	17,000	17,000
Payload Module	22 x 14 Dia	32,000	32,000
Logistic Module	22 x 14 Dia	50,000	50,000
Service (Berthing) Structure	30	3,000	3,000
Other Equip. & Struc. Weight	236	40 Lbs/Ft	9,440
Total Weight, Lbs	223,440		
Total Mass, Slugs	6,946		

*Weight of solar arrays and radiators are included in the resource modules.

Table 2

Component Self Moment of Inertia for Four-Panel Configuration

Component	I_{SXX} Slug-Ft^2	I_{SYY} Slug-Ft^2	I_{SZZ} Slug-Ft^2
Solar Panels	5.180×10^4	2.072×10^5	2.590×10^5
Radiators	1.030×10^5	7.772×10^3	9.520×10^4
Resource Modules*	7.274×10^4	3.390×10^4	7.274×10^4
Laboratory Modules	4.500×10^4	8.500×10^4	3.960×10^4
Habitat Modules	2.779×10^4	2.779×10^4	1.295×10^4
Payload Module	2.437×10^4	5.637×10^4	5.637×10^4
Logistic Module	3.807×10^4	8.171×10^4	8.171×10^4
Service Structure Equip. & Main Structure	3.046×10^3	5.284×10^3	5.284×10^3

*Masses of solar panels and radiators are excluded for this computation

Table 3

Component Moment of Inertia w.r.t. the Center of Reference Frame for the Four-Panel Configuration

Component	I_{XX} Slug-Ft^2	I_{YY} Slug-Ft^2	I_{ZZ} Slug-Ft^2
Solar Panels	4.926×10^6	1.256×10^6	6.184×10^6
Radiators	7.790×10^5	1.010×10^5	6.780×10^5
Resource Modules*	2.177×10^6	3.390×10^4	2.177×10^6
Laboratory Modules	8.673×10^5	8.673×10^5	3.960×10^4
Habitat Modules	2.779×10^4	2.779×10^4	1.295×10^4
Payload Module	2.437×10^4	3.787×10^5	3.787×10^5
Logistic Module	3.807×10^4	5.852×10^5	5.852×10^5
Service Structure	3.046×10^3	1.068×10^5	1.068×10^5
Equip. & Main Structure	6.096×10^6	9.586×10^3	6.096×10^6
Total Station	1.494×10^7	3.368×10^6	1.626×10^7

CHAPTER III

DYNAMIC MODELS FOR SPACE STATIONS

The development of space station control technology requires results of the following nature:

(1) First - order assessment of problems that will have significant effects on the space station designs. In order to guide the concept formulation and design, these types of results must be generated at a high rate of return.

(2) Analysis of problems that involve multiple interactive elements which require somewhat complex implementation. Because of the complexity of the problem, more time will be required for development and implementation.

For the first purpose stated above, a 6-DOF finite-element dynamic model is developed for the two-panel space station. Because of its tractability and reasonable simulation turnaround time and cost, it is used extensively to evaluate adaptive control problems and performance. For the second purpose, a 19-DOF finite-element dynamic model is developed for the four-panel space station. However, the analysis in this report is, in general, configuration independent.

3.1 Finite-Element Model for the Two-Panel Station Configuration

3.1.1 Dynamic Variables, Coordinates, and Parameters

The 6-DOF finite-element model is shown in Fig. 6, in which only plane motions are considered. The motions of interest are the rotations about the X-axis which are tightly coupled with the displacements along the Z-axis. Hence, this model has six degrees of

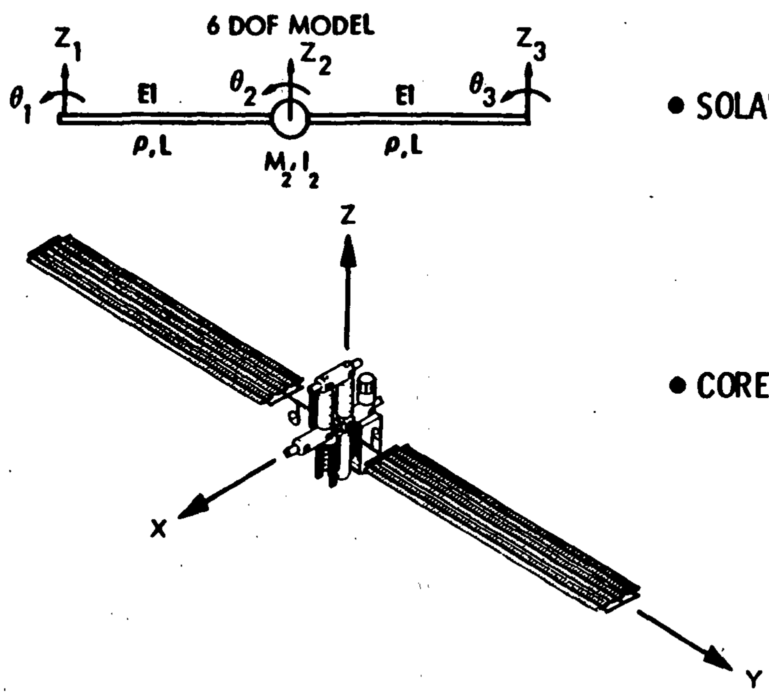

MODEL PARAMETERS

- SOLAR ARRAYS
  - $(EI) = 9.48 \times 10^6$ LB-FT^2
  - $L = 250$ FT
  - $\rho = 0.497$ SLUGS/FT
- CORE STATION
  - $M_2 = 3905.35$ SLUGS
  - $I_2 = 2.89 \times 10^6$ SLUG-FT^2

Figure 6 6-DOF Finite-Element Model for the Two-Panel Configuration freedom — three linear displacements Z_1, Z_2, Z_3 and three bending angles θ_1, θ_2, θ_3 of the central bus and the two outer tips of the solar panels. The solar panels are modeled as two uniform beams with length L, linear mass density ρ, and flexural rigidity EI. The bus and modules are modeled as a rigid core body with mass M_2 and moment of inertia I_2 located at the center of the structure.

3.1.2 The Stiffness Matrix

A finite-element technique is used to derive the stiffness and mass matrices for the model [50]. To obtain the stiffness matrix by using this technique, one starts by dividing the structure into a finite number of elements, the properties of each element are then determined. The properties of the entire structure are obtained by superimposing those of the elements at the associated nodes. There are two nodal points associated with each element, and two degrees of freedom at each node if only transverse plane displacements are considered. The deflected shape of the beam element may be described by a set of cubic Hermitian polynomials, as follows, when unit displacement is applied at the left end,

$$\psi_1 (x) = 1 - 3\left(\frac{x}{L}\right)^2 + 2\left(\frac{x}{L}\right)^3 \qquad (3.1)$$

$$\psi_3 (x) = x\left(1 - \frac{x}{L}\right)^2 \qquad (3.2)$$

The shape functions for unit displacement at the right end are,

$$\psi_2 (x) = 3 \left(\frac{x}{L}\right)^2 - 2 \left(\frac{x}{L}\right)^3 \tag{3.3}$$

$$\psi_4 (x) = \frac{x^2}{L} \left(\frac{x}{L} - 1\right) \tag{3.4}$$

The general shape expression is the superposition of these functions,

$$\nu (x) = \psi_1 (x) \nu_a + \psi_2 (x) \nu_b + \psi_3 (x) \theta_a + \psi_4 (x) \theta_b \tag{3.5}$$

The stiffness coefficient associated with the beam flexure is

$$k_{ij} = \int_o^L EI (x) \psi_i'' (x) \psi_j'' (x) dx = k_{ji} \tag{3.6}$$

For a uniform beam segment, the stiffness matrix becomes

$$\begin{bmatrix} F_a \\ F_b \\ T_a \\ T_b \end{bmatrix} = \frac{2EI}{L^3} \begin{bmatrix} 6 & -6 & 3L & 3L \\ -6 & 6 & -3L & -3L \\ 3L & -3L & 2L^2 & L^2 \\ 3L & -3L & L^2 & 2L^2 \end{bmatrix} \begin{bmatrix} \nu_a \\ \nu_b \\ \theta_a \\ \theta_b \end{bmatrix} \tag{3.7}$$

where F_a, F_b, T_a, and T_b are the nodal forces and torques at nodes a and b, respectively, and ν_a, ν_b, θ_a, and θ_b are the corresponding nodal displacements -- translation and rotation. The stiffness of the complete structure is obtained by adding the element stiffness appropriately. For instance, the structural stiffness of node i at which elements l, m, and n are attached is

$$k_{ii} = \hat{k}_{ii}^{(l)} + \hat{k}_{ii}^{(m)} + \hat{k}_{ii}^{(n)} \tag{3.8}$$

where the hat implies that all the variables are expressed in a common global coordinate system, or they have been transformed to a common system from their local systems.

Now we shall use Eqs. (3.7) and (3.8) to derive the stiffness matrix for the 6-DOF model. Consider the uniform beam element in Fig. 7. If the two nodal points taken are located at its ends, there will be a total of four DOF -- one translation and one rotation at each node. Through the finite-element method the stiffness matrix K_A is

$$\begin{bmatrix} F_1 \\ T_1 \\ F_2 \\ T_2 \end{bmatrix} = K_A \begin{bmatrix} Z_1 \\ \theta_1 \\ Z_2 \\ \theta_2 \end{bmatrix} = \frac{2EI}{L^3} \begin{bmatrix} 6 & 3L & -6 & 3L \\ 3L & 2L^2 & -3L & L^2 \\ -6 & -3L & 6 & -3L \\ 3L & L^2 & -3L & 2L^2 \end{bmatrix} \begin{bmatrix} Z_1 \\ \theta_1 \\ Z_2 \\ \theta_2 \end{bmatrix} \tag{3.9}$$

where F_1 and F_2 are the forces, T_1 and T_2 are the torques applied at the nodes. For a similar beam element (see Fig. 7), the stiffness matrix K_B is

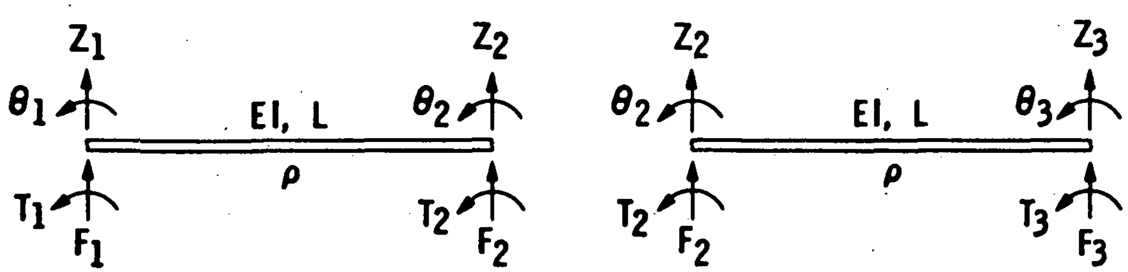

Figure 7 Uniform Beam Elements

$$\begin{bmatrix} F_2 \\ T_2 \\ F_3 \\ T_3 \end{bmatrix} = K_B \begin{bmatrix} Z_2 \\ \theta_2 \\ Z_3 \\ \theta_3 \end{bmatrix} = \frac{2EI}{L^3} \begin{bmatrix} 6 & 3L & -6 & 3L \\ 3L & 2L^2 & -3L & L^2 \\ -6 & -3L & 6 & -3L \\ 3L & L^2 & -3L & 2L^2 \end{bmatrix} \begin{bmatrix} Z_2 \\ \theta_2 \\ Z_3 \\ \theta_3 \end{bmatrix} \tag{3.10}$$

By using Eq. (3.8) to combine Eqs. (3.9) and (3.10), i.e., adding the element stiffness at the joining point, the stiffness matrix K for the combined uniform beam elements (Fig. 8) is obtained as

$$\begin{bmatrix} F_1 \\ T_1 \\ F_2 \\ T_2 \\ F_3 \\ T_3 \end{bmatrix} = K \begin{bmatrix} Z_1 \\ \theta_1 \\ Z_2 \\ \theta_2 \\ Z_3 \\ \theta_3 \end{bmatrix}$$

$$= \frac{2EI}{L^3} \left[\begin{array}{cc:cc:cc} 6 & 3L & -6 & 3L & 0 & 0 \\ 3L & 2L^2 & -3L & L^2 & 0 & 0 \\ \hdashline -6 & -3L & 12 & 0 & -6 & 3L \\ 3L & L^2 & 0 & 4L^2 & -3L & L^2 \\ \hdashline 0 & 0 & -6 & -3L & 6 & -3L \\ 0 & 0 & 3L & L^2 & -3L & 2L^2 \end{array}\right] \begin{bmatrix} Z_1 \\ \theta_1 \\ Z_2 \\ \theta_2 \\ Z_3 \\ \theta_3 \end{bmatrix} \tag{3.11}$$

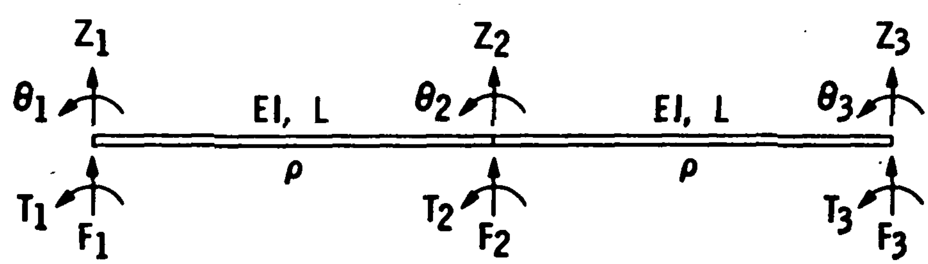

Figure 8 Combined Uniform Beam Elements

3.1.3 The Consistent-Mass Matrix

The consistent-mass matrix is the mass matrix for the distributed mass of the flexible structure. For a beam element of length L, mass density $\rho(x)$, the mass influence coefficient m_{ij} can be expressed as

$$m_{ij} = \int_o^L \rho(x)\, \psi_i(x)\, \psi_j(x)\, dx = m_{ji} \tag{3.12}$$

where $\psi_i(x)$ and $\psi_j(x)$ are the shape functions. The term "consistent" signifies that this mass matrix is obtained using the same shape functions $\psi_{\bullet}(x)$ as those used for deriving the stiffness matrix. The cubic Hermitian polynomials are generally used for straight beams. Therefore, for the straight uniformly distributed beam element shown in Fig. 7, the consistent-mass matrix M_A is

$$\begin{bmatrix} F_1 \\ T_1 \\ F_2 \\ T_2 \end{bmatrix} = M_A \begin{bmatrix} \ddot{Z}_1 \\ \ddot{\theta}_1 \\ \ddot{Z}_2 \\ \ddot{\theta}_2 \end{bmatrix} = \frac{\rho L}{420} \begin{bmatrix} 156 & 22L & 54 & -13L \\ 22L & 4L^2 & 13L & -3L^2 \\ 54 & -13L & 156 & -22L \\ -13L & -3L^2 & -22L & 4L^2 \end{bmatrix} \begin{bmatrix} \ddot{Z}_1 \\ \ddot{\theta}_1 \\ \ddot{Z}_2 \\ \ddot{\theta}_2 \end{bmatrix} \tag{3.13}$$

Similarly, the consistent-mass matrix M_B for the adjoining beam element is

$$\begin{bmatrix} F_2 \\ T_2 \\ F_3 \\ T_3 \end{bmatrix} = M_B \begin{bmatrix} \ddot{Z}_2 \\ \ddot{\theta}_2 \\ \ddot{Z}_3 \\ \ddot{\theta}_3 \end{bmatrix} = \frac{\rho L}{420} \begin{bmatrix} 156 & 22L & 54 & -13L \\ 22L & 4L^2 & 13L & -3L^2 \\ 54 & -13L & 156 & -22L \\ -13L & -3L^2 & -22L & 4L^2 \end{bmatrix} \begin{bmatrix} \ddot{Z}_2 \\ \ddot{\theta}_2 \\ \ddot{Z}_3 \\ \ddot{\theta}_3 \end{bmatrix} \tag{3.14}$$

Hence, the combined consistent-mass matrix M_C for the 6-DOF model can be obtained by using an approach similar to that for obtaining the stiffness matrix as,

$$\begin{bmatrix} F_1 \\ T_1 \\ F_2 \\ T_2 \\ F_3 \\ T_3 \end{bmatrix} = M_C \begin{bmatrix} \ddot{Z}_1 \\ \ddot{\theta}_1 \\ \ddot{Z}_2 \\ \ddot{\theta}_2 \\ \ddot{Z}_3 \\ \ddot{\theta}_3 \end{bmatrix}$$

$$= \frac{\rho L}{420} \begin{bmatrix} 156 & 22L & 54 & -13L & 0 & 0 \\ 22L & 4L^2 & 13L & -3L^2 & 0 & 0 \\ 54 & 13L & 312 & 0 & 54 & -13L \\ -13L & -3L^2 & 0 & 8L^2 & 13L & -3L^2 \\ 0 & 0 & 54 & 13L & 156 & -22L \\ 0 & 0 & -13L & -3L^2 & -22L & 4L^2 \end{bmatrix} \begin{bmatrix} \ddot{Z}_1 \\ \ddot{\theta}_1 \\ \ddot{Z}_2 \\ \ddot{\theta}_2 \\ \ddot{Z}_3 \\ \ddot{\theta}_3 \end{bmatrix} \tag{3.15}$$

3.1.4 The Lumped-Mass Matrix and System Mass Matrix

The consistent-mass matrix accounts for the effect of distributed mass only, the effect of concentrated mass is accounted for by the lumped-mass matrix M_D,

$$M_D = \text{diag}\ (0,\ 0,\ M_2,\ I_2,\ 0,\ 0) \tag{3.16}$$

The total system mass matrix is, then

$$M = M_C + M_D \tag{3.17}$$

3.1.5 Equations of Motion

The equations of motion for the 6-DOF model can then be written as

$$\begin{cases} M\ \ddot{Z}_p + K\ Z_p = F = B\ u_p & (3.18) \\ y_p = C(\alpha\ Z_p + \dot{Z}_p) & (3.19) \end{cases}$$

where

$$Z_p = [Z_{p1}\ \theta_{p1}\ Z_{p2}\ \theta_{p2}\ Z_{p3}\ \theta_{p3}]^T$$

$$= [Z_1\ \theta_1\ Z_2\ \theta_2\ Z_3\ \theta_3]^T$$

$$F = [F_1\ T_1\ F_2\ T_2\ F_3\ T_3]^T$$

u_p = M-dimensional plant control input vector

y_p = M-dimensional plant output vector

B = 6 x M control influence matrix

C = M x 6 measurement distribution matrix

α is the weighting factor of the position vs. rate measurement

3.1.6 Modal Coordinates and Modal Properties

To carry out the analysis of this dissertation, modal coordinates are used. The modal model is obtained by setting $F = 0$ in Eq. (3.18) and solving the eigenvalue problem. Let ϕ be the normalized eigenvector matrix which is selected such that

$$\phi^T M \phi = I \tag{3.20}$$

$$\phi^T K \phi = \Lambda \tag{3.21}$$

where Λ is the diagonal eigenvalue matrix. Let η be the modal amplitude vector, and $Z_p = \phi\eta$. Substitute this into Eq. (3.18) and premultiply both sides by ϕ^T, one has the following dynamical equation in modal form,

$$\ddot{\eta} + \Lambda\eta = \phi^T B u_p \tag{3.22}$$

After adding damping terms, Eq. (3.22) becomes

$$\ddot{\eta} + \mathrm{diag}\,(2\zeta_1\omega_1, \ldots 2\zeta_6\omega_6)\dot{\eta} + \mathrm{diag}(\omega_1^2, \ldots, \omega_6^2)\eta = \phi^T B u_p \tag{3.23}$$

The corresponding damped dynamical equation in physical coordinates can be obtained through transformation. Let D be the damping factor matrix, one has

$$D = \phi^{-T} \text{ diag } (2\zeta_1\omega_1, \ldots, 2\zeta_6\omega_6)\phi^{-1} \tag{3.24}$$

Hence, the system equations of motion in physical and modal coordinates are, respectively

$$\begin{cases} M\ddot{Z}_p + D\dot{Z}_p + KZ_p = Bu_p & (3.25a) \\ y_p = C\,(\alpha Z_p + \dot{Z}_p) & (3.25b) \end{cases}$$

and

$$\begin{cases} \ddot{\eta} + \text{diag }(2\zeta_1\omega_1, \ldots, 2\zeta_6\omega_6)\dot{\eta} + \text{diag }(\omega_1^2, \ldots, \omega_6^2)\eta = \phi^T Bu_p & (3.26a) \\ y_p = C(\alpha\phi\eta + \phi\dot{\eta}) & (3.26b) \end{cases}$$

The modal properties of the 6-DOF model are obtained by using the parameters given in Fig. 6. The modal frequencies are,

$$\begin{aligned} \omega_1 &= 0 \\ \omega_2 &= 0 \\ \omega_3 &= 0.04 \text{ Hz} \\ \omega_4 &= 0.0637 \text{ Hz} \\ \omega_5 &= 0.3885 \text{ Hz} \\ \omega_6 &= 0.3947 \text{ Hz} \end{aligned} \tag{3.27a}$$

and the mode shape matrix (eigenvector matrix) ϕ is

$$\phi = \begin{bmatrix} .872E-1 & .194E-1 & -.127 & -.961E-1 & .178 & .178 \\ -.352E-3 & -.157E-4 & .720E-3 & .719E-3 & -.545E-2 & -.549E-2 \\ -.693E-3 & .155E-1 & .301E-2 & -.360E-7 & .151E-2 & -.174E-5 \\ -.352E-3 & -.157E-4 & .727E-8 & -.450E-3 & .126E-6 & -.117E-3 \\ -.886E-1 & .116E-1 & -.127 & .961E-1 & .179 & -.117 \\ -.352E-3 & -.157E-4 & -.720E-3 & .719E-3 & .546E-2 & -.548E-2 \end{bmatrix} . \tag{3.27b}$$

Figure 9 shows the mode shapes corresponding to the above mode shape matrix. Of the six modes, there are two zero-frequency rigid body rotational and translational modes, two first bending modes — symmetric and antisymmetric, and two second bending modes.

3.2 Finite-Element Model for the Four-Panel Station Configuration

3.2.1 Dynamic Variables, Coordinates, and Parameters

Referring to Fig. 10, the main or backbone structure is modeled as two flexible beams rigidly attached to the core body (the bus); and the solar panels are also modeled as flexible beams with two beams jointed together and attached to the ends of the main structure. The two payloads, assumed rigid here, are hinge connected to the core body to form a balanced structure. To keep the model to a tractable size, the beams are assumed torsionally stiff, and hence, only bending angles and the associated deflections are modeled here.

This model consists of 19 dynamic variables, 7 translations and 12 rotations, as indicated in Fig. 10. Since the beams are assumed torsionally stiff, ϕ_2 (ϕ_6) represents the roll angles for the entire length of the beams associated with the south (north) panels. For

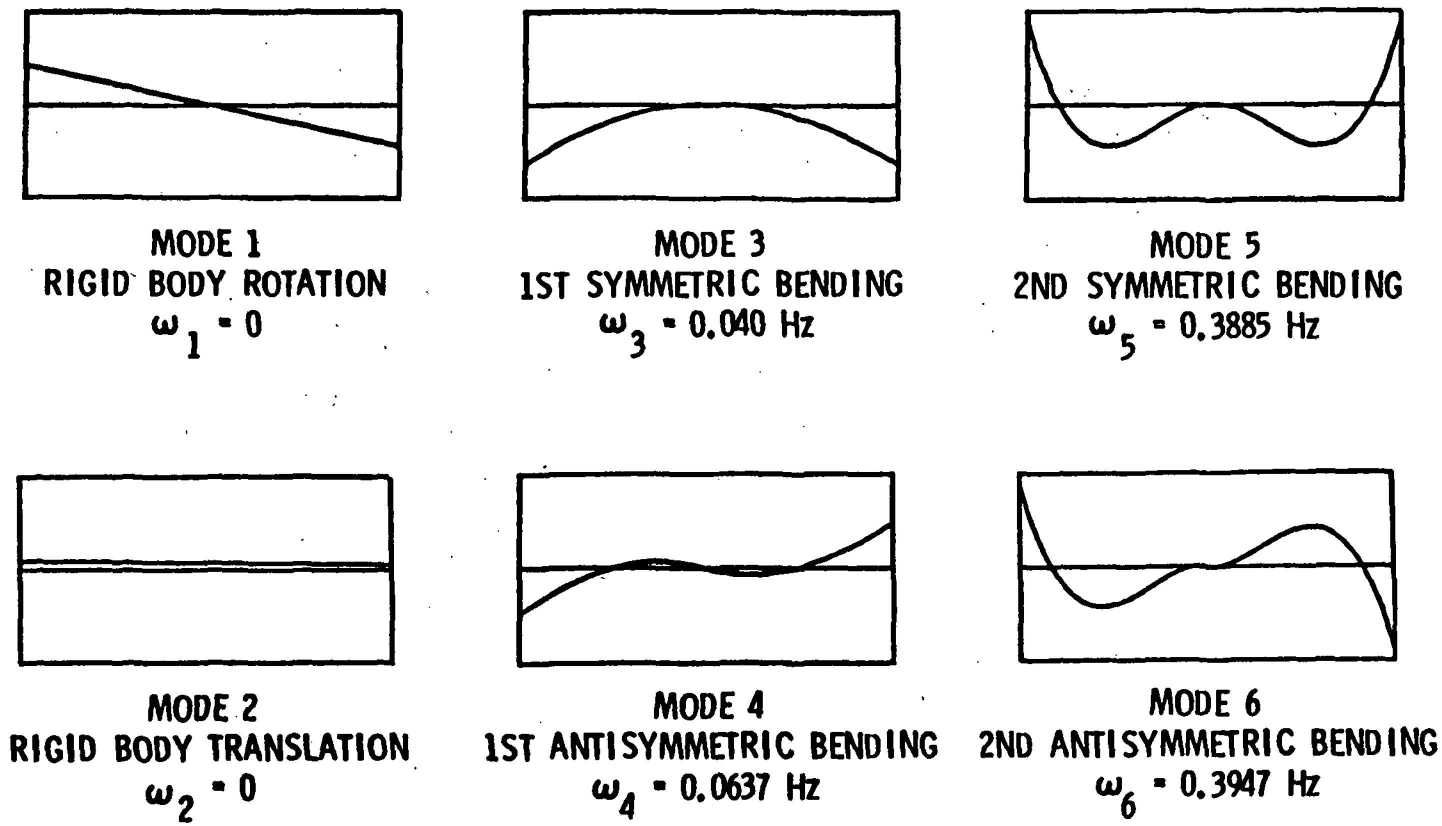

Figure 9 Modal Properties for the 6-DOF Two-Panel Configuration Model

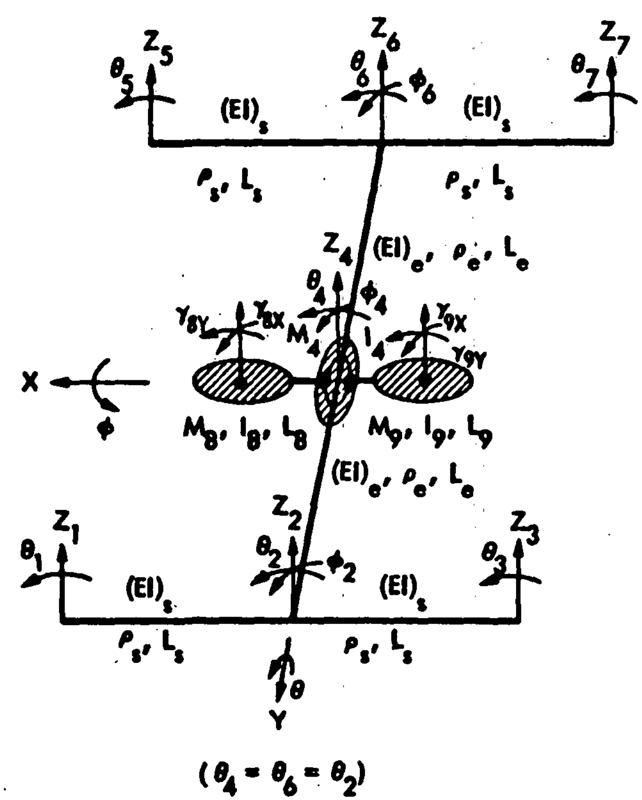

MODEL PARAMETERS

- SOLAR ARRAYS
  - $(EI)_s = 9.48 \times 10^6$ LB-FT^2
  - $L_s = 115$ FT
  - $\rho_s = 0.541$ SLUG/FT
- MAIN STRUCTURE
  - $(EI)_e = 9.48 \times 10^7$ LB-FT^2
  - $L_e = 140$ FT
  - $\rho_e = 1.048$ SLUG/FT
- CORE STATION
  - $M_4 = 4165.35$ SLUGS
  - $I_{4XX} = 3.869 \times 10^6$ SLUG-FT^2
  - $I_{4YY} = 1.343 \times 10^6$ SLUG-FT^2
- PAYLOADS
  - $M_8 = M_9 = 994.72$ SLUGS
  - $L_8 = L_9 = 18$ ft
  - $I_{8XS} = I_{9XS} = 2.437 \times 10^4$ SLUG-FT^2
  - $I_{8YS} = I_{9YS} = 5.637 \times 10^4$ SLUG-FT^2

Figure 10 19-DOF Finite-Element Model for the Four-Panel Planar Configuration the same reason, θ_4 is the pitch angle for the entire main structure, therefore, the following constraints apply:

$$\theta_2 = \theta_6 = \theta_4 \tag{3.28}$$

The payload motions are modeled by the hinge angles, γ'_{8x}, γ'_{8y}, γ'_{9x}, γ'_{9y}, where in Fig. 10, γ_{8x}, γ_{8y}, γ_{9x}, γ_{9y} are the corresponding inertial attitude angles. The translations at the c.m. of the payloads can be computed using the hinge angles. Therefore, the translation variables are Z_1, Z_2, Z_3, Z_4, Z_5, Z_6, Z_7, and the rotation variables are θ_1, ϕ_2, θ_3, θ_4, ϕ_4, θ_5, ϕ_6, θ_7, γ'_{8x}, γ'_{8y}, γ'_{9x}, and γ'_{9y}.

The model parameters are basically the flexural rigidity (EI), the length, and the mass density for the beam elements in the model; the mass, moment of inertia and length for the payloads and the core station. The values for the mass-related parameters are computed based on information discussed in Chapter II.

3.2.2 The Stiffness Matrix

First, the 19-DOF model is divided into three parts, the solar panels -- south, the solar panels -- north, and the main structure. The payloads will not be considered until later. The finite-element technique used is the same as that for the 6-DOF model.

Consider Fig. 11, the two "south" panels are modeled as two uniform beams, each 115 ft in length. Referring to Eq. (3.11), one has

$$
\begin{bmatrix} F_1 \\ T_{1\theta} \\ F_2 \\ T_{2\theta} \\ F_3 \\ T_{3\theta} \end{bmatrix}
= \frac{2(EI)_s}{L_s^3}
\begin{bmatrix}
6 & 3L_s & -6 & 3L_s & 0 & 0 \\
3L_s & 2L_s^2 & -3L_s & L_s^2 & 0 & 0 \\
-6 & -3L_s & 12 & 0 & -6 & 3L_s \\
3L_s & L_s^2 & 0 & 4L_s^2 & -3L_s & L_s^2 \\
0 & 0 & -6 & -3L_s & 6 & -3L_s \\
0 & 0 & 3L_s & L_s^2 & -3L_s & 2L_s^2
\end{bmatrix}
\begin{bmatrix} Z_1 \\ \theta_1 \\ Z_2 \\ \theta_2 \\ Z_3 \\ \theta_3 \end{bmatrix}
\tag{3.29}
$$

Similarly, referring to Fig. 12, the stiffness matrix for the north panels is obtained as

$$
\begin{bmatrix} F_5 \\ T_{5\theta} \\ F_6 \\ T_{6\theta} \\ F_7 \\ T_{7\theta} \end{bmatrix}
= \frac{2(EI)_s}{L_s^3}
\begin{bmatrix}
6 & 3L_s & -6 & 3L & 0 & 0 \\
3L_s & 2L_s^2 & -3L_s & L_s^2 & 0 & 0 \\
-6 & -3L_s & 12 & 0 & -6 & 3L_s \\
3L_s & L_s^2 & 0 & 4L_s^2 & -3L_s & L_s^2 \\
0 & 0 & -6 & -3L_s & 6 & -3L_s \\
0 & 0 & 3L & L_s^2 & -3L_s & 2L_s^2
\end{bmatrix}
\begin{bmatrix} Z_5 \\ \theta_5 \\ Z_6 \\ \theta_6 \\ Z_7 \\ \theta_7 \end{bmatrix}
\tag{3.30}
$$

The elastic model for the main structure is shown in Fig. 13. The main structure is also modeled as two flexible beams, but with higher flexural rigidity than those of the solar panels. These beams are uniform and have a length of 140 ft each. The stiffness matrix for this structure is shown in the following equation,

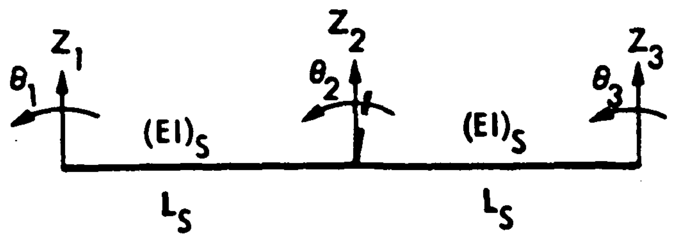

Figure 11 Elastic Model for Solar Panels -- South

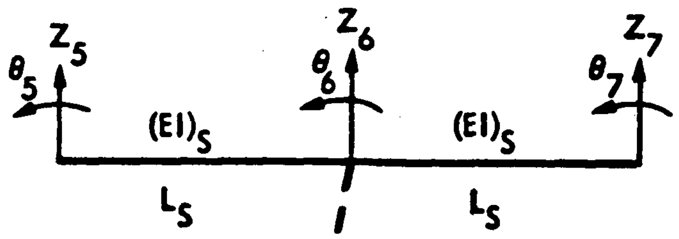

Figure 12 Elastic Model for Solar Panels — North

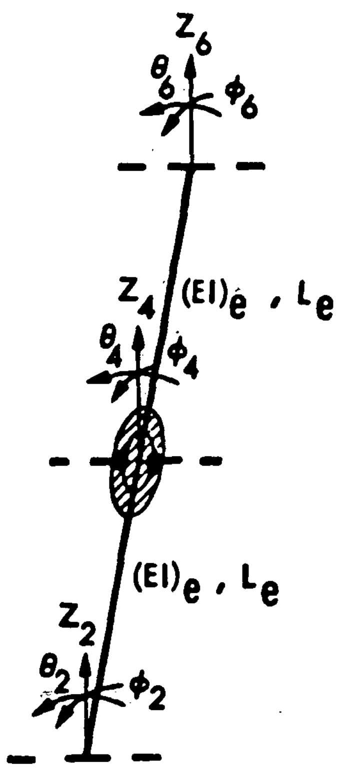

Figure 13 Elastic Model for the Main Structure

$$\begin{bmatrix} F_2 \\ T_{2\phi} \\ F_4 \\ T_{4\phi} \\ F_6 \\ T_{6\phi} \end{bmatrix} = \frac{2(EI)_e}{L_e^3} \left[\begin{array}{cc|cc|cc} 6 & 3L_e & -6 & 3L_e & 0 & 0 \\ 3L_e & 2L_e^2 & -3L_e & L_e^2 & 0 & 0 \\ \hline -6 & -3L_e & 12 & 0 & -6 & 3L_e \\ 3L_e & L_e^2 & 0 & 4L_e^2 & -3L_e & L_e^2 \\ \hline 0 & 0 & -6 & -3L_e & 6 & -3L_e \\ 0 & 0 & 3L_e & L_e^2 & -3L_e & 2L_e^2 \end{array}\right] \begin{bmatrix} Z_2 \\ \phi_2 \\ Z_4 \\ \phi_4 \\ Z_6 \\ \phi_6 \end{bmatrix} \tag{3.31}$$

Applying the same principle of Eq. (3.8), the stiffness matrices of Eqs. (3.29), (3.30) and (3.31) can be combined to yield the system stiffness matrix. Reorder the force and displacement vectors and the corresponding rows and columns of Eq. (3.29) as follows,

$$\begin{bmatrix} T_{2\theta} \\ F_1 \\ T_{1\theta} \\ F_3 \\ T_{3\theta} \\ F_2 \end{bmatrix} = \frac{2(EI)_s}{L_s^3} \left[\begin{array}{ccccc|c} 4L_s^2 & 3L_s & L_s^2 & -3L_s & L_s^2 & 0 \\ 3L_s & 6 & 3L_s & 0 & 0 & -6 \\ L_s^2 & 3L_s & 2L_s^2 & 0 & 0 & -3L_s \\ -3L_s & 0 & 0 & 6 & -3L_s & -6 \\ L_s^2 & 0 & 0 & -3L_s & 2L_s^2 & -3L_s \\ \hline 0 & -6 & -3L_s & -6 & 3L_s & 12 \end{array}\right] \begin{bmatrix} \theta_2 \\ Z_1 \\ \theta_1 \\ Z_3 \\ \theta_3 \\ Z_2 \end{bmatrix} \tag{3.32}$$

The purpose of this reordering process is to move $T_{2\theta}$ and θ_2 to the top for later use and F_2 and Z_2 to the bottom so that the "south" panels can be combined with the main structure.

Reorder the rows and columns of Eq. (3.31) so that F_2 and Z_2 are placed on the top and F_6 and Z_6 are on the bottom,

$$\begin{bmatrix} F_2 \\ T_{2\phi} \\ F_4 \\ T_{4\phi} \\ T_{6\phi} \\ F_6 \end{bmatrix} = \frac{2(EI)_e}{L_e^3} \left[\begin{array}{c|ccccc|c} 6 & 3L_e & -6 & 3L_e & 0 & & 0 \\ \hline 3L_e & 2L_e^2 & -3L_e & L_e^2 & 0 & & 0 \\ -6 & -3L_e & 12 & 0 & 3L_e & & -6 \\ 3L_e & L_e^2 & 0 & 4L_e^2 & L_e^2 & & -3L_e \\ 0 & 0 & 3L_e & L_e^2 & 2L_e^2 & & -3L_e \\ \hline 0 & 0 & -6 & -3L_e & -3L_e & & 6 \end{array}\right] \begin{bmatrix} Z_2 \\ \phi_2 \\ Z_4 \\ \phi_4 \\ \phi_6 \\ Z_6 \end{bmatrix} \tag{3.33}$$

Reorder Eq. (3.30) so that F_6 and Z_6 sit on the top and $T_{6\theta}$ and θ_6 at the bottom,

$$\begin{bmatrix} F_6 \\ F_5 \\ T_{5\theta} \\ F_7 \\ T_{7\theta} \\ T_{6\theta} \end{bmatrix} = \frac{2(EI)_s}{L_s^3} \left[\begin{array}{c|ccccc} 12 & -6 & -3L_s & -6 & 3L_s & 0 \\ \hline -6 & 6 & 3L_s & 0 & 0 & 3L_s \\ -3L_s & 3L_s & 2L_s^2 & 0 & 0 & L_s^2 \\ -6 & 0 & 0 & 6 & -3L_s & -3L_s \\ 3L_s & 0 & 0 & -3L_s & 2L_s^2 & L_s^2 \\ 0 & 3L_s & L_s^2 & -3L_s & L_s^2 & 4L_s^2 \end{array}\right] \begin{bmatrix} Z_6 \\ Z_5 \\ \theta_5 \\ Z_7 \\ \theta_7 \\ \theta_6 \end{bmatrix} \tag{3.34}$$

Let

$$\alpha = \frac{2(EI)_s}{L_s^3}, \quad \text{and} \quad \beta = \frac{2(EI)_e}{L_e^3} \tag{3.35}$$

combine Eqs. (3.32), (3.33) and (3.34) one has

$$\begin{bmatrix} T_{2\theta} \\ F_1 \\ T_{1\theta} \\ F_3 \\ T_{3\theta} \\ F_2 \\ T_{2\phi} \\ F_4 \\ T_{4\phi} \\ T_{6\phi} \\ F_6 \\ F_5 \\ T_{5\theta} \\ F_7 \\ T_{7\theta} \\ T_{6\theta} \end{bmatrix} = \left[\begin{array}{cccccccccccccccc}
4L_s^2\alpha & 3L_s\alpha & L_s^2\alpha & -3L_s\alpha & L_s^2\alpha & 0 & & & & & & & & & & \\
3L_s\alpha & 6\alpha & 3L_s\alpha & 0 & 0 & -6\alpha & & & & & & & & & & \\
L_s^2\alpha & 3L_s\alpha & 2L_s^2\alpha & 0 & 0 & -3L_s\alpha & & & & & & & & & & \\
-3L_s\alpha & 0 & 0 & 6\alpha & -3L_s\alpha & -6\alpha & & & & & & & & & & \\
L_s^2\alpha & 0 & 0 & -3L_s\alpha & 2L_s^2\alpha & 3L_s\alpha & & & & & & & & & & \\
0 & -6\alpha & -3L_s\alpha & -6\alpha & 3L_s\alpha & 12\alpha+6\beta & 3L_e\beta & -6\beta & 3L_e\beta & 0 & 0 & & & & & \\
 & & & & & 3L_e\beta & 2L_e^2\beta & -3L_e\beta & L_e^2\beta & 0 & 0 & & & & & \\
 & & & & & 6\beta & -3L_e\beta & 12\beta & 0 & 3L_e\beta & -6\beta & & & & & \\
 & & & & & 3L_e\beta & L_e^2\beta & 0 & 4L_e^2\beta & L_e^2\beta & -3L_e\beta & & & & & \\
 & & & & & 0 & 0 & 3L_e\beta & L_e^2\beta & 2L_e^2\beta & -3L_e\beta & & & & & \\
 & & & & & 0 & 0 & -6\beta & -3L_e\beta & -3L_e\beta & 6\beta+12\alpha & -6\alpha & -3L_s\alpha & -6\alpha & 3L_s\alpha & 0 \\
 & & & & & & & & & & -6\alpha & 6\alpha & 3L_s\alpha & 0 & 0 & 3L_s\alpha \\
 & & & & & & & & & & -3L_s\alpha & 3L_s\alpha & 2L_s^2\alpha & 0 & 0 & L_s^2\alpha \\
 & & & & & & & & & & -6\alpha & 0 & 0 & 6\alpha & -3L_s\alpha & -3L_s\alpha \\
 & & & & & & & & & & 3L_s\alpha & 0 & 0 & -3L_s\alpha & 2L_s^2\alpha & L_s^2\alpha \\
 & & & & & & & & & & 0 & 3L_s\alpha & L_s^2\alpha & -3L_s\alpha & L_s^2\alpha & 4L_s^2\alpha
\end{array}\right] \begin{bmatrix} \theta_2 \\ z_1 \\ \theta_1 \\ z_3 \\ \theta_3 \\ z_2 \\ \phi_2 \\ z_4 \\ \phi_4 \\ \phi_6 \\ z_6 \\ z_5 \\ \theta_5 \\ z_7 \\ \theta_7 \\ \theta_6 \end{bmatrix} \tag{3.36}$$

Now we shall use the constraints of Eq. (3.28) and

$$T_{2\theta} = T_{6\theta} = T_{4\theta} \tag{3.37}$$

to combine $T_{6\theta}$ and $T_{2\theta}$ and rename it as $T_{4\theta}$, and θ_6 and θ_2 and rename it as θ_4 and rearrange the rows and columns so that they appear between F_4 and $T_{4\phi}$ and between Z_4 and ϕ_4, respectively. In addition, we also exchange the orders of $T_{6\phi}$ and F_6, and ϕ_6 and Z_6. Thus if we let F_s, Z_s, and K_s be the force vector, displacement vector, and the stiffness matrix, respectively, Eq. (3.36) becomes

$$F_s = K_s\, Z_s \tag{3.38}$$

where

$$F_s = (F_1\ T_{1\theta}\ F_3\ T_{3\theta}\ F_2\ T_{2\phi}\ F_4\ T_{4\theta}\ T_{4\phi}\ F_6\ T_{6\phi}\ F_5\ T_{5\theta}\ F_7\ T_{7\theta})^T \tag{3.39}$$

$$Z_s = (Z_1\ \theta_1\ Z_3\ \theta_3\ Z_2\ \phi_2\ Z_4\ \theta_4\ \phi_4\ Z_6\ \phi_6\ Z_5\ \theta_5\ Z_7\ \theta_7)^T \tag{3.40}$$

and K_s is shown in Eq. (3.41).

$$K_s = \begin{bmatrix}
6\alpha & 3L_s\alpha & 0 & 0 & -6\alpha & 0 & 0 & 3L_s\alpha & 0 & 0 & 0 & 0 & 0 & 0 & 0 \\
3L_s\alpha & 2L_s^2\alpha & 0 & 0 & -3L_s\alpha & 0 & 0 & L_s^2\alpha & 0 & 0 & 0 & 0 & 0 & 0 & 0 \\
0 & 0 & 6\alpha & -3L_s\alpha & -6\alpha & 0 & 0 & -3L_s\alpha & 0 & 0 & 0 & 0 & 0 & 0 & 0 \\
0 & 0 & -3L_s\alpha & 2L_s^2\alpha & 3L_s\alpha & 0 & 0 & L_s^2\alpha & 0 & 0 & 0 & 0 & 0 & 0 & 0 \\
-6\alpha & -3L_s\alpha & -6\alpha & 3L_s\alpha & 12\alpha+6\beta & 3L_e\beta & -6\beta & 0 & 3L_e\beta & 0 & 0 & 0 & 0 & 0 & 0 \\
0 & 0 & 0 & 0 & 3L_e\beta & 2L_e^2\beta & -3L_e\beta & 0 & L_e^2\beta & 0 & 0 & 0 & 0 & 0 & 0 \\
0 & 0 & 0 & 0 & -6\beta & -3L_e\beta & 12\beta & 0 & 0 & -6\beta & 3L_e\beta & 0 & 0 & 0 & 0 \\
3L_s\alpha & L_s^2\alpha & -3L_s\alpha & L_s^2\alpha & 0 & 0 & 0 & 8L_s^2\alpha & 0 & 0 & 0 & 3L_s\alpha & L_s^2\alpha & -3L_s\alpha & L_s^2\alpha \\
0 & 0 & 0 & 0 & 3L_e\beta & L_e^2\beta & 0 & 0 & 4L_e^2\beta & -3L_e\beta & L_e^2\beta & 0 & 0 & 0 & 0 \\
0 & 0 & 0 & 0 & 0 & 0 & -6\beta & 0 & -3L_e\beta & 12\alpha+6\beta & -3L_e\beta & -6\alpha & -3L_s\alpha & -6\alpha & 3L_s\alpha \\
0 & 0 & 0 & 0 & 0 & 0 & 3L_e\beta & 0 & L_e^2\beta & -3L_e\beta & 2L_e^2\beta & 0 & 0 & 0 & 0 \\
0 & 0 & 0 & 0 & 0 & 0 & 0 & 3L_s\alpha & 0 & -6\alpha & 0 & 6\alpha & 3L_s\alpha & 0 & 0 \\
0 & 0 & 0 & 0 & 0 & 0 & 0 & L_s^2\alpha & 0 & -3L_s\alpha & 0 & 3L_s\alpha & 2L_s^2\alpha & 0 & 0 \\
0 & 0 & 0 & 0 & 0 & 0 & 0 & -3L_s\alpha & 0 & -6\alpha & 0 & 0 & 0 & 6\alpha & 3L_s\alpha \\
0 & 0 & 0 & 0 & 0 & 0 & 0 & L_s^2\alpha & 0 & 3L_s\alpha & 0 & 0 & 0 & -3L_s\alpha & 2L_s^2\alpha
\end{bmatrix} \tag{3.41}$$

where $\alpha = \dfrac{2(EI)_s}{L_s^3}$ and $\beta = \dfrac{2(EI)_e}{L_e^3}$.

A quick check of symmetry, K_s is symmetric as it is supposed to be.

3.2.3 The Consistent-Mass Matrix

Consider Figs. 14, 15, and 16 which show the distributed mass models for the south and north solar panels and the main structure, respectively. By using the same finite-element technique, the consistent-mass matrices for the component structures are,

a. Solar Panel — South

$$\begin{bmatrix} F_1 \\ T_{1\theta} \\ F_2 \\ T_{2\theta} \\ F_3 \\ T_{3\theta} \end{bmatrix} = \frac{\rho_s L_s}{420} \begin{bmatrix} 156 & 22L_s & 54 & -13L_s & 0 & 0 \\ 22L_s & 4L_s^2 & 13L_s & -3L_s^2 & 0 & 0 \\ 54 & 13L_s & 312 & 0 & 54 & -13L_s \\ -13L_s & -3L_s^2 & 0 & 8L_s^2 & 13L_s & -3L_s^2 \\ 0 & 0 & 54 & 13L_s & 156 & -22L_s \\ 0 & 0 & -13L_s & -3L_s^2 & -22L_s & 4L_s^2 \end{bmatrix} \begin{bmatrix} \ddot{Z}_1 \\ \ddot{\theta}_1 \\ \ddot{Z}_2 \\ \ddot{\theta}_2 \\ \ddot{Z}_3 \\ \ddot{\theta}_3 \end{bmatrix} \tag{3.42}$$

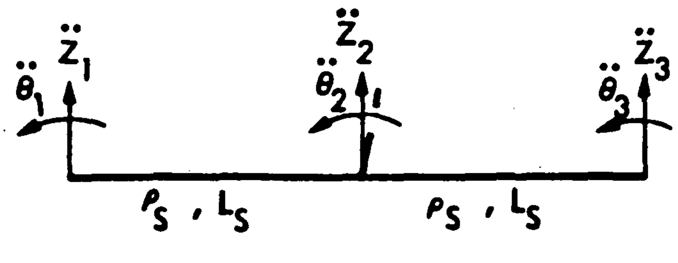

Figure 14 Distributed Mass Model for Solar Panels — South

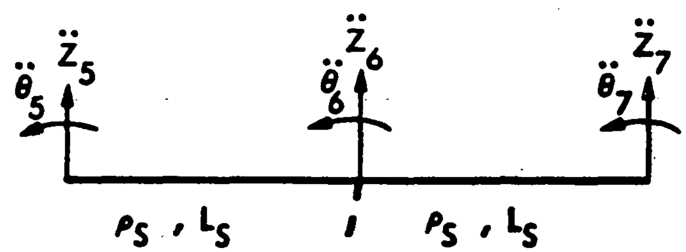

Figure 15 Distributed Mass Model for Solar Panels — North

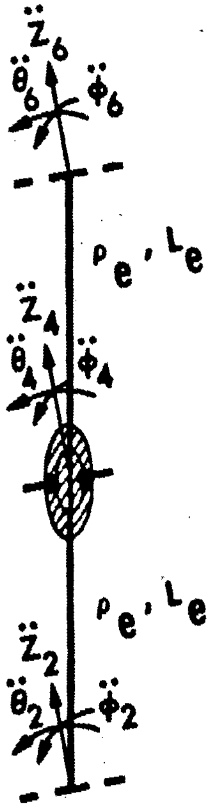

Figure 16 Distributed Mass Model for the Main Structure

b. Solar Panel — North

$$\begin{bmatrix} F_5 \\ T_{5\theta} \\ F_6 \\ T_{6\theta} \\ F_7 \\ T_{7\theta} \end{bmatrix} = \frac{\rho_s L_s}{420} \begin{bmatrix} 156 & 22L_s & 54 & -13L_s & 0 & 0 \\ 22L_s & 4L_s^2 & 13L_s & -3L_s^2 & 0 & 0 \\ 54 & 13L_s & 312 & 0 & 54 & -13L_s \\ -13L_s & -3L_s^2 & 0 & 8L_s^2 & 13L_s & -3L_s^2 \\ 0 & 0 & 54 & 13L_s & 156 & -22L_s \\ 0 & 0 & -13L_s & -3L_s^2 & -22L_s & 4L_s^2 \end{bmatrix} \begin{bmatrix} \ddot{Z}_5 \\ \ddot{\theta}_5 \\ \ddot{Z}_6 \\ \ddot{\theta}_6 \\ \ddot{Z}_7 \\ \ddot{\theta}_7 \end{bmatrix} \tag{3.43}$$

c. Main Structure

$$\begin{bmatrix} F_2 \\ T_{2\phi} \\ F_4 \\ T_{4\phi} \\ F_6 \\ T_{6\phi} \end{bmatrix} = \frac{\rho_e L_e}{420} \begin{bmatrix} 156 & 22L_e & 54 & -13L_e & 0 & 0 \\ 22L_e & 4L_e^2 & 13L_e & -3L_e^2 & 0 & 0 \\ 54 & 13L_e & 312 & 0 & 54 & -13L_e \\ -13L_e & -3L_e^2 & 0 & 8L_e^2 & 13L_e & -3L_e^2 \\ 0 & 0 & 54 & 13L_e & 156 & -22L_e \\ 0 & 0 & -13L_e & -3L_e^2 & -22L_e & 4L_e^2 \end{bmatrix} \begin{bmatrix} \ddot{Z}_2 \\ \ddot{\phi}_2 \\ \ddot{Z}_4 \\ \ddot{\phi}_4 \\ \ddot{Z}_6 \\ \ddot{\phi}_6 \end{bmatrix} \tag{3.44}$$

Employing a similar approach for obtaining the stiffness matrix, the following equation can be obtained:

$$F_s = M_{sc} \ddot{Z}_s \tag{3.45}$$

where

ORIGINAL PAGE IS
OF POOR QUALITY

$$\bar{F}_s = (F_1 \; T_{1\theta} \; F_3 \; T_{3\theta} \; F_2 \; T_{2\phi} \; F_4 \; T_{4\theta} \; T_{4\phi} \; F_6 \; T_{6\phi} \; F_5 \; T_{5\theta} \; F_7 \; T_{7\theta})^T$$

$$\ddot{Z}_s = (\ddot{Z}_1 \; \ddot{\theta}_1 \; \ddot{Z}_3 \; \ddot{\theta}_3 \; \ddot{Z}_2 \; \ddot{\phi}_2 \; \ddot{Z}_4 \; \ddot{\theta}_4 \; \ddot{\phi}_4 \; \ddot{Z}_6 \; \ddot{\phi}_6 \; \ddot{Z}_5 \; \ddot{\theta}_5 \; \ddot{Z}_7 \; \ddot{\theta}_7)^T$$

and the consistent-mass matrix M_{SC} is shown in Eqs. (3.46) and (3.47).

$$M_{SC} = \begin{bmatrix}
156a & 22L_sa & 0 & 0 & 54a & 0 & 0 & -13L_sa & 0 & 0 & 0 & 0 & 0 & 0 & 0 \\
-22L_sa & 4L_s^2a & 0 & 0 & 13L_sa & 0 & 0 & -3L_s^2a & 0 & 0 & 0 & 0 & 0 & 0 & 0 \\
0 & 0 & 156a & -22L_sa & 54a & 0 & 0 & 13L_sa & 0 & 0 & 0 & 0 & 0 & 0 & 0 \\
0 & 0 & -22L_sa & 4L_s^2a & -13L_sa & 0 & 0 & -3L_s^2a & 0 & 0 & 0 & 0 & 0 & 0 & 0 \\
54a & 13L_sa & 54a & -13L_sa & 312a+156b & 22L_eb & 54b & 0 & -13L_eb & 0 & 0 & 0 & 0 & 0 & 0 \\
0 & 0 & 0 & 0 & 22L_eb & 4L_e^2b & 13L_eb & 0 & -3L_e^2b & 0 & 0 & 0 & 0 & 0 & 0 \\
0 & 0 & 0 & 0 & 54b & 13L_eb & 312b & 0 & 0 & 54b & -13L_eb & 0 & 0 & 0 & 0 \\
-13L_sa & -3L_s^2a & 13L_sa & -3L_s^2a & 0 & 0 & 0 & 16L_s^2a & 0 & 0 & 0 & -13L_sa & -3L_s^2a & 13L_sa & -3L_s^2a \\
0 & 0 & 0 & 0 & -13L_eb & 3L_e^2b & 0 & 0 & 8L_e^2b & 13L_eb & -3L_e^2b & 0 & 0 & 0 & 0 \\
0 & 0 & 0 & 0 & 0 & 0 & 54b & 0 & 13L_eb & 156b+312a & -22L_eb & 54a & 13L_sa & 54a & -13L_sa \\
0 & 0 & 0 & 0 & 0 & 0 & -13L_eb & 0 & -3L_e^2b & -22L_eb & 4L_e^2b & 0 & 0 & 0 & 0 \\
0 & 0 & 0 & 0 & 0 & 0 & 0 & -13L_sa & 0 & 54a & 0 & 156a & 22L_sa & 0 & 0 \\
0 & 0 & 0 & 0 & 0 & 0 & 0 & -3L_s^2a & 0 & 13L_sa & 0 & 22L_sa & 4L_s^2a & 0 & 0 \\
0 & 0 & 0 & 0 & 0 & 0 & 0 & 13L_sa & 0 & 54a & 0 & 0 & 0 & 156a & -22L_sa \\
0 & 0 & 0 & 0 & 0 & 0 & 0 & -3L_s^2a & 0 & -13L_sa & 0 & 0 & 0 & -22L_sa & 4L_s^2a
\end{bmatrix} \tag{3.46}$$

$$\text{where} \quad a = \frac{\rho_s L_s}{420} \quad \text{and} \quad b = \frac{\rho_e L_e}{420} \; . \tag{3.47}$$

3.2.4 The Lumped-Mass Matrix and System Mass Matrix

M_{SC} accounts for the distributed mass for the flexible structure but not the lumped mass associated with the rigid bodies. Let M_{SD} be the lumped-mass matrix for the station excluding the payloads, then

$$M_{SD} = \mathrm{diag}\ (0,0,0,0,0,0,M_4,I_{4yy},I_{4xx},0,0,0,0,0,0) \qquad (3.48)$$

where M_4, I_{4xx}, and I_{4yy} are the mass and moments of inertia of the core station defined in Fig. 10.

The total mass matrix, excluding payloads is,

$$M_S = M_{SC} + M_{SD} \qquad (3.49)$$

The corresponding dynamic equation due to mass and inertia is

$$F_S = M_S \ddot{Z}_S \qquad (3.50)$$

3.2.5 Payload Dynamics and Hinge Torque Model

The dynamic model for the payloads (identified as bodies 8 and 9) and the hinge coordinates are shown in Fig. 17.

To include the payload dynamics and the dynamic interactions between the payloads and the station, the following expressions are obtained using the Lagrangian approach:

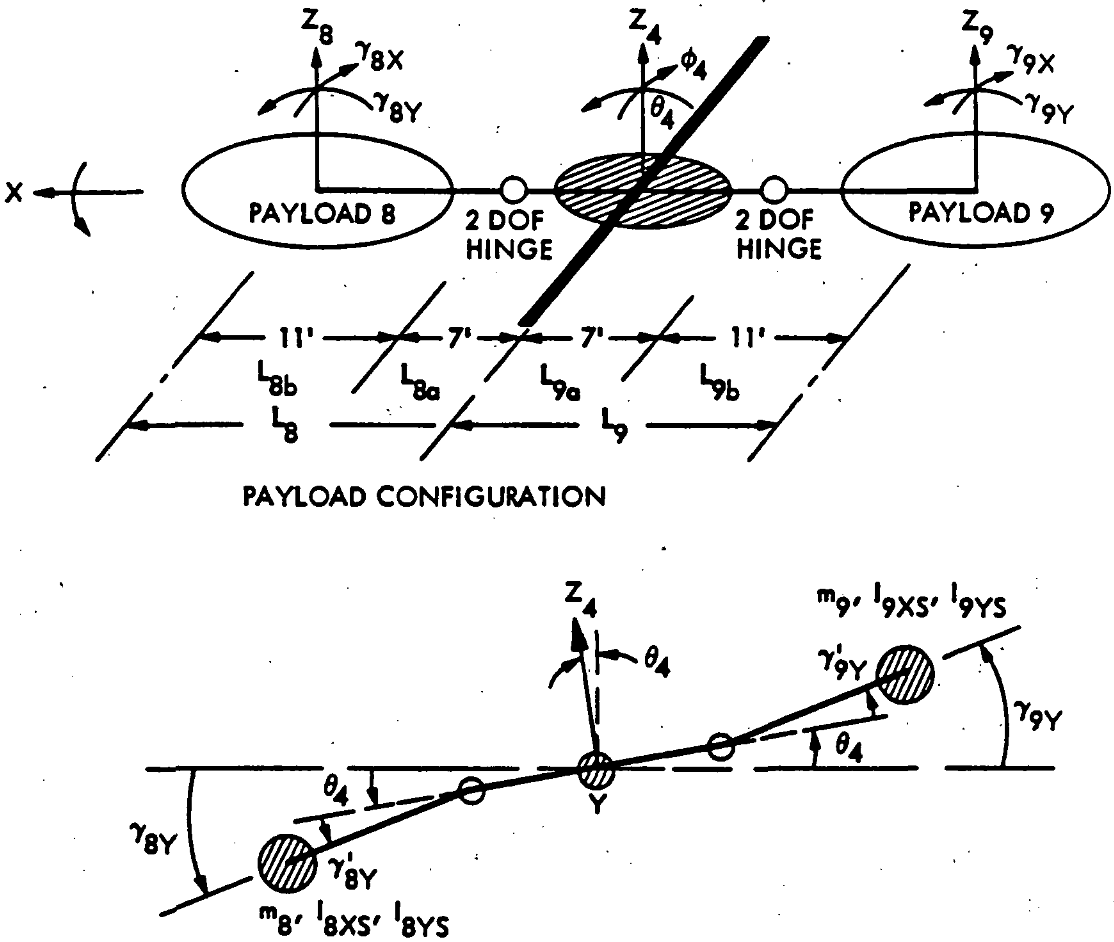

$\gamma'_{8X} = \gamma_{8X} - \phi_4$ = HINGE ANGLE FOR "PAYLOAD 8" ABOUT X-AXIS

$\gamma'_{8Y} = \gamma_{8Y} - \theta_4$ = HINGE ANGLE FOR "PAYLOAD 8" ABOUT Y-AXIS

$\gamma'_{9X} = \gamma_{9X} - \phi_4$ = HINGE ANGLE FOR "PAYLOAD 9" ABOUT X-AXIS

$\gamma'_{9Y} = \gamma_{9Y} - \theta_4$ = HINGE ANGLE FOR "PAYLOAD 9" ABOUT Y-AXIS

Figure 17 Payload Dynamics and Hinge Model

$$F_4 - (M_8+M_9)\ddot{Z}_4 + (M_8L_8-M_9L_9)\ddot{\theta}_4 + M_8L_{8b}\ddot{\gamma}'_{8y}-M_9L_{9b}\ddot{\gamma}'_{9y} \tag{3.51}$$

$$T_{4\theta} + (M_8L_8-M_9L_9)\ddot{Z}_4 - (I_{8ys}+M_8L_8^2 + I_{9ys}+M_9L_9^2)\ddot{\theta}_4 \tag{3.52}$$
$$- (I_{8ys} + M_8L_{8a}L_{8b} + M_8L_{8b}^2)\ddot{\gamma}'_{8y} - (I_{9ys}+M_9L_{9a}L_{9b}+M_9L_{9b}^2)\ddot{\gamma}'_{9y}$$

$$T_{4\phi} - (I_{8xs} + I_{9xs})\ddot{\phi}_4 - I_{8xs}\ddot{\gamma}'_{8x} - I_{9xs}\ddot{\gamma}'_{9x} \tag{3.53}$$

Eqs. (3.51), (3.52) and (3.53) are used to replace F_4, $T_{4\theta}$, and $T_{4\phi}$ in Eq. (3.50).

The torques applied at the payload hinges are,

$$T_{8x} = I_{8xs}\ddot{\phi}_4 + I_{8xs}\ddot{\gamma}'_{8x} \tag{3.54}$$

$$T_{9x} = I_{9xs}\ddot{\phi}_4 + I_{9xs}\ddot{\gamma}'_{9x} \tag{3.55}$$

$$T_{8y} = - M_8L_{8b}\ddot{Z}_4 + (I_{8ys}+M_8L_{8a}L_{8b}+M_8L_{8b}^2)\ddot{\theta}_4 + (I_{8ys}+M_8L_{8b}^2)\ddot{\gamma}'_{8y} \tag{3.56}$$

$$T_{9y} = M_9L_{9b}\ddot{Z}_4 + (I_{9ys}+M_9L_{9a}L_{9b}+M_9L_{9b}^2)\ddot{\theta}_4 + (I_{9ys}+M_9L_{9b}^2)\ddot{\gamma}'_{9y} \tag{3.57}$$

where γ'_{8x}, γ'_{8y}, γ'_{9x}, and γ'_{9y} are the hinge angles for payloads 8 and 9 about the X- and Y-axes.

The above equations are derived using the Lagrangian approach with more general assumptions and then linearized for small angles. The detailed derivation is shown in Appendix A.

3.2.6 Equations of Motion

Let $F_p = (T_{8x}, T_{9x}, T_{8y}, T_{9y})^T$ and $Z_p = (\gamma'_{8x}, \gamma'_{9x}, \gamma'_{8y}, \gamma'_{9y})^T$ be the payload forcing and displacement vectors, the corresponding vectors for the system can be partitioned as follows,

$$F = \begin{bmatrix} F_s \\ \hline F_p \end{bmatrix} \text{ and } Z = \begin{bmatrix} Z_s \\ \hline Z_p \end{bmatrix} \tag{3.58}$$

The system mass matrix becomes,

$$M = M_C + M_D \tag{3.59}$$

where

$$M_C = \left[\begin{array}{c|c} M_{SC} & 0_{15x4} \\ \hline 0_{4x15} & 0_{4x4} \end{array}\right] \tag{3.60}$$

and

$$M_D = \left[\begin{array}{c|c} M_{SD}+M'_{SD} & M^T_{PSD} \\ \hline M_{PSD} & M_{PD} \end{array}\right] \tag{3.61}$$

M_{SC} is defined in Eq. (3.46) and M_{SD} in Eq. (3.48), and M'_{SD}, M_{PD}, M_{PSD} are,

$$M'_{SD} = \left[\begin{array}{c|ccc|c} 0_{6x6} & & 0_{6x3} & & 0_{6x6} \\ \hline & m_8+m_9 & m_9L_9-m_8L_8 & 0 & \\ 0_{3x6} & m_9L_9-m_8L_8 & m_8L_8^2+m_9L_9^2+I_{8yS}+I_{9yS} & 0 & 0_{3x6} \\ & 0 & 0 & I_{8yS}+I_{9yS} & \\ \hline 0_{6x6} & & 0_{6x3} & & 0_{6x6} \end{array}\right]$$

(3.62)

$$
M_{PD} = \begin{bmatrix} I_{8xS} & 0 & 0 & 0 \\ 0 & I_{9xS} & 0 & 0 \\ 0 & 0 & I_{8yS}+m_8L_{8b}^2 & 0 \\ 0 & 0 & 0 & I_{9yS}+m_9L_{9b}^2 \end{bmatrix} \tag{3.63}
$$

$$
M_{PSD} = \left[\begin{array}{c|ccc|c} & 0 & 0 & I_{8xS} & \\ & 0 & 0 & I_{9xS} & \\ 0_{4x6} & -m_8L_{8b} & I_{8yS}+m_8L_{8a}L_{8b}+m_8L_{8b}^2 & 0 & 0_{4x6} \\ & m_9L_{9b} & I_{9yS}+m_9L_{9a}L_{9b}+m_9L_{9b}^2 & 0 & \end{array}\right] \tag{3.64}
$$

The system stiffness matrix is

$$
K = \left[\begin{array}{c|c} K_s & 0_{15x4} \\ \hline 0_{4x15} & 0_{4x4} \end{array}\right] \tag{3.65}
$$

where K_s is defined in Eq. (3.41).

The equation of motion is

$$
M\ddot{Z} + KZ = F \tag{3.66}
$$

3.2.7 Modal Coordinates and Modal Properties

Let $\eta(t)$, Λ, and ϕ be the modal amplitude vector, eigenvalue matrix, and normalized eigenvector matrix, respectively. Let $Z(t) = \phi\eta(t)$, substitute this into Eq. (3.66) and premultiply Eq. (3.66) by ϕ^T, then $\phi^T M \phi = I$ and $\phi^T K \phi = \Lambda$, one has the following dynamical equation in modal form,

$$\ddot{\eta} + \Lambda\eta = \phi^T F \tag{3.67}$$

where $\Lambda = \text{diag}\ (\omega_1^2,\ldots,\omega_{19}^2)$. Adding damping terms, Eq. (3.67) becomes,

$$\ddot{\eta} + \text{diag}\ (2\zeta_1\omega_1,\ldots,2\zeta_{19}\omega_{19})\dot{\eta} + \text{diag}(\omega_1^2,\ldots,\omega_{19}^2)\eta = \phi^T F \tag{3.68}$$

The corresponding damped dynamical equation in physical coordinates can be obtained through transformation. Let D be the damping factor matrix, one has

$$D = \phi^{-T}\ \text{diag}\ (2\zeta_1\omega_1,\ldots,2\zeta_{19}\omega_{19})\phi^{-1} \tag{3.69}$$

and the equation of motion becomes,

$$M\ddot{Z} + D\dot{Z} + KZ = F \tag{3.70}$$

For the purpose of control, let B and C be the control influence matrix and measurement distribution matrix, respectively, the system equation in physical and modal coordinates are, respectively,

$$
\begin{cases}
M\ddot{Z} + D\dot{Z} + KZ = Bu_p & (3.71) \\
\\
y_p = C\,(\alpha Z_p + \dot{Z}_p) & (3.72)
\end{cases}
$$

and

$$
\begin{cases}
\ddot{\eta} + \text{diag}\,(2\zeta_1\omega_1,\ldots,2\zeta_{19}\omega_{19})\dot{\eta} + \text{diag}\,(\omega_1^2,\ldots,\omega_{19}^2)\eta = \phi^T Bu_p & (3.73) \\
\\
y_p = C(\alpha\phi\eta + \phi\dot{\eta}) & (3.74)
\end{cases}
$$

To obtain the modal properties, i.e., to determine the eigenvalues and eigenvectors, for the open-loop system, one can either free the hinges for the payloads or clamp them. For the latter case, a 15-DOF system results with 12 flexible modes and 3 rigid body modes. For the former case, however, a 19-DOF system results since the payloads are considered rigid bodies and the hinges are freed, it ends up with 4 additional rigid or zero frequency modes. Since this does not yield additional information, only the clamped-hinge case is considered in this dissertation.

The modal frequencies and mode shapes for the four-panel configuration with clamped-hinge case are shown in Fig. 18. These modes are divided into three groups. The first bending group consists of 6 modes with frequencies ranging from 0.115 Hz to 0.302 Hz. These modes are formed with the first symmetric or antisymmetric bending of the three major structures, i.e., the two solar panel pairs and the main structure. The second bending group is caused by

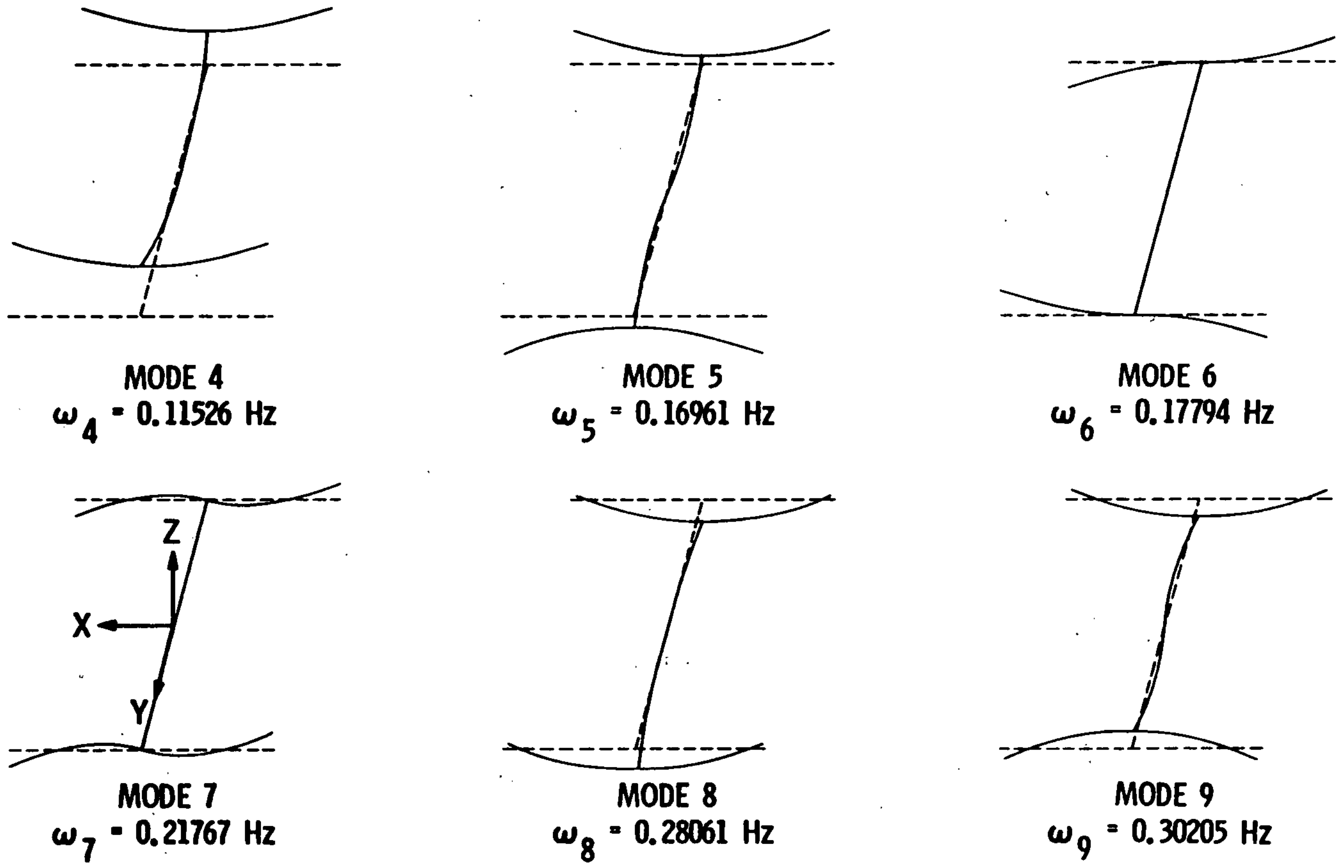

(a) First Bending Group

Figure 18 Modal Properties for the Four-Panel Configuration Model

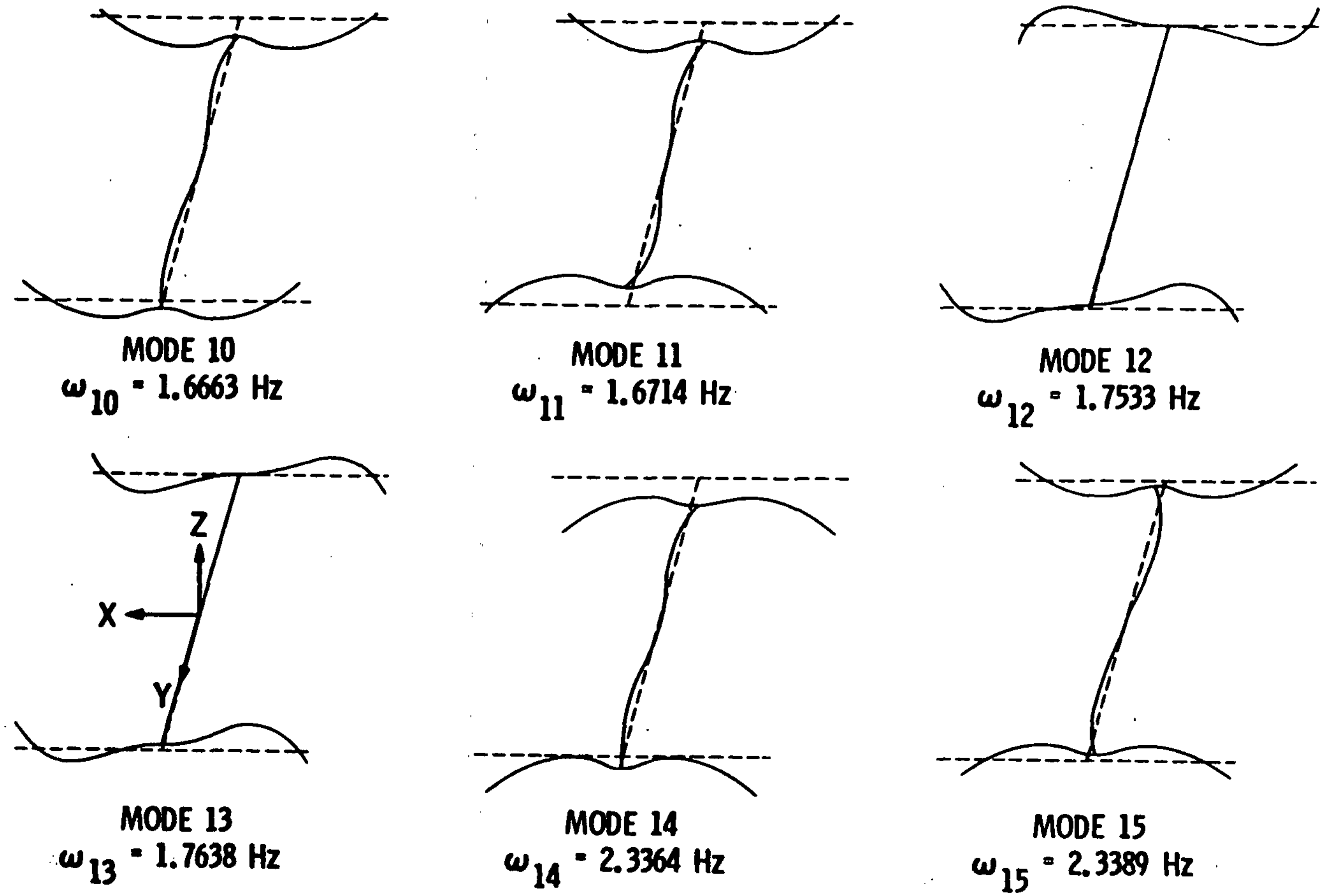

(b) Second Bending Group

Figure 18 Continued

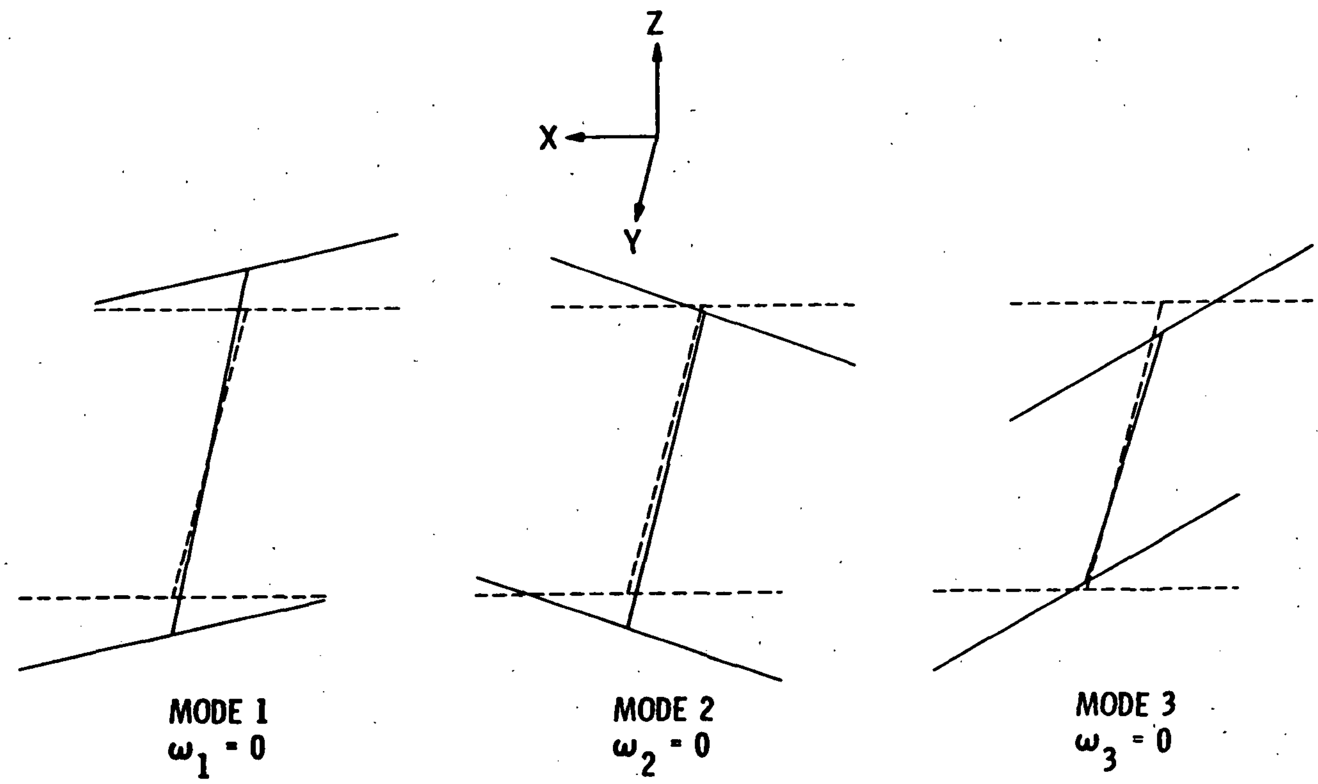

(c) Rigid Body Modes

Figure 18 Continued

the second symmetric or the antisymmetric bending of the three major structures. The frequencies for this group are much higher than those of the first group, ranging from 1.67 Hz to 2.34 Hz. The third group consists of three rigid body modes with zero frequency.

The structural and mass parameters used for generating these modes are shown in Fig. 10. The flexural rigidity $(EI)_s = 9.48 \times 10^6$ lb-ft^2 has been used for the solar panels and a value of an order of magnitude higher has been used for the main structure.

3.3 Frequency Characterization of Space Station Dynamical Systems

With the availability of these space station models, the frequency characteristics of the various dynamical systems in the space station environment are identified as shown in Fig. 19.

For a nominal orbital altitude of 400 km, the orbital period is 92.61 minutes or 1.8×10^{-4} Hz rate. For an altitude close to 400 km, the orbital rate will be inside the shaded narrow region in Fig. 19. The solar panel libration frequency for quasi-solar-inertial pointing [51] will be twice the orbital rate, as shown in Fig. 19. A low bandwidth attitude control system for the space station will have a bandwidth in the range of 0.001 Hz to 0.005 Hz. The two-panel low DOF model and the four-panel finite-element model are shown in Fig. 19 with their modeled frequencies identified by vertical lines. The dashed regions extending the modeled modes represent the modal spectra that are not included in the models. The payload attitude control systems for a range of applications will have bandwidth in a range centered at 1 Hz. The core body including the pressurized modules should have structural frequencies above 9 Hz. The figure

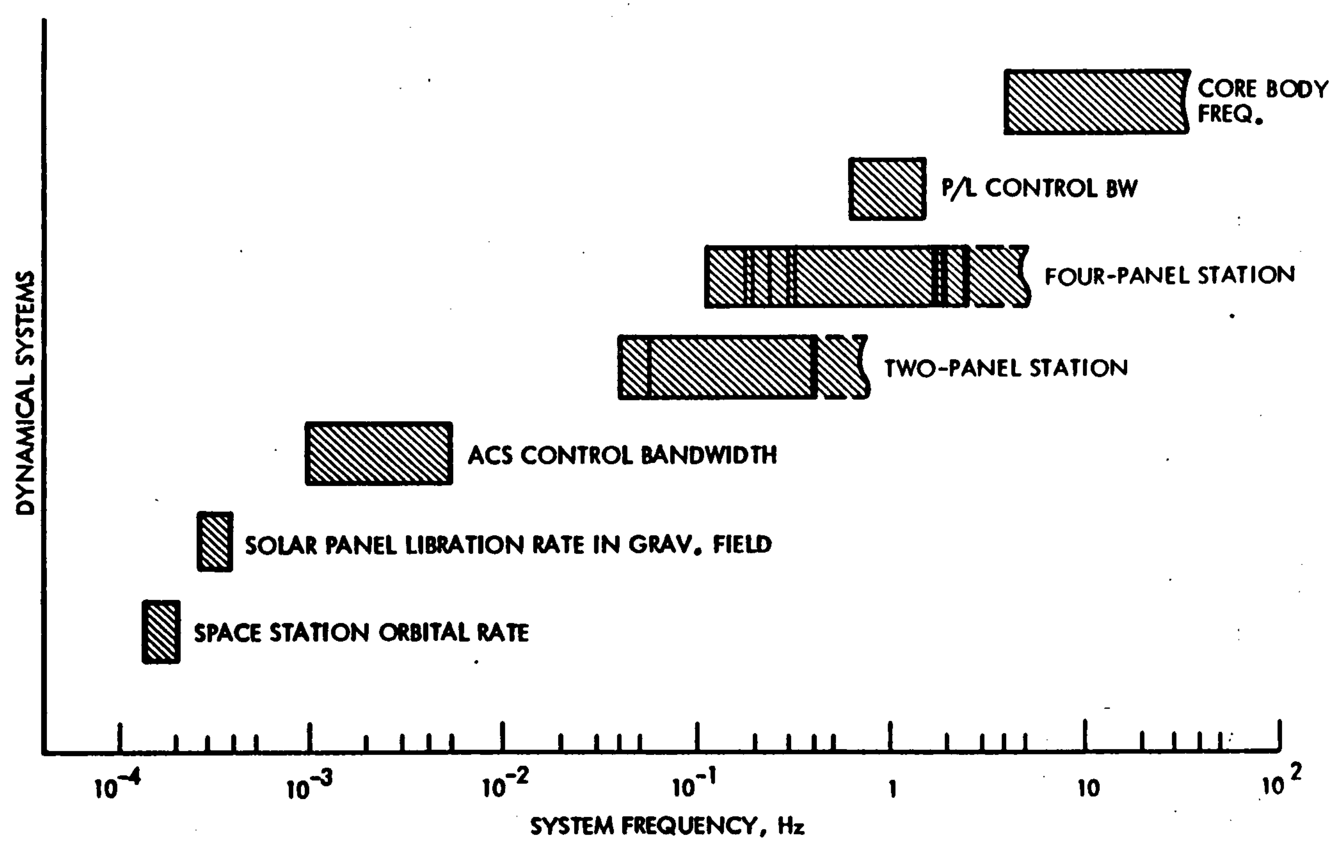

Figure 19 Frequency Characteristics of Space Station Dynamical Systems

indicates that the spectral separations of the orbital rate, the attitude controllers, and the low frequency modes of the station structure are reasonable. However, the same cannot be said about the structural modes and the payload controls. For instance, the payload controller bandwidth falls between the modes of the first and the second bending groups. This result strongly suggests that decoupling control for the payload is required.

CHAPTER IV

PROBLEM FORMULATION

The space station, or the controlled plant can be represented by the following state space model:

$$\begin{cases} \dot{x}_p(t) = A_p\, x_p(t) + B_p\, u_p(t) & (4.1) \\ y_p(t) = C_p\, x_p(t) & (4.2) \end{cases}$$

where $x_p(t)$ is the N_p-dimensional plant states, $u_p(t)$ is the M-dimensional plant control inputs, and $y_p(t)$ is the M-dimensional plant outputs. Here it has been implicitly assumed that the number of inputs equals the number of outputs. Physically, control inputs are the forces and torques generated by actuators, such as thrusters, proof masses, Control Moment Gyros, and momentum wheels. The outputs are measurements such as linear and angular displacements and rates measured by accelerometers, rate and integration gyros, etc. A_p, B_p, C_p are the state, control influence, and measurement distribution matrices of appropriate dimensions. (A_p,B_p) is controllable and (A_p, C_p) is observable.

A reference model that serves as a performance measure is required. This model is chosen to be asymptotically stable and can be represented by the following equations:

$$\begin{cases} \dot{x}_m(t) = A_m\, x_m(t) + B_m\, u_m(t) & (4.3) \\ y_m(t) = C_m\, x_m(t) & (4.4) \end{cases}$$

where $x_m(t)$ is the N_m-dimensional model states, $u_m(t)$ is the M-dimensional model commands, and $y_m(t)$ is the M-dimensional model outputs. A_m, B_m, C_m are matrices of appropriate dimensions.

Since the space station is infinitely dimensional while the dimension of the reference model has to be reasonably small for practical implementation, the following condition will be necessary for any adaptive algorithms for LSS (large space structures) or space stations:

$$N_p \gg N_m \tag{4.5}$$

Define the output error between the plant and the model as

$$e_y(t) = y_m(t) - y_p(t) \tag{4.6}$$

Since the reference model specifies the desired performance of the plant (space station), the objective is then, without assuming the complete knowledge of the plant, to design an adaptation mechanism to generate a suitable plant control input $u_p(t)$, so that the plant output tracks the model output asymptotically, i.e.,

$$\lim_{t\to\infty} e_y(t) = 0 \tag{4.7}$$

CHAPTER V

CONTROL ARCHITECTURE

5.1 Control Architecture for the Two-Panel Configuration

Referring to Fig. 6, the most rigid location on the station is its core on which inertial sensors, accelerometers and actuators are located. Control Moment Gyros (CMG's) are assumed and they are effective only for antisymmetric modes; the symmetric modes are controlled by the thrusters or proof masses. To gain controllability and compensate for vibrations of the large flexible panel structure, reaction wheels at the tips of the panels are postulated. Accelerometers and a target set of vibration sensors for relative attitude and rate measurements are also placed at the panel tips. Although the panel tips are far from ideal for locating hardware components, the choice is nil. For translational control, force actuators are required at the bus.

With the above control architectural design, the control input and output vectors are defined as follows:

$$u_p = \begin{bmatrix} u_{p1} \\ u_{p2} \\ u_{p3} \\ u_{p4} \end{bmatrix} = \begin{bmatrix} T_1 \\ F_2 \\ T_2 \\ T_3 \end{bmatrix} = \begin{bmatrix} \text{control torque at left panel tip} \\ \text{control force at central bus} \\ \text{control torque at central bus} \\ \text{control torque at right panel tip} \end{bmatrix} \tag{5.1}$$

and

$$y_p = \begin{bmatrix} y_{p1} \\ y_{p2} \\ y_{p3} \\ y_{p4} \end{bmatrix} = \begin{bmatrix} \alpha\theta_{p1} + \dot{\theta}_{p1} \\ \alpha Z_{p2} + \dot{Z}_{p2} \\ \alpha\theta_{p2} + \dot{\theta}_{p2} \\ \alpha\theta_{p3} + \dot{\theta}_{p3} \end{bmatrix} \tag{5.2}$$

In order to apply adaptive control techniques to this 6-DOF model, Eqs. (3.26a) and (3.26b), i.e., the plant equations, are written in state space form. Let η_p be the modal amplitude vector, and define the plant state vector x_p as,

$$x_p = \begin{bmatrix} \eta_p \\ \hline \dot{\eta}_p \end{bmatrix} \tag{5.3}$$

we have

$$\left\{ \begin{aligned} \dot{x}_p &= \left[\begin{array}{cc|cc} \multicolumn{2}{c|}{0} & \multicolumn{2}{c}{I} \\ \hline -\omega_{p1}^2 & 0 & -2\zeta_{p1}\omega_{p1} & 0 \\ 0 & -\omega_{p6}^2 & 0 & -2\zeta_{p6}\omega_{p6} \end{array}\right] \begin{bmatrix} \eta_p \\ \hline \dot{\eta}_p \end{bmatrix} + \begin{bmatrix} 0 \\ \hline \phi_p^T B \end{bmatrix} u_p & (5.4) \\ y_p &= \left[\begin{array}{c|c} \alpha C\phi_p & C\phi_p \end{array}\right] \begin{bmatrix} \eta_p \\ \hline \dot{\eta}_p \end{bmatrix} & (5.5) \end{aligned} \right.$$

the corresponding A_p, B_p, and C_p matrices are

$$A_p = \left[\begin{array}{cc|cc} \multicolumn{2}{c|}{0_{6x6}} & \multicolumn{2}{c}{I_{6x6}} \\ \hline -\omega_{p1}^2 & 0 & -2\zeta_{p1}\omega_{p1} & 0 \\ 0 & -\omega_{p6}^2 & 0 & -2\zeta_{p6}\omega_{p6} \end{array}\right] \tag{5.6}$$

$$B_p = \begin{bmatrix} 0 \\ \hline \phi_p^T B \end{bmatrix} \tag{5.7}$$

$$C_p = [\alpha C\phi_p \mid C\phi_p] \tag{5.8}$$

where ϕ_p is the mode shape (eigenvector) matrix for the plant, ω_{pk} and ζ_{pk} are the modal frequencies and damping ratios, respectively.

Based on the control input vector u_p given in Eq. (5.1), the control influence matrix B is given by

$$B = \begin{bmatrix} 0 & 0 & 0 & 0 \\ 1 & 0 & 0 & 0 \\ 0 & 1 & 0 & 0 \\ 0 & 0 & 1 & 0 \\ 0 & 0 & 0 & 0 \\ 0 & 0 & 0 & 1 \end{bmatrix} \tag{5.9}$$

Since the sensors and actuators are colocated, we have, in Eqs. (5.7) and (5.8)

$$C = B^T \tag{5.10}$$

5.2 Control Architecture for the Four-Panel Configuration

With a similar but more complicated control architectural design than that used for the two-panel configuration, the control input and output vectors for the four-panel configuration are defined as follows:

$$
u_p = \begin{bmatrix} u_{p1} \\ u_{p2} \\ u_{p3} \\ u_{p4} \\ u_{p5} \\ u_{p6} \\ u_{p7} \\ u_{p8} \\ u_{p9} \\ u_{p10} \\ u_{p11} \end{bmatrix} = \begin{bmatrix} T_{1\theta} \\ T_{3\theta} \\ F_2 \\ T_{2\phi} \\ F_4 \\ T_{4\theta} \\ T_{4\phi} \\ F_6 \\ T_{6\phi} \\ T_{5\theta} \\ T_{7\theta} \end{bmatrix} = \begin{bmatrix} \text{Y-torque at left south panel tip} \\ \text{Y-torque at right south panel tip} \\ \text{Z-force at the root of south panel} \\ \text{X-torque (bending) at the root of south panel} \\ \text{Z-force at central bus} \\ \text{Y-torque (twisting) at central bus} \\ \text{X-torque (bending) at central bus} \\ \text{Z-force at the root of north panel} \\ \text{X-torque (bending) at the root of north panel} \\ \text{Y-torque at left north panel tip} \\ \text{Y-torque at right north panel tip} \end{bmatrix}
$$

and

(5.11)

$$
y_p = \begin{bmatrix} y_{p1} \\ y_{p2} \\ y_{p3} \\ y_{p4} \\ y_{p5} \\ y_{p6} \\ y_{p7} \\ y_{p8} \\ y_{p9} \\ y_{p10} \\ y_{p11} \end{bmatrix} = \begin{bmatrix} \alpha\theta_{p1} + \dot{\theta}_{p1} \\ \alpha\theta_{p3} + \dot{\theta}_{p3} \\ \alpha Z_{p2} + \dot{Z}_{p2} \\ \alpha\phi_{p2} + \dot{\phi}_{p2} \\ \alpha Z_{p4} + \dot{Z}_{p4} \\ \alpha\theta_{p4} + \dot{\theta}_{p4} \\ \alpha\phi_{p4} + \dot{\phi}_{p4} \\ \alpha Z_{p6} + \dot{Z}_{p6} \\ \alpha\phi_{p6} + \dot{\phi}_{p6} \\ \alpha\theta_{p5} + \dot{\theta}_{p5} \\ \alpha\theta_{p7} + \dot{\theta}_{p7} \end{bmatrix} \tag{5.12}
$$

11 sets of sensors and actuators are used at 7 locations. The problem becomes more involved now because of the more complicated

structure and the three-dimensional motion instead of plane motion only.

Again, for the application of adaptive control, state-space representations of Eqs. (3.73) and (3.74) are obtained. Let η_p be the modal amplitude vector, and define the plant state vector x_p as,

$$x_p = \left[\begin{array}{c} \eta_p \\ \hline \dot{\eta}_p \end{array}\right] \tag{5.13}$$

we have

$$\dot{x}_p = \left[\begin{array}{cc|cc} \multicolumn{2}{c|}{0} & \multicolumn{2}{c}{I} \\ \hline -\omega_{p1}^2 & 0 & -2\zeta_{p1}\omega_{p1} & 0 \\ 0 & -\omega_{p15}^2 & 0 & -2\zeta_{p15}\omega_{p15} \end{array}\right] \left[\begin{array}{c} \eta_p \\ \hline \dot{\eta}_p \end{array}\right] + \left[\begin{array}{c} 0 \\ \hline \phi_p^T B \end{array}\right] u_p \tag{5.14}$$

$$y_p = \left[\begin{array}{c|c} \alpha C\phi_p & C\phi_p \end{array}\right] \left[\begin{array}{c} \eta_p \\ \hline \dot{\eta}_p \end{array}\right] \tag{5.15}$$

the corresponding A_p, B_p, and C_p matrices are

$$A_p = \left[\begin{array}{cc|cc} \multicolumn{2}{c|}{0_{15x15}} & \multicolumn{2}{c}{I_{15x15}} \\ \hline -\omega_{p1}^2 & 0 & -2\zeta_{p1}\omega_{p1} & 0 \\ 0 & -\omega_{p15}^2 & 0 & -2\zeta_{p15}\omega_{p15} \end{array}\right] \tag{5.16}$$

$$B_p = \left[\begin{array}{c} 0 \\ \hline \phi_p^T B \end{array}\right] \tag{5.17}$$

$$C_p = [\alpha C\phi_p \quad C\phi_p] \tag{5.18}$$

where ϕ_p, ω_{pk}, and ζ_{pk} are the eigenvector matrix, modal frequencies and damping ratios, respectively, and the control influence matrix B is

$$B = \begin{bmatrix} 0&0&0&0&0&0&0&0&0&0&0 \\ 1&0&0&0&0&0&0&0&0&0&0 \\ 0&0&0&0&0&0&0&0&0&0&0 \\ 0&1&0&0&0&0&0&0&0&0&0 \\ 0&0&1&0&0&0&0&0&0&0&0 \\ 0&0&0&1&0&0&0&0&0&0&0 \\ 0&0&0&0&1&0&0&0&0&0&0 \\ 0&0&0&0&0&1&0&0&0&0&0 \\ 0&0&0&0&0&0&1&0&0&0&0 \\ 0&0&0&0&0&0&0&1&0&0&0 \\ 0&0&0&0&0&0&0&0&1&0&0 \\ 0&0&0&0&0&0&0&0&0&0&0 \\ 0&0&0&0&0&0&0&0&0&1&0 \\ 0&0&0&0&0&0&0&0&0&0&0 \\ 0&0&0&0&0&0&0&0&0&0&1 \end{bmatrix} \tag{5.19}$$

Again, the sensors and actuators are colocated, hence

$$C = B^T \tag{5.20}$$

in Eqs. (5.17) and (5.18).

CHAPTER VI

ADAPTIVE CONTROL ALGORITHM

The equations of the plant (space station) and the reference model are described in Eqs. (4.1)-(4.4), and are repeated below for convenience:

$$\text{plant} \begin{cases} \dot{x}_p(t) = A_p\, x_p(t) + B_p\, u_p(t) & (6.1) \\ y_p(t) = C_p\, x_p(t) & (6.2) \end{cases}$$

$$\text{model} \begin{cases} \dot{x}_m(t) = A_m\, x_m(t) + B_m\, u_m(t) & (6.3) \\ y_m(t) = C_m\, x_m(t) & (6.4) \end{cases}$$

The output error is

$$e_y(t) = y_m(t) - y_p(t) \tag{6.5}$$

The objective is to find u_p such that

$$\lim_{t \to \infty} e_y(t) = 0 \tag{6.6}$$

with the requirement that dimension $N_p >> N_m$ and A_p, B_p, C_p are not completely known.

The adaptive control algorithm under consideration here is an extension of that developed in Ref. 42. Since the Command Generator Tracker theory [43] formed the basis of that algorithm, it is introduced first in the following.

6.1 The Command Generator Tracker Theory

The Command Generator Tracker (CGT) concept developed by Broussard is a type of model reference control. What makes it attractive is that it allows perfect model output tracking even though the plant and the model are not of the same order. The basic idea of CGT is to generate a plant input $u_p(t)$ as a linear combination of the model states $x_m(t)$, model inputs $u_m(t)$, and the output tracking error $e_y(t)$, i.e.,

$$u_p(t) = S_{21}x_m(t) + S_{22}u_m(t) + K_e\, e_y(t) \tag{6.7}$$

so that the output tracking error asymptotically approaches zero. The gain matrices S_{21} and S_{22} are referred to as the CGT gains, and K_e is selected to stabilize $(A_p-B_pK_eC_p)$.

When $y_p(t) = y_m(t)$ (i.e., perfect tracking occurs), the corresponding plant state and control trajectories are called "ideal trajectories" and are denoted as $x_p^*(t)$ and $u_p^*(t)$, respectively. When $u_m(t)$ is constant+, $x_p^*(t)$ and $u_p^*(t)$ are assumed to be linearly related to the model command u_m and model state $x_m(t)$ as shown in the following equations:

$$\begin{bmatrix} x_p^*(t) \\ u_p^*(t) \end{bmatrix} = \begin{bmatrix} S_{11} & S_{12} \\ S_{21} & S_{22} \end{bmatrix} \begin{bmatrix} x_m(t) \\ u_m(t) \end{bmatrix} \tag{6.8}$$

where S_{11}, S_{12}, S_{21} and S_{22} are matrices with appropriate dimensions. By definition, the ideal trajectory $x_p^*(t)$ is such that

+For the more general case, refer to Ref. 54.

$$y_p^*(t) = C_p\, x_p^*(t) = C_m\, x_m(t) = y_m(t) \tag{6.9}$$

and

$$\dot{x}_p^*(t) = A_p\, x_p^*(t) + B_p\, u_p^*(t) \tag{6.10}$$

To find the CGT gains S_{21} and S_{22}, we first substitute Eq. (6.8) into Eq. (6.9). Thus,

$$C_p\, x_p^*(t) = C_p(S_{11}\, x_m(t) + S_{12}\, u_m) = C_m\, x_m \tag{6.11}$$

Hence,

$$C_p\, S_{11} = C_m \tag{6.12}$$

$$C_p\, S_{12} = 0 \tag{6.13}$$

Differentiating Eq. (6.8),

$$\dot{x}_p^*(t) = S_{11}\dot{x}_m(t) + S_{12}\,\dot{u}_m = S_{11}\,\dot{x}_m(t) = S_{11}(A_m x_m(t) + B_m u_m) \tag{6.14}$$

and substituting Eq. (6.8) into Eq. (6.10)

$$\begin{aligned}\dot{x}_p^*(t) &= A_p(S_{11}\, x_m(t) + S_{12}\, u_m) + B_p(S_{21}\, x_m(t) + S_{22}\, u_m)\\ &= (A_p\, S_{11} + B_p\, S_{21})\, x_m(t) + (A_p\, S_{12} + B_p\, S_{22})\, u_m\end{aligned} \tag{6.15}$$

and comparing Eqs. (6.14) and (6.15), we have

$$S_{11} A_m = A_p S_{11} + B_p S_{21} \tag{6.16}$$

$$S_{11} B_m = A_p S_{12} + B_p S_{22} \tag{6.17}$$

Rewriting Eqs. (6.12), (6.13), (6.16) and (6.17) in matrix form, we obtain

$$\begin{bmatrix} A_p & B_p \\ C_p & 0 \end{bmatrix} \cdot \begin{bmatrix} S_{11} & S_{12} \\ S_{12} & S_{22} \end{bmatrix} = \begin{bmatrix} S_{11}A_m & S_{11}B_m \\ C_m & 0 \end{bmatrix} \tag{6.18}$$

and then define

$$\begin{bmatrix} \Omega_{11} & \Omega_{12} \\ \Omega_{21} & \Omega_{22} \end{bmatrix} = \begin{bmatrix} A_p & B_p \\ C_p & 0 \end{bmatrix}^{-1} \tag{6.19}$$

The resulting CGT equations become

$$S_{11} = \Omega_{11}S_{11}A_m + \Omega_{12}C_m \tag{6.20a}$$

$$S_{12} = \Omega_{11}S_{11}B_m \tag{6.20b}$$

$$S_{21} = \Omega_{21}S_{11}A_m + \Omega_{22}C_m \tag{6.20c}$$

$$S_{22} = \Omega_{21}S_{11}B_m \tag{6.20d}$$

The so-called perfect model following (PMF) conditions are a special case of the CGT when the state vector is available and it is assumed that $x_p^*(t) = x_m(t)$. Since $x_p^*(t) = S_{11}x_m(t) + S_{12}u_m$, the PMF conditions imply that $S_{11} = I$ and $S_{12} = 0$. Also, since

$$\dot{x}_p^*(t) = \dot{x}_m(t) \tag{6.21}$$

i.e.,

$$A_p x_p^*(t) + B_p u_p^*(t)$$

$$= A_p\, x_m(t) + B_p(S_{21}\, x_m(t) + S_{22}\, u_m)$$

$$= (A_p + B_p\, S_{21})\, x_m(t) + B_p\, S_{22}\, u_m$$

$$= A_m\, x_m(t) + B_m\, u_m \tag{6.22}$$

From Eq. (6.22), it is found that

$$B_p\, S_{21} = A_m - A_p \tag{6.23a}$$

$$B_p\, S_{22} = B_m \tag{6.23b}$$

If the CGT gains S_{21} and S_{22} which satisfy the PMF conditions (Eq. (6.23)) exist, a valid PMF controller then becomes

$$u_p(t) = u_p^*(t) + K(x_m(t) - x_p(t)) \tag{6.24}$$

where K is a stabilizing feedback gain.

Back to the general CGT, we define the state error as $e_x(t) = x_p^*(t) - x_p(t)$ and seek a controller which guarantees that $e_x(t) \to 0$ as $t \to \infty$. Because when $x_p(t) = x_p^*(t)$, we have $C_p\, x_p(t) = C_p\, x_p^*(t)$, hence

$$y_p(t) \triangleq C_p\, x_p(t) = C_p\, x_p^*(t) \triangleq C_m x_m(t) \triangleq y_m(t) \tag{6.25}$$

and that is exactly the desired result we require.

With the error defined as $e_x(t) = x_p^*(t) - x_p(t)$, the error dynamics becomes

$$\dot{e}_x(t) = A_p x_p^*(t) + B_p u_p^*(t) - A_p\, x_p(t) - B_p\, u_p(t)$$

$$= A_p\, e_x(t) + B_p[u_p^*\,(t) - u_p(t)] \qquad (6.26)$$

Note that

$$e_y(t) = y_m(t) - y_p(t) = C_p(x_p^*(t) - x_p(t)) = C_p\, e_x(t) \qquad (6.27)$$

Equation (6.26) will be used in the subsequent stability analysis.

The CGT concept stated above is, however, non-adaptive. The purpose of adaptive control is to eliminate the need for a priori knowledge of the plant that is required in CGT.

6.2 Direct Model Reference Adaptive Control

Based on the CGT concept, Sobel et al. [42] developed the following adaptive control law:

$$u_p(t) = K_e(t)\, e_y(t) + K_x(t)\, x_m(t) + K_u(t)\, u_m(t) \qquad (6.28)$$

or, let $r(t)$ be a $2M + N_m$ vector defined as

$$r^T(t) = [e_y{}^T(t)\; x_m{}^T(t)\; u_m{}^T(t)] \qquad (6.29)$$

and $K(t)$ be the $M \times (2M+N_m)$ adaptive gain matrix defined as

$$K(t) = [K_e(t)\ K_x(t)\ K_u(t)] \tag{6.30}$$

Then

$$u_p(t) = K(t)\ r(t) \tag{6.31}$$

where $K(t)$ is a combination of two types of gains, i.e.,

$$K(t) = K_p(t) + K_I(t) \tag{6.32}$$

and $K_p(t)$ is the direct gain, $K_I(t)$ is the integral gain defined as follows:

$$K_p(t) = e_y(t)\ r^T(t)\bar{T} \tag{6.33}$$

$$\dot{K}_I(t) = e_y(t)\ r^T(t)T \tag{6.34}$$

with

$$K_I(0) = K_{IO} \tag{6.35}$$

where T and $\bar{T}$ are the $(2M+N_m) \times (2M+N_m)$ gain weighting matrices. K_{IO} is the initial integral gain. Note that $u_p(t)$ is highly nonlinear and its values are, in part, proportional to the cube of the output error $e_y(t)\ e_y^T(t)\ e_y(t)$.

The stability conditions of the adaptive controller are established via the Lyapunov direct method by considering a positive definite function given by

$$V(e_x,K_I) = e_x^T(t)\ P\ e_x(t) + \mathrm{Tr}[S(K_I-\tilde{K})T^{-1}(K_I-\tilde{K})^T S^T] \tag{6.36}$$

where

P is a $N_p \times N_p$ positive definite symmetric matrix

$\tilde{K}$ is a $M \times (2M+N_m)$ dummy gain matrix

S is a $M \times M$ nonsingular matrix

Note that dummy gain matrix $\tilde{K}$ does not appear in the control algorithm. It can be partitioned as $\tilde{K} = [\tilde{K}_e, \tilde{K}_x, \tilde{K}_u]$ so that

$$\tilde{K}\, r(t) = \tilde{K}_e\, C_p\, e_x(t) + \tilde{K}_x\, x_m(t) + \tilde{K}_u\, u_m \tag{6.37}$$

where $\tilde{K}_e$, $\tilde{K}_x$ and $\tilde{K}_u$ are, like $\tilde{K}$, dummy gains.

Introducing the control algorithm into the error equation given by Eq. (6.26), using Eqs. (6.31) to (6.33) and recalling from Eq. (6.8) that $u_p^*(t) = S_{21}\, x_m(t) + S_{22}\, u_m$, gives:

$$\begin{aligned}\dot{e}_x(t) = A_p\, e_x(t) + B_p[&S_{21}\, x_m(t) + S_{22}\, u_m \\ &- K_I(t) r(t) - C_p\, e_x(t)\, r^T(t)\, \bar{T}\, r(t)]\end{aligned} \tag{6.38}$$

The time dependence of the variables is omitted in the sequel for brevity. Thus the adaptive system is described by

$$\dot{e}_x = A_p e_x + B_p[S_{21} x_m + S_{22} u_m - K_I r - C_p e_x r^T \bar{T} r] \tag{6.39}$$

and

$$\dot{K}_I = C_p e_x r^T T \tag{6.40}$$

For the positive definite function given in Eq. (6.36), its time derivative is given by

$$\dot{V} = e_x^T P \dot{e}_x + \dot{e}_x^T P e_x + 2\ \mathrm{Tr}[S(K_I - \tilde{K})T^{-1}\dot{K}_I^T S^T] \tag{6.41}$$

Substituting Eqs. (6.39) and (6.40) into Eq. (6.41), we have

$$\begin{aligned}
\dot{V} = {} & e_x^T P[A_p e_x + B_p S_{21} x_m + B_p S_{22} u_m - B_p K_I r - B_p C_p e_x r^T \bar{T} r] \\
& + [A_p e_x + B_p S_{21} x_m + B_p S_{22} u_m - B_p K_I r - B_p C_p e_x r^T \bar{T} r]^T P e_x \\
& + 2\ e_x^T\ C_p^T\ S^T\ S(K_I - \tilde{K})r \\
= {} & e_x^T(PA_p + A_p^T P)e_x - e_x^T(PB_p C_p + C_p^T B_p^T P)e_x r^T \bar{T} r \\
& - 2\ e_x^T P B_p\ K_I r + 2 e_x^T P B_p (S_{21} x_m + S_{22} u_m) \\
& + 2\ e_x^T\ C_p^T\ S^T\ S(K_I - \tilde{K})r \\
= {} & e_x^T(PA_p + A_p^T P)e_x - e_x^T(PB_p C_p + C_p^T B_p^T P)e_x r^T \bar{T} r \\
& - 2\ e_x^T[C_p^T\ S^T\ S - PB_p]K_I r - 2\ e_x^T\ C_p^T\ S^T\ S\ \tilde{K}\ r \\
& + 2\ e_x^T\ P\ B_p(S_{21} x_m + S_{22} u_m)
\end{aligned} \tag{6.42}$$

Choosing C_p such that $C_p^T\ S^T\ S = P\ B_p$, Eq. (6.42) becomes

$$\begin{aligned}
\dot{V} = {} & e_x^T(PA_p + A_p^T P)e_x - 2\ e_x^T P B_p (S^T S)^{-1}\ B_p^T\ P\ e_x\ r^T\ \bar{T}\ r \\
& - 2\ e_x^T\ C_p^T\ S^T\ S\ \tilde{K}\ r + 2\ e_x^T\ PB_p(S_{21} x_m + S_{22} u_m)
\end{aligned} \tag{6.43}$$

Substituting Eq. (6.37) into Eq. (6.43), we obtain

$$\dot{V} = e_x^T[P(A_p - B_p\tilde{K}_eC_p) + (A_p - B_p\tilde{K}_eC_p)^TP]e_x$$
$$- 2\ e_x^TPB_p(S^TS)^{-1}B_p^T\ P\ e_x\ r^T\ \bar{T}\ r$$
$$+ 2\ e_x^T\ PB_p[(S_{21}-\tilde{K}_x)x_m + (S_{22} - \tilde{K}_u)u_m] \tag{6.44}$$

with the choice $\tilde{K}_x = S_{21}$ and $\tilde{K}_u = S_{22}$, Eq. (6.44) reduces to

$$\dot{V} = e_x^T[P(A_p - B_p\tilde{K}_eC_p) + (A_p - B_p\tilde{K}_eC_p)^TP]e_x$$
$$- 2\ e_x^TPB_p(S^TS)^{-1}B_p^T\ P\ e_x\ r^T\ \bar{T}\ r \tag{6.45}$$

Let $$Q = - P(A_p - B_p\tilde{K}_eC_p) - (A_p - B_p\tilde{K}_eC_p)^T\ P \tag{6.46}$$

Eq. (6.45) becomes

$$\dot{V} = - e_x^T\ Q\ e_x - 2\ e_x^T\ P\ B_p(S^TS)^{-1}\ B_p^T\ P\ e_x\ r^T\ \bar{T}\ r \tag{6.47}$$

If $\bar{T}$ is chosen to be positive semidefinite, the second term in Eq. (6.47) will be negative semidefinite in e_x. Then we choose P such that for some $\tilde{K}_e$, Q is positive definite. Consequently, $\dot{V}$ is negative definite in e_x, and V is a Lyapunov function for establishing the asymptotic stability of the zero state of Eqs. (6.39) and (6.40).

C-2

To summarize, a sufficient condition for asymptotic stability is

(1) T is positive definite

(2) $\bar{T}$ is positive semidefinite

(3) $P\,B_p = C_p^T(S^TS)$

(4) P is chosen such that $P(A_p-B_p\,\tilde{K}_e\,C_p) + (A_p-B_p\,\tilde{K}_e\,C_p)^TP$ is negative definite for some $\tilde{K}_e$.

Under the above conditions, the plant output will asymptotically track the model output. Furthermore, since the derivative of V is negative semidefinite in the augmented state $[e_x(t), K_I(t)]$, the adaptive gains will be bounded.

It should be noted that conditions (3) and (4) together are equivalent to requiring that the plant transfer matrix $Z(s) = C_p(sI-A_p + B_p\,\tilde{K}_e\,C_p)^{-1}\,B_p$ be strictly positive real for some feedback gain matrix $\tilde{K}_e$. For the definition of positive realness and strictly positive realness of matrices, see Appendix B.

6.3 Instability Problem Caused by Rigid Body Modes

It is well-known that the zero frequency rigid body modes are unstable modes. Simulation results show that this adaptive control algorithm fails to stabilize these modes and yield stable states or outputs. These problems may be verified analytically. They are treated as critical cases of stability problems for autonomous differential equations developed in Ref. 52. Let

$$\dot{x} = Ax + g(x) \tag{6.48}$$

be the given differential equation, where Ax represents the linear part and g(x) the nonlinear part. The real parts of the eigenvalues of A are assumed to be nonpositive. The critical case refers to the situation where some of the eigenvalues have zero real parts. If the matrix A has a double zero eigenvalue and if the reduced equation can be written in the form

$$\dot{\omega}_1=\omega_2 + g(\omega_1,\omega_2) \tag{6.49}$$

$$\dot{\omega}_2=a\omega_1^{\gamma}+a'\omega_1^{\gamma+1}+\ldots+\omega_2(b\omega_1^{\delta}+b'\omega_1^{\delta+1}+\ldots)+\omega_2^2h(\omega_1,\omega_2) \tag{6.50}$$

(where g is at least of second order, γ and δ are positive integers), then we have the following sufficient conditions for instability due to Lyapunov [53].

The equilibrium is unstable, if one of the following conditions is satisfied:

(1) γ even;

(2) γ odd, $a>0$;

(3) γ odd, $a<0$, δ even, $\gamma \geq \delta + 1$, $b>0$;

(4) γ odd, $a<0$, δ odd, $\gamma \geq 2\delta + 2$;

(5) γ odd, $a<0$, δ odd, $\gamma = 2\delta + 1$, $b^2+4(\delta+1)\gamma \geq 0$;

(6) the equation for $\dot{\omega}_2$ contains only the term $h(\omega_1,\omega_2)$.

To apply the above criteria to our case, the system equations are rewritten in the form of Eqs. (6.49) and (6.50) by defining

$$J = [C_m \quad -C_p] \tag{6.51}$$

$$\hat{x} = \begin{bmatrix} x_m \\ x_p \end{bmatrix} \tag{6.52}$$

Then

$$e_y = C_m x_m - C_p x_p = J\hat{x} \tag{6.53}$$

since

$$r = \begin{bmatrix} e_y \\ x_m \\ u_m \end{bmatrix} \tag{6.54}$$

$$\bar{T} = \begin{bmatrix} \bar{T}_{ey} & & 0 \\ & \bar{T}_{xm} & \\ 0 & & \bar{T}_{um} \end{bmatrix} \tag{6.55}$$

Hence

$$\begin{aligned} r^T \bar{T} r &= e_y^T \bar{T}_{ey} e_y + x_m^T \bar{T}_{xm} x_m + u_m^T \bar{T}_{um} u_m \\ &= \hat{x}^T J^T \bar{T}_{ey} J\hat{x} + x_m^T \bar{T}_{xm} x_m + C \text{ (constant)} \end{aligned} \tag{6.56}$$

Therefore the system equations (6.1) and (6.3) can be rewritten as,

$$
\dot{\hat{x}} = \begin{bmatrix} \dot{x}_m \\ \dot{x}_p \end{bmatrix} = \begin{bmatrix} A_m & 0 \\ 0 & A_p \end{bmatrix} \hat{x} + \begin{bmatrix} B_m u_m \\ B_p J\hat{x}\ (\hat{x}^T J^T\ \overline{T}_{ey}\ J\hat{x} + x_m{}^T\ \overline{T}_{xm} X_m + C) \end{bmatrix}
$$

$$
+ \begin{bmatrix} 0 \\ B_p K_I\ r \end{bmatrix} \tag{6.57}
$$

$$
\dot{K}_I = e_y\ r^T\ T \tag{6.58}
$$

As stated in Chapter VII, in the present study, we concentrate on the space station attitude hold only, i.e., $u_m = 0$. In this special case, the corresponding ω_1's are x_{pi} (modal amplitudes) and ω_2's are $\dot{x}_{pi}$ (modal amplitude rates), respectively. For a certain mode, its corresponding block in matrix A is

$$
\begin{bmatrix} 0 & 1 \\ -2\zeta_i\omega_i & \omega_i^2 \end{bmatrix}
$$

Hence for rigid body modes, it becomes $\begin{bmatrix} 0 & 1 \\ 0 & 0 \end{bmatrix}$ which is exactly the form represented by Eqs. (6.49) and (6.50). Taking the 6-DOF model as an example, it is found through tedious expansion that $\gamma = 3$, and $a < 0$; hence, the possibilities of satisfying condition 1 or 2 are excluded. One of the remaining conditions may still be satisfied although the expansion will be extremely tedious and is not done here. Note that the above conditions are sufficient conditions;

therefore, the equilibrium state of the system may still be unstable even though none of them are satisfied.

If u_m is equal to some constant instead of zero, the analysis of stability will be different. Since the term $B_pJ\hat{x}C$ in Eq. (6.57) is linear in x_p, it should be added to A_p. This changes the corresponding matrix A in Eq. (6.48) and its eigenvalues. The zero frequency modes would disappear, and the stability of the system will be entirely determined by the eigenvalues of matrix A. If any of them has a positive real part, instability of the system can be concluded immediately.

6.4 Plant Augmentation

To solve this unstable rigid body modes problem, a method referred to as plant augmentation is proposed. The plant augmentation is accomplished by introducing an inner control loop in the plant.

Consider the equation of motion (Eq. (3.18) or (3.66)) before the damping term is added,

$$M\ddot{Z}_p + KZ_p = Bu_p \tag{6.59}$$

After the inner loop is introduced, the above equation becomes

$$M\ddot{Z}_p + KZ_p = Bu_p - K_{IL}\, Z_p \tag{6.60}$$

where K_{IL} is the inner loop control gain matrix. By rewriting Eq. (6.60) as follows,

$$M\ddot{Z}_p + (K + K_{IL})Z_p = Bu_p \tag{6.61}$$

one can see that the modal characteristics of the plant have been altered due to K_{IL}. By choosing the values and structure of K_{IL}, the rigid body modes will no longer have zero frequencies. As a result of this plant characteristic change, a stable adaptive control system can be realized. It is important to note that to design such an inner loop, one does not require accurate knowledge of the plant. This is because the inner loop controller can be made very robust by choosing the loop only at the location where the controllability is the highest for the rigid body modes. Furthermore, the exact values of the augmented rigid mode frequencies are not important and what is important is that they are different from zero. Looking from another point of view, the stability of the adaptive system has been improved by the highly robust inner control loop.

Taking the two-panel configuration as an example, the inner loop gain K_{IL} is chosen to have the following form:

$$K_{IL} = \mathrm{diag}(0,\ 0,\ K_{Z2},\ K_{\theta 2},\ 0,\ 0) \tag{6.62}$$

This selection is based on the fact that the rigid body modes are largely determined by the core body of the space station. To determine K_{Z2}, we refer to the following block diagram:

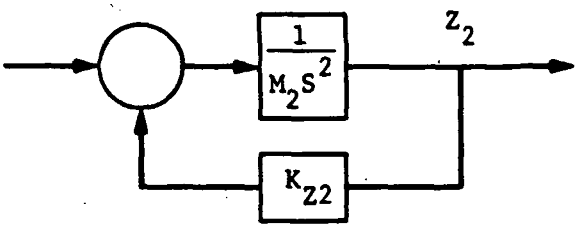

Since the transfer function H can be written as

$$H = \frac{1}{M_2 S^2 + K_{Z2}} \tag{6.63}$$

the natural frequency ω_{Z2} for the rigid body translational mode can then be estimated as,

$$\omega_{Z2} \cong \sqrt{\frac{K_{Z2}}{M_2}} \tag{6.64}$$

Similarly, the natural frequency $\omega_{\theta 2}$ for the rigid body rotational mode is

$$\omega_{\theta 2} \cong \sqrt{\frac{K_{\theta 2}}{I_2}} \tag{6.65}$$

Hence, the selection of ω_{Z2} and $\omega_{\theta 2}$ determines the values of K_{Z2} and $K_{\theta 2}$.

Extending the above approach to the four-panel configuration is straightforward. K_{IL} is now of the form:

$$K_{IL} = \text{diag}(0,\ 0,\ 0,\ 0,\ 0,\ 0,\ K_{Z4},\ K_{\theta 4},\ K_{\phi 4},\ 0,\ 0,\ 0,\ 0,\ 0,\ 0) \tag{6.66}$$

Including the effects of payloads, the natural frequencies of the rigid body modes are estimated as follows,

$$\omega_{Z4} \cong \sqrt{\frac{K_{Z4}}{M_4+M_8+M_9}} \tag{6.67}$$

$$\omega_{\theta 4} \cong \sqrt{\frac{K_{\theta 4}}{I_{4yy}+M_8L_8^{\ 2}+M_9L_9^{\ 2}+I_{8ys}+I_{9ys}}} \tag{6.68}$$

$$\omega_{\phi 4} \cong \sqrt{\frac{K_{\phi 4}}{I_{4xx}+I_{8xs}+I_{9xs}}} \tag{6.69}$$

Again the selection of ω_{Z4}, $\omega_{\theta 4}$ and $\omega_{\phi 4}$ determines the values of K_{Z4}, $K_{\theta 4}$, and $K_{\phi 4}$, respectively.

With the inner loop introduced, the space station adaptive control system block diagram is shown in Fig. 20.

6.5 Sufficient Conditions for Global Asymptotic Stability

After solving the problem of zero frequency rigid body modes via plant augmentation, we need to find sufficient conditions that will make the space station adaptive control system globally asymptotically stable. Referring to Section 6.2, we have to select a positive definite P satisfying $PB_p = C_p^{\ T}(S^TS)$, and for which $Q = -P(A_p-B_p\tilde{K}_e C_p)-(A_p-B_p\tilde{K}_eC_p)^TP$ is positive definite for some $\tilde{K}_e$.

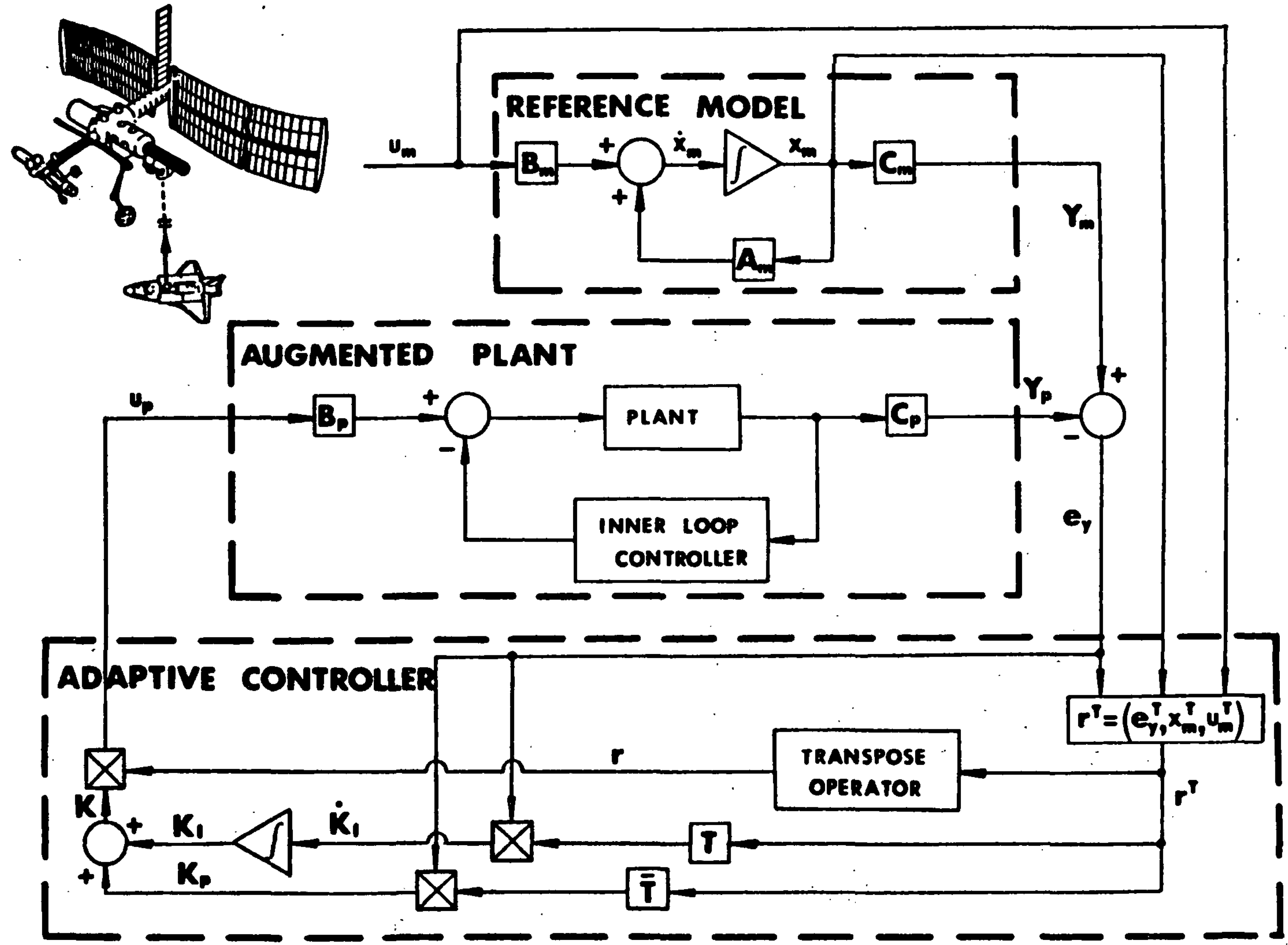

Figure 20 Space Station Adaptive Control System Block Diagram

Before deriving the sufficient conditions for globally asymptotic stability, we consider first the characteristic equation of a symmetric matrix for determining its eigenvalues.

Let W be a symmetric matrix having the following partitioned form:

$$W = \begin{bmatrix} \Lambda_1 & \Lambda_3 \\ \Lambda_3 & \Lambda_2 \end{bmatrix} \tag{6.70}$$

Let λ be an eigenvalue of W. Then

$$\begin{bmatrix} \Lambda_1 & \Lambda_3 \\ \Lambda_3 & \Lambda_2 \end{bmatrix} \begin{bmatrix} \nu_1 \\ \nu_2 \end{bmatrix} = \lambda \begin{bmatrix} \nu_1 \\ \nu_2 \end{bmatrix} \tag{6.71}$$

where $[\nu_1 \quad \nu_2]^T$ is an eigenvector of W corresponding to λ, i.e.,

$$\Lambda_1 \nu_1 + \Lambda_3 \nu_2 = \lambda \ \nu_1 \tag{6.72}$$

$$\Lambda_3 \nu_1 + \Lambda_2 \nu_2 = \lambda \ \nu_2 \tag{6.73}$$

From Eq. (6.73)

$$\Lambda_3 \ \nu_1 = (\lambda \ I - \Lambda_2) \ \nu_2 \tag{6.74}$$

Hence

$$\nu_1 = \Lambda_3^{-1} \ (\lambda I - \Lambda_2) \nu_2 \tag{6.75}$$

Substituting Eq. (6.75) into Eq. (6.72), we have

$$\begin{aligned} \Lambda_3 \nu_2 &= (\lambda I - \Lambda_1)\nu_1 \\ &= (\lambda I - \Lambda_1)\Lambda_3^{-1} (\lambda I - \Lambda_2)\nu_2 \end{aligned} \tag{6.76}$$

i.e.,

$$[\Lambda_3 - (\lambda I - \Lambda_1)\Lambda_3^{-1} (\lambda I - \Lambda_2)]\nu_2 = 0 \tag{6.77}$$

Define the matrix inside the brackets in Eq. (6.77) as $\tilde{\Lambda}$, i.e.,

$$\tilde{\Lambda} = \Lambda_3 - (\lambda I - \Lambda_1)\Lambda_3^{-1} (\lambda I - \Lambda_2) \tag{6.78}$$

Since $\tilde{\Lambda}$ is a diagonal matrix, in order to have a nontrivial solution ν_2, at least one element of $\tilde{\Lambda}$ must be zero.

Expanding Eq. (6.78), we have

$$\tilde{\Lambda} = \lambda^2\Lambda_3^{-1} - \lambda\Lambda_3^{-1} (\Lambda_1+\Lambda_2) + (\Lambda_3^{-1}\Lambda_1\Lambda_2 - \Lambda_3) \tag{6.79}$$

To find the first set of sufficient conditions, let

$$P = \begin{bmatrix} I & \alpha I \\ \alpha I & I \end{bmatrix} \tag{6.80}$$

$$S^T S = I \tag{6.81}$$

$$\tilde{K}_e = K_1^T K_1 \tag{6.82}$$

then

$$PB_p = \begin{bmatrix} I & \alpha I \\ \alpha I & I \end{bmatrix} \begin{bmatrix} 0 \\ \phi_p{}^T B_p \end{bmatrix} = \begin{bmatrix} I & \alpha I \\ \alpha I & I \end{bmatrix} \begin{bmatrix} 0 \\ \phi_p{}^T C^T \end{bmatrix}$$

$$= \begin{bmatrix} \alpha\phi_p{}^T C^T \\ \phi_p{}^T C^T \end{bmatrix} = C_p{}^T \tag{6.83}$$

and the condition $PB_p = C_p{}^T(S^TS)$ is satisfied.

Since P is required to be positive definite, all of its eigenvalues must be positive. Referring to Eqs. (6.70) and (6.80), the corresponding Λ_1, Λ_2 and Λ_3 here are

$$\Lambda_1 = I \tag{6.84}$$

$$\Lambda_2 = I \tag{6.85}$$

$$\Lambda_3 = \alpha I \tag{6.86}$$

In view of Eq. (6.79), we have

$$\tilde{\Lambda} = \frac{\lambda^2}{\alpha} I - \frac{\lambda}{\alpha}(2I) + (\frac{1}{\alpha} I - \alpha I) \tag{6.87}$$

or

$$\tilde{\Lambda} = \lambda^2 I - 2\lambda I + (I - \alpha^2 I) \tag{6.88}$$

Hence a typical pair of eigenvalues are found by

$$\lambda^2 - 2\lambda + (1 - \alpha^2) = 0 \tag{6.89}$$

The roots of Eq. (6.89) are given by

$$\lambda_{1,2} = \frac{2 \pm \sqrt{4-4(1-\alpha^2)}}{2} = 1 \pm \alpha \tag{6.90}$$

Note that $\alpha > 0$, hence

$$\lambda_1 = 1 + \alpha > 0 \tag{6.91}$$

For $\lambda_2 = 1 - \alpha > 0$, we require

$$\alpha < 1 \tag{6.92}$$

Referring to Eq. (5.6) or (5.16), we define

$$\Lambda = \begin{bmatrix} \omega_1^2 & & 0 \\ & \ddots & \\ 0 & & \omega_{Np}^2 \end{bmatrix} \tag{6.93}$$

and assume the same damping for all modes,

$$\zeta = \zeta_1 = \zeta_2 = \dots = \zeta_{Np} \tag{6.94}$$

Then the matrix A_p can be written as

$$A_p = \begin{bmatrix} 0 & I \\ -\Lambda & -2\zeta\Lambda^{1/2} \end{bmatrix} \tag{6.95}$$

Substituting P, A_p, B_p, C_p and $\tilde{K}_e$ into the equation for Q,

$$Q = -P(A_p-B_p\tilde{K}_eC_p)-(A_p-B_p\tilde{K}_eC_p)^TP$$

$$= -\begin{bmatrix} I & \alpha I \\ \alpha I & I \end{bmatrix}\left(\begin{bmatrix} 0 & I \\ -\Lambda & -2\zeta\Lambda^{1/2} \end{bmatrix} - \begin{bmatrix} 0 \\ \phi_p^TC^T \end{bmatrix} K_1{}^TK_1 \begin{bmatrix} \alpha C\phi_p & C\phi_p \end{bmatrix}\right)$$

$$-\left(\begin{bmatrix} 0 & I \\ -\Lambda & -2\zeta\Lambda^{1/2} \end{bmatrix} - \begin{bmatrix} 0 \\ \phi_p{}^TC^T \end{bmatrix} K_1{}^TK_1 \begin{bmatrix} \alpha C\phi_p & C\phi_p \end{bmatrix}\right)^T \begin{bmatrix} I & \alpha I \\ \alpha I & I \end{bmatrix}$$

$$= -\begin{bmatrix} I & \alpha I \\ \alpha I & I \end{bmatrix}\left(\begin{bmatrix} 0 & I \\ -\Lambda & -2\zeta\Lambda^{1/2} \end{bmatrix} - \begin{bmatrix} 0 & 0 \\ \alpha\phi_p{}^TC^TK_1{}^TK_1C\phi_p & \phi_p{}^TC^TK_1{}^TK_1C\phi_p \end{bmatrix}\right)$$

$$-\left(\begin{bmatrix} 0 & I \\ -\Lambda & -2\zeta\Lambda^{1/2} \end{bmatrix} - \begin{bmatrix} 0 & 0 \\ \alpha\phi_p{}^TC^TK_1{}^TK_1C\phi_p & \phi_p{}^TC^TK_1{}^TK_1C\phi_p \end{bmatrix}\right)^T \begin{bmatrix} I & \alpha I \\ \alpha I & I \end{bmatrix}$$

$$= -\begin{bmatrix} I & \alpha I \\ \alpha I & I \end{bmatrix}\begin{bmatrix} 0 & I \\ -\Lambda-\alpha\phi_p{}^TC^TK_1{}^TK_1C\phi_p & -2\zeta\Lambda^{1/2}-\phi_p{}^TC^TK_1{}^TK_1C\phi_p \end{bmatrix}$$

$$-\begin{bmatrix} 0 & -\Lambda-\alpha\phi_p{}^TC^TK_1{}^TK_1C\phi_p \\ I & -2\zeta\Lambda^{1/2}-\phi_p{}^TC^TK_1{}^TK_1C\phi_p \end{bmatrix}\begin{bmatrix} I & \alpha I \\ \alpha I & I \end{bmatrix}$$

$$= - \begin{bmatrix} -\alpha\Lambda-\alpha^2\phi_p{}^T C^T K_1{}^T K_1 C\phi_p & I-2\alpha\zeta\Lambda^{1/2}-\alpha\phi_p{}^T C^T K_1{}^T K_1 C\phi_p \\ -\Lambda-\alpha\phi_p{}^T C^T K_1{}^T K_1 C\phi_p & \alpha I-2\zeta\Lambda^{1/2}-\phi_p{}^T C^T K_1{}^T K_1 C\phi_p \end{bmatrix}$$

$$- \begin{bmatrix} -\alpha\Lambda-\alpha^2\phi_p{}^T C^T K_1{}^T K_1 C\phi_p & -\Lambda-\alpha\phi_p{}^T C^T K_1{}^T K_1 C\phi_p \\ I-2\alpha\zeta\Lambda^{1/2}-\alpha\phi_p{}^T C^T K_1{}^T K_1 C\phi_p & \alpha I-2\zeta\Lambda^{1/2}-\phi_p{}^T C^T K_1{}^T K_1 C\phi_p \end{bmatrix}$$

$$= \begin{bmatrix} \alpha\Lambda+\alpha^2\phi_p{}^T C^T K_1{}^T K_1 C\phi_p & -I+2\alpha\zeta\Lambda^{1/2}+\alpha\phi_p{}^T C^T K_1{}^T K_1 C\phi_p \\ \Lambda+\alpha\phi_p{}^T C^T K_1{}^T K_1 C\phi_p & -\alpha I+2\zeta\Lambda^{1/2}+\phi_p{}^T C^T K_1{}^T K_1 C\phi_p \end{bmatrix}$$

$$+ \begin{bmatrix} \alpha\Lambda+\alpha^2\phi_p{}^T C^T K_1{}^T K_1 C\phi_p & \Lambda+\alpha\phi_p{}^T C^T K_1{}^T K_1 C\phi_p \\ -I+2\alpha\zeta\Lambda^{1/2}+\alpha\phi_p{}^T C^T K_1{}^T K_1 C\phi_p & -\alpha I+2\zeta\Lambda^{1/2}+\phi_p{}^T C^T K_1{}^T K_1 C\phi_p \end{bmatrix}$$

$$= \begin{bmatrix} 2\alpha\Lambda & \Lambda-I+2\alpha\zeta\Lambda^{1/2} \\ \Lambda-I+2\alpha\zeta\Lambda^{1/2} & -2\alpha I+4\zeta\Lambda^{1/2} \end{bmatrix} + 2 \begin{bmatrix} \alpha^2\phi_p{}^T C^T K_1{}^T K_1 C\phi_p & \alpha\phi_p{}^T C^T K_1{}^T K_1 C\phi_p \\ \alpha\phi_p{}^T C^T K_1{}^T K_1 C\phi_p & \phi_p{}^T C^T K_1{}^T K_1 C\phi_p \end{bmatrix}$$

$$= \begin{bmatrix} 2\alpha\Lambda & \Lambda-I+2\alpha\zeta\Lambda^{1/2} \\ \Lambda-I+2\alpha\zeta\Lambda^{1/2} & -2\alpha I+4\zeta\Lambda^{1/2} \end{bmatrix} + 2 \begin{bmatrix} \phi_p{}^T C^T & 0 \\ 0 & \phi_p{}^T C^T \end{bmatrix} \begin{bmatrix} \alpha K_1{}^T \\ K_1{}^T \end{bmatrix} X$$

$$\begin{bmatrix} \alpha K_1 & K_1 \end{bmatrix} \begin{bmatrix} C\phi_p & 0 \\ 0 & C\phi_p \end{bmatrix} \tag{6.96}$$

The second term in Eq. (6.96) is apparently positive semidefinite. Hence in order to make Q positive definite, the first term must be positive definite. Let

$$Q_1 = \begin{bmatrix} 2\alpha\Lambda & \Lambda - I + 2\alpha\zeta\Lambda^{1/2} \\ \Lambda - I + 2\alpha\zeta\Lambda^{1/2} & -2\alpha I + 4\zeta\Lambda^{1/2} \end{bmatrix} \tag{6.97}$$

referring to Eq. (6.70), the corresponding Λ_1, Λ_2 and Λ_3 here are

$$\Lambda_1 = 2\alpha\Lambda \tag{6.98}$$

$$\Lambda_2 = -\ 2\alpha I + 4\zeta\Lambda^{1/2} \tag{6.99}$$

$$\Lambda_3 = \Lambda - I + 2\alpha\zeta\Lambda^{1/2} \tag{6.100}$$

Substituting them into Eq. (6.79), we have

$$\tilde{\Lambda} = \lambda^2(\Lambda - I + 2\alpha\zeta\Lambda^{1/2})^{-1} - \lambda(\Lambda - I + 2\alpha\zeta\Lambda^{1/2})^{-1}(2\alpha\Lambda - 2\alpha I + 4\zeta\Lambda^{1/2})$$

$$+ (\Lambda - I + 2\alpha\zeta\Lambda^{1/2})^{-1}(2\alpha\Lambda)\ (-2\alpha I + 4\zeta\Lambda^{1/2}) - (\Lambda - I + 2\alpha\zeta\Lambda^{1/2}) \tag{6.101}$$

In order that $(\Lambda - I + 2\alpha\zeta\Lambda^{1/2})^{-1}$ exists,

$$|\Lambda - I + 2\alpha\zeta\Lambda^{1/2}| \neq 0 \tag{6.102}$$

i.e., $\omega_i^{\,2} - 1 + 2\alpha\zeta\omega_i \neq 0$, for $i = 1, \ldots N_p$ (6.103) i.e., $\alpha \neq \dfrac{1-\omega_i^{\,2}}{2\zeta\omega_i}$, for $i = 1, \ldots, N_p$ (6.104)

Expanding Eq. (6.101), we have

$$\tilde{\Lambda} = \lambda^2 \begin{bmatrix} \frac{1}{\omega_1^{\,2}-1+2\alpha\zeta\omega_1} & & 0 \\ & \ddots & \\ 0 & & \frac{1}{\omega_{Np}^{\,2}-1+2\alpha\zeta\omega_{Np}} \end{bmatrix} - \lambda \begin{bmatrix} \frac{1}{\omega_1^{\,2}-1+2\alpha\zeta\omega_1} & & 0 \\ & \ddots & \\ 0 & & \frac{1}{\omega_{Np}^{\,2}-1+2\alpha\zeta\omega_{Np}} \end{bmatrix} \begin{bmatrix} 2\alpha\omega_1^{\,2}-2\alpha+4\zeta\omega_1 & & 0 \\ & \ddots & \\ 0 & & 2\alpha\omega_{Np}^{\,2}-2\alpha+4\zeta\omega_{Np} \end{bmatrix}$$

$$+ \begin{bmatrix} \frac{2\alpha\omega_1^{\,2}(-2\alpha+4\zeta\omega_1)}{\omega_1^{\,2}-1+2\alpha\zeta\omega_1} & & 0 \\ & \ddots & \\ 0 & & \frac{2\alpha\omega_{Np}^{\,2}(-2\alpha+4\zeta\omega_{Np})}{\omega_{Np}^{\,2}-1+2\alpha\zeta\omega_{Np}} \end{bmatrix} - \begin{bmatrix} \omega_1^{\,2}-1+2\alpha\zeta\omega_1 & & \\ & \ddots & \\ & & \omega_{Np}^{\,2}-1+2\alpha\zeta\omega_{Np} \end{bmatrix} \qquad (6.105)$$

i.e., the characteristic equations are,

$$\frac{1}{\omega_i^{\,2}-1+2\alpha\zeta\omega_i}\,\lambda^2 - \frac{2\alpha\omega_i^{\,2}-2\alpha+4\zeta\omega_i}{\omega_i^{\,2}-1+2\alpha\zeta\omega_i}\,\lambda + \frac{2\alpha\omega_i^{\,2}(-2\alpha+4\zeta\omega_i)-(\omega_i^{\,2}-1+2\alpha\zeta\omega_i)^2}{\omega_i^{\,2}-1+2\alpha\zeta\omega_i} = 0$$

for $i = 1, \ldots, N_p$ (6.106)

or

$$\lambda^2-(2\alpha\omega_i^{\,2}-2\alpha+4\zeta\omega_i)\lambda-(\omega_i^{\,4}+1+4\alpha^2\zeta^2\omega_i^{\,2}-2\omega_i^{\,2}-4\alpha\zeta\omega_i+4\alpha^2\omega_i^{\,2}-4\alpha\zeta\omega_i^{\,3}) = 0$$

for $i = 1, \ldots, N_p$ (6.107)

Note that for the quadratic equation:

$$a\lambda^2 + b\lambda + C = 0 \qquad (6.108)$$

the roots are,

$$\lambda_1 = \frac{-b+\sqrt{b^2-4ac}}{2a} \tag{6.109}$$

$$\lambda_2 = \frac{-b-\sqrt{b^2-4ac}}{2a} \tag{6.110}$$

Hence, in order to have $\lambda_1 > 0$ and $\lambda_2 > 0$ we must have

$$b < 0 \tag{6.111}$$

$$ac > 0 \tag{6.112}$$

Referring to Eq. (6.107), the conditions for positive λ_i's are then,

$$2\zeta\omega_i - \alpha(1-\omega_i^2) > 0 \quad , \qquad \text{for } i = 1,\dots, N_p \tag{6.113}$$

$$1-4\alpha\zeta\omega_i-(2-4\alpha^2-4\alpha^2\zeta^2)\omega_i^2-4\alpha\zeta\omega_i^3+\omega_i^4<0 \; , \quad \text{for } i = 1, \dots, N_p \tag{6.114}$$

To summarize, the first set of sufficient conditions for globally asymptotic stability is given by

T is positive definite

$\bar{T}$ is positive semidefinite

$$\alpha < 1 \tag{6.115}$$

$$\alpha \neq \frac{1-\omega_i^2}{2\zeta\omega_i} \tag{6.116}$$

$$2\zeta\omega_i - \alpha(1-\omega_i^2) > 0 \tag{6.117}$$

$$1-4\alpha\zeta\omega_i-(2-4\alpha^2-4\alpha^2\zeta^2)\omega_i^2-4\alpha\zeta\omega_i^3+\omega_i^4 < 0 \tag{6.118}$$

for $i = 1, \dots, N_p$.

To find the second set of sufficient conditions, we select

$$P = \begin{bmatrix} \beta I & \alpha I \\ \alpha I & I \end{bmatrix} \tag{6.119}$$

$$S^T S = I \tag{6.120}$$

$$\tilde{K}_e = K_1^T K_1 \tag{6.121}$$

Then

$$PB_p = \begin{bmatrix} \beta I & \alpha I \\ \alpha I & I \end{bmatrix} \begin{bmatrix} 0 \\ \phi_p^T C^T \end{bmatrix} = \begin{bmatrix} \alpha\phi_p^T C^T \\ \phi_p^T C^T \end{bmatrix} = C_p^T \tag{6.122}$$

and the condition $PB_p = C_p^T(S^T S)$ is satisfied.

Since P is required to be positive definite, we have, first of all,

$$\beta > 0 \tag{6.123}$$

and the eigenvalues of P must be positive. Referring to Eq. (6.70), the corresponding Λ_1, Λ_2 and Λ_3 here are

$$\Lambda_1 = \beta I \tag{6.124}$$

$$\Lambda_2 = I \tag{6.125}$$

$$\Lambda_3 = \alpha I \tag{6.126}$$

Substituting them into Eq. (6.79), it becomes

$$\tilde{\Lambda} = \frac{\lambda^2}{\alpha} I - \frac{\lambda}{\alpha} (\beta I + I) + (\frac{\beta}{\alpha} I - \alpha I) \tag{6.127}$$

or

$$\tilde{\Lambda} = \lambda^2 I - (\beta+1)I + (\beta-\alpha^2)I \tag{6.128}$$

Hence, a typical pair of eigenvalues are determined by

$$\lambda^2 - (\beta+1)\lambda + (\beta-\alpha^2) = 0 \tag{6.129}$$

Referring to Eqs. (6.111) and (6.112), the conditions for positive λ_i's are

$$\beta > -1 \quad \text{(automatically satisfied)} \tag{6.130}$$

and

$$\beta > \alpha^2 \tag{6.131}$$

Substituting P, A_p, B_p, C_p and $\tilde{K}_e$ into the equation for Q, we have

$$Q = - P(A_p - B_p\tilde{K}_e C_p) - (A_p - B_p\tilde{K}_e C_p)^T P$$

$$= - \begin{bmatrix} \beta I & \alpha I \\ \alpha I & I \end{bmatrix} \begin{bmatrix} 0 & I \\ -\Lambda - \alpha\phi_p{}^T C^T K_1{}^T K_1 C\phi_p & -2\zeta\Lambda^{1/2} - \phi_p{}^T C^T K_1{}^T K_1 C\phi_p \end{bmatrix}$$

$$
-\begin{bmatrix} 0 & -\Lambda-\alpha\phi_p{}^TC^TK_1{}^TK_1C\phi_p \\ I & -2\zeta\Lambda^{1/2}-\phi_p{}^TC^TK_1{}^TK_1C\phi_p \end{bmatrix}\begin{bmatrix} \beta I & \alpha I \\ \alpha I & I \end{bmatrix}
$$

$$
= -\begin{bmatrix} -\alpha\Lambda-\alpha^2\phi_p{}^TC^TK_1{}^TK_1C\phi_p & \beta I-2\alpha\zeta\Lambda^{1/2}-\alpha\phi_p{}^TC^TK_1{}^TK_1C\phi_p \\ -\Lambda-\alpha\phi_p{}^TC^TK_1{}^TK_1C\phi_p & \alpha I-2\zeta\Lambda^{1/2}-\phi_p{}^TC^TK_1{}^TK_1C\phi_p \end{bmatrix}
$$

$$
-\begin{bmatrix} -\alpha\Lambda-\alpha^2\phi_p{}^TC^TK_1{}^TK_1C\phi_p & -\Lambda-\alpha\phi_p{}^TC^TK_1{}^TK_1C\phi_p \\ \beta I-2\alpha\zeta\Lambda^{1/2}-\alpha\phi_p{}^TC^TK_1{}^TK_1C\phi_p & \alpha I-2\zeta\Lambda^{1/2}-\phi_p{}^TC^TK_1{}^TK_1C\phi_p \end{bmatrix}
$$

$$
= \begin{bmatrix} \alpha\Lambda+\alpha^2\phi_p{}^TC^TK_1{}^TK_1C\phi_p & -\beta I+2\alpha\zeta\Lambda^{1/2}+\alpha\phi_p{}^TC^TK_1{}^TK_1C\phi_p \\ \Lambda+\alpha\phi_p{}^TC^TK_1{}^TK_1C\phi_p & -\alpha I+2\zeta\Lambda^{1/2}+\phi_p{}^TC^TK_1{}^TK_1C\phi_p \end{bmatrix}
$$

$$
+\begin{bmatrix} \alpha\Lambda+\alpha^2\phi_p{}^TC^TK_1{}^TK_1C\phi_p & \Lambda+\alpha\phi_p{}^TC^TK_1{}^TK_1C\phi_p \\ -\beta I+2\alpha\zeta\Lambda^{1/2}+\alpha\phi_p{}^TC^TK_1{}^TK_1C\phi_p & -\alpha I+2\zeta\Lambda^{1/2}+\phi_p{}^TC^TK_1{}^TK_1C\phi_p \end{bmatrix}
$$

$$
= \begin{bmatrix} 2\alpha\Lambda+2\alpha^2\phi_p{}^TC^TK_1{}^TK_1C\phi_p & \Lambda-\beta I+2\alpha\zeta\Lambda^{1/2}+2\alpha\phi_p{}^TC^TK_1{}^TK_1C\phi_p \\ \Lambda-\beta I+2\alpha\zeta\Lambda^{1/2}+2\alpha\phi_p{}^TC^TK_1{}^TK_1C\phi_p & -2\alpha I+4\zeta\Lambda^{1/2}+2\phi_p{}^TC^TK_1{}^TK_1C\phi_p \end{bmatrix}
$$

$$= \begin{bmatrix} 2\alpha\Lambda & \Lambda-\beta I+2\alpha\zeta\Lambda^{1/2} \\ \Lambda-\beta I+2\alpha\zeta\Lambda^{1/2} & -2\alpha I+4\zeta\Lambda^{1/2} \end{bmatrix} +2 \begin{bmatrix} \phi_p{}^T C^T & 0 \\ 0 & \phi_p{}^T C^T \end{bmatrix} \begin{bmatrix} \alpha K_1{}^T \\ K_1{}^T \end{bmatrix}$$

$$\begin{bmatrix} \alpha K_1 & K_1 \end{bmatrix} \begin{bmatrix} C\phi_p & 0 \\ 0 & C\phi_p \end{bmatrix} \tag{6.132}$$

Again the second term in Eq. (6.132) is apparently positive semidefinite. Hence in order to make Q positive definite, the first term must be positive definite. Let

$$Q_2 = \begin{bmatrix} 2\alpha\Lambda & \Lambda-\beta I+2\alpha\zeta\Lambda^{1/2} \\ \Lambda-\beta I+2\alpha\zeta\Lambda^{1/2} & -2\alpha I+4\zeta\Lambda^{1/2} \end{bmatrix} \tag{6.133}$$

referring to Eq. (6.70), the corresponding Λ_1, Λ_2 and Λ_3 here are

$$\Lambda_1 = 2\alpha\Lambda \tag{6.134}$$

$$\Lambda_2 = -\ 2\alpha I+4\zeta\Lambda^{1/2} \tag{6.135}$$

$$\Lambda_3 = \Lambda-\beta I+2\alpha\zeta\Lambda^{1/2} \tag{6.136}$$

Substituting them into Eq. (6.79), we have

$$\tilde{\Lambda} = \lambda^2(\Lambda-\beta I+2\alpha\zeta\Lambda^{1/2})^{-1}-\lambda(\Lambda-\beta I+2\alpha\zeta\Lambda^{1/2})^{-1}(2\alpha\Lambda-2\alpha I+4\zeta\Lambda^{1/2})$$

$$+\ (\Lambda-\beta I+2\alpha\zeta\Lambda^{1/2})^{-1}(2\alpha\Lambda)(-2\alpha I+4\zeta\Lambda^{1/2})-(\Lambda-\beta I+2\alpha\zeta\Lambda^{1/2}) \tag{6.137}$$

In order that $(\Lambda-\beta I+2\alpha\zeta\Lambda^{1/2})^{-1}$ exists, we must have

$$|\Lambda-\beta I+2\alpha\zeta\Lambda^{1/2}| \neq 0$$

$$\text{i.e.,}\quad \omega_i^{\,2}-\beta+2\alpha\zeta\omega_i \neq 0 \qquad \text{for } i = 1, \ldots, N_p \tag{6.138}$$

$$\text{i.e.,}\quad \alpha \neq \frac{\beta-\omega_i^{\,2}}{2\zeta\omega_i} \qquad \text{for } i = 1, \ldots, N_p \tag{6.139}$$

Expanding Eq. (6.137), we have

$$\tilde{\Lambda} = \lambda^2\begin{bmatrix} \frac{1}{\omega_1^{\,2}-\beta+2\alpha\zeta\omega_1} & & 0 \\ & \ddots & \\ 0 & & \frac{1}{\omega_{Np}^{\,2}-\beta+2\alpha\zeta\omega_{Np}} \end{bmatrix} - \lambda\begin{bmatrix} \frac{1}{\omega_1^{\,2}-\beta+2\alpha\zeta\omega_1} & & 0 \\ & \ddots & \\ 0 & & \frac{1}{\omega_{Np}^{\,2}-\beta+2\alpha\zeta\omega_{Np}} \end{bmatrix}\begin{bmatrix} 2\alpha\omega_1^{\,2}-2\alpha+4\zeta\omega_1 & & 0 \\ & \ddots & \\ 0 & & 2\alpha\omega_{Np}^{\,2}-2\alpha+4\zeta\omega_{Np} \end{bmatrix}$$

$$+\begin{bmatrix} \frac{2\alpha\omega_1^{\,2}(-2\alpha+4\zeta\omega_1)}{\omega_1^{\,2}-\beta+2\alpha\zeta\omega_1} & & 0 \\ & \ddots & \\ 0 & & \frac{2\alpha\omega_{Np}^{\,2}(-2\alpha+4\zeta\omega_{Np})}{\omega_{Np}^{\,2}-\beta+2\alpha\zeta\omega_{Np}} \end{bmatrix} - \begin{bmatrix} \omega_1^{\,2}-\beta+2\alpha\zeta\omega_1 & & 0 \\ & \ddots & \\ 0 & & \omega_{Np}^{\,2}-\beta+2\alpha\zeta\omega_{Np} \end{bmatrix} \tag{6.140}$$

Thus, the characteristic equations are,

$$\frac{1}{\omega_i^2-\beta+2\alpha\zeta\omega_i}\lambda^2-\frac{2\alpha\omega_i^2-2\alpha+4\zeta\omega_i}{\omega_i^2-\beta+2\alpha\zeta\omega_i}\lambda+\frac{2\alpha\omega_i^2(-2\alpha+4\zeta\omega_i)-(\omega_i^2-\beta+2\alpha\zeta\omega_i)^2}{\omega_i^2-\beta+2\alpha\zeta\omega_i}=0$$

for $i = 1, \ldots, N_p$ (6.141)

i.e.,

$$\lambda^2-(2\alpha\omega_i^2-2\alpha+4\zeta\omega_i)\lambda-(\omega_i^4+\beta^2+4\alpha^2\zeta^2\omega_i^2-2\beta\omega_i^2-4\alpha\beta\zeta\omega_i+4\alpha^2\omega_i^2-4\alpha\zeta\omega_i^3)=0$$

for $i = 1, \ldots, N_p$ (6.142)

Referring to Eqs. (6.111) and (6.112), the conditions for positive λ_i's are then,

$$2\zeta\omega_i - \alpha(1-\omega_i^2) > 0, \qquad \text{for } i = 1, \ldots, N_p \qquad (6.143)$$

$$\beta^2-4\alpha\beta\zeta\omega_i-(2\beta-4\alpha^2-4\alpha^2\zeta^2)\omega_i^2 - 4\alpha\zeta\omega_i^3+\omega_i^4 < 0,$$

for $i = 1, \ldots, N_p$ (6.144)

In summary, the second set of sufficient conditions for globally asymptotic stability is given by

T is positive definite

$\overline{T}$ is positive semidefinite

$$\beta > \alpha^2 \tag{6.145}$$

$$\alpha \neq \frac{\beta-\omega_i^{\ 2}}{2\zeta\omega_i} \tag{6.146}$$

$$2\zeta\omega_i - \alpha(1-\omega_i^{\ 2}) > 0 \tag{6.147}$$

$$\beta^2 - 4\alpha\beta\zeta\omega_i - (2\beta-4\alpha^2-4\alpha^2\zeta^2)\omega_i^{\ 2} - 4\alpha\zeta\omega_i^{\ 3}+\omega_i^{\ 4} < 0 \tag{6.148}$$

for $i = 1, \ldots, N_p$

As we compare the above two sets of sufficient conditions, it is apparent that the second set gives us more freedom for selecting the system parameters.

CHAPTER VII

PERFORMANCE ANALYSIS AND PRACTICAL CONSIDERATIONS

The purpose of this chapter is to investigate the dynamic responses of the space stations under the severe disturbances as the adaptive controller described above is applied without assuming the complete knowledge of the system parameters. In addition, from the point of view of practical implementation, means of reducing the control efforts and their effects on the performance of the system are studied.

Crew motion, reboost, and vehicle docking are the major disturbance sources. They will also cause changes of mass property. Crew motion will shift the center of mass, reboost will result in gradual mass reduction, and vehicle docking will spontaneously increase mass and inertia of the system. From the point of view of time-varying effect and the level of disturbances, space shuttle docking is by far the most significant source of disturbance. Since most of the cases studied here are related to shuttle docking, the docking characteristics and devices are described first in the following sections.

The simulation programs are written in Advanced Continuous Simulation Language (ACSL). The program and numerical results of the simulation of adaptive control during shuttle docking for the 19-DOF four-panel space station are listed in Appendices D and E, respectively.

7.1 Shuttle Reaction Control Subsystem Residual Rates

The shuttle Reaction Control Subsystem (RCS) consists of two major parts, the primary (PRCS) and the vernier (VRCS) subsystems. There are a total of 44 thrusters, 38 of them are associated with the PRCS, each has a nominal thrust level of 870 lbs; and the other 6 are associated with the VRCS with a thrust level of 24 lbs each. Phase plane control laws are employed to determine when actuations are needed and jet select logics are used to determine what thrusters are to turn on. The states of the system are estimated by a two-stage state estimator with a dual cycle time of 80 ms and 160 ms.

PRCS is normally employed for ΔV change, attitude maneuvers, and coarse attitude control; and the VRCS is for fine attitude control. Since shuttle docking requires maneuvers, PRCS must be used. Due to the high thrust level of the PRCS, and with more than one jet used at the same time to maintain attitude and approach rate while maneuvering, large residual rates result. The best achievable (minimum) residual rates, i.e., rates obtained under ideal conditions, are $\Delta V = 0.05$ ft/sec and $\Delta\omega = 0.20$ deg/sec. However, these minimum rates are difficult to realize under nominal operational conditions and much higher rates are expected. These expected rates are on the order of $\Delta V = 0.50$ ft/sec and $\Delta\omega = 1.00$ deg/sec. Figure 21 shows the shuttle control system block diagram and residual rates.

For the purpose of performance analysis, the following assumptions are made regarding the shuttle and space station docking:

- PRIMARY REACTION CONTROL SUBSYSTEM: FOR ΔV CHANGES, ATTITUDE MANEUVERS, AND GROSS ATTITUDE CONTROL FUNCTIONS

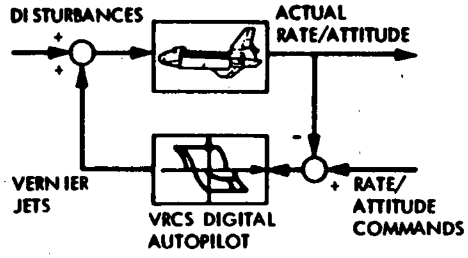

SHUTTLE CONTROL SYSTEM
BLOCK DIAGRAM

MINIMUM THRUST FORCE
FOR PRCS JETS: 870 LBS

- RESIDUAL RATES

BEST ACHIEVABLE RATES	EXPECTED RATES
ΔV = 0.05 FT/SEC	ΔV = 0.50 FT/SEC
$\Delta\omega$ = 0.20 DEG/SEC	$\Delta\omega$ = 1.00 DEG/SEC

Figure 21 Shuttle Reaction Control Subsystem (RCS) Residual Rates

(1) Throughout the docking period, the space station attitude control system will maintain operational on attitude hold mode.

(2) Just prior to the contact, the shuttle RCS is set at passive mode, i.e., no thrusters are allowed to fire.

(3) Once contact is made, latching is assumed, i.e., no separation is allowed.

7.2 Design of Shuttle Docking Devices

Shuttle hard docking is a rather idealized condition. Under this condition, the shuttle momentum is transferred to the space station for a short period of time, Δt. At the end of Δt, the station and the shuttle are latched together as one integrated body. The initial momentum of the shuttle is determined by the shuttle mass, $M_s = 7.81 \times 10^3$ slugs (2.52×10^5 lbs) and inertia, $I_s = 7.54 \times 10^6$ slug-ft^2, and the shuttle residual rate ΔV and $\Delta\omega$ (see Fig. 21). The final velocities are, of course, determined by the combined system mass and inertia.

The concept and design of a shuttle docking device which can simulate both hard and soft docking is shown in Fig. 22. The space station and shuttle are considered as two separate bodies coupled by a set of angular and rectilinear springs and dampers. Let M_s and I_s be the shuttle mass and inertia, and M_2 and I_2 the mass and inertia of the station. The values of the spring constants and damping factors can be computed using the following equations:

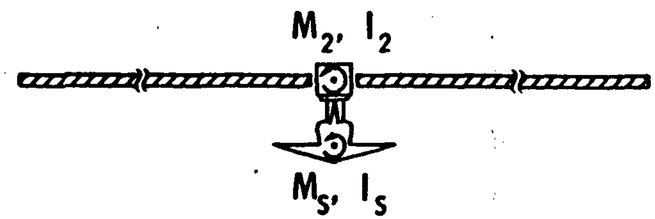

(NOT IN PROPORTION)

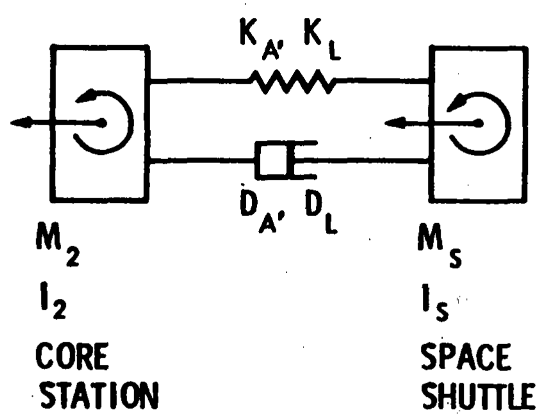

DOCKING SYSTEM PARAMETERS

- ANGULAR STIFFNESS AND DAMPING

$$K_A = \omega_A^2 \left(\frac{I_2 \, I_S}{I_2 + I_S} \right) \qquad \text{FT-LB/RAD}$$

$$D_A = 2 \zeta_A \omega_A \left(\frac{I_2 \, I_S}{I_2 + I_S} \right) \qquad \text{FT-LB/RAD/SEC}$$

- LINEAR STIFFNESS AND DAMPING

$$K_L = \omega_L^2 \left(\frac{M_2 \, M_S}{M_2 + M_S} \right) \qquad \text{LB/FT}$$

$$D_L = 2 \zeta_L \omega_L \left(\frac{M_2 \, M_S}{M_2 + M_S} \right) \qquad \text{LB/FT/SEC}$$

Figure 22 Concept and Design of Shuttle Docking Device

$$K_A = \omega_A{}^2\left(\frac{I_2\, I_s}{I_2 + I_s}\right) \tag{7.1}$$

$$D_A = 2\zeta_A\omega_A\left(\frac{I_2\, I_s}{I_2 + I_s}\right) \tag{7.2}$$

$$K_L = \omega_L{}^2\left(\frac{M_2\, M_s}{M_2 + M_s}\right) \tag{7.3}$$

$$D_L = 2\zeta_L\omega_L\left(\frac{M_2\, M_s}{M_2 + M_s}\right) \tag{7.4}$$

where K_A, D_A, ω_A, ζ_A are the spring constant, damping factor, natural frequency and damping ratio for the set of rotational spring and damper, respectively. Similarly, K_L, D_L, ω_L, ζ_L are for the set of rectilinear spring and damper. The detailed derivation of Eqs. (7.1) - (7.4) is given in Appendix C.

With this design, shuttle hard docking can be simulated by using extremely stiff springs and dampers while for soft docking, much weaker springs and dampers are employed.

7.3 Performance of Adaptive Control on the Two-Panel Space Station

As stated in Chapter III, the 6-DOF two-panel space station is used extensively to evaluate adaptive control problems and performance because of the associated reasonable simulation turnaround time and cost. These results provide valuable guidance to the understanding of the performance of space station adaptive control systems.

7.3.1 Augmented Plant Modal Properties

Following the approach described in Section 6.4, the following inner-loop control gains are chosen:

$K_{\theta 2} = 45662$ ft-lb/rad

$K_{Z2} = 4464$ lb/ft

This plant augmentation has caused changes of modal properties from those shown in Eq. (3.27) of the unaugmented plant. The modal frequencies and mode shape matrix for this augmented plant are,

$$\begin{aligned} \omega_{p1} &= 0.01163 \text{ Hz} \\ \omega_{p2} &= 0.039 \text{ Hz} \\ \omega_{p3} &= 0.0656 \text{ Hz} \\ \omega_{p4} &= 0.1684 \text{ Hz} \\ \omega_{p5} &= 0.3892 \text{ Hz} \\ \omega_{p6} &= 0.3947 \text{ Hz} \end{aligned} \tag{7.5}$$

and

$$\phi_p = \begin{bmatrix} -.921E-1 & .128 & -.922E-1 & .144E-1 & .178 & .178 \\ .382E-3 & -.704E-3 & .705E-3 & -.264E-3 & -.544E-2 & -.549E-2 \\ .382E-9 & .177E-3 & .641E-8 & -.158E-1 & .185E-2 & .226E-5 \\ .332E-3 & -.745E-8 & -.465E-3 & -.959E-9 & .135E-6 & -.117E-3 \\ .921E-1 & .128 & .922E-1 & .144E-1 & .178 & -.177 \\ .382E-3 & .704E-3 & .705E-3 & .264E-3 & .546E-2 & -.548E-2 \end{bmatrix} \tag{7.6}$$

The corresponding mode shapes are plotted in Fig. 23. As can be seen, the four lower frequency modes have changed substantially, and most importantly, the two evolved rigid body modes no longer have zero frequencies.

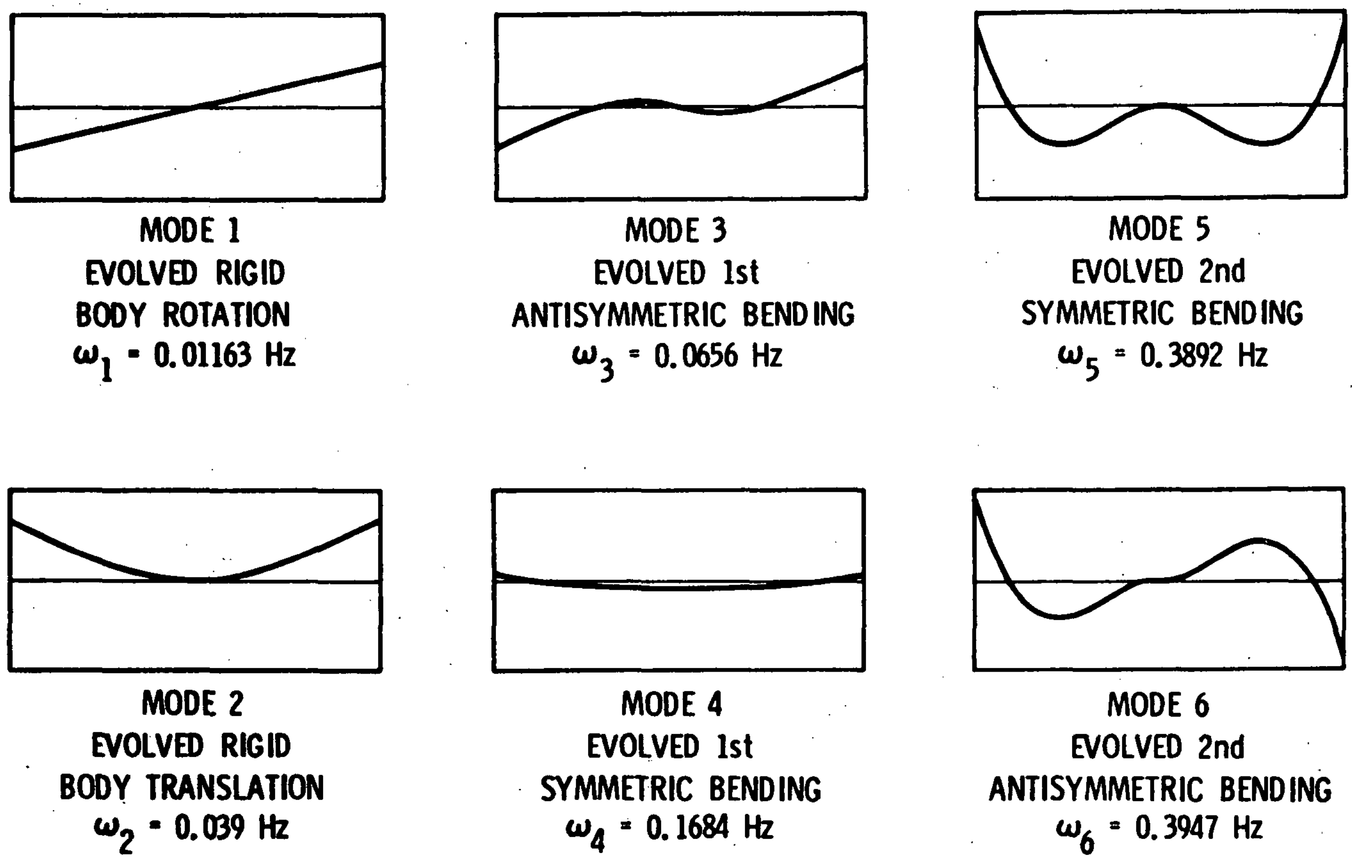

Figure 23 Augmented Plant Modal Properties for the 6-DOF Two-Panel Configuration Model

With the modal dampings assumed to be $\zeta_{pk} = 0.5\%$ for all modes, the A_p, B_p, and C_p matrices in Eqs. (5.6), (5.7) and (5.8) can be readily determined.

7.3.2 The Selection of the Reference Model

To evaluate the performance of the adaptive controller, the reference model is selected to have lower order, significantly different model parameters, and high damping. It consists of 4 modes (corresponding to the 4 low frequency modes of the plant) or 8 states x_m, 4 inputs u_m, and 4 outputs y_m which are defined as follows,

$$x_m = \left[\begin{array}{c} \eta_m \\ \hline \dot{\eta}_m \end{array}\right] \tag{7.7}$$

$$u_m = \begin{bmatrix} u_{m1} \\ u_{m2} \\ u_{m3} \\ u_{m4} \end{bmatrix} \tag{7.8}$$

$$y_m = \begin{bmatrix} y_{m1} \\ y_{m2} \\ y_{m3} \\ y_{m4} \end{bmatrix} = \begin{bmatrix} \alpha\theta_{m1} + \dot{\theta}_{m1} \\ \alpha Z_{m2} + \dot{Z}_{m2} \\ \alpha\theta_{m2} + \dot{\theta}_{m2} \\ \alpha\theta_{m3} + \dot{\theta}_{m3} \end{bmatrix} \tag{7.9}$$

the corresponding system matrices A_m, B_m and C_m are

$$A_m = \left[\begin{array}{c|c} 0_{4x4} & I_{4x4} \\ \hline \begin{matrix} -\omega_{m1}^2 & & \\ & \ddots & \\ & & -\omega_{m4}^2 \end{matrix} & \begin{matrix} -2\zeta_{m1}\omega_{m1} & & \\ & \ddots & \\ & & -2\zeta_{m4}\omega_{m4} \end{matrix} \end{array}\right] \tag{7.10}$$

$$B_m = \begin{bmatrix} 0 \\ ---- \\ \phi_m{}^T B \end{bmatrix} \quad (7.11)$$

$$C_m = \begin{bmatrix} \alpha C\phi_m & C\phi_m \end{bmatrix} \quad (7.12)$$

where B and C are shown in Eqs. (5.9) and (5.10), respectively. The modal frequencies for the reference model are,

$$\begin{aligned} \omega_{m1} &= 0.02 \text{ Hz} \\ \omega_{m2} &= 0.03 \text{ Hz} \\ \omega_{m3} &= 0.04 \text{ Hz} \\ \omega_{m4} &= 0.06 \text{ Hz} \end{aligned} \quad (7.13)$$

The modal dampings are $\zeta_{mk} = 0.707$ for all modes. The position to rate measurement weighting factor $\alpha = 0.2$ and the gain weighting matrices $T = \bar{T} = \text{diag}\ (2.5 \times 10^9,\ 2.5 \times 10^9,\ 2.5 \times 10^{11},\ 2.5 \times 10^9,$ 1000, 1000, 1000, 1000, 1000, 1000, 1000, 1000, 400, 400, 400, 400) are used.

7.3.3 Adaptive Regulator Control

7.3.3.1 Controller Performance with High Initial Transient

The purpose here is to evaluate the convergence property of the adaptive controller for the attitude hold and vibration suppression under very large initial transient conditions. The initial conditions for the plant are:

$$
\begin{aligned}
Z_{p1} &= -\ 3.699 \text{ ft} & \dot{Z}_{p1} &= -\ 0.877 \text{ ft/sec} \\
\theta_{p1} &= 0.860 \text{ deg} & \dot{\theta}_{p1} &= 0.336 \text{ deg/sec} \\
Z_{p2} &= 0.345 \text{ ft} & \dot{Z}_{p2} &= 0.035 \text{ ft/sec} \\
\theta_{p2} &= 0.937 \text{ deg} & \dot{\theta}_{p2} &= 0.037 \text{ deg/sec} \\
Z_{p3} &= 4.071 \text{ ft} & \dot{Z}_{p3} &= 1.045 \text{ ft/sec} \\
\theta_{p3} &= 0.723 \text{ deg} & \dot{\theta}_{p3} &= 0.387 \text{ deg/sec}
\end{aligned}
\tag{7.14}
$$

These conditions were taken 10 seconds after the shuttle docked to the space station with the shuttle initial approaching rates of 0.2 deg/sec and 0.05 ft/sec. The corresponding values in the modal coordinates are obtained through the following transformation,

$$
\begin{aligned}
\eta_p &= \phi_p^{-1}\, Z_p \\
\dot{\eta}_p &= \phi_p^{-1}\, \dot{Z}_p
\end{aligned}
\tag{7.15}
$$

The initial conditions for the reference model are

$$
\begin{aligned}
\eta_{mi} &= 0.9\ \eta_{pi} \\
\dot{\eta}_{mi} &= 0.9\ \dot{\eta}_{pi}
\end{aligned}
\tag{7.16}
$$

for $i = 1, \ldots, 4$.

The simulation results for this case are shown in Figs. 24-29.* Figure 24 shows the outputs of the plant and the model. The model outputs damp out quickly because of its high damping, and the plant

*The remaining figures are at the end of this report.

outputs track them asymptotically and converge within 100 seconds from the transient starts. The same behavior is observed in Figs. 25 and 26 for the plant and model physical states. In Fig. 25, Z_{2p} follows Z_{2m} better than Z_{1p} to Z_{1m} or Z_{3p} to Z_{3m} because a force actuator is employed at the central bus; thus, at this position, linear displacement can be controlled more effectively. Figure 27 indicates that the four lower frequency modes of the plant also closely follow the corresponding modes of the model although mode 2 damps out at a slower pace. Mode 1, the rigid body rotational mode, is apparently the dominant mode of the system. The two high frequency modes shown in Fig. 28 also converge to zero within 100 seconds. The required adaptive control inputs, u_{pi}, are plotted in Fig. 29. The demand on bus control torque is quite high, almost 3,000 ft-lb under these high initial transient conditions.

7.3.3.2 Controller Performance with High Initial Transient and Measurement Noise

The measurement noises of the sensors are assumed to be zero-mean gaussian white processes. The level of the noises are taken to be two orders of magnitude lower than those of the peak outputs. Under these assumptions, the measurement uncertainties for the accelerometers are 0.012 inch and for the gyros are 20.63 $\widehat{\text{sec}}$. The qualities for the sensors in existence today are much better than these. For instance, the accuracy of the gyro used on High Energy Astronomy Observatory - 1 (HEAO-1) is 0.5 $\widehat{\text{sec}}$.

The plant and model outputs are shown in Fig. 30. Apparently, the measurement noises have no significant effects on the high rate of convergence and stability of the system although y_{p3} has some noticeable fluctuations throughout the time history. Figure 31 shows the adaptive control inputs. The bus control force u_{p2} fluctuates highly during the first 25 seconds which is quite different from that of the case without measurement noises. After the initial transient, all the control inputs are associated with sustaining or even increasing fluctuations. Control energy is wasted by reacting to noises after the steady state is reached. One way to solve this problem is to employ a threshold at the actuator input. Control is applied to the system only when the input exceeds the threshold levels. Nevertheless, controller robustness is observed even with a high degree of measurement noises applied to the system.

7.3.4 Adaptive Control During Shuttle Docking

The following simulations are designed to test the controller performance and stability using shuttle docking dynamics. To simulate these cases, a docking disturbance term $B_d u_d$ is added to the right-hand side of Eq. (3.18), where

$$B_d = \begin{bmatrix} 0 & 0 \\ 0 & 0 \\ 1 & 0 \\ 0 & 1 \\ 0 & 0 \\ 0 & 0 \end{bmatrix} , \qquad u_d = \begin{bmatrix} F_d \\ T_d \end{bmatrix} \tag{7.17}$$

and F_d is the docking force, T_d is the docking torque applied to the space station. F_d and T_d are determined by the following equations:

$$F_d = D_L(\dot{Z}_{shuttle} - \dot{Z}_{p2}) + K_L(Z_{shuttle} - Z_{p2}) \tag{7.18}$$

$$T_d = D_A(\dot{\theta}_{shuttle} - \dot{\theta}_{p2}) + K_A(\theta_{shuttle} - \theta_{p2}) \tag{7.19}$$

and the equations of motion of the shuttle are characterized by

$$\ddot{Z}_{shuttle} = - F_d/M_s \tag{7.20}$$

$$\ddot{\theta}_{shuttle} = - T_d/I_s \tag{7.21}$$

where M_s is the mass and I_s is the moment of inertia of the shuttle. The shuttle residual rates (rates prior to docking) are:

$$\dot{Z}_{shuttle}(0) = 0.05 \text{ ft/sec} \tag{7.22}$$

$$\dot{\theta}_{shuttle}(0) = 0.2 \text{ deg/sec} \tag{7.23}$$

7.3.4.1 Shuttle Hard Docking

The control objective here is to stabilize the space station so that it returns to its prior docking condition after docking occurs. Thus all of the initial conditions for the plant and the model are set to zero. For regulator control, the input command u_m to the model is zero. Since there are no model disturbances employed under the "unscheduled event," the reference model stays at its quiescent state throughout the simulation period. Thus the plant, while under the influence of the docking disturbances, is commanded to follow the zero output.

The following docking parameters are used in this case:

$$
\begin{aligned}
D_L &= 2.313 \times 10^3 \text{ lb/ft/sec} \\
K_L &= 1.028 \times 10^3 \text{ lb/ft} \\
D_A &= 1.86 \times 10^7 \text{ ft-lb/rad/sec} \\
K_A &= 8.25 \times 10^7 \text{ ft-lb/rad}
\end{aligned}
\tag{7.24}
$$

the corresponding damping ratios and natural frequencies are

$$
\text{linear:} \quad
\begin{aligned}
\zeta_L &= 0.707 \\
\omega_L &= 0.1 \text{ Hz}
\end{aligned}
\tag{7.25}
$$

$$
\text{angular:} \quad
\begin{aligned}
\zeta_A &= 0.707 \\
\omega_A &= 1.0 \text{ Hz}
\end{aligned}
\tag{7.26}
$$

This case is termed "simulated hard docking" because the springs and dampers used are extremely stiff. The simulation results are plotted in Figs. 32-39. Figure 32 shows that all of the plant outputs converge to zero within 100 seconds after docking begins. The results here are surprisingly good since, in addition to the high docking disturbances and the parameter and truncation errors, we also deal with a sudden increase of plant mass and inertia by more than 100%. The same performance is observed for the plant and model physical states in Figs. 33 and 34. In Fig. 35, all but mode 2 are well damped. Mode 2 shows a very lightly damped oscillation, however, since the amplitude of this mode is very small and it presents no noticeable effects on any of the physical outputs. At higher amplitude, the damping is also higher, the oscillation will be decayed at a faster rate and it will pose no real problem to the system. The two high frequency modes in Fig. 36 also show good convergence rates. Figure 37 illustrates the time history of shuttle angular position and rate. It is not surprising to note that they appear almost exactly the same as the central bus angular position and rate (Figs. 34(b) and (d)) because after the hard docking, the shuttle and the station are supposed to combine and become one body. Figure 38 indicates that the peak of the docking torque is 63,158 ft-lb.

To achieve the above performance, a peak torque as high as 7500 ft-lb has to be generated by the bus torque actuator (u_{p3}) as shown in Fig. 39. This is extremely high and presents an implementation problem. Of course, hard docking will not be a realistic docking option due to its high transient loads to the space station. Under soft docking conditions, the torque should be much less.

7.3.4.2 Shuttle Soft Docking

The conditions for the shuttle soft docking simulation are the same as those of shuttle hard docking except that much weaker springs and dampers are employed here. Specifically, the following docking interface parameters are used:

$$
\begin{aligned}
D_L &= 693.8 \text{ lb/ft/sec} \\
K_L &= 92.49 \text{ lb/ft} \\
D_A &= 5.57 \times 10^4 \text{ ft-lb/rad/sec} \\
K_A &= 742 \text{ ft-lb/rad}
\end{aligned}
\tag{7.27}
$$

the corresponding damping ratios and natural frequencies are

$$
\text{linear:} \quad \zeta_L = 0.707, \quad \omega_L = 0.03 \text{ Hz} \tag{7.28}
$$

$$
\text{angular:} \quad \zeta_A = 0.707, \quad \omega_A = 0.003 \text{ Hz} \tag{7.29}
$$

Because of the very low system natural frequencies yielded under soft docking, it will take a much longer time for the space station to reach its quiescent state. Hence, the simulation time of 400 seconds is used in this case. The simulation results are shown in Figs. 40-49. Referring to Fig. 40, all plant outputs except y_{p2} converge slower than those of the hard docking case, especially y_{p3}. In Figs. 41 and 42, Z_{p1}, Z_{p3} and θ_{p2} also show a significantly slower convergence rate. The same behavior is observed for modes 1, 2, 3 and 6 in Figs. 43 and 44. In contrast to the hard docking case as expected, the shuttle angular position and rate as shown in Fig. 45 have experienced high excursions. However, with the adaptive control system on the space station, the angular position and rate of the central bus have deviated very little from their nominal values (Figs. 42 (b) and (d)). Figure 46 indicates that the peak of the docking torque is 190 ft-lb, substantially lower than the 63,158 ft-lb of the hard docking -- a factor of 332.

What makes the soft docking a desirable docking option is, in addition to the reduced shock load, that the demand of control efforts drops drastically. For instance, the peak of u_{p3} drops to 300 ft-lb from 7,500 ft-lb of hard docking (Fig. 47). The comparison of relative panel tip displacement and acceleration by employing adaptive control vs. low gain bus control are shown in Figs. 48 and 49, respectively. The dynamic load and panel deflection are markedly reduced by using adaptive control. For example, with the adaptive control, the peak panel deflection drops to 0.41 ft. from 6.6 ft.

7.3.4.3 Shuttle Hard Docking with Actuator Saturation

One way to relieve the high actuation demand on the control hardware is to employ actuator saturation through gain limiting. To study the effect of actuator saturation, shuttle hard docking is again employed here (for soft docking will take too long to simulate). The following limits for the control inputs are used:

$$\begin{aligned} \max \left| u_{p1} \right| &= 50 \text{ ft-lb} \\ \max \left| u_{p2} \right| &= 12 \text{ lbs} \\ \max \left| u_{p3} \right| &= 1000 \text{ ft-lb} \\ \max \left| u_{p4} \right| &= 50 \text{ ft-lb} \end{aligned} \tag{7.30}$$

Figures 50-54 indicate that the system performance has degraded compared with those without saturation (Figs. 32-36), as expected. The peaks of the responses are higher and it takes longer time periods for them to converge. It is also seen that the responses are more jittering due to the bang-bang effect. Larger angular excursion of the shuttle is also observed in Fig. 55. The docking force and torque remain unchanged (Fig. 56). Figure 57 shows that the control inputs u_{p1} and u_{p4} have not yet totally stayed within their linear operation region at the end of 150 sec.

As the gain limit becomes more severe (one half the values shown in Eq. (7.30)), the system performance degrades further as indicated in Fig. 58. Though it is believed that the outputs will still converge, it will take a much longer time than the above cases. Moreover, only u_{p2} stayed within the linear operation during the simulation period (Fig. 59).

Regardless of the severe actuation saturations applied, the results show no sign of threatening the system stability.

7.3.4.4 Shuttle Hard Docking with Model Switching and Disturbance Modeling

Intuitively it is true that the control effort can be reduced if after the shuttle docking contact is made with the space station, one uses a new reference model in which the shuttle mass and inertia are incorporated and a simulated disturbance similar to the docking disturbance is injected. The plant outputs will now follow the new model transient instead of the zero model outputs. The reason for the control inputs to be smaller is because of the expected smaller output errors. This has motivated us to study the effect of model switching and disturbance modeling.

Since the plant is assumed to be poorly known, after incorporating the shuttle mass properties, the mode shapes and modal frequencies of the 4 modes of the model are deliberately selected with an error up to 20%. The disturbance force and torque inputs to the reference model are taken to be 2.25 sec-pulse of 173.78 lbs and 0.225 sec-pulse of 116953 ft-lb amplitude, respectively.

The simulation results are shown in Figs. 60-65. The plant outputs follow the reference model outputs reasonably well. By comparing Figs. 60-64 with Figs. 32-36, it is found that the convergence rates are about the same for the two cases. As far as the peak control inputs are concerned, u_{p3} drops significantly from 7500 ft-lb to 2880 ft-lb, and u_{p2} drops from 120 lbs to 75 lbs as shown in Fig. 65. However, u_{p1} and u_{p4} rise from 230 ft-lb to about 800 ft-lb. These results indicate that the concept of model switching is more involved than one may think. More study in the area of peak control effort reduction will be required. In general, one should not expect to reduce all the control efforts, but only the critical ones.

7.4 Performance of Adaptive Control on the Four-Panel Space Station

The purpose of this section is to demonstrate the performance of adaptive control on the much more complex 19-DOF four-panel space station model.

7.4.1 Augmented Plant Modal Properties

Plant augmentation has altered the modal properties from those of the original plant. The new modal frequencies and mode shapes are shown in Fig. 66. The three evolved rigid body modes no longer have zero frequencies, and the evolved modes 1 and 2 become pure rotation about the X and Y axes, respectively. Note that the frequencies of the modes in the first bending group are also pushed higher while those of the modes in the second bending group remain unchanged due to the fact that the inner-loop controller is a low-bandwidth system.

With the modal dampings assumed to be $\zeta_{pk} = 0.5\%$ for all modes, the A_p, B_p and C_p matrices in Eqs. (5.16), (5.17) and (5.18) can be readily determined.

7.4.2 The Selection of the Reference Model

Again, to evaluate the performance of the adaptive controller on the four-panel space station, the reference model is selected to be a lower order system with high damping and significantly different parameters from those of the plant. It consists of 9 modes (corresponding to the rigid body modes and the modes in the first bending group of the plant) or 18 states x_m, 11 inputs u_m and 11 outputs y_m which are defined as follows

$$x_m = \begin{bmatrix} \eta_m \\ --- \\ \dot{\eta}_m \end{bmatrix} \tag{7.31}$$

$$u_m = \begin{bmatrix} u_{m1} \\ u_{m2} \\ u_{m3} \\ u_{m4} \\ u_{m5} \\ u_{m6} \\ u_{m7} \\ u_{m8} \\ u_{m9} \\ u_{m10} \\ u_{m11} \end{bmatrix} \tag{7.32}$$

$$y_m = \begin{bmatrix} y_{m1} \\ y_{m2} \\ y_{m3} \\ y_{m4} \\ y_{m5} \\ y_{m6} \\ y_{m7} \\ y_{m8} \\ y_{m9} \\ y_{m10} \\ y_{m11} \end{bmatrix} = \begin{bmatrix} \alpha\theta_{m1} + \dot{\theta}_{m1} \\ \alpha\theta_{m3} + \dot{\theta}_{m3} \\ \alpha Z_{m2} + \dot{Z}_{m2} \\ \alpha\phi_{m2} + \dot{\phi}_{m2} \\ \alpha Z_{m4} + \dot{Z}_{m4} \\ \alpha\theta_{m4} + \dot{\theta}_{m4} \\ \alpha\phi_{m4} + \dot{\phi}_{m4} \\ \alpha Z_{m6} + \dot{Z}_{m6} \\ \alpha\phi_{m6} + \dot{\phi}_{m6} \\ \alpha\theta_{m5} + \dot{\theta}_{m5} \\ \alpha\theta_{m7} + \dot{\theta}_{m7} \end{bmatrix} \tag{7.33}$$

The corresponding system matrices A_m, B_m and C_m are,

$$A_m = \left[\begin{array}{c|c} 0_{9x9} & I_{9x9} \\ \hline \begin{matrix} -\omega_{m1}^2 & & \\ & \ddots & \\ & & -\omega_{m9}^2 \end{matrix} & \begin{matrix} -2\zeta_{m1}\omega_{m1} & & \\ & \ddots & \\ & & -2\zeta_{m9}\omega_{m9} \end{matrix} \end{array}\right] \tag{7.34}$$

$$B_m = \left[\begin{array}{c} 0 \\ \hline \phi_m^T B \end{array}\right] \tag{7.35}$$

$$C_m = \left[\alpha C\phi_m \quad C\phi_m\right] \tag{7.36}$$

where B and C are shown in Eqs. (5.19) and (5.20), respectively. To show the breadth of the controller performance, the modal frequencies are selected to have a 40% error and mode shapes a 30% error. The high modal damping ratios $\zeta_{mk} = 0.707$ for all modes and position to rate measurement weighting factor $\alpha = 0.2$ are employed.

7.4.3 Adaptive Regulator Control with High Initial Transient

The purpose here is to evaluate the convergence property of the adaptive controller for the attitude hold and vibration suppression under very large initial transient conditions.

The initial conditions for the plant are:

$$
\begin{aligned}
Z_{p1} &= -\ 1.649 \text{ ft} & \dot{Z}_{p1} &= \ \ 0.283 \text{ ft/sec} \\
\theta_{p1} &= \ \ 0.845 \text{ deg} & \dot{\theta}_{p1} &= -\ 0.179 \text{ deg/sec} \\
Z_{p3} &= \ \ 1.617 \text{ ft} & \dot{Z}_{p3} &= -\ 0.284 \text{ ft/sec} \\
\theta_{p3} &= \ \ 0.830 \text{ deg} & \dot{\theta}_{p3} &= -\ 0.180 \text{ deg/sec} \\
Z_{p2} &= -\ 0.004 \text{ ft} & \dot{Z}_{p2} &= \ \ 0.002 \text{ ft/sec} \\
\phi_{p2} &= -\ 0.004 \text{ deg} & \dot{\phi}_{p2} &= \ \ 0.017 \text{ deg/sec} \\
Z_{p4} &= -\ 0.001 \text{ ft} & \dot{Z}_{p4} &= \ \ 0.0002 \text{ ft/sec} \\
\theta_{p4} &= \ \ 0.722 \text{ deg} & \dot{\theta}_{p4} &= -\ 0.029 \text{ deg/sec} \\
\phi_{p4} &= \ \ 0.012 \text{ deg} & \dot{\phi}_{p4} &= -\ 0.035 \text{ deg/sec} \\
Z_{p6} &= \ \ 0.004 \text{ ft} & \dot{Z}_{p6} &= -\ 0.001 \text{ ft/sec} \\
\phi_{p6} &= -\ 0.003 \text{ deg} & \dot{\phi}_{p6} &= \ \ 0.017 \text{ deg/sec} \\
Z_{p5} &= -\ 1.618 \text{ ft} & \dot{Z}_{p5} &= \ \ 0.283 \text{ ft/sec} \\
\theta_{p5} &= \ \ 0.830 \text{ deg} & \dot{\theta}_{p5} &= -\ 0.180 \text{ deg/sec} \\
Z_{p7} &= \ \ 1.649 \text{ ft} & \dot{Z}_{p7} &= -\ 0.284 \text{ ft/sec} \\
\theta_{p7} &= \ \ 0.846 \text{ deg} & \dot{\theta}_{p7} &= -\ 0.179 \text{ deg/sec}
\end{aligned}
\tag{7.37}
$$

These dynamical conditions were taken 10 seconds after the shuttle docked to the space station with the following initial approaching rates:

$$
\begin{aligned}
\dot{Z}_{shuttle} &= 0.05 \text{ ft/sec} \\
\dot{\theta}_{shuttle} &= 0.2 \text{ deg/sec} \\
\dot{\phi}_{shuttle} &= 0.2 \text{ deg/sec}
\end{aligned}
\tag{7.38}
$$

The corresponding initial values in the modal coordinates are obtained through the following transformation,

$$\begin{aligned} \eta_p &= \phi_p^{-1}\, z_p \\ \dot{\eta}_p &= \phi_p^{-1}\, \dot{z}_p \end{aligned} \tag{7.39}$$

The initial conditions for the reference model are,

$$\begin{aligned} \eta_{mi} &= 0.8\ \eta_{pi} \\ \dot{\eta}_{mi} &= 0.8\ \dot{\eta}_{pi} \end{aligned} \tag{7.40}$$

for $i = 1, \ldots, 9$.

The gain weighting matrices $T = \overline{T} = \text{diag}\,(2.5 \times 10^8,\ 2.5 \times 10^8,\ 2.5 \times 10^6,\ 2.5 \times 10^6,\ 2.5 \times 10^6,\ 2.5 \times 10^9,\ 2.5 \times 10^8,\ 2.5 \times 10^6,\ 2.5 \times 10^6,\ 2.5 \times 10^8,\ 2.5 \times 10^8,$ 100, 100, 100, 100, 100, 100, 100, 100, 100, 100, 100, 100, 100, 100, 100, 100, 100, 100, 400, 400, 400, 400, 400, 400, 400, 400, 400, 400, 400, 400) are used.

The adaptive system simulation for the four-panel configuration is implemented in a fashion similar to that for the two-panel configuration except that the dimension and complexity are much greater and the execution time and cost are high. Because of this, relatively fewer cases have been studied here. However, the results are very encouraging as shown in Figs. 67-73. The simulation period is 75 seconds. Figure 67 indicates that the plant outputs closely track the model outputs; and with the exception of y_{p4}, y_{p7} and y_{p9}, all outputs converge within 75 seconds. Figures 68 and 69 also show excellent physical state responses. The three bending angles ϕ_2, ϕ_4, ϕ_6 and their rates $\dot{\phi}_2$, $\dot{\phi}_4$, $\dot{\phi}_6$ converge slower than other states and rates. The modal responses are shown in Figs. 70-72. All except mode 5 show relatively high damping rates. Mode 2, the rigid Y-rotational mode, strongly dominates the system dynamics and has a very high rate of damping. This mode is excited due to the fact that the simulation assumes a huge shuttle angular momentum about the pitch axis. The demand for control efforts shown in Fig. 73 is substantially lower than that required for the two-panel configuration. The peak of control torque is 400 ft-lb at the central bus and 350 ft-lb at the panel tips as compared with 3,000 ft-lb and 1,000 ft-lb, respectively, for the two-panel configuration. This is because the four-panel configuration is much more stiff and massive.

7.4.4 Adaptive Control During Shuttle Hard Docking

Unlike the hard docking case for the two-panel configuration, it is assumed here that the residual angular momenta of the shuttle are about its roll and pitch axes. The docking disturbance term $B_d u_d$ is then defined as

$$
B_d = \begin{bmatrix} 0 & 0 & 0 \\ 0 & 0 & 0 \\ 0 & 0 & 0 \\ 0 & 0 & 0 \\ 0 & 0 & 0 \\ 0 & 0 & 0 \\ 1 & 0 & 0 \\ 0 & 1 & 0 \\ 0 & 0 & 1 \\ 0 & 0 & 0 \\ 0 & 0 & 0 \\ 0 & 0 & 0 \\ 0 & 0 & 0 \\ 0 & 0 & 0 \\ 0 & 0 & 0 \end{bmatrix} \qquad u_d = \begin{bmatrix} F_d \\ T_d \\ P_d \end{bmatrix} \tag{7.41}
$$

where F_d is the docking force, T_d is the docking torque about the pitch axis (Y-axis), and P_d is the docking torque about the roll axis (X-axis). Again the shuttle is assumed to dock with the space station at the central bus (the core). F_d, T_d and P_d are determined by the following equations:

$$
F_d = D_F\,(\dot{Z}_{shuttle} - \dot{Z}_{p4}) + K_F\,(Z_{shuttle} - Z_{p4}) \tag{7.42}
$$

$$
T_d = D_T\,(\dot{\theta}_{shuttle} - \dot{\theta}_{p4}) + K_T\,(\theta_{shuttle} - \theta_{p4}) \tag{7.43}
$$

$$
P_d = D_P\,(\dot{\phi}_{shuttle} - \dot{\phi}_{p4}) + K_p\,(\phi_{shuttle} - \phi_{p4}) \tag{7.44}
$$

and the equations of motion of the shuttle are characterized by

$$\ddot{Z}_{shuttle} = - F_d/M_s \tag{7.45}$$

$$\ddot{\theta}_{shuttle} = - T_d/I_\theta \tag{7.46}$$

$$\ddot{\phi}_{shuttle} = - P_d/I_\phi \tag{7.47}$$

where M_s = 7820 slugs is the mass; $I_\theta = 7.54 \times 10^6$ slug-ft^2 is the moment of inertia about the pitch axis; and $I_\phi = 1.0 \times 10^6$ slug-ft^2 is the moment of inertia about the roll axis of the shuttle.

The shuttle residual rates (rates prior to docking) are:

$$\dot{Z}_{shuttle}\,(0) = 0.05 \text{ ft/sec} \tag{7.48}$$

$$\dot{\theta}_{shuttle}\,(0) = 0.2 \text{ deg/sec} \tag{7.49}$$

$$\dot{\phi}_{shuttle}\,(0) = 0.2 \text{ deg/sec} \tag{7.50}$$

Again all of the initial conditions for the plant and the model are set to zero, and since there are no reference model disturbances, the reference model stays at its quiescent state throughout the simulation period. Thus the plant is commanded to follow the zero output at the presence of docking disturbances.

The docking parameters used and the corresponding damping ratios and natural frequencies are listed as follows:

$$
\begin{aligned}
\text{linear:}\quad & D_F = 3.06 \times 10^3 \text{ lb/ft/sec} \\
& K_F = 1.36 \times 10^3 \text{ lb/ft} \\
& \zeta_F = 0.707 \\
& \omega_F = 0.1 \text{ Hz}
\end{aligned}
\tag{7.51}
$$

$$
\begin{aligned}
\text{angular:}\quad & D_T = 1.46 \times 10^7 \text{ ft-lb/rad/sec} \\
\text{(pitch)}\quad & K_T = 6.48 \times 10^7 \text{ ft-lb/rad} \\
& \zeta_T = 0.707 \\
& \omega_T = 1.0 \text{ Hz}
\end{aligned}
\tag{7.52}
$$

$$
\begin{aligned}
\text{angular:}\quad & D_P = 7.08 \times 10^6 \text{ ft-lb/rad/sec} \\
\text{(roll)}\quad & K_P = 3.15 \times 10^7 \text{ ft-lb/rad} \\
& \zeta_P = 0.707 \\
& \omega_P = 1.0 \text{ Hz}
\end{aligned}
\tag{7.53}
$$

The gain weighting matrices are $T = \bar{T} = \text{diag}\,(2.5 \times 10^6, 2.5 \times 10^6, 2.5 \times 10^6, 2.5 \times 10^6, 2.5 \times 10^6, 2.5 \times 10^8, 2.5 \times 10^8, 2.5 \times 10^6, 2.5 \times 10^6, 2.5 \times 10^6, 2.5 \times 10^6, 1000, 1000, 1000, 1000, 1000, 1000, 1000, 1000, 1000, 1000, 1000, 1000, 1000, 1000, 1000, 1000, 1000, 1000, 400, 400, 400, 400, 400, 400, 400, 400, 400, 400, 400)$.

The simulation results are shown in Figs. 74-82. Figure 74 shows that all of the plant outputs converge to equilibrium state within 300 seconds after docking begins. The same performance is observed for the plant states and their rates in Figs. 75 and 76. In Figs. 77-79, all but mode 5 are well damped. However, the amplitude of mode 5 is very small and it is believed that it will converge after some longer period of time. Mode 2 strongly dominates the system dynamics due to the huge shuttle angular momentum applied about the pitch axis. Due to the higher structural stiffness, the required control efforts (Fig. 80) drop drastically compared with those in the hard docking case for the two-panel configuration while the docking force and torque maintain unchanged (see Figs. 38 and 82). The linear and angular positions of the shuttle shown in Fig. 81 are practically the same as those of the station central bus (Figs. 75(d), (j) and (n)), as expected.

CHAPTER VIII

CONCLUSIONS

The feature of a large space deployable structure is its complex flexible dynamics. Flexible dynamics are characterized by extremely high system dimensions and parameter uncertainties. Model truncation plays an important role in spacecraft control due to the limited computer capability and related hardware available today or in the near future. Control systems that can adequately deal with truncated dynamics and model parameter errors are necessary for large space structural systems. Space stations, among all large space structural systems, have stringent operational requirements and present a unique challenge for control engineers and researchers. For space stations, in addition to the parameter uncertainties and truncation errors, the control system has also to deal with the growth, time-varying dynamics, and high-intensity environmental disturbances. Adaptive control provides a potential solution to these problems. A direct model reference adaptive control algorithm for the control of space stations is investigated. This algorithm along with the proposed inner-loop plant augmentation technique (for the unstable rigid body dynamics) form a potentially robust control system for space stations. Two sufficient conditions have been derived to assure the globally asymptotic stability. Extensive control simulations and analyses have been conducted for two space station configurations with emphasis on generic properties and practical implementation issues.

The adaptive system developed here has exhibited high performance and robustness. However, in common with all other adaptive control algorithms, this one is also nonlinear, complex, and high gain. The demand on control effort, especially during stringent high disturbance operations, is so high that it has exceeded the capability of the realistic hardware. To cope with this problem, a number of solutions have been proposed and investigated. These solutions are gain limiting, reference model switching, disturbance modeling, and disturbance load reduction (e.g., soft space shuttle docking). With these methods integrated into the controller, the required hardware capability has been drastically reduced yet stability and robust performance of the system are still observed. Further research in this area is required and fruitful results are expected.

Specific conclusions are summarized as follows:

(1) The study results show promising potential application of adaptive control techniques to space stations.

(2) The proposed inner-loop plant augmentation method as part of the adaptive system has improved the system convergence significantly and stabilized the rigid body modes.

(3) High rates of convergence and robustness have been observed throughout the simulated cases.

Specifically,

(i) The system is robust a) in the presence of unmodeled dynamics -- model truncation, b) with poorly known plant dynamics, and c) in the event of instant change of system mass property by more than 100%.

(ii) It shows a good convergence property even under severe dynamic conditions including a) high initial elastic deformation and initial attitude errors, b) strong shuttle docking disturbances and dynamic interactions.

(4) Shuttle hard docking is an example of the harsh space station operational environment. The high gain requirement associated with the adaptive controller will far exceed hardware limitations. Two methods of reducing the control demand have been investigated. Gain limitation can be applied to set a practical limit to the control effort and maintain stability of the system at the expense of higher transient and longer settling time. Model switching together with disturbance modeling provides a means for output error reduction and hence, the reduced control demand. However, since our knowledge about the plant is incomplete, tuning through simulation is required to achieve good results.

(5) It is believed that a combination of load reduction (e.g., shuttle soft docking), gain limiting, model switching, and disturbance modeling will result in satisfactory system performance with realistic hardware implementation.

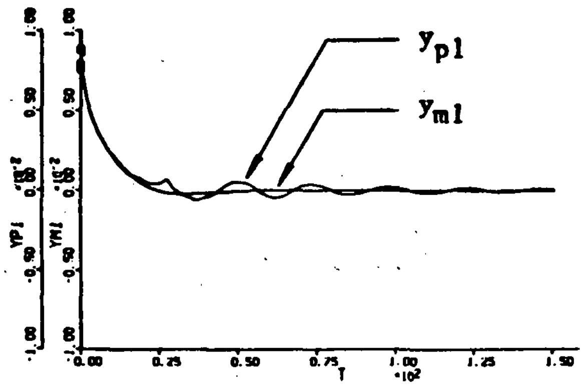

(a) $y_{p1} = \alpha\,\theta_{p1} + \dot{\theta}_{p1}$ (rad)

$y_{m1} = \alpha\,\theta_{m1} + \dot{\theta}_{m1}$ (rad)

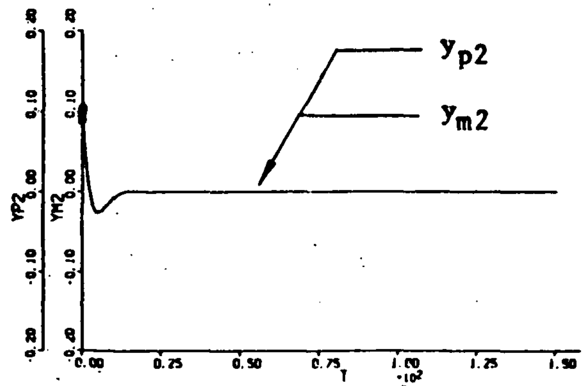

(b) $y_{p2} = \alpha\, Z_{p2} + \dot{Z}_{p2}$ (ft)

$y_{m2} = \alpha\, Z_{m2} + \dot{Z}_{m2}$ (ft)

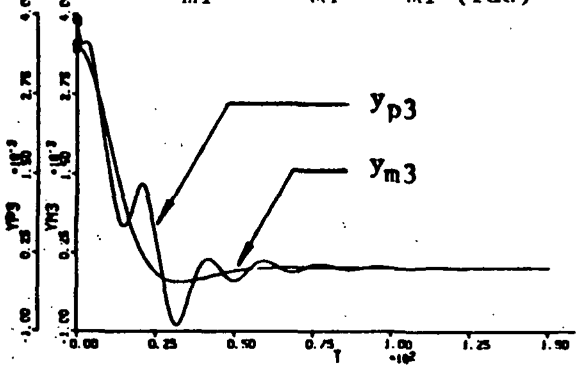

(c) $y_{p3} = \alpha\,\theta_{p2} + \dot{\theta}_{p2}$ (rad)

$y_{m3} = \alpha\,\theta_{m2} + \dot{\theta}_{m2}$ (rad)

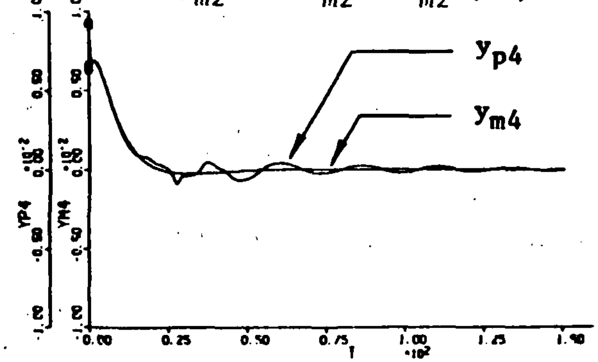

(d) $y_{p4} = \alpha\,\theta_{p3} + \dot{\theta}_{p3}$ (rad)

$y_{m4} = \alpha\,\theta_{m3} + \dot{\theta}_{m3}$ (rad)

Figure 24 Adaptive Regulator Control for Two-Panel Configuration

-- Plant and Model Outputs

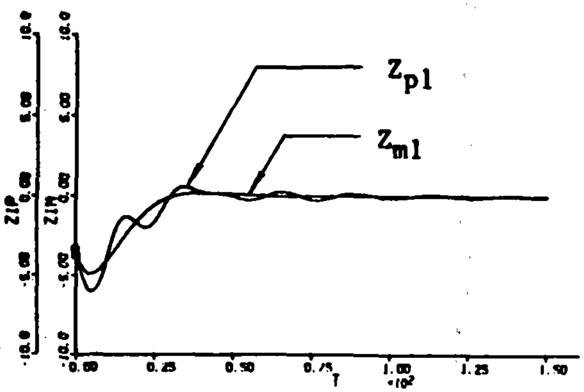

(a) Z_{p1}, Z_{m1} (ft)

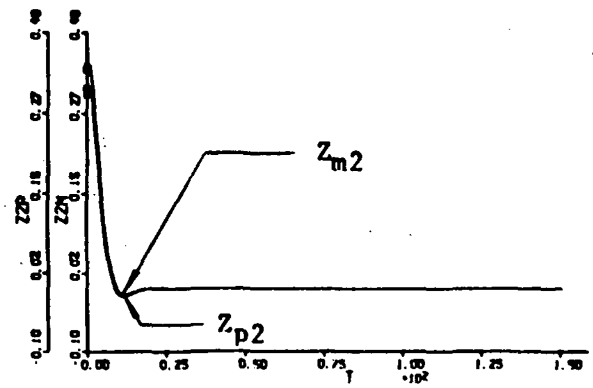

(b) Z_{p2}, Z_{m2} (ft)

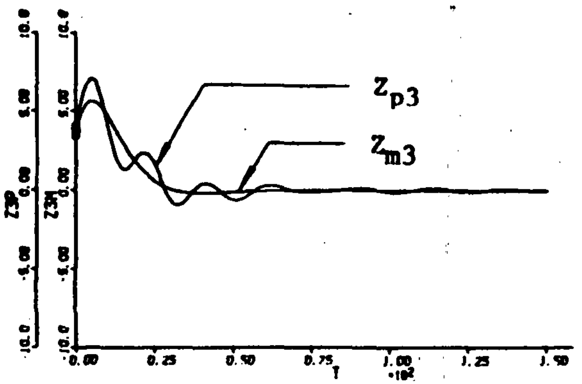

(c) Z_{p3}, Z_{m3} (ft)

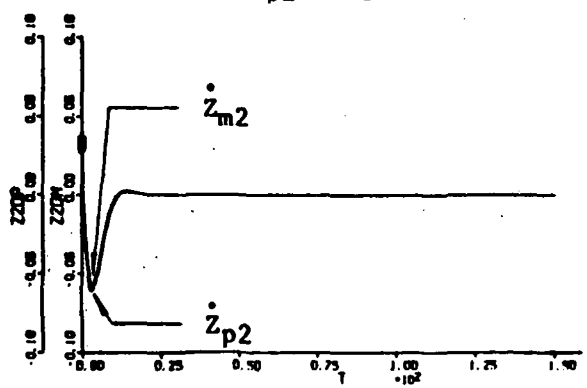

(d) $\dot{Z}_{p2}$, $\dot{Z}_{m2}$ (ft/sec)

Figure 25 Adaptive Regulator Control for Two-Panel Configuration

-- Plant and Model Translational State Responses

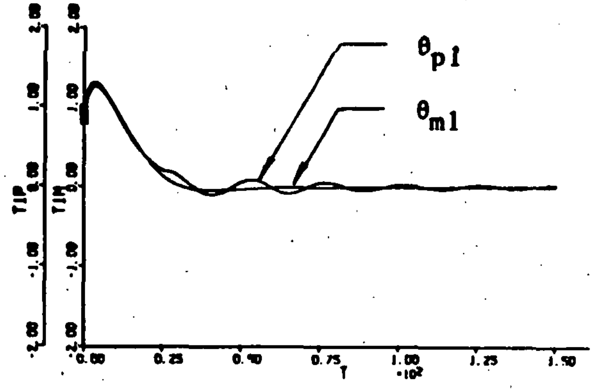

(a) θ_{p1}, θ_{m1} (deg)

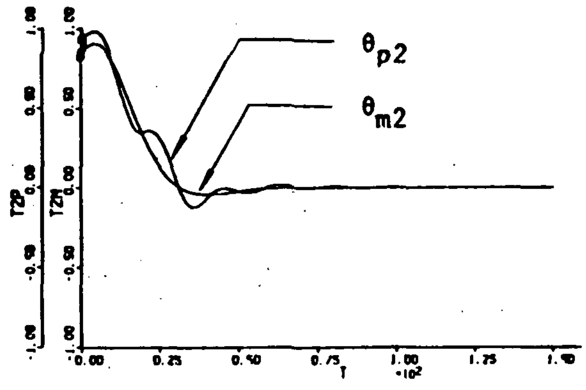

(b) θ_{p2}, θ_{m2} (deg)

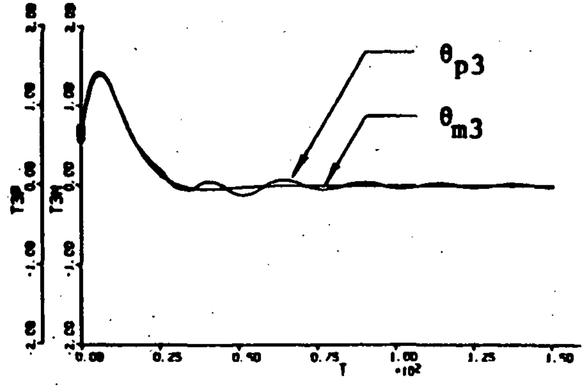

(c) θ_{p3}, θ_{m3} (deg)

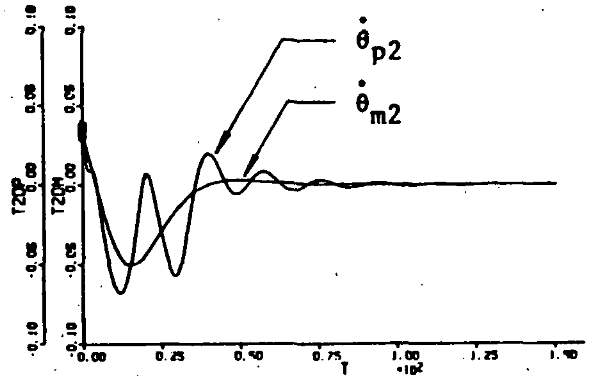

(d) $\dot{\theta}_{p2}$, $\dot{\theta}_{m2}$ (deg/sec)

Figure 26 Adaptive Regulator Control for Two-Panel Configuration

-- Plant and Model Rotational State Responses

ORIGINAL PAGE IS
OF POOR QUALITY

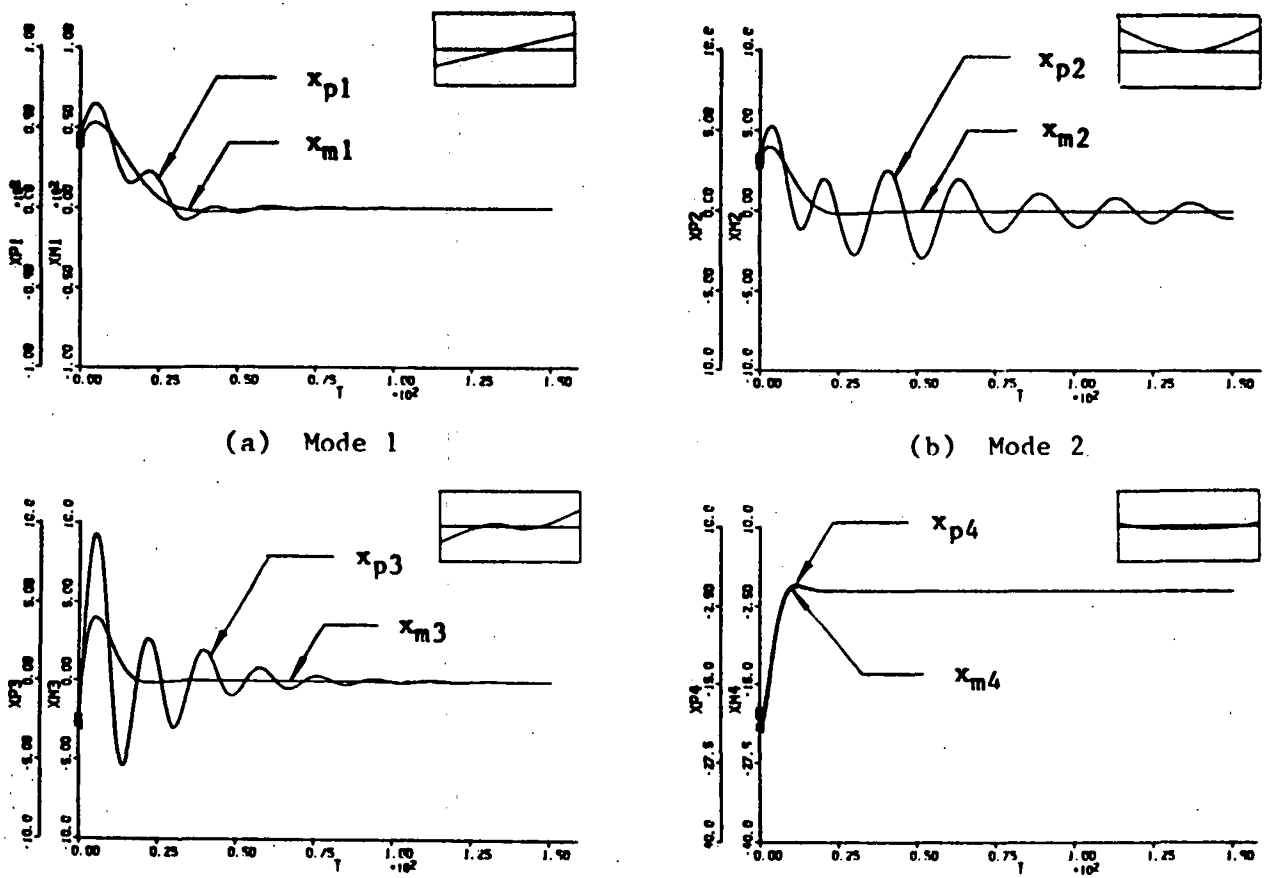

(a) Mode 1 (b) Mode 2

(c) Mode 3 (d) Mode 4

Figure 27 Adaptive Regulator Control for Two-Panel Configuration

-- Plant and Model Modal Responses

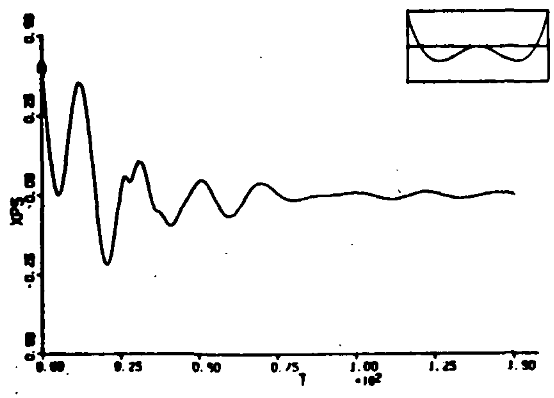

(a) Mode 5

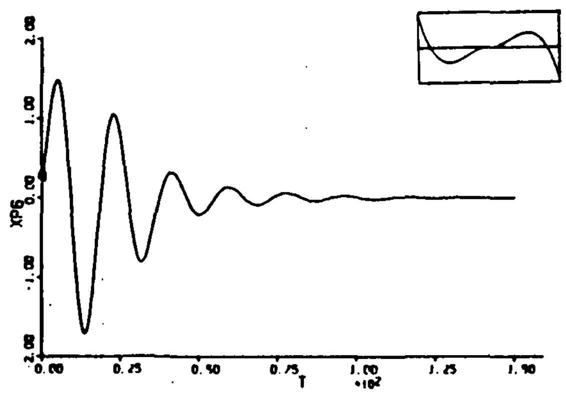

(b) Mode 6

Figure 28 Adaptive Regulator Control for Two-Panel Configuration

-- High Frequency Plant Modal Responses

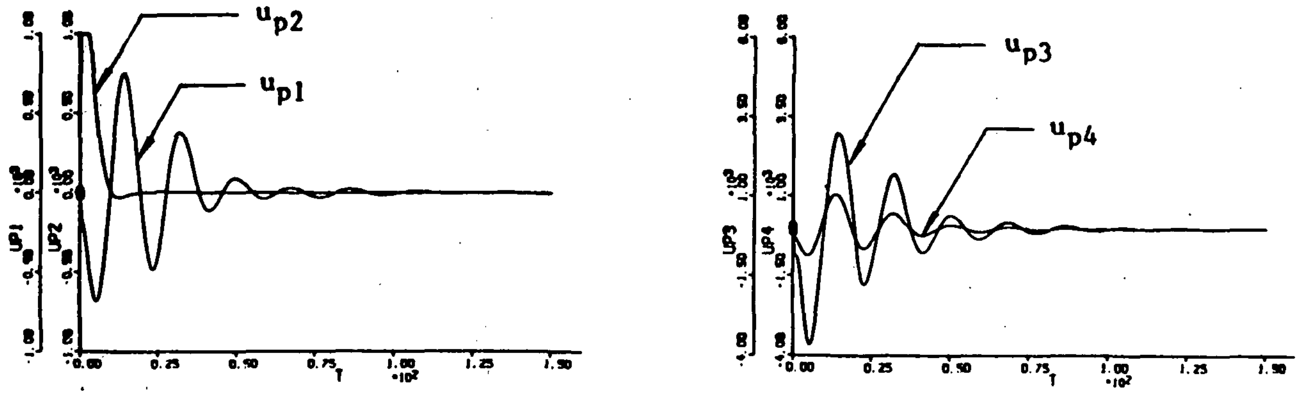

(a) u_{p1}: Left Panel Tip Control Torque (ft-lb)

u_{p2}: Bus Control Force (lb)

(b) u_{p3}: Bus Control Torque (ft-lb)

u_{p4}: Right Panel Tip Control Torque (ft-lb)

Figure 29 Adaptive Regulator Control for Two-Panel Configuration -- Adaptive Control Inputs

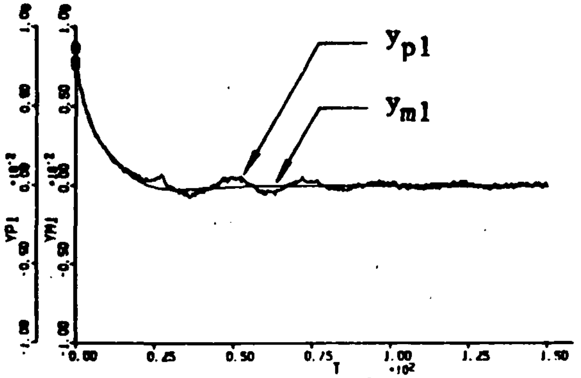

(a) $y_{p1} = \alpha\ \theta_{p1} + \dot{\theta}_{p1} + \nu_1$ (rad)

$y_{m1} = \alpha\ \theta_{m1} + \dot{\theta}_{m1}$ (rad)

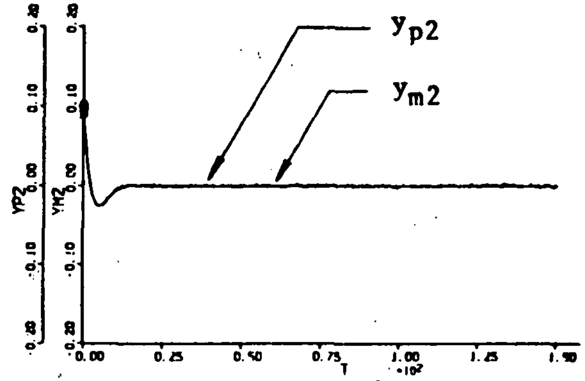

(b) $y_{p2} = \alpha\ Z_{p2} + \dot{Z}_{p2} + \nu_2$ (ft)

$y_{m2} = \alpha\ Z_{m2} + \dot{Z}_{m2}$ (ft)

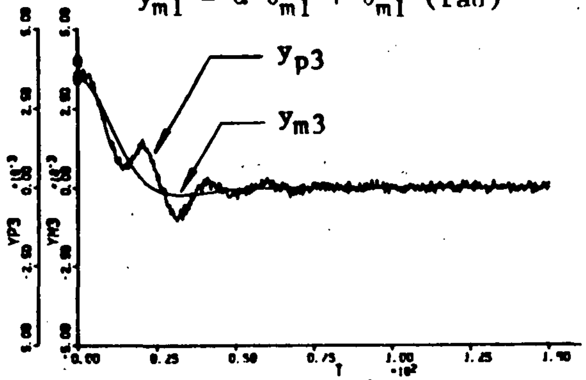

(c) $y_{p3} = \alpha\ \theta_{p2} + \dot{\theta}_{p2} + \nu_3$ (rad)

$y_{m3} = \alpha\ \theta_{m2} + \dot{\theta}_{m2}$ (rad)

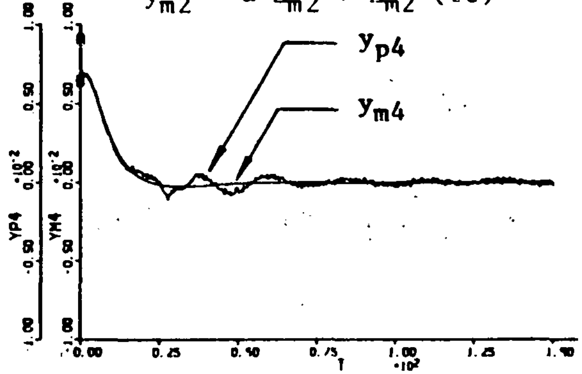

(d) $y_{p4} = \alpha\ \theta_{p3} + \dot{\theta}_{p3} + \nu_4$ (rad)

$y_{m4} = \alpha\ \theta_{m3} + \dot{\theta}_{m3}$ (rad)

Figure 30 Adaptive Regulator Control with Measurement Noise for Two-Panel Configuration -- Plant and Model Outputs

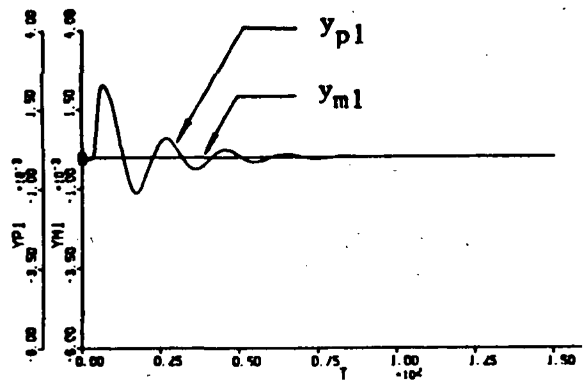

(a) $y_{p1} = \alpha\,\theta_{p1} + \dot{\theta}_{p1}$ (rad)

$y_{m1} = \alpha\,\theta_{m1} + \dot{\theta}_{m1}$ (rad)

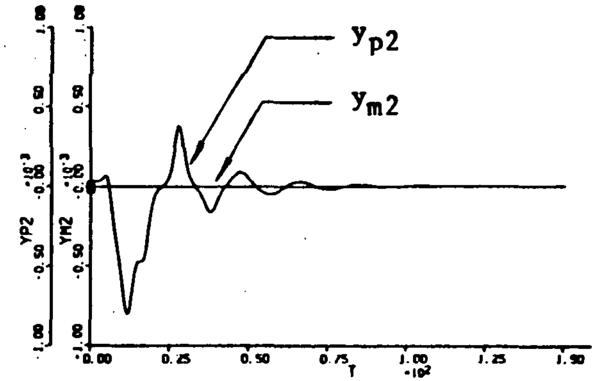

(b) $y_{p2} = \alpha\,Z_{p2} + \dot{Z}_{p2}$ (ft)

$y_{m2} = \alpha\,Z_{m2} + \dot{Z}_{m2}$ (ft)

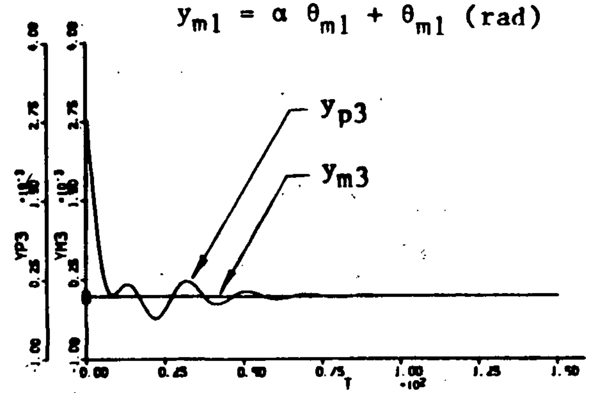

(c) $y_{p3} = \alpha\,\theta_{p2} + \dot{\theta}_{p2}$ (rad)

$y_{m3} = \alpha\,\theta_{m2} + \dot{\theta}_{m2}$ (rad)

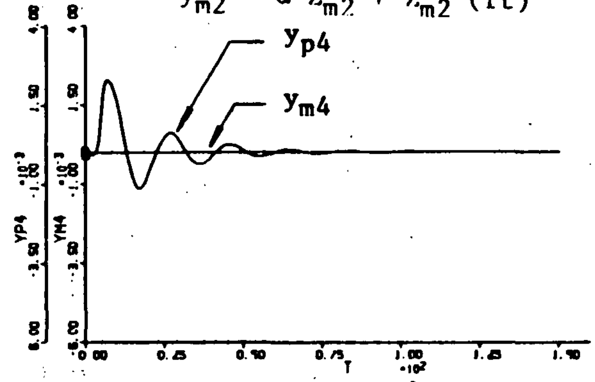

(d) $y_{p4} = \alpha\,\theta_{p3} + \dot{\theta}_{p3}$ (rad)

$y_{m4} = \alpha\,\theta_{m3} + \dot{\theta}_{m3}$ (rad)

Figure 32 Adaptive Control During Shuttle Hard Docking for Two-Panel Configuration -- Plant and Model Outputs

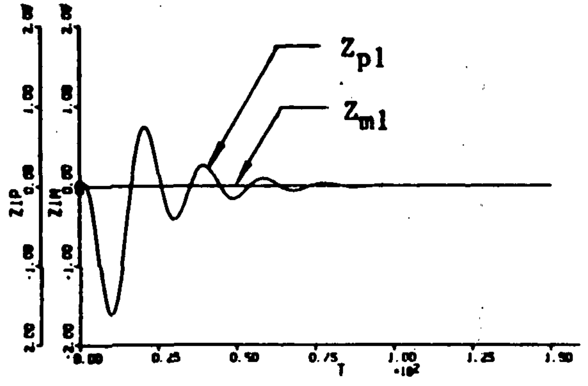

(a) Z_{p1}, Z_{m1} (ft)

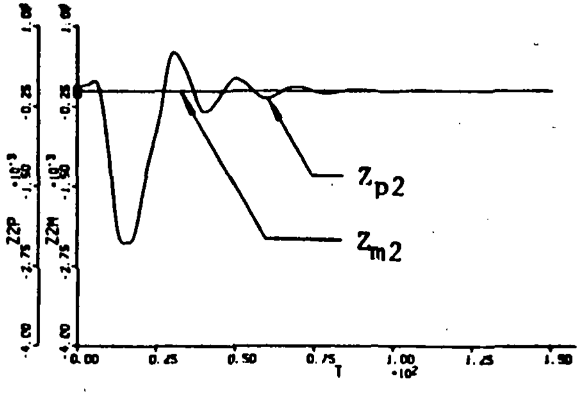

(b) Z_{p2}, Z_{m2} (ft)

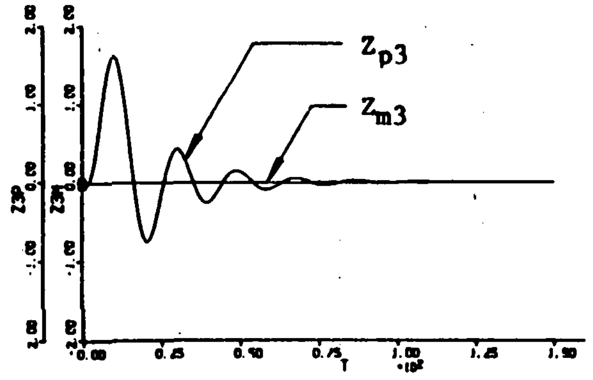

(c) Z_{p3}, Z_{m3} (ft)

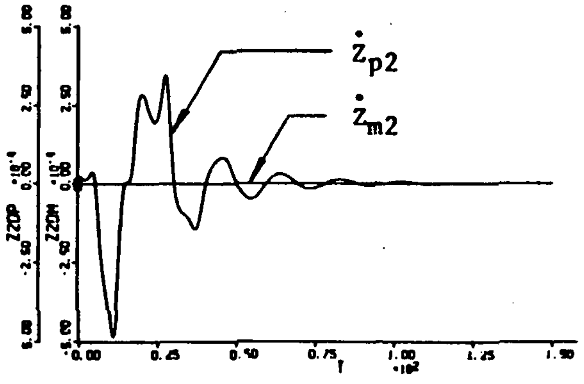

(d) $\dot{Z}_{p2}$, $\dot{Z}_{m2}$ (ft/sec)

Figure 33 Adaptive Control During Shuttle Hard Docking for Two-Panel Configuration

-- Plant and Model Translational State Responses

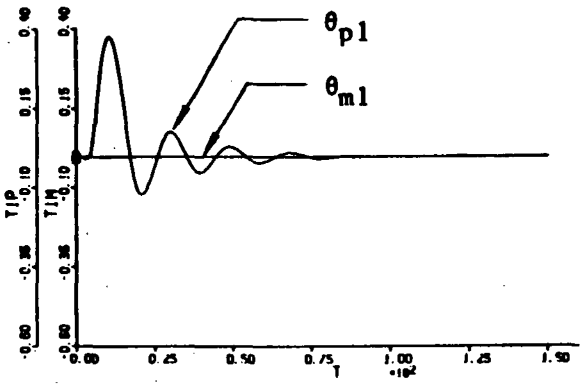

(a) θ_{p1}, θ_{m1} (deg)

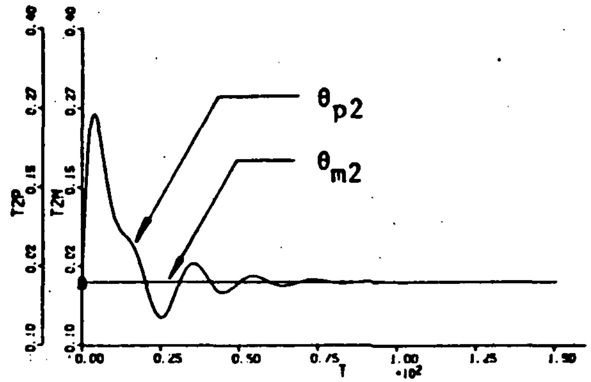

(b) θ_{p2}, θ_{m2} (deg)

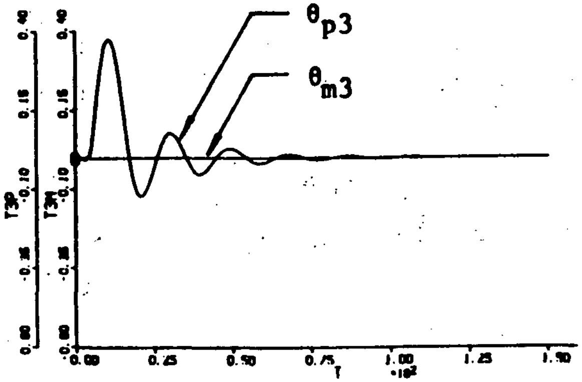

(c) θ_{p3}, θ_{m3} (deg)

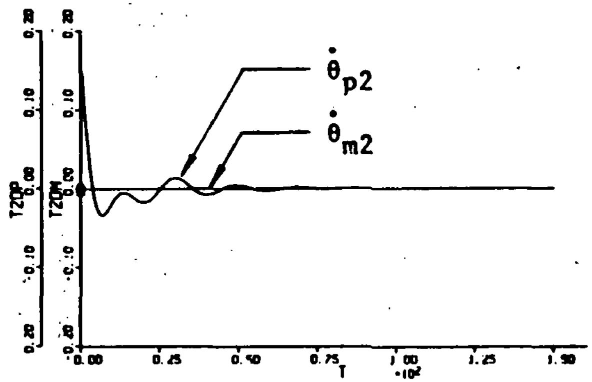

(d) $\dot{\theta}_{p2}$, $\dot{\theta}_{m2}$ (deg/sec)

Figure 34 Adaptive Control During Shuttle Hard Docking for Two-Panel Configuration -- Plant and Model Rotational State Responses

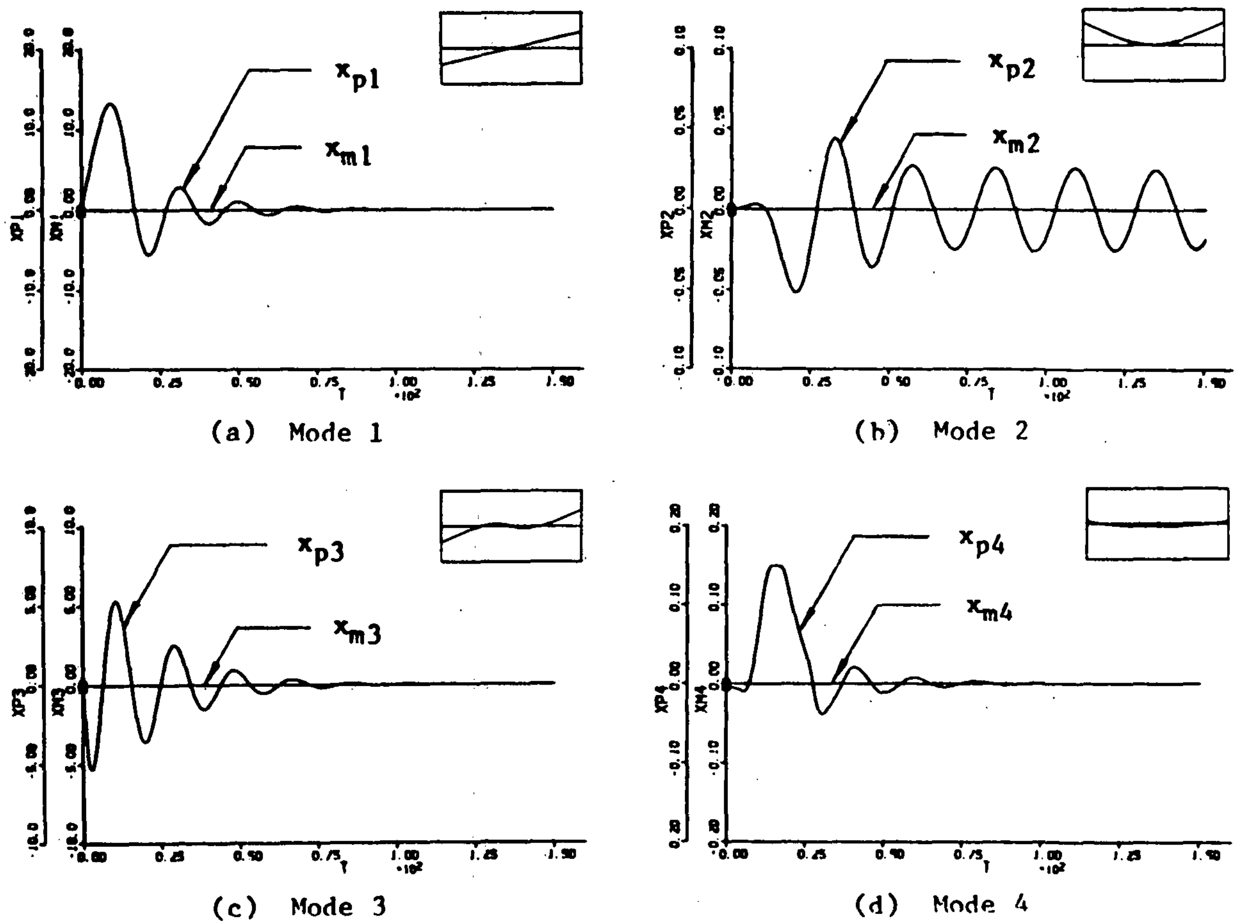

Figure 35 Adaptive Control During Shuttle Hard Docking for Two-Panel Configuration -- Plant and Model Modal Responses

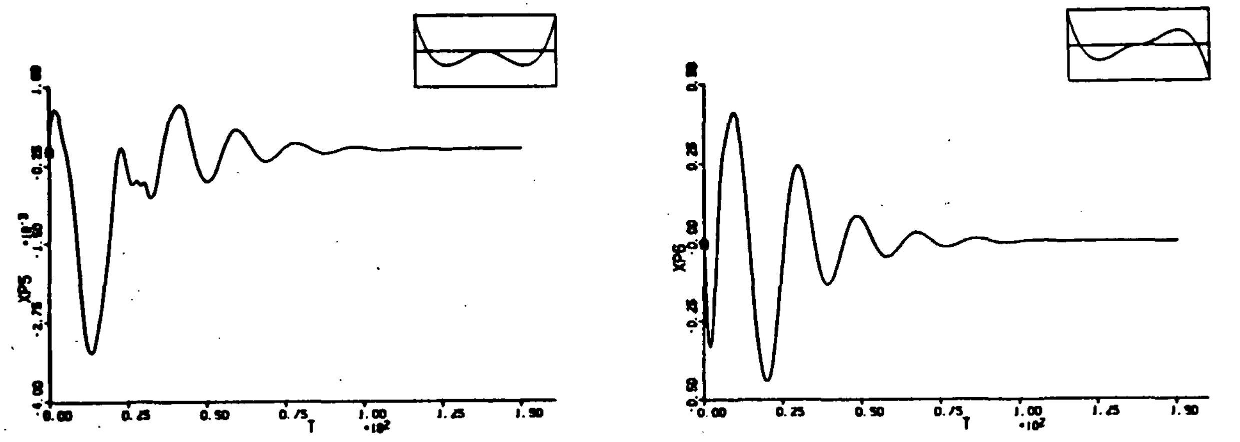

(a) Mode 5

(b) Mode 6

Figure 36 Adaptive Control During Shuttle Hard Docking for Two-Panel Configuration

— High Frequency Plant Modal Responses

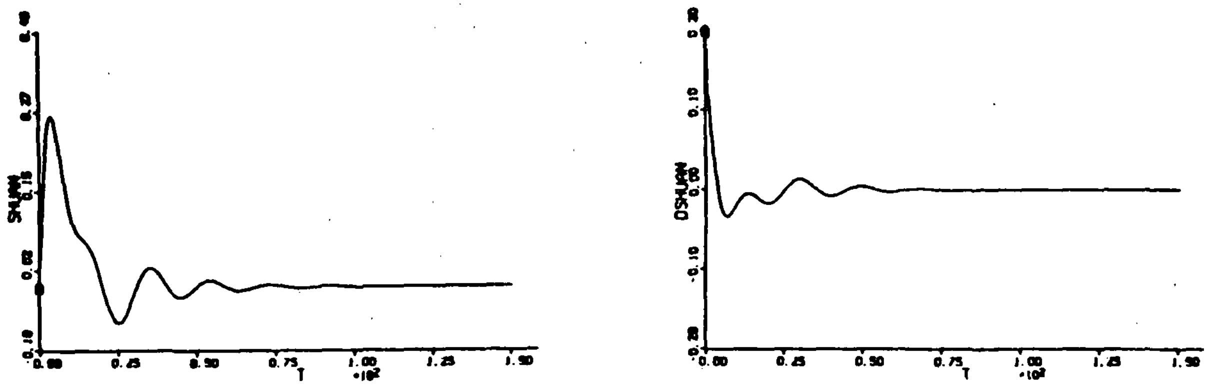

(a) $\theta_{shuttle}$ (deg)

(b) $\dot{\theta}_{shuttle}$ (deg/sec)

Figure 37 Adaptive Control During Shuttle Hard Docking for Two-Panel Configuration

— Shuttle Angular Position and Rate

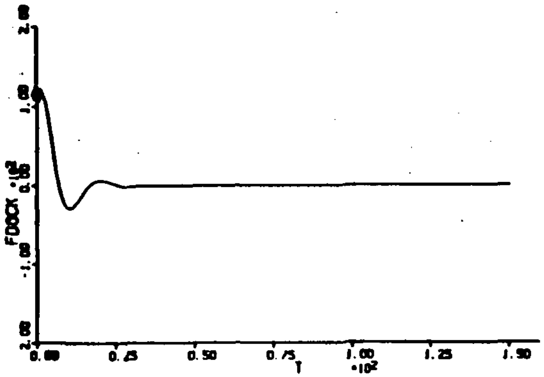

(a) Docking Force F_d (lb)

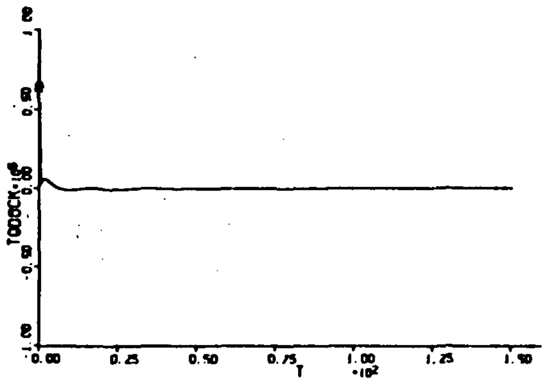

(b) Docking Torque T_d (ft-lb)

Figure 38 Adaptive Control During Shuttle Hard Docking for Two-Panel Configuration

-- Docking Force and Torque

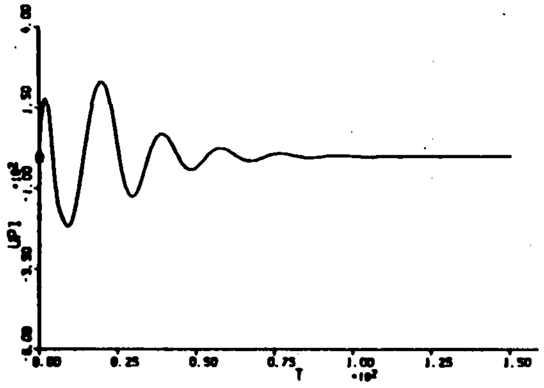

(a) u_{p1}: Left Panel Tip Control Torque (ft-lb)

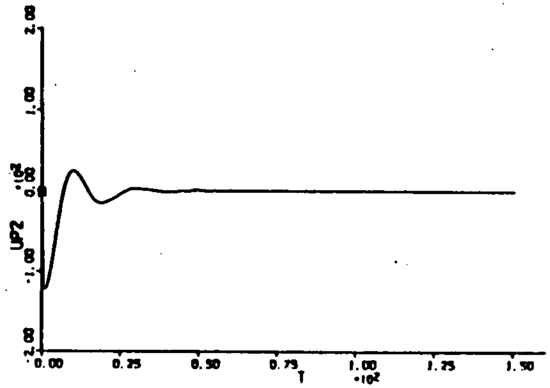

(b) u_{p2}: Bus Control Force (lb)

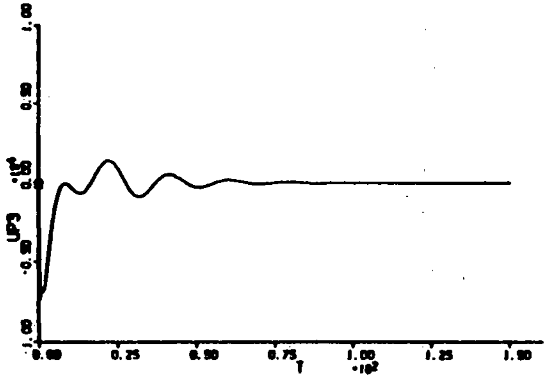

(c) u_{p3}: Bus Control Torque (ft-lb)

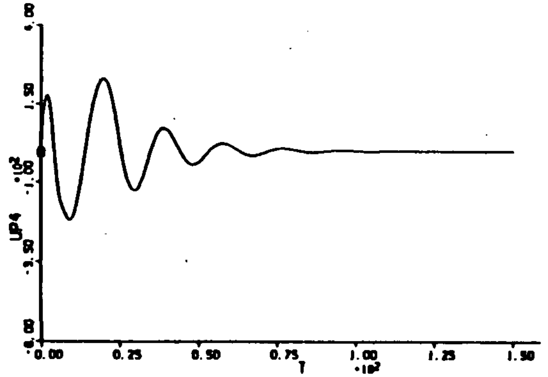

(d) u_{p4}: Right Panel Tip Control Torque (ft-lb)

Figure 39 Adaptive Control During Shuttle Hard Docking for Two-Panel Configuration -- Adaptive Control Inputs

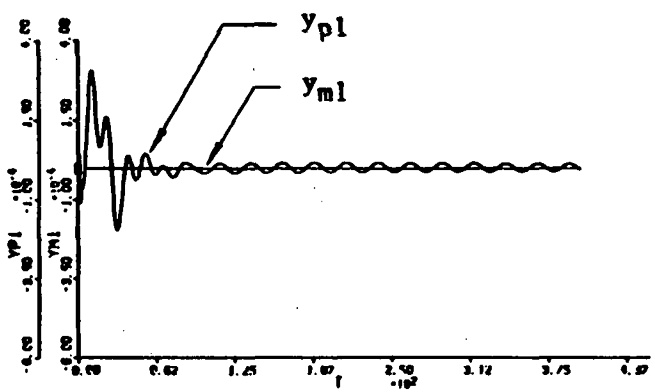

(a) $y_{p1} = \alpha\ \theta_{p1} + \dot{\theta}_{p1}$ (rad)

$y_{m1} = \alpha\ \theta_{m1} + \dot{\theta}_{m1}$ (rad)

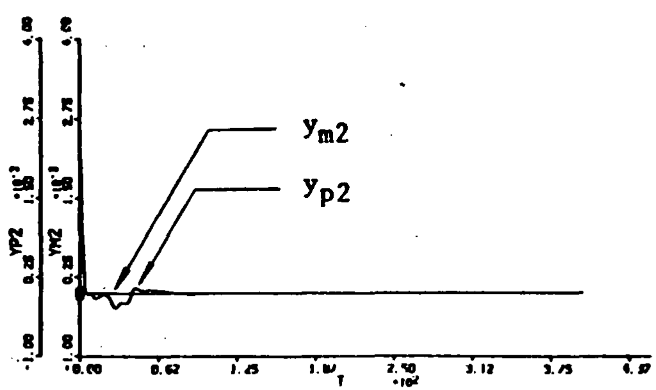

(b) $y_{p2} = \alpha\ Z_{p2} + \dot{Z}_{p2}$ (ft)

$y_{m2} = \alpha\ Z_{m2} + \dot{Z}_{m2}$ (ft)

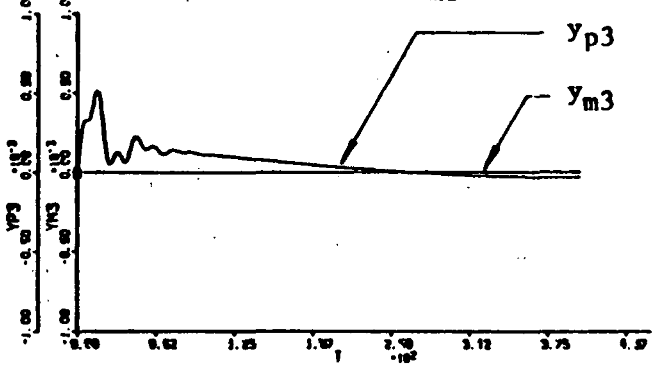

(c) $y_{p3} = \alpha\ \theta_{p2} + \dot{\theta}_{p2}$ (rad)

$y_{m3} = \alpha\ \theta_{m2} + \dot{\theta}_{m2}$ (rad)

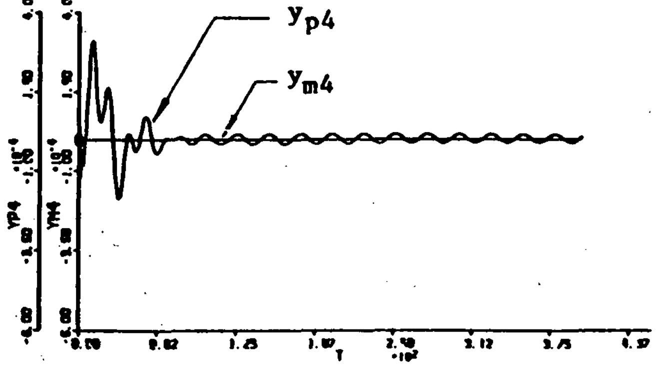

(d) $y_{p4} = \alpha\ \theta_{p3} + \dot{\theta}_{p3}$ (rad)

$y_{m4} = \alpha\ \theta_{m3} + \dot{\theta}_{m3}$ (rad)

Figure 40 Adaptive Control During Shuttle Soft Docking for Two-Panel Configuration -- Plant and Model Outputs

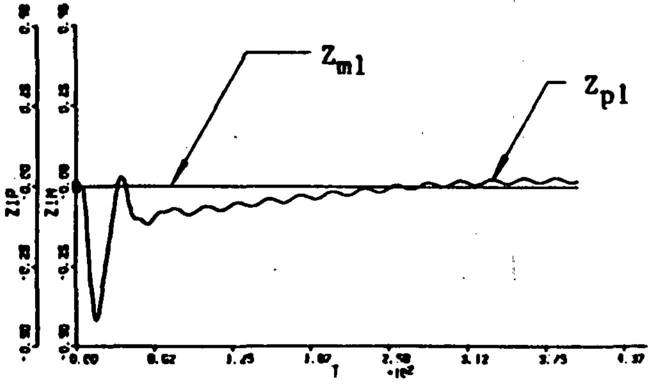

(a) Z_{p1}, Z_{m1} (ft)

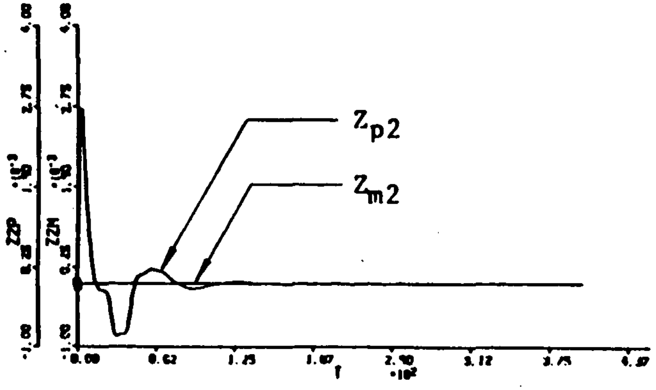

(b) Z_{p2}, Z_{m2} (ft)

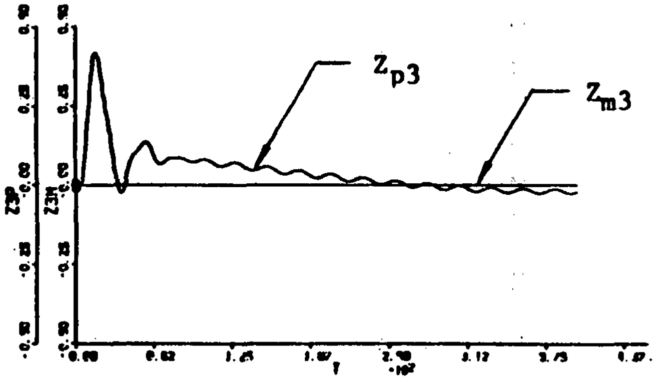

(c) Z_{p3}, Z_{m3} (ft)

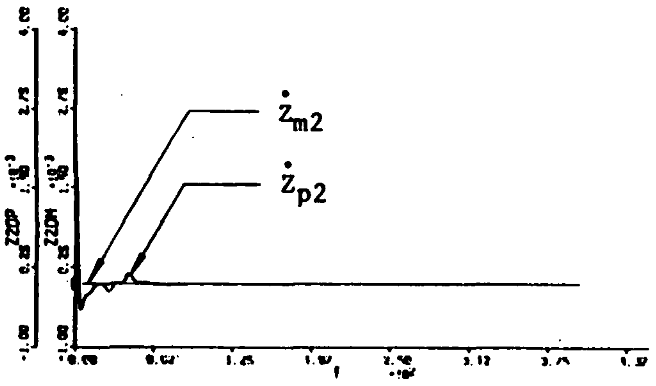

(d) $\dot{Z}_{p2}$, $\dot{Z}_{m2}$ (ft/sec)

Figure 41 Adaptive Control During Shuttle Soft Docking for Two-Panel Configuration -- Plant and Model Translational State Responses

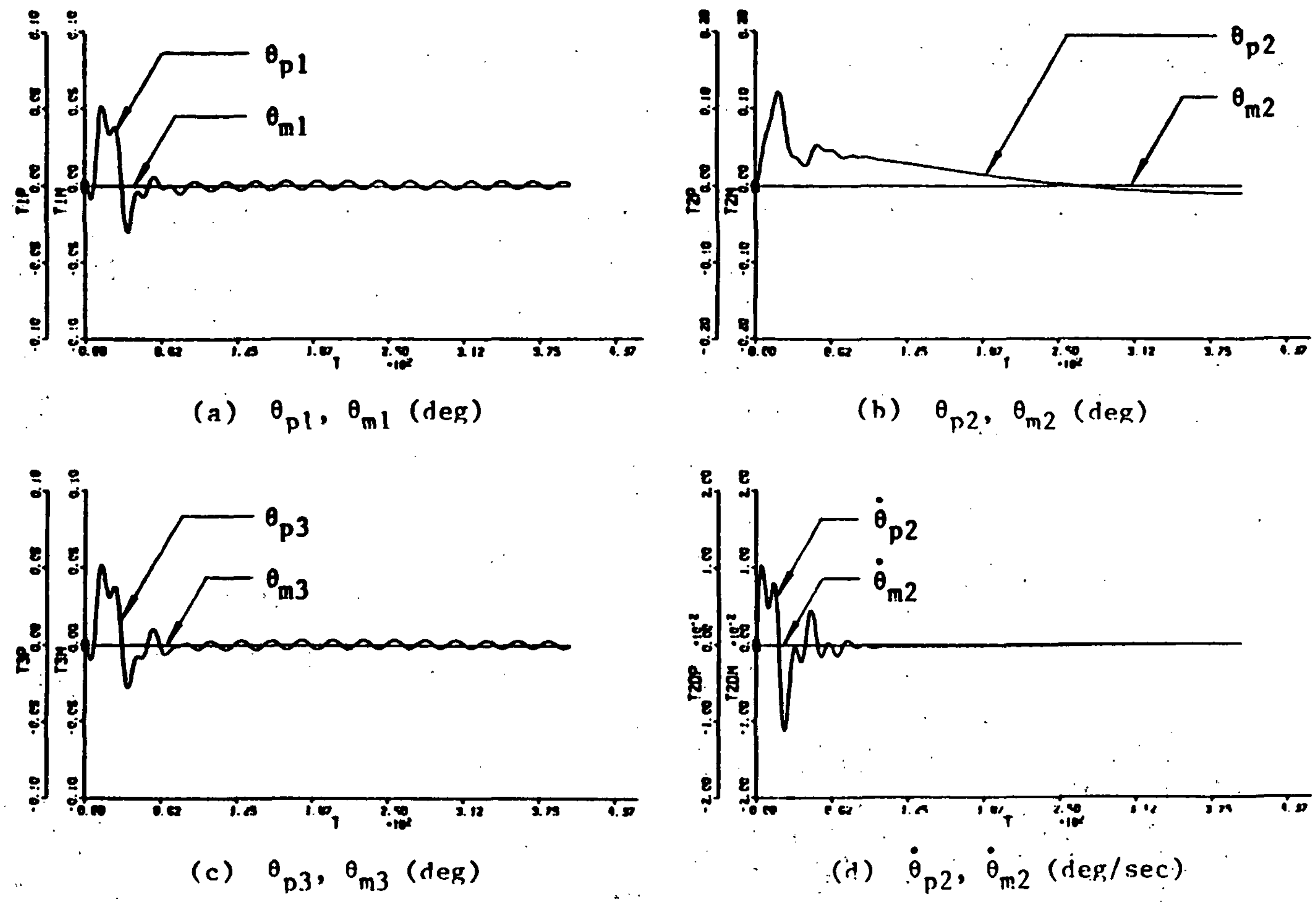

Figure 42 Adaptive Control During Shuttle Soft Docking for Two-Panel Configuration -- Plant and Model Rotational State Responses

ORIGINAL PAGE IS
OF POOR QUALITY

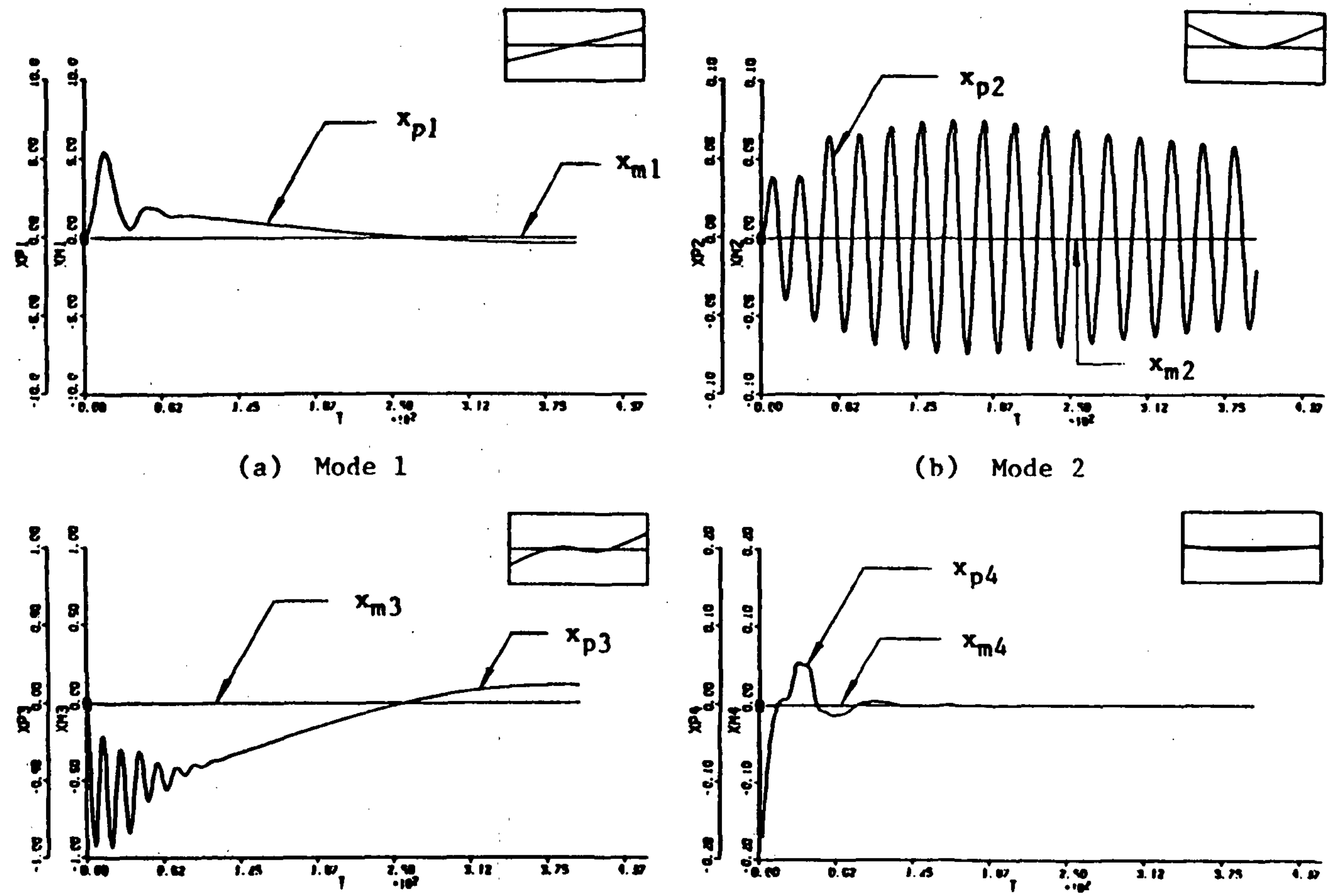

(a) Mode 1 (b) Mode 2 (c) Mode 3 (d) Mode 4

Figure 43 Adaptive Control During Shuttle Soft Docking for Two-Panel Configuration -- Plant and Model Modal Responses

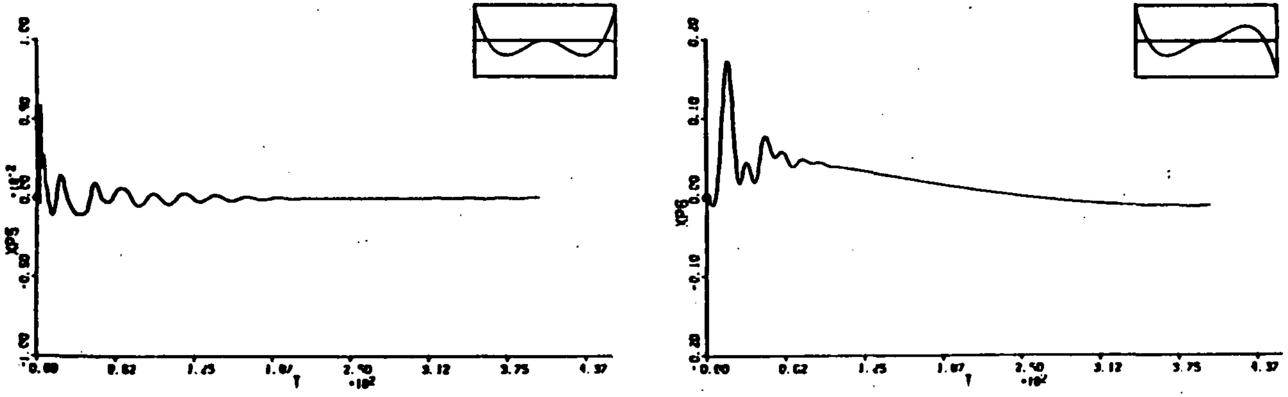

(a) Mode 5 (b) Mode 6

Figure 44 Adaptive Control During Shuttle Soft Docking for Two-Panel Configuration

— High Frequency Plant Modal Responses

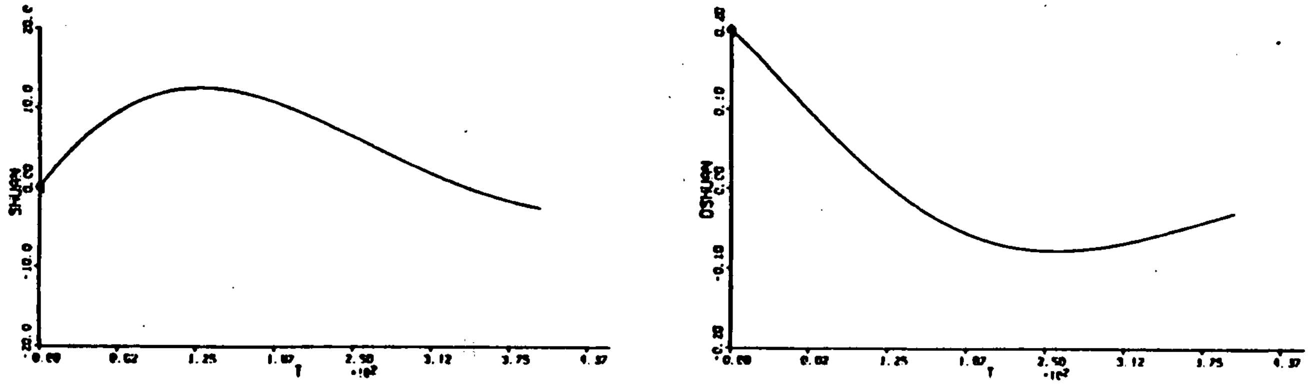

(a) $\theta_{shuttle}$ (deg)

(b) $\dot{\theta}_{shuttle}$ (deg/sec)

Figure 45 Adaptive Control During Shuttle Soft Docking for Two-Panel Configuration

— Shuttle Angular Position and Rate

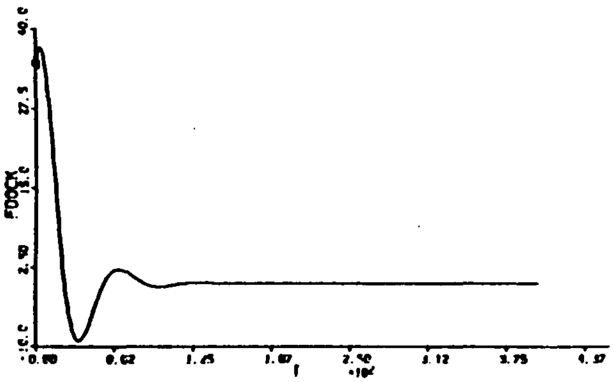

(a) Docking Force F_d (lb)

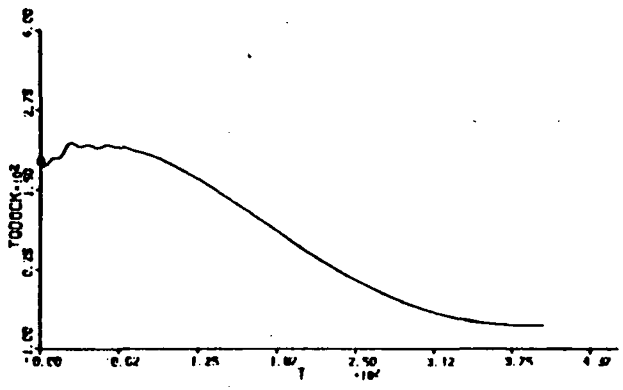

(b) Docking Torque T_d (ft-lb)

Figure 46 Adaptive Control During Shuttle Soft Docking for Two-Panel Configuration

-- Docking Force and Torque

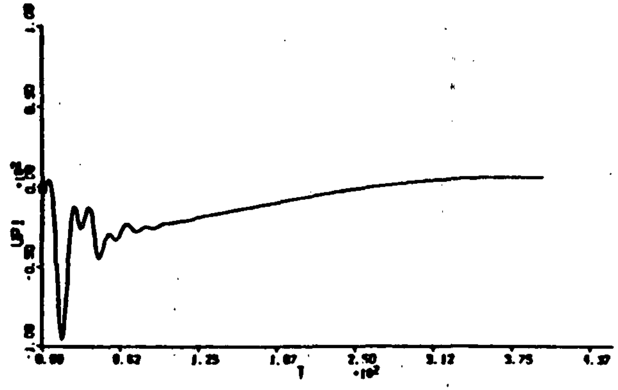

(a) u_{p1}: Left Panel Tip Control Torque (ft-lb)

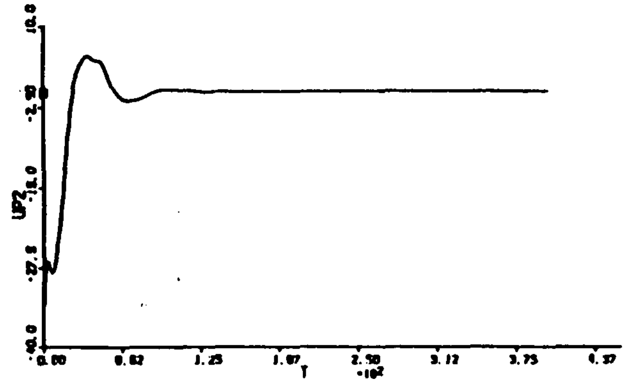

(b) u_{p2}: Bus Control Force (lb)

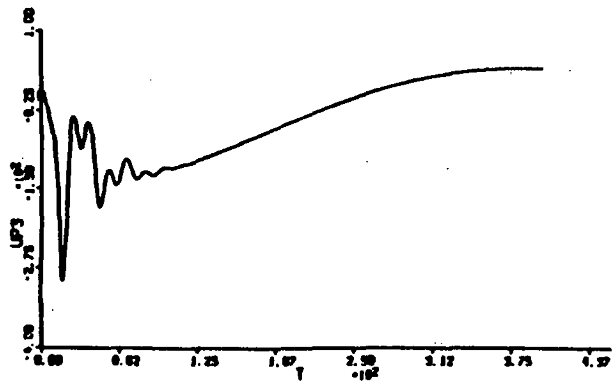

(c) u_{p3}: Bus Control Torque (ft-lb)

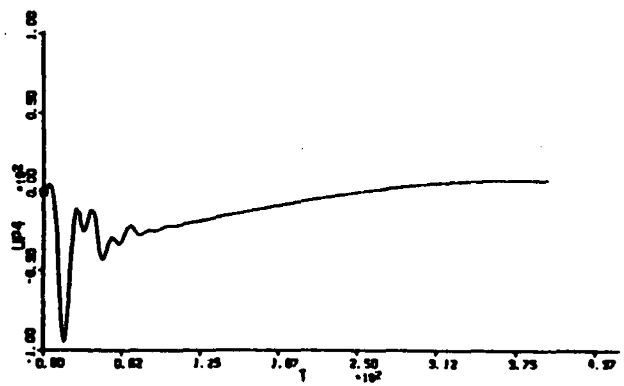

(d) u_{p4}: Right Panel Tip Control Torque (ft-lb)

Figure 47 Adaptive Control During Shuttle Soft Docking for Two-Panel Configuration -- Adaptive Control Inputs

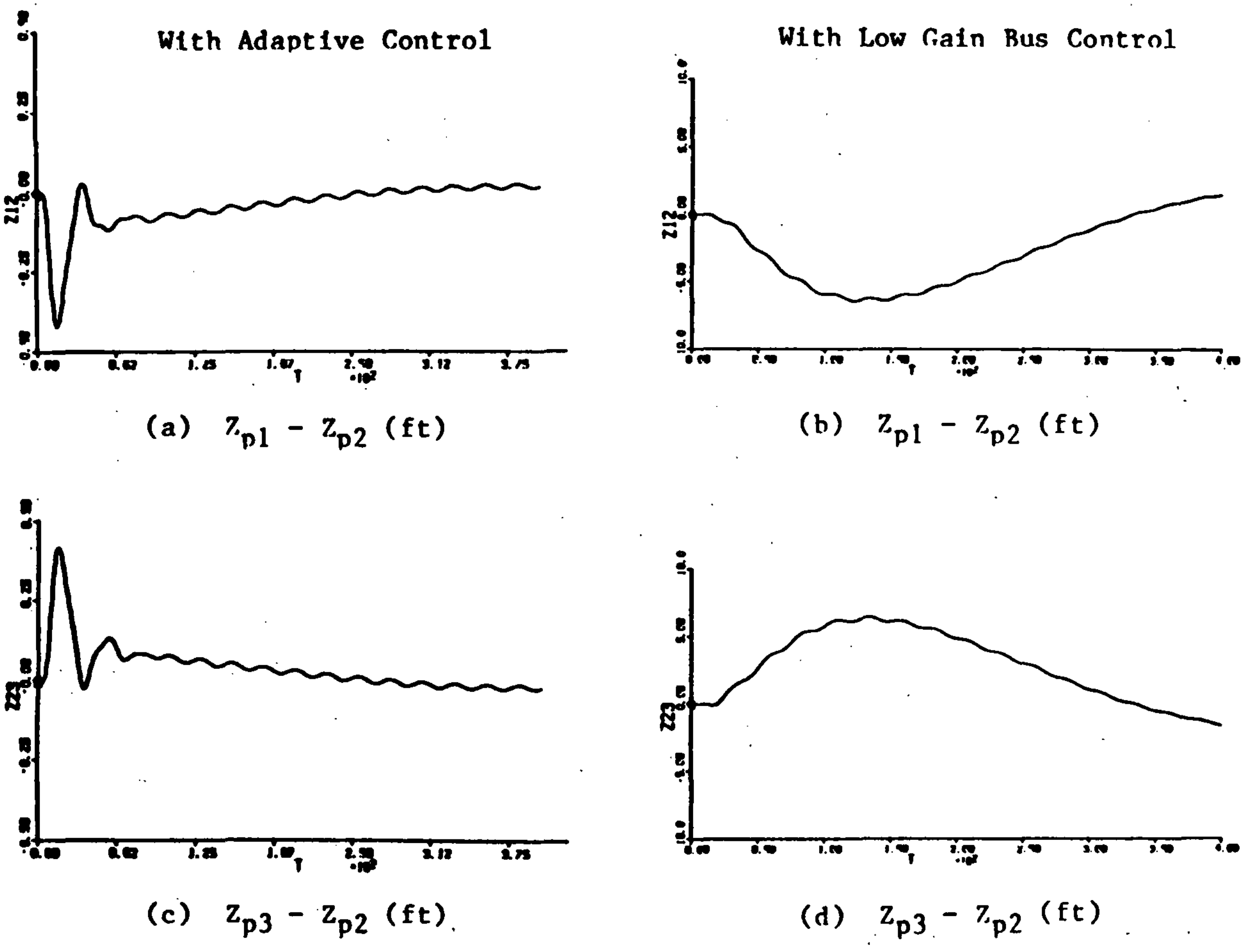

Figure 48 Comparative Shuttle Soft Docking Responses

— Relative Panel Tip Displacements

With Adaptive Control

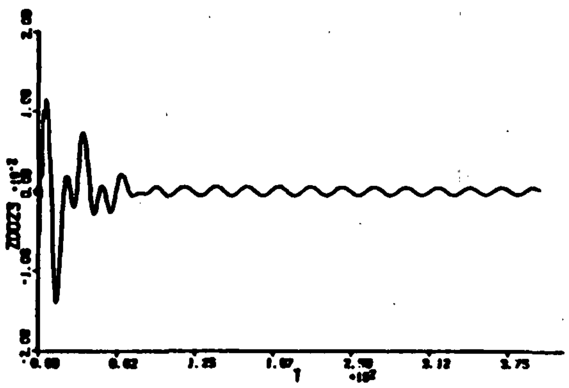

(a) $\ddot{Z}_{p3} - \ddot{Z}_{p2}$ (ft/sec/sec)

With Low Gain Bus Control

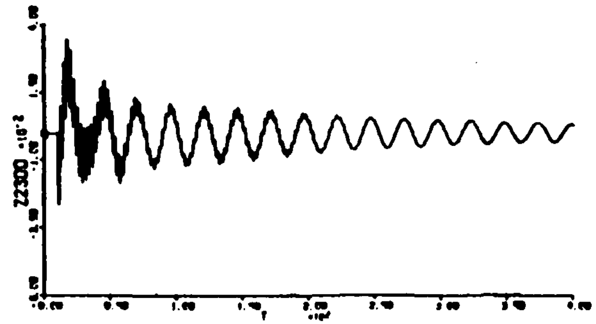

(b) $\ddot{Z}_{p3} - \ddot{Z}_{p2}$ (ft/sec/sec)

Figure 49 Comparative Shuttle Soft Docking Responses

— Relative Panel Tip Acceleration

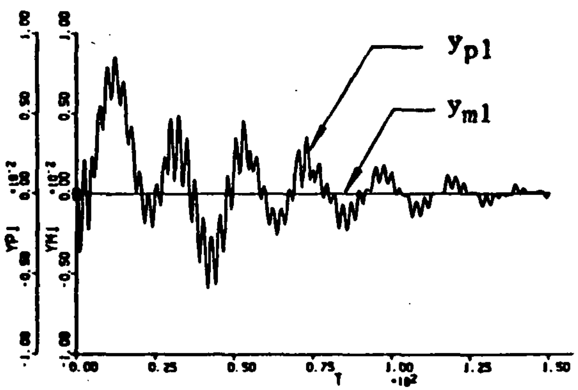

(a) $y_{p1} = \alpha\ \theta_{p1} + \dot{\theta}_{p1}$ (rad)

$y_{m1} = \alpha\ \theta_{m1} + \dot{\theta}_{m1}$ (rad)

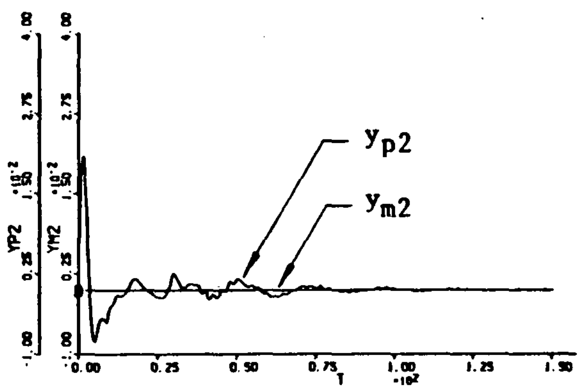

(b) $y_{p2} = \alpha\ Z_{p2} + \dot{Z}_{p2}$ (ft)

$y_{m2} = \alpha\ Z_{m2} + \dot{Z}_{m2}$ (ft)

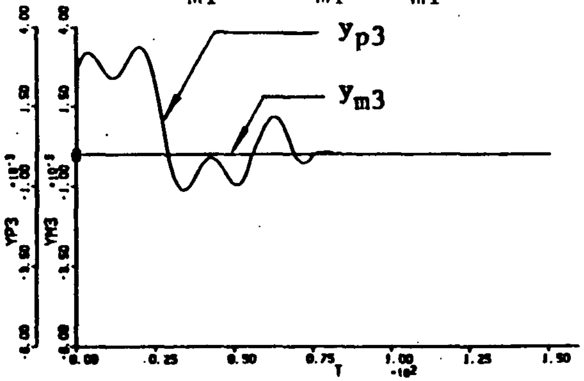

(c) $y_{p3} = \alpha\ \theta_{p2} + \dot{\theta}_{p2}$ (rad)

$y_{m3} = \alpha\ \theta_{m2} + \dot{\theta}_{m2}$ (rad)

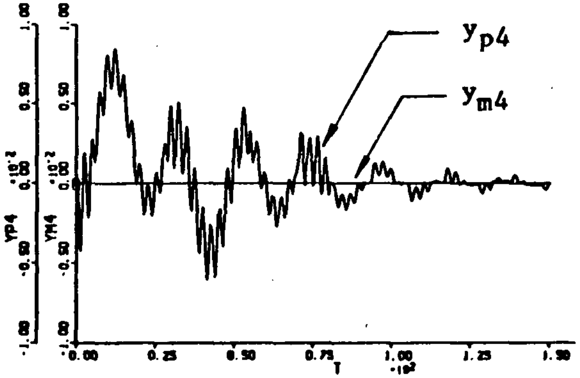

(d) $y_{p4} = \alpha\ \theta_{p3} + \dot{\theta}_{p3}$ (rad)

$y_{m4} = \alpha\ \theta_{m3} + \dot{\theta}_{m3}$ (rad)

Figure 50 Adaptive Control During Shuttle Hard Docking with Actuator Saturation for Two-Panel Configuration — Plant and Model Outputs

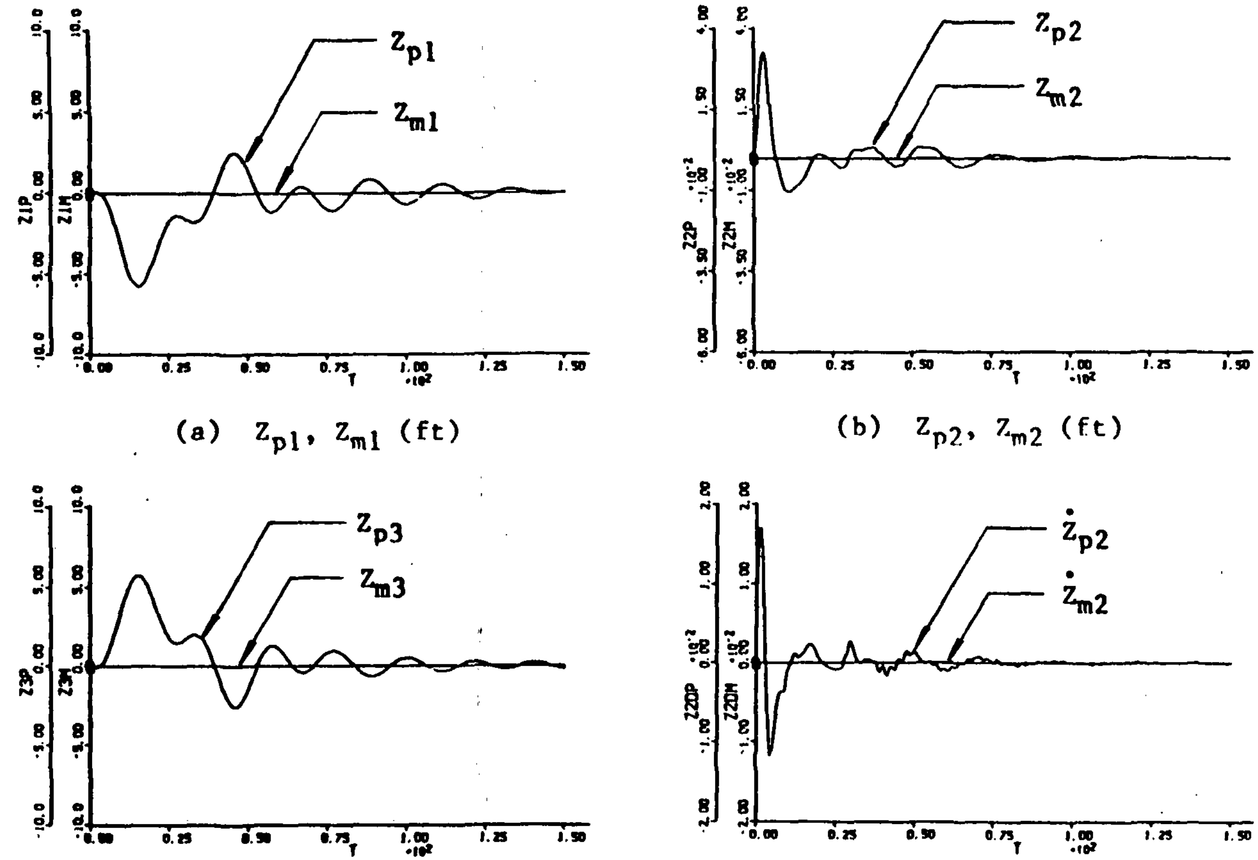

(a) Z_{p1}, Z_{m1} (ft)

(b) Z_{p2}, Z_{m2} (ft)

(c) Z_{p3}, Z_{m3} (ft)

(d) $\dot{Z}_{p2}$, $\dot{Z}_{m2}$ (ft/sec)

Figure 51 Adaptive Control During Shuttle Hard Docking with Actuator Saturation for Two-Panel Configuration — Plant and Model Translational State Responses

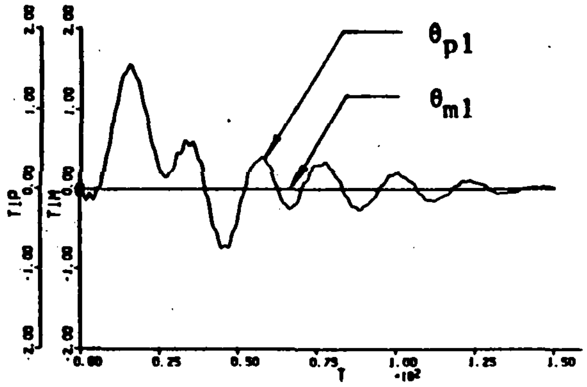

(a) θ_{p1}, θ_{m1} (deg)

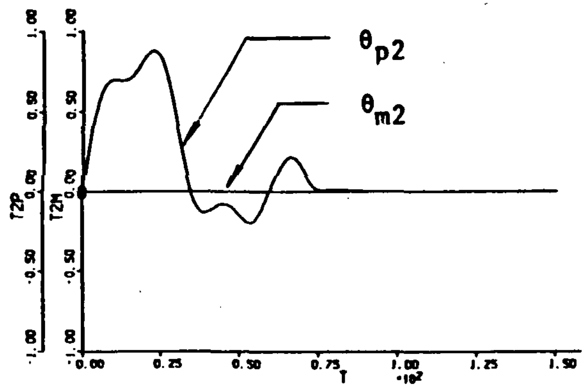

(b) θ_{p2}, θ_{m2} (deg)

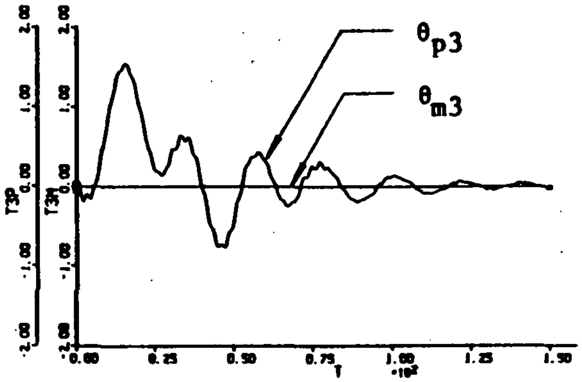

(c) θ_{p3}, θ_{m3} (deg)

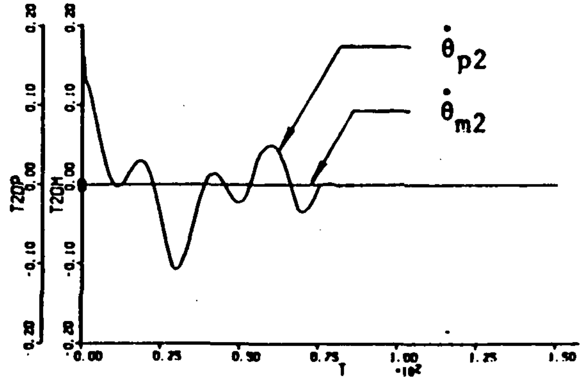

(d) $\dot{\theta}_{p2}$, $\dot{\theta}_{m2}$ (deg/sec)

Figure 52 Adaptive Control During Shuttle Hard Docking with Actuator Saturation for Two-Panel Configuration -- Plant and Model Rotational State Responses

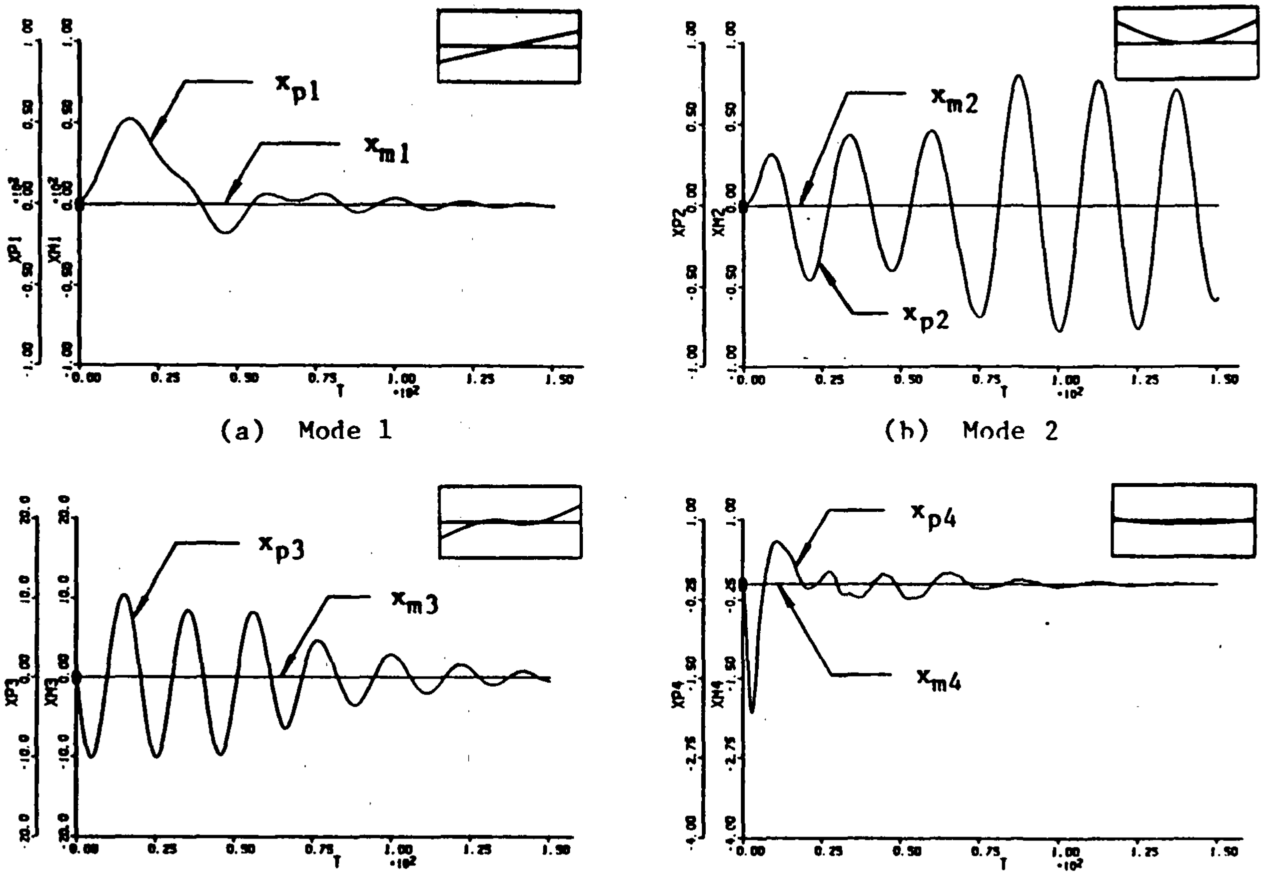

(a) Mode 1 (b) Mode 2

(c) Mode 3 (d) Mode 4

Figure 53 Adaptive Control During Shuttle Hard Docking with Actuator Saturation for Two-Panel Configuration — Plant and Model Modal Responses

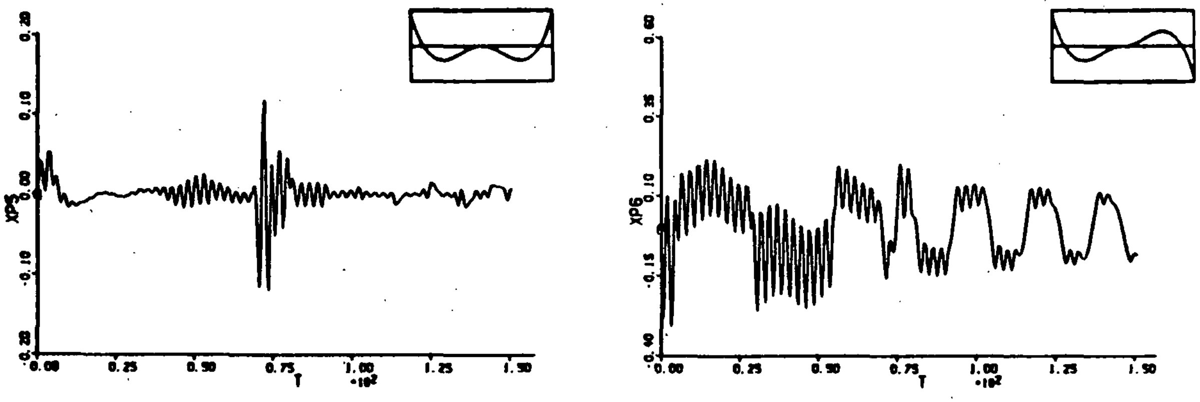

(a) Mode 5

(b) Mode 6

Figure 54 Adaptive Control During Shuttle Hard Docking with Actuator Saturation for Two-Panel Configuration -- High Frequency Plant Modal Responses

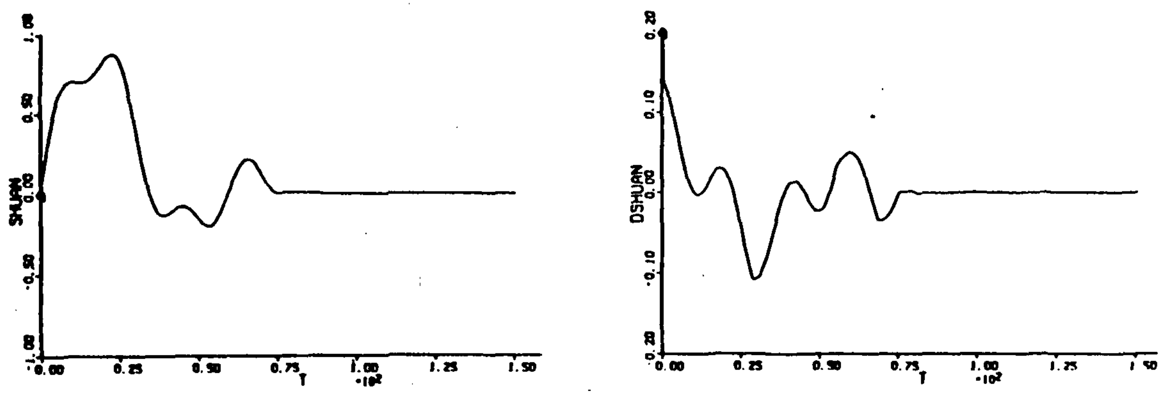

(a) $\theta_{shuttle}$ (deg)

(b) $\dot{\theta}_{shuttle}$ (deg/sec)

Figure 55 Adaptive Control During Shuttle Hard Docking with Actuator Saturation for Two-Panel Configuration — Shuttle Angular Position and Rate

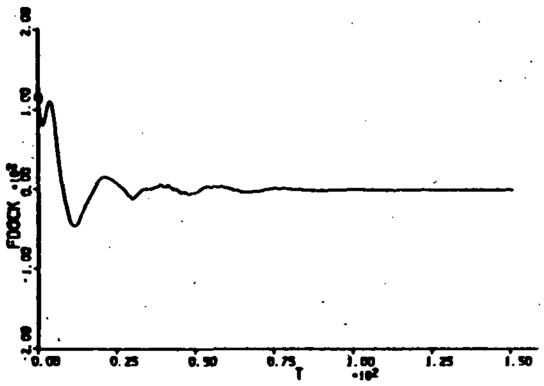

(a) Docking Force F_d (lb)

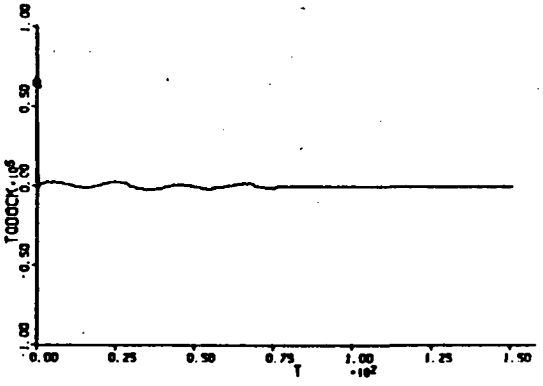

(b) Docking Torque T_d (ft-lb)

Figure 56 Adaptive Control During Shuttle Hard Docking with Actuator Saturation for Two-Panel Configuration — Docking Force and Torque

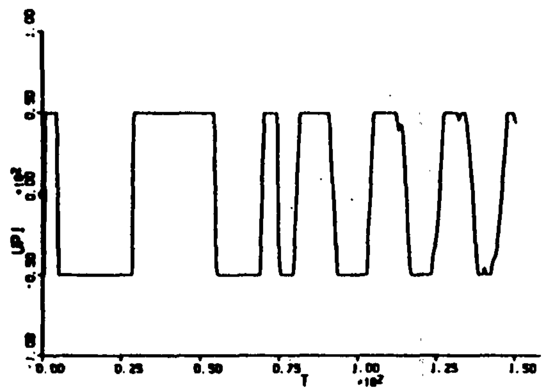

(a) u_{p1}: Left Panel Tip Control Torque (ft-lb)

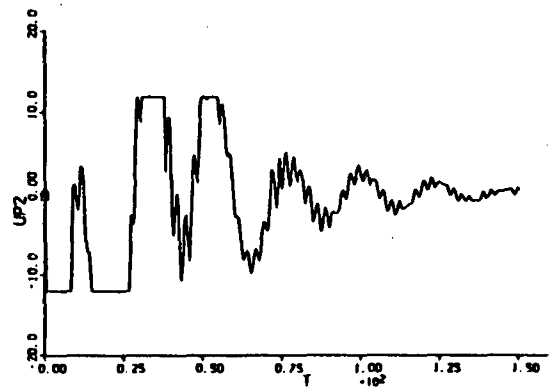

(b) u_{p2}: Bus Control Force (lb)

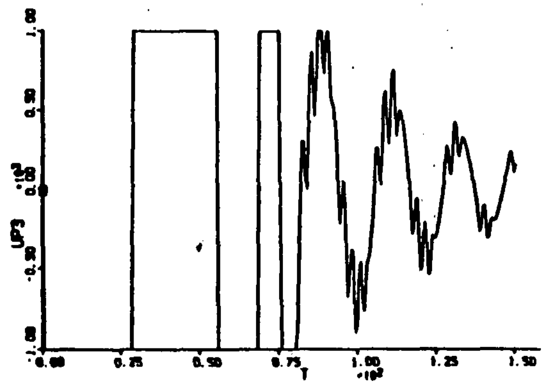

(c) u_{p3}: Bus Control Torque (ft-lb)

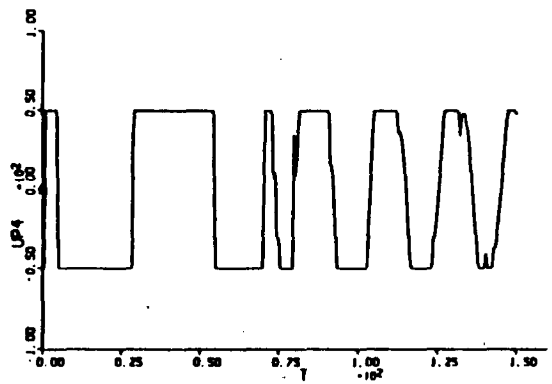

(d) u_{p4}: Right Panel Tip Control Torque (ft-lb)

Figure 57 Adaptive Control During Shuttle Hard Docking with Actuator Saturation for Two-Panel Configuration — Adaptive Control Inputs

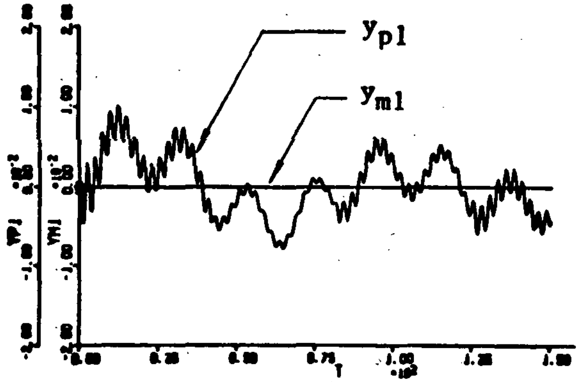

(a) $y_{p1} = \alpha\ \theta_{p1} + \dot{\theta}_{p1}$ (rad)

$y_{m1} = \alpha\ \theta_{m1} + \dot{\theta}_{m1}$ (rad)

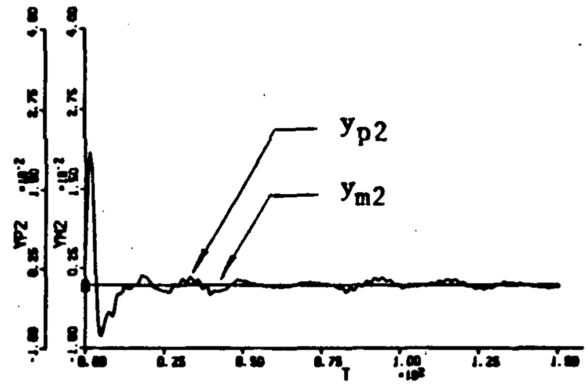

(b) $y_{p2} = \alpha\ Z_{p2} + \dot{Z}_{p2}$ (ft)

$y_{m2} = \alpha\ Z_{m2} + \dot{Z}_{m2}$ (ft)

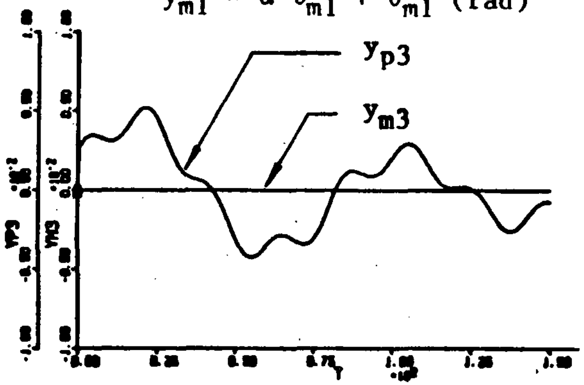

(c) $y_{p3} = \alpha\ \theta_{p2} + \dot{\theta}_{p2}$ (rad)

$y_{m3} = \alpha\ \theta_{m2} + \dot{\theta}_{m2}$ (rad)

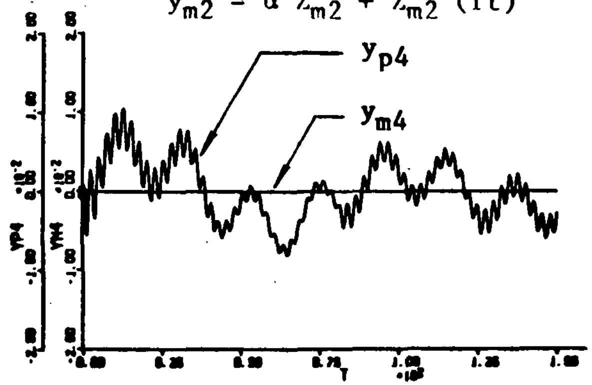

(d) $y_{p4} = \alpha\ \theta_{p3} + \dot{\theta}_{p3}$ (rad)

$y_{m4} = \alpha\ \theta_{m3} + \dot{\theta}_{m3}$ (rad)

Figure 58 Adaptive Control During Shuttle Hard Docking with More Severe Actuator Saturation for Two-Panel Configuration — Plant and Model Outputs

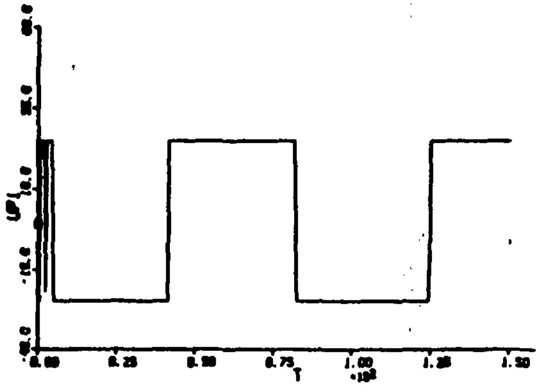

(a) u_{p1}: Left Panel Tip Control Torque (ft-lb)

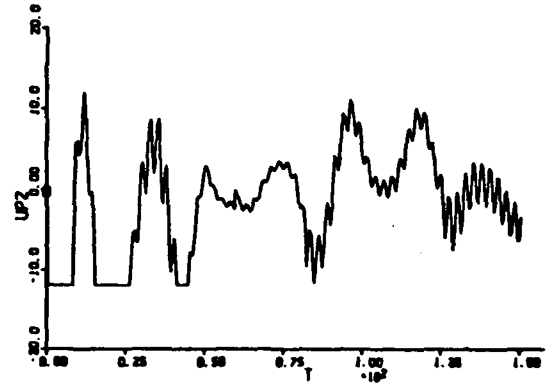

(b) u_{p2}: Bus Control Force (lb)

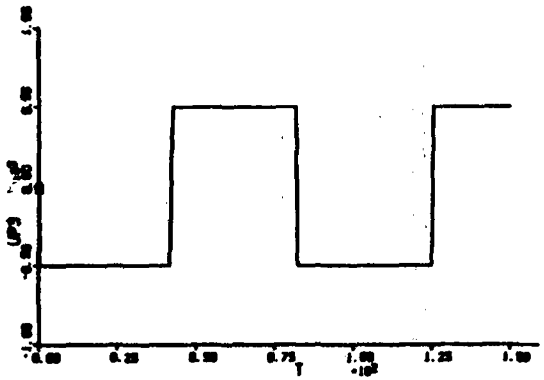

(c) u_{p3}: Bus Control Torque (ft-lb)

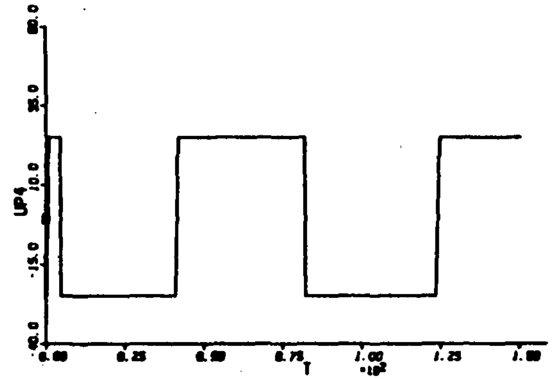

(d) u_{p4}: Right Panel Tip Control Torque (ft-lb)

Figure 59 Adaptive Control During Shuttle Hard Docking with More Severe Actuator Saturation for Two-Panel Configuration — Adaptive Control Inputs

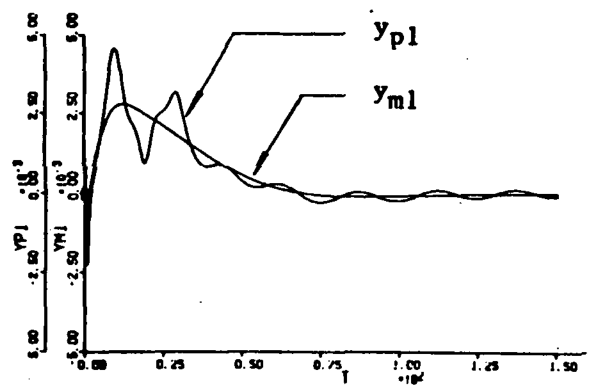

(a) $y_{p1} = \alpha\ \theta_{p1} + \dot{\theta}_{p1}$ (rad)

$y_{m1} = \alpha\ \theta_{m1} + \dot{\theta}_{m1}$ (rad)

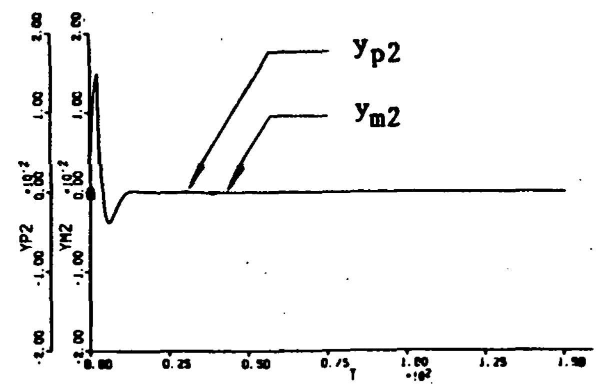

(b) $y_{p2} = \alpha\ Z_{p2} + \dot{Z}_{p2}$ (ft)

$y_{m2} = \alpha\ Z_{m2} + \dot{Z}_{m2}$ (ft)

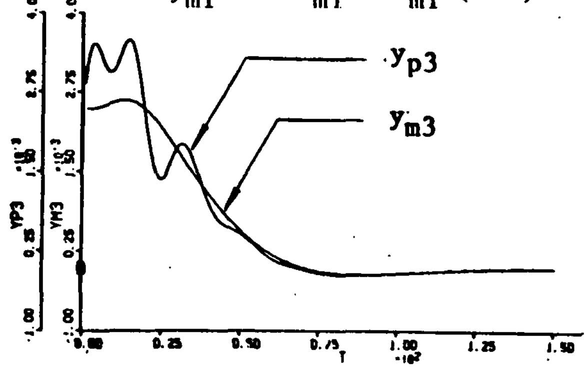

(c) $y_{p3} = \alpha\ \theta_{p2} + \dot{\theta}_{p2}$ (rad)

$y_{m3} = \alpha\ \theta_{m2} + \dot{\theta}_{m2}$ (rad)

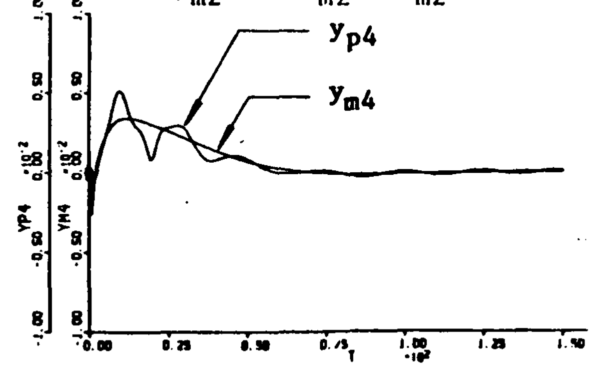

(d) $y_{p4} = \alpha\ \theta_{p3} + \dot{\theta}_{p3}$ (rad)

$y_{m4} = \alpha\ \theta_{m3} + \dot{\theta}_{m3}$ (rad)

Figure 60 Adaptive Control During Shuttle Hard docking with Model Switching and Disturbance Modeling for Two-Panel Configuration — Plant and Model Outputs

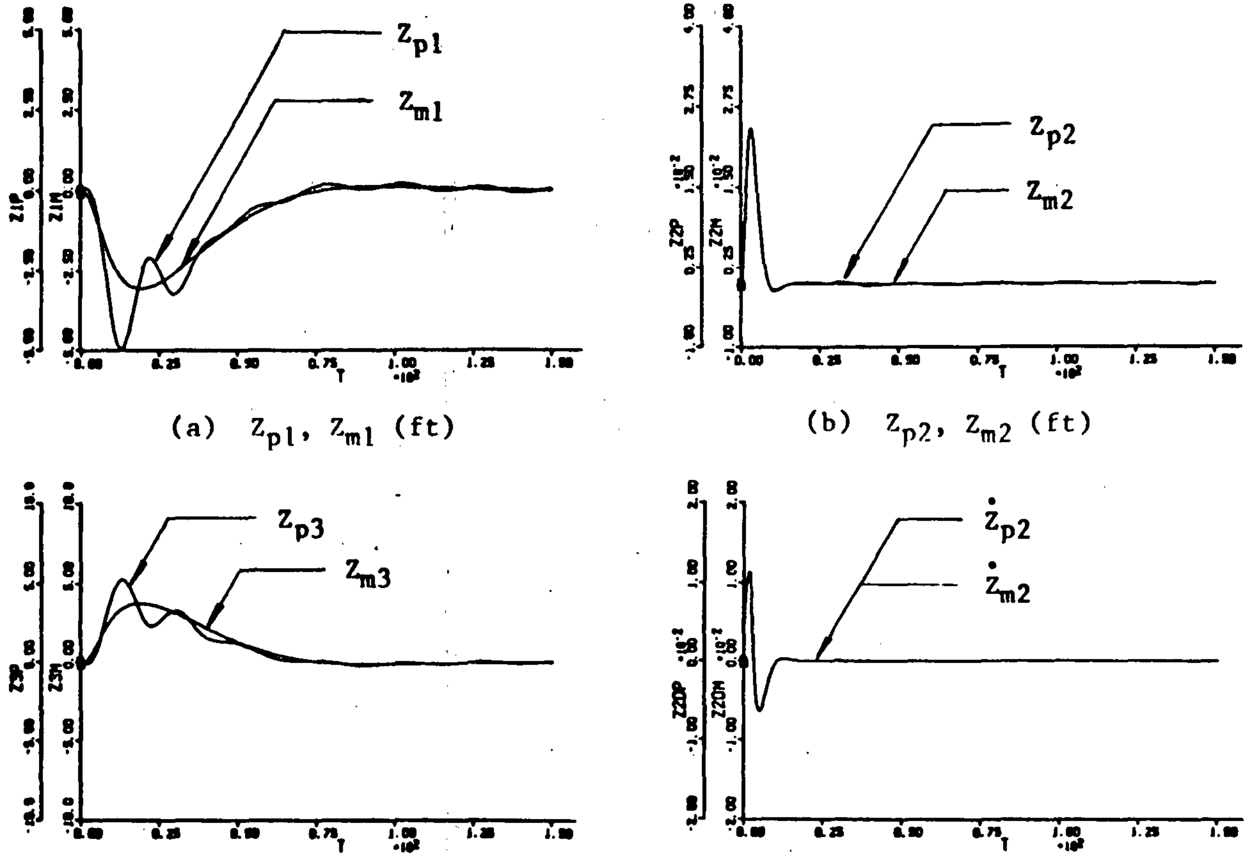

(a) Z_{p1}, Z_{m1} (ft)

(b) Z_{p2}, Z_{m2} (ft)

(c) Z_{p3}, Z_{m3} (ft)

(d) $\dot{Z}_{p2}$, $\dot{Z}_{m2}$ (ft/sec)

Figure 61 Adaptive Control During Shuttle Hard Docking with Model Switching and Disturbance Modeling for Two-Panel Configuration — Plant and Model Translational State Responses

ORIGINAL PAGE IS
OF POOR QUALITY

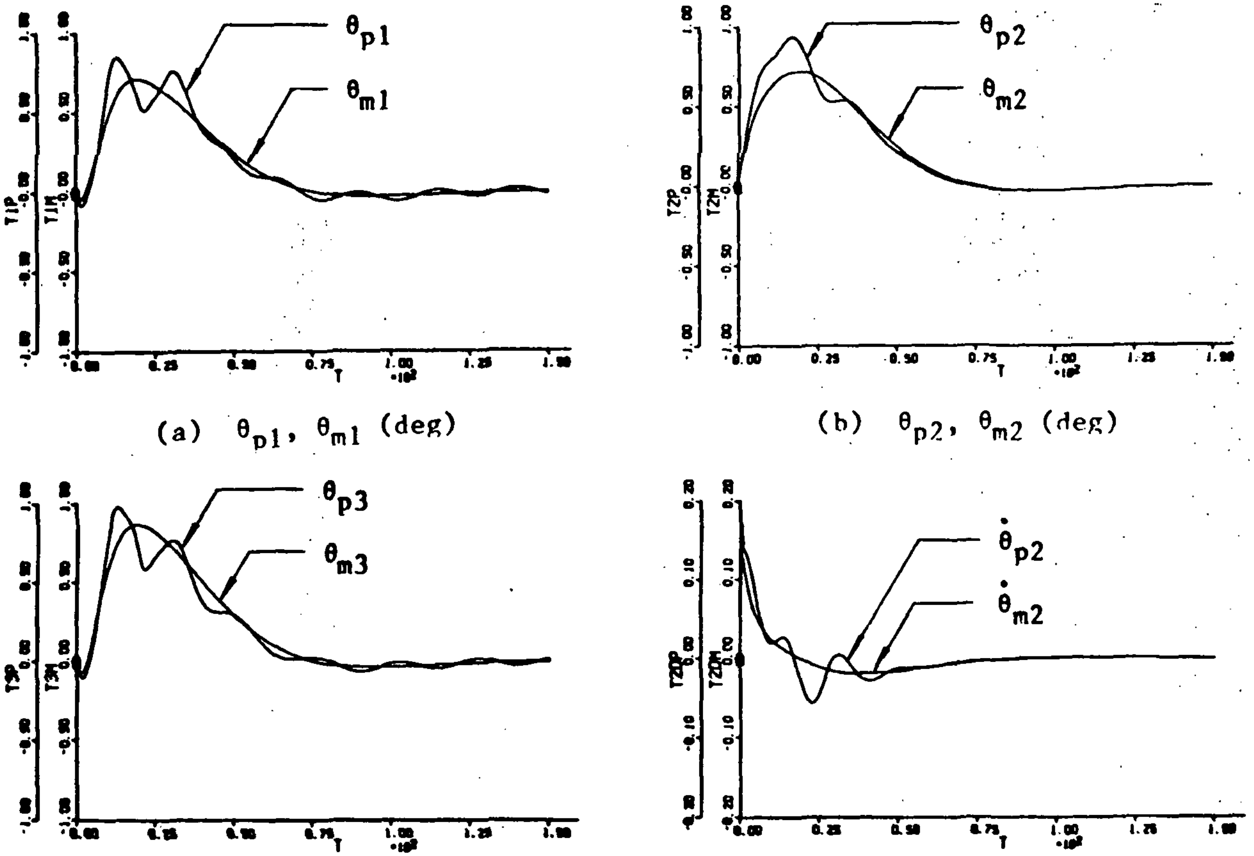

(a) θ_{p1}, θ_{m1} (deg)

(b) θ_{p2}, θ_{m2} (deg)

(c) θ_{p3}, θ_{m3} (deg)

(d) $\dot{\theta}_{p2}$, $\dot{\theta}_{m2}$ (deg/sec)

Figure 62 Adaptive Control During Shuttle Hard Docking with Model Switching and Disturbance Modeling for Two-Panel Configuration -- Plant and Model Rotational State Responses

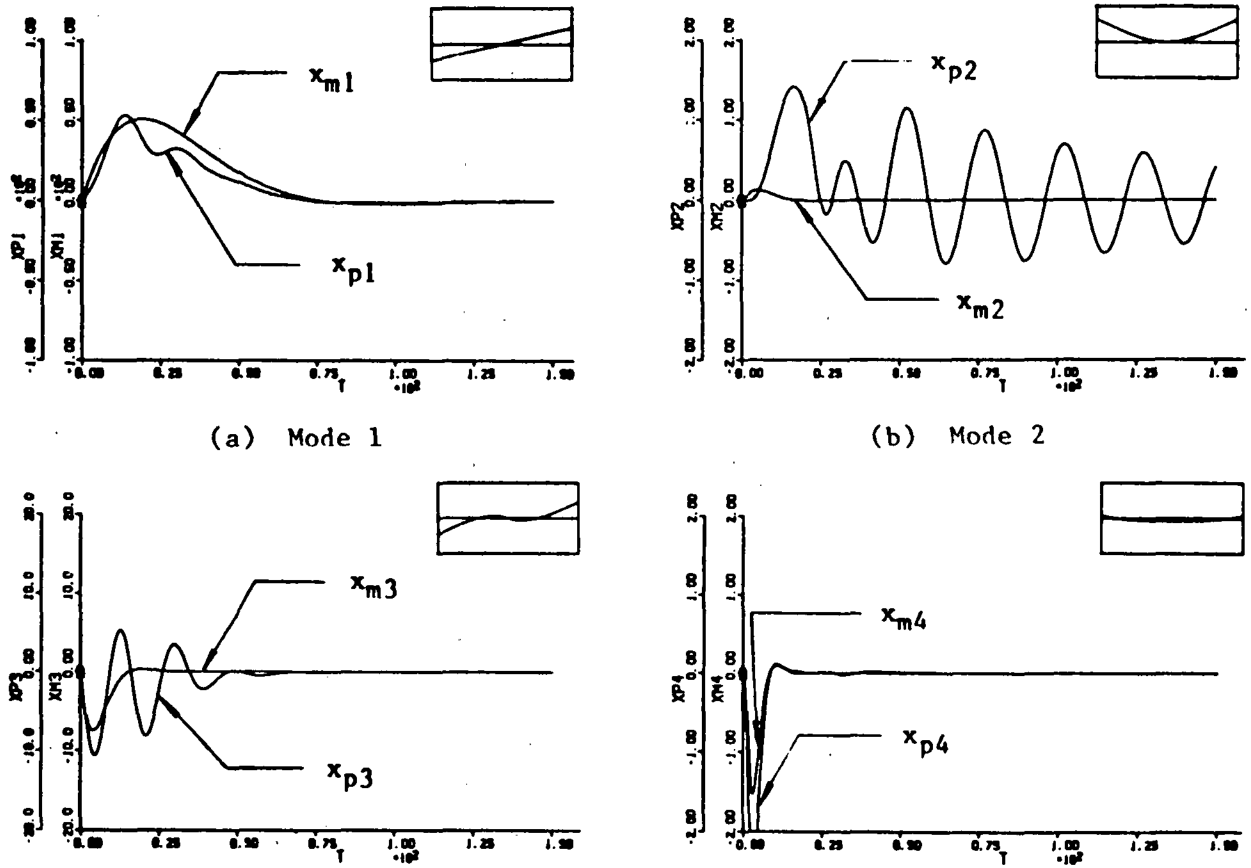

(a) Mode 1

(b) Mode 2

(c) Mode 3

(d) Mode 4

Figure 63 Adaptive Control During Shuttle Hard Docking with Model Switching and Disturbance Modeling for Two-Panel Configuration — Plant and Model Modal Responses

C-3

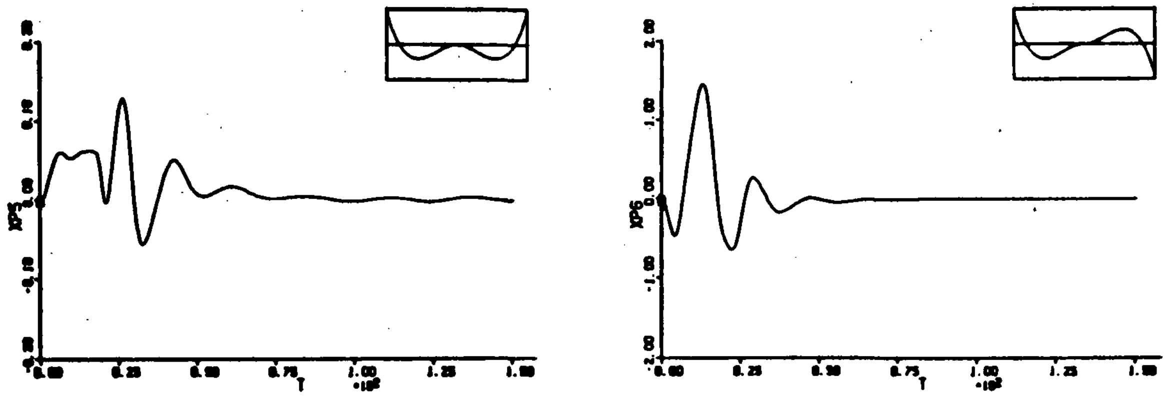

(a) Mode 5 (b) Mode 6

Figure 64 Adaptive Control During Shuttle Hard Docking with Model Switching and Disturbance Modeling for Two-Panel Configuration -- High Frequency Plant Modal Responses

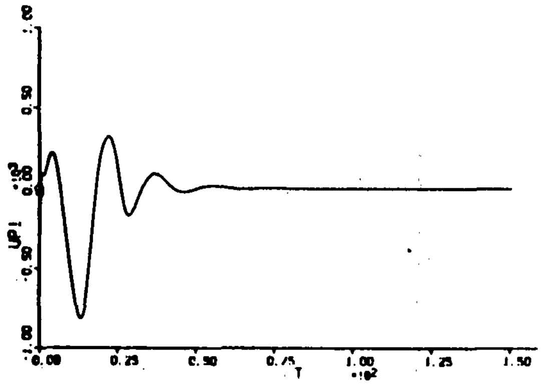

(a) u_{p1}: Left Panel Tip Control Torque (ft-lb)

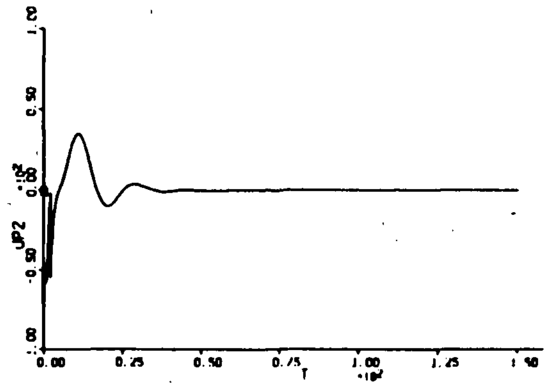

(b) u_{p2}: Bus Control Force (lb)

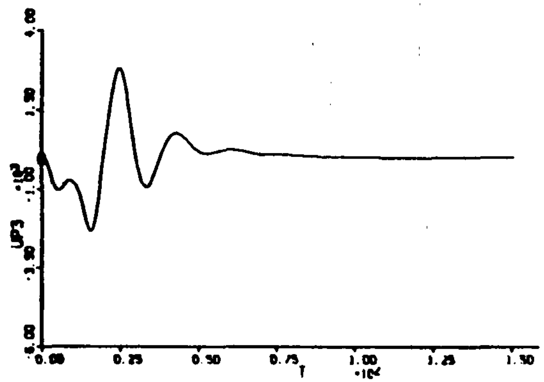

(c) u_{p3}: Bus Control Torque (ft-lb)

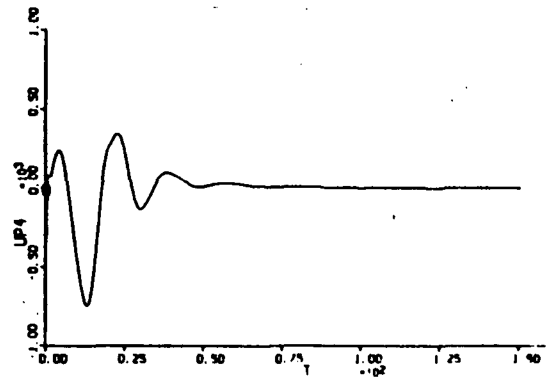

(d) u_{p4}: Right Panel Tip Control Torque (ft-lb)

Figure 65 Adaptive Control During Shuttle Hard Docking with Model Switching and Disturbance Modeling for Two-Panel Configuration — Adaptive Control Inputs

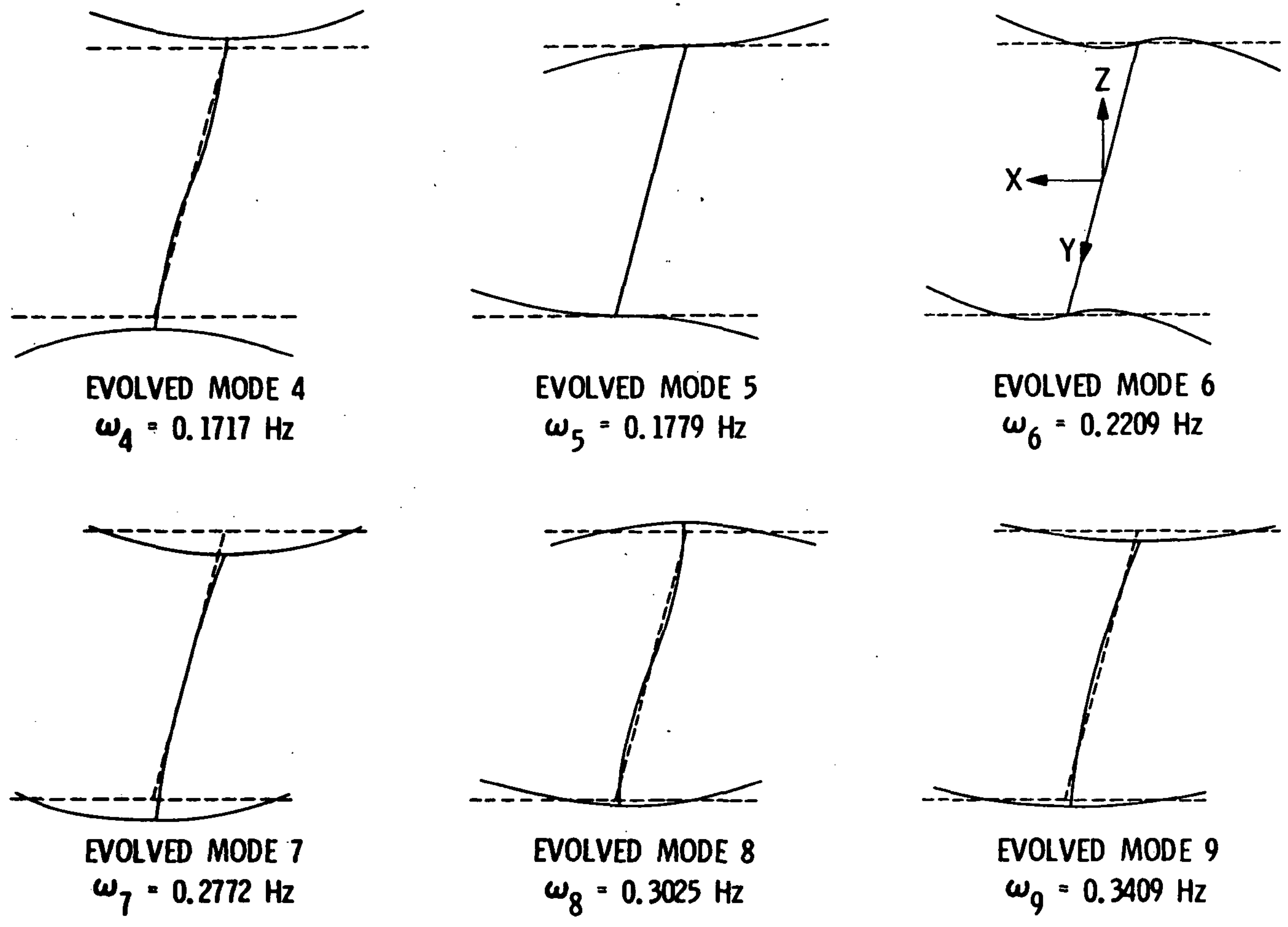

(a) Evolved First Bending Group

Figure 66 Augmented Plant Modal Properties for the Four-Panel Configuration Model

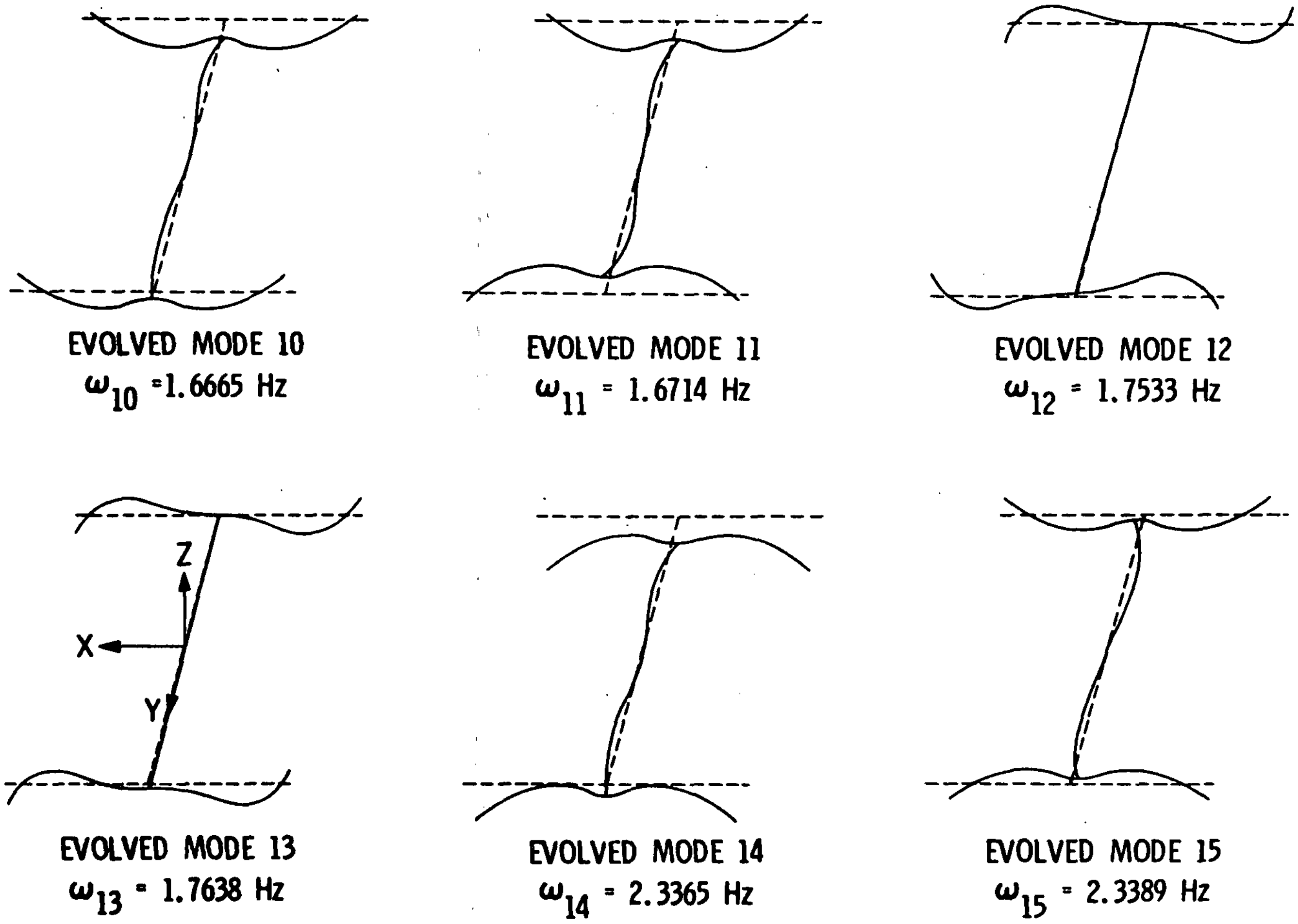

(h) Evolved Second Bending Group

Figure 66 Continued

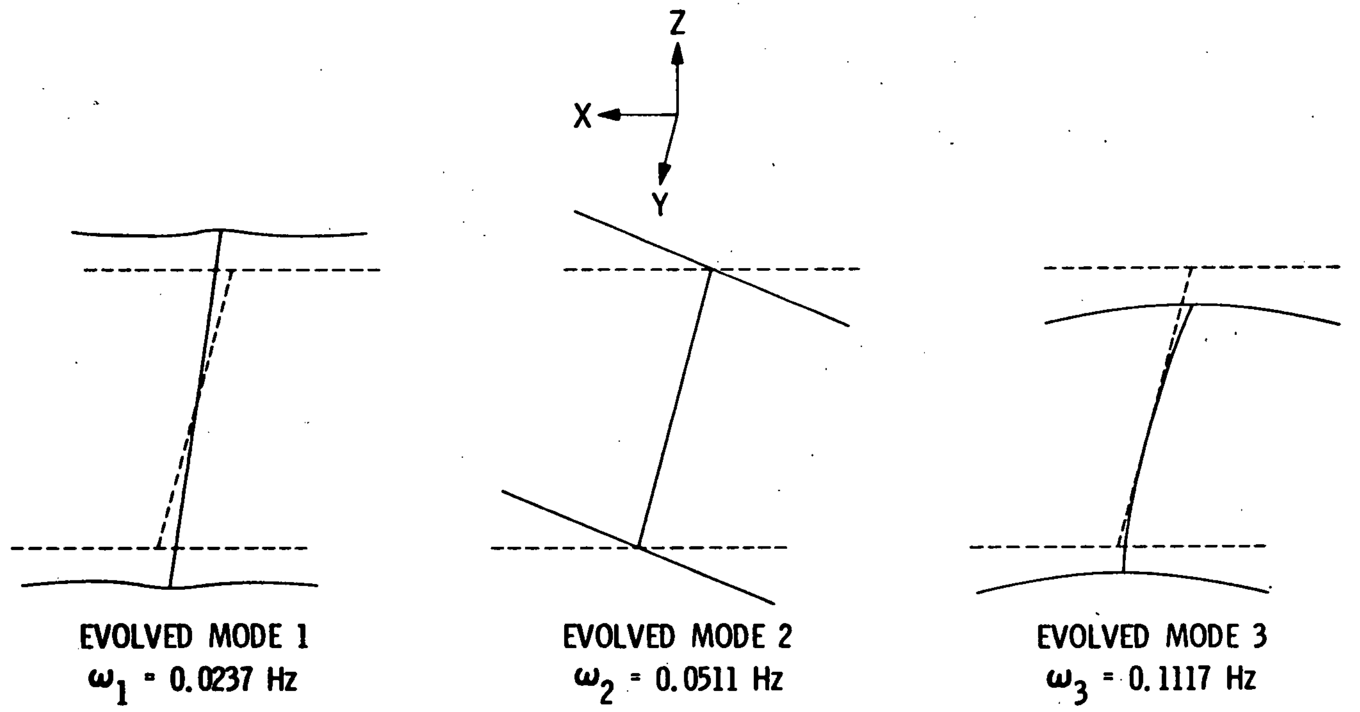

(c) Evolved Rigid Body Modes

Figure 66 Continued

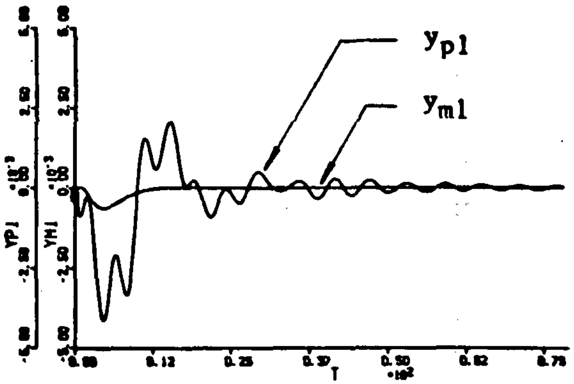

(a) $y_{p1} = \alpha\ \theta_{p1} + \dot{\theta}_{p1}$ (rad)

$y_{m1} = \alpha\ \theta_{m1} + \dot{\theta}_{m1}$ (rad)

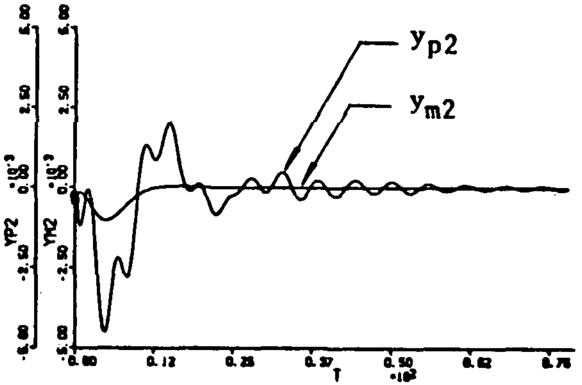

(b) $y_{p2} = \alpha\ \theta_{p3} + \dot{\theta}_{p3}$ (rad)

$y_{m2} = \alpha\ \theta_{m3} + \dot{\theta}_{m3}$ (rad)

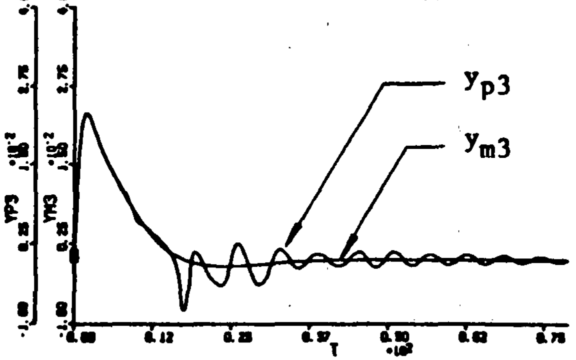

(c) $y_{p3} = \alpha\ Z_{p2} + \dot{Z}_{p2}$ (ft)

$y_{m3} = \alpha\ Z_{m2} + \dot{Z}_{m2}$ (ft)

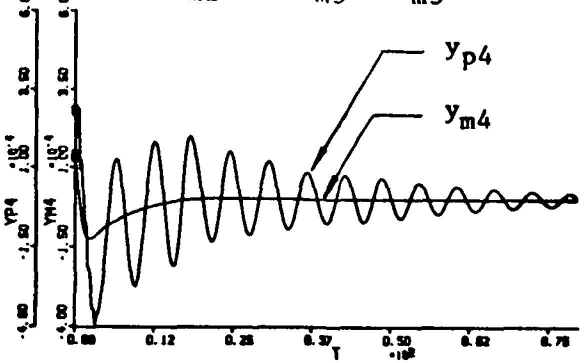

(d) $y_{p4} = \alpha\ \phi_{p2} + \dot{\phi}_{p2}$ (rad)

$y_{m4} = \alpha\ \phi_{m2} + \dot{\phi}_{m2}$ (rad)

Figure 67 Adaptive Regulator Control for Four-Panel Configuration

-- Plant and Model Outputs

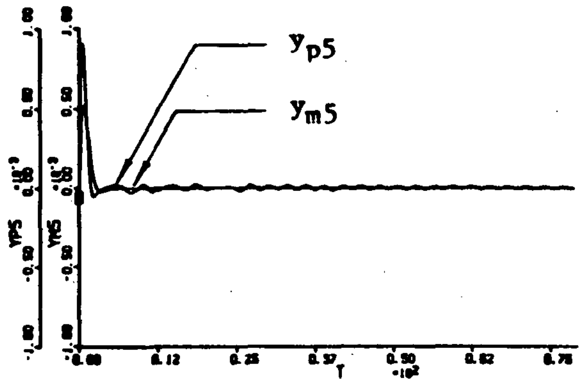

(e) $y_{p5} = \alpha\, Z_{p4} + \dot{Z}_{p4}$ (ft)

$y_{m5} = \alpha\, Z_{m4} + \dot{Z}_{m4}$ (ft)

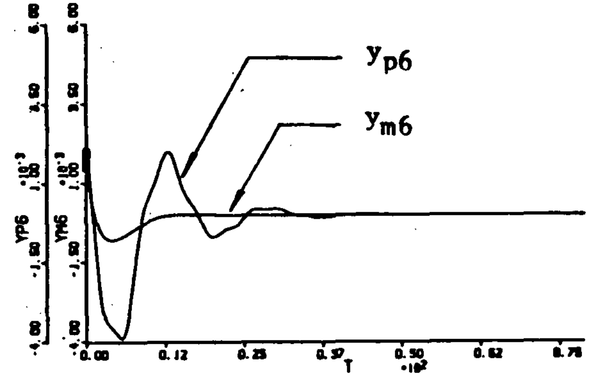

(f) $y_{p6} = \alpha\, \theta_{p4} + \dot{\theta}_{p4}$ (rad)

$y_{m6} = \alpha\, \theta_{m4} + \dot{\theta}_{m4}$ (rad)

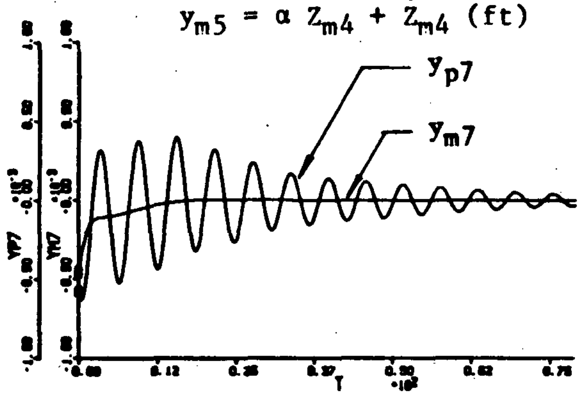

(g) $y_{p7} = \alpha\, \phi_{p4} + \dot{\phi}_{p4}$ (rad)

$y_{m7} = \alpha\, \phi_{m4} + \dot{\phi}_{m4}$ (rad)

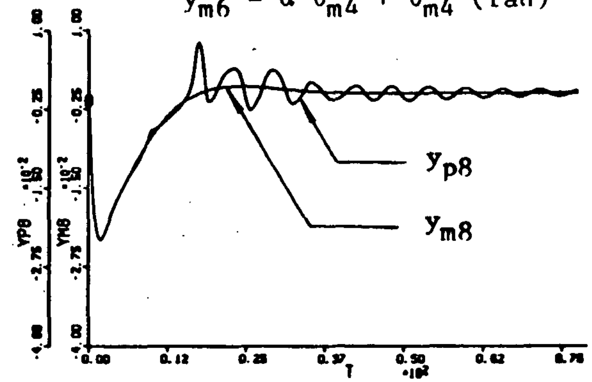

(h) $y_{p8} = \alpha\, Z_{p6} + \dot{Z}_{p6}$ (ft)

$y_{m8} = \alpha\, Z_{m6} + \dot{Z}_{m6}$ (ft)

Figure 67 Continued -

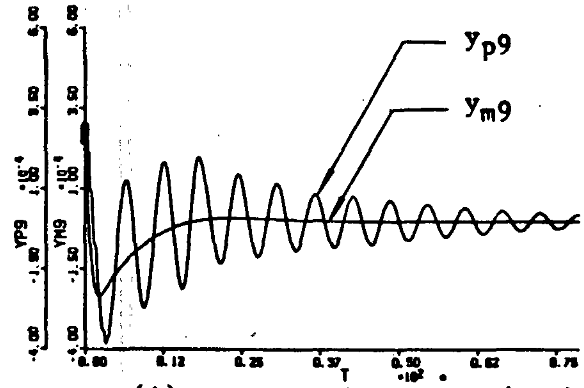

(i) $y_{p9} = \alpha\ \phi_{p6} + \dot{\phi}_{p6}$ (rad)

$y_{m9} = \alpha\ \phi_{m6} + \dot{\phi}_{m6}$ (rad)

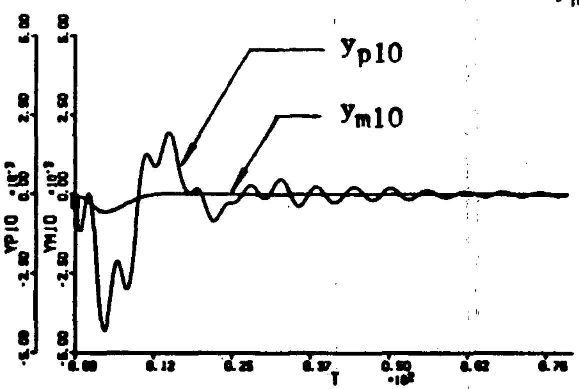

(j) $y_{p10} = \alpha\ \theta_{p5} + \dot{\theta}_{p5}$ (rad)

$y_{m10} = \alpha\ \theta_{m5} + \dot{\theta}_{m5}$ (rad)

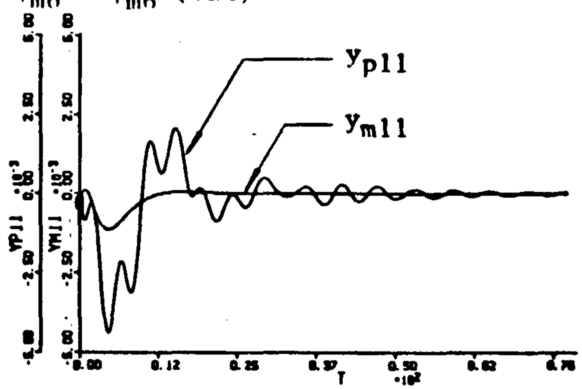

(k) $y_{p11} = \alpha\ \theta_{p7} + \dot{\theta}_{p7}$ (rad)

$y_{m11} = \alpha\ \theta_{m7} + \dot{\theta}_{m7}$ (rad)

Figure 67 Continued

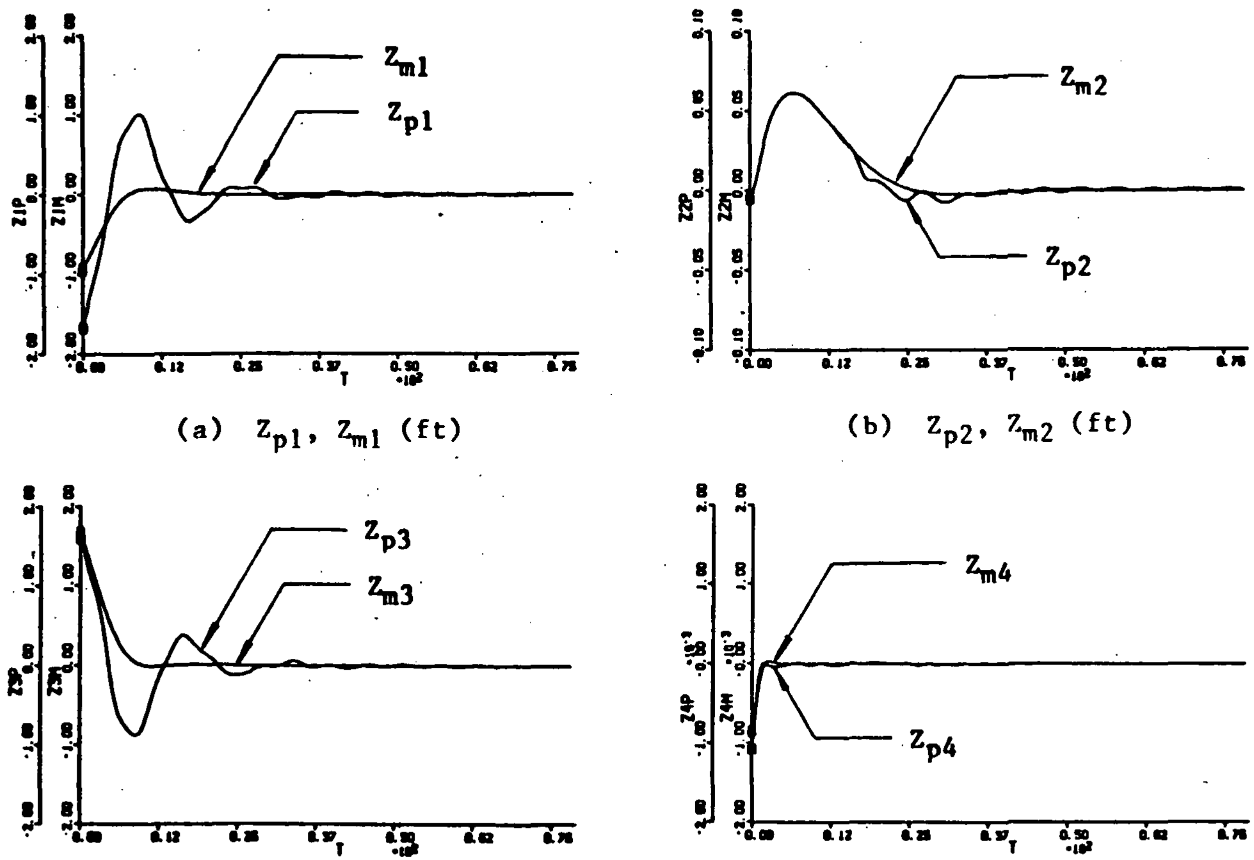

(a) Z_{p1}, Z_{m1} (ft)

(b) Z_{p2}, Z_{m2} (ft)

(c) Z_{p3}, Z_{m3} (ft)

(d) Z_{p4}, Z_{m4} (ft)

Figure 68 Adaptive Regulator Control for Four-Panel Configuration

-- Plant and Model Physical State Responses

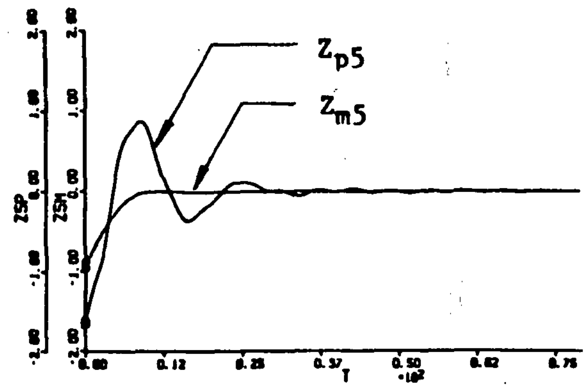

(e) Z_{p5}, Z_{m5} (ft)

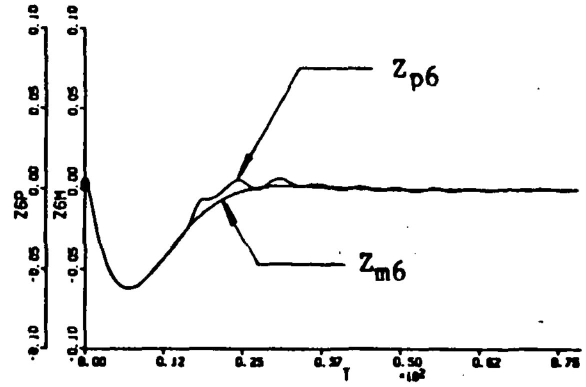

(f) Z_{p6}, Z_{m6} (ft)

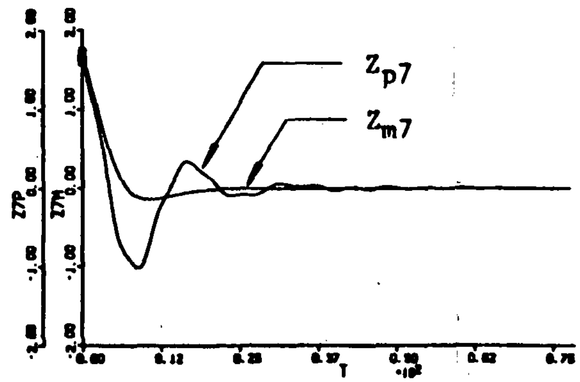

(g) Z_{p7}, Z_{m7} (ft)

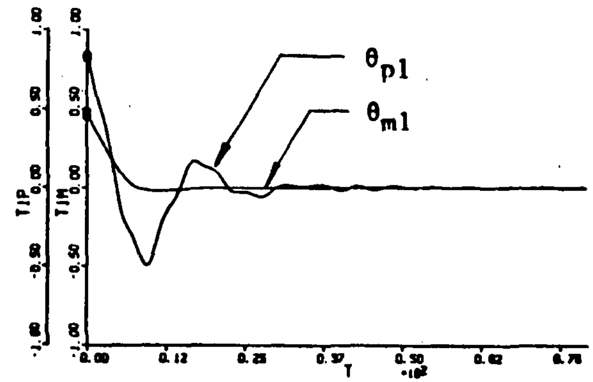

(h) θ_{p1}, θ_{m1} (deg)

Figure 68 Continued

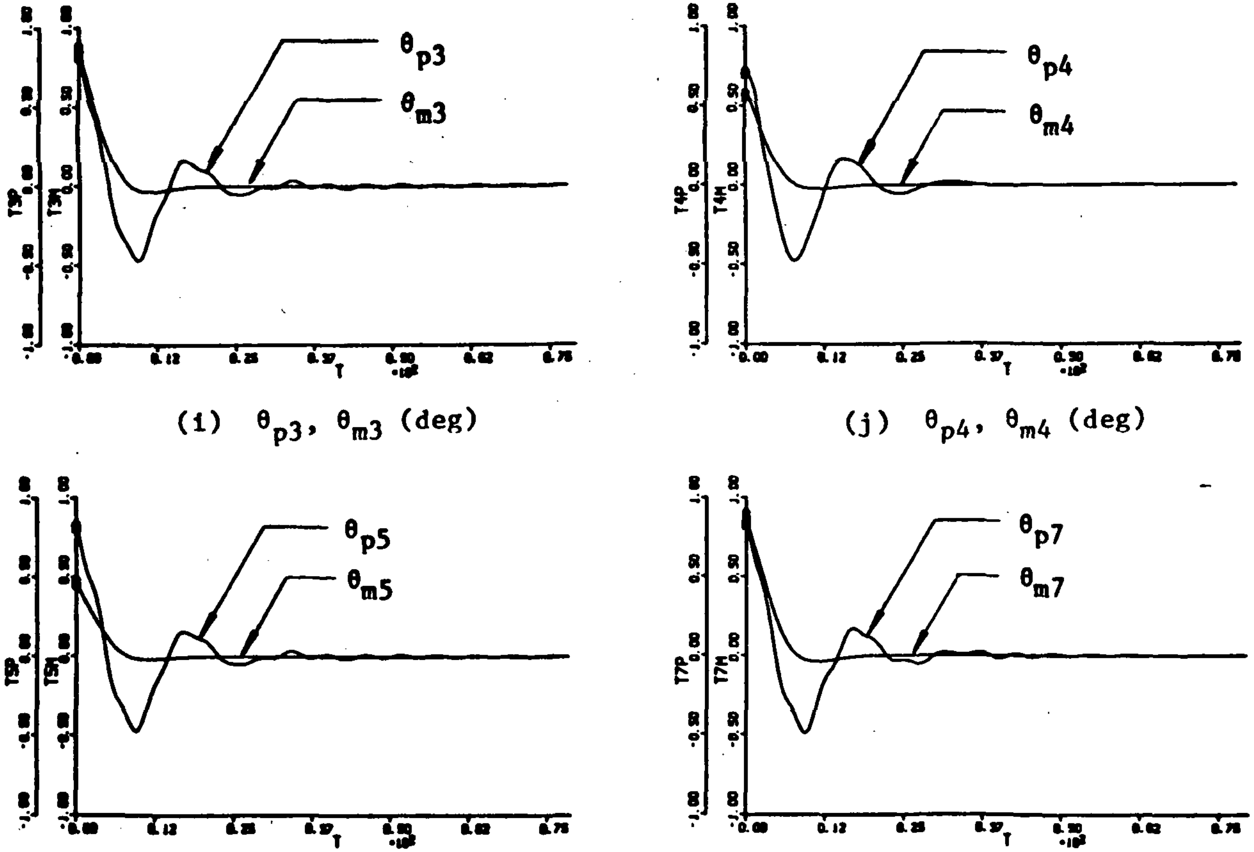

(i) θ_{p3}, θ_{m3} (deg)

(j) θ_{p4}, θ_{m4} (deg)

(k) θ_{p5}, θ_{m5} (deg)

(l) θ_{p7}, θ_{m7} (deg)

Figure 68 Continued

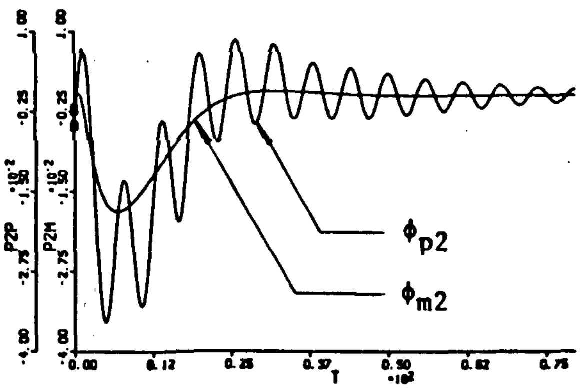

(m) ϕ_{p2}, ϕ_{m2} (deg)

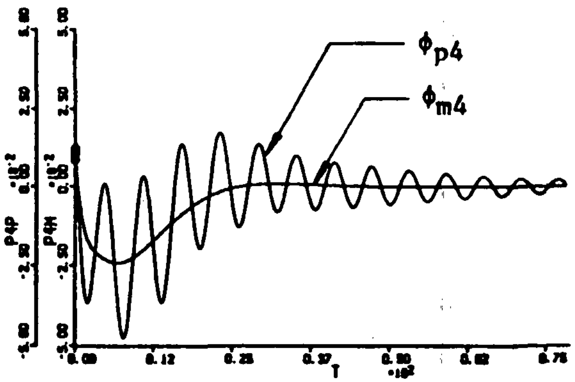

(n) ϕ_{p4}, ϕ_{m4} (deg)

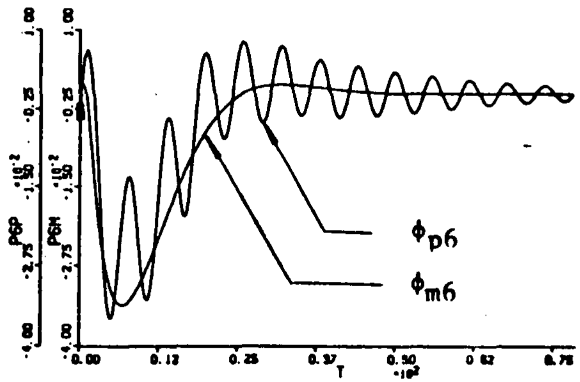

(o) ϕ_{p6}, ϕ_{m6} (deg)

Figure 68 Continued

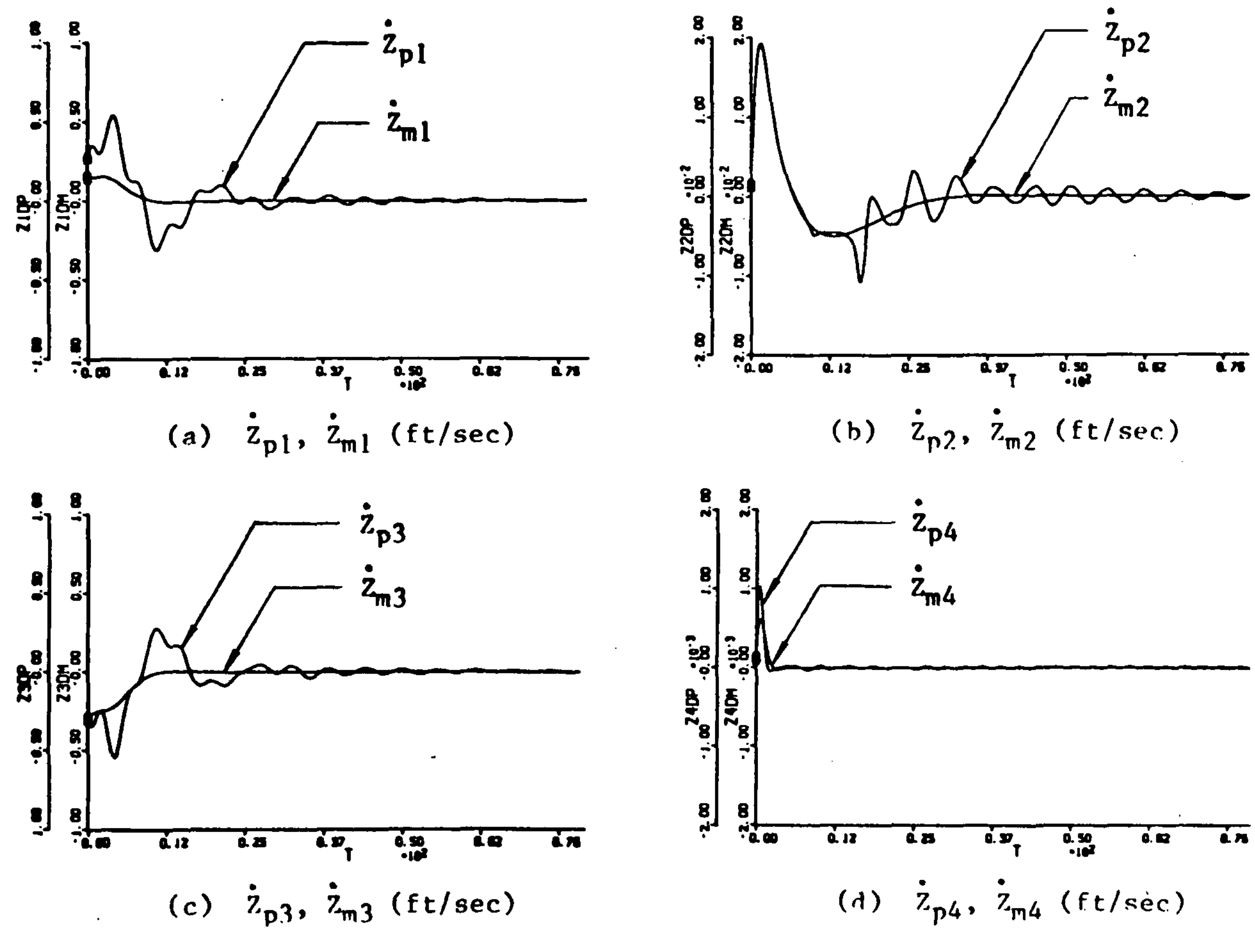

(a) $\dot{Z}_{p1}$, $\dot{Z}_{m1}$ (ft/sec)

(b) $\dot{Z}_{p2}$, $\dot{Z}_{m2}$ (ft/sec)

(c) $\dot{Z}_{p3}$, $\dot{Z}_{m3}$ (ft/sec)

(d) $\dot{Z}_{p4}$, $\dot{Z}_{m4}$ (ft/sec)

Figure 69 Adaptive Regulator Control for Four-Panel Configuration
-- Plant and Model Physical State Rate Responses

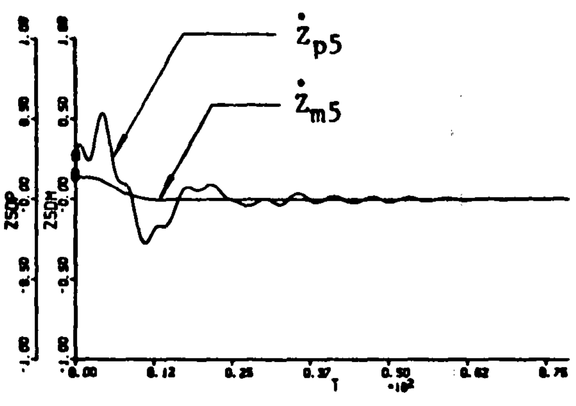

(e) $\dot{Z}_{p5}$, $\dot{Z}_{m5}$ (ft/sec)

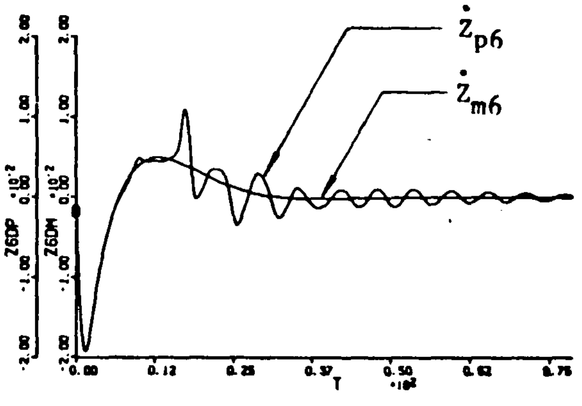

(f) $\dot{Z}_{p6}$, $\dot{Z}_{m6}$ (ft/sec)

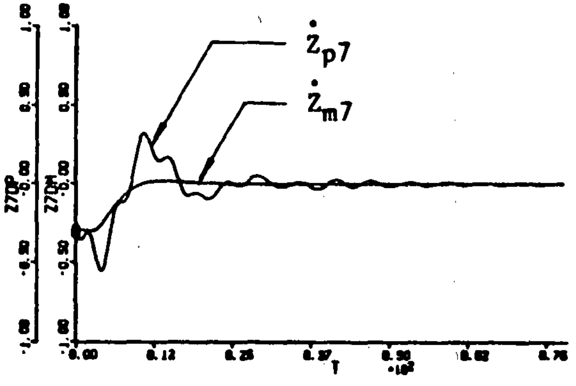

(g) $\dot{Z}_{p7}$, $\dot{Z}_{m7}$ (ft/sec)

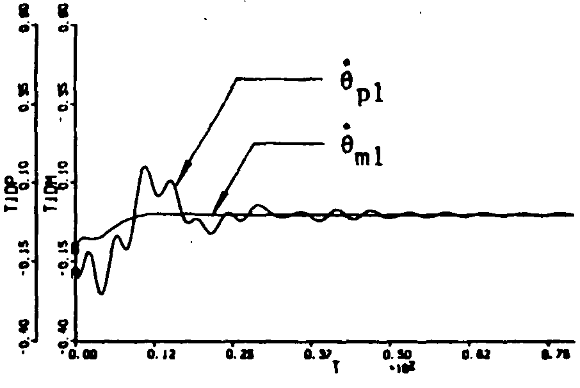

(h) $\dot{\theta}_{p1}$, $\dot{\theta}_{m1}$ (deg/sec)

Figure 69. Continued

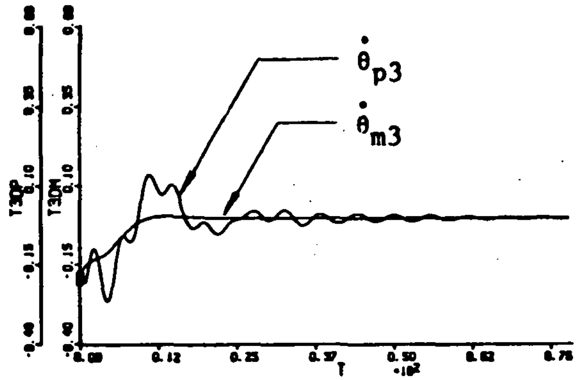

(i) $\dot{\theta}_{p3}$, $\dot{\theta}_{m3}$ (deg/sec)

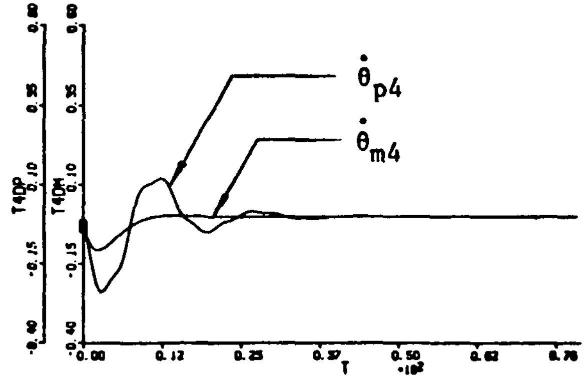

(j) $\dot{\theta}_{p4}$, $\dot{\theta}_{m4}$ (deg/sec)

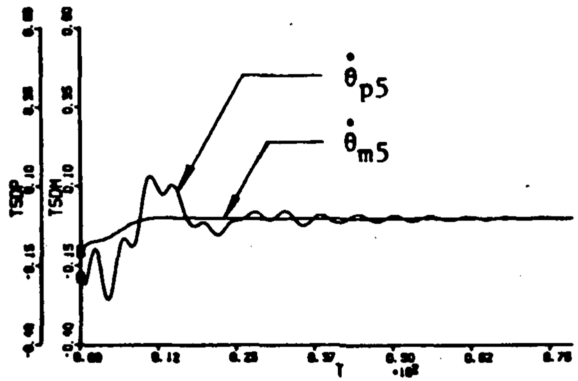

(k) $\dot{\theta}_{p5}$, $\dot{\theta}_{m5}$ (deg/sec)

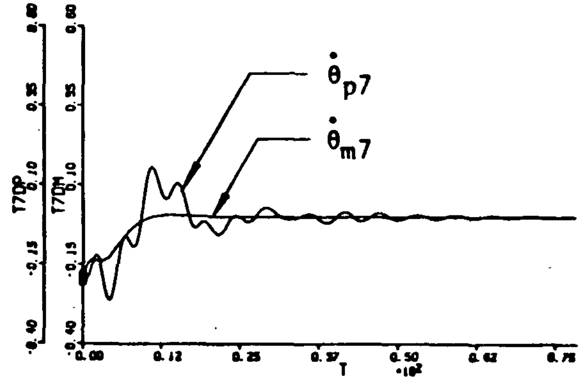

(l) $\dot{\theta}_{p7}$, $\dot{\theta}_{m7}$ (deg/sec)

Figure 69 Continued

ORIGINAL PAGE IS
OF POOR QUALITY

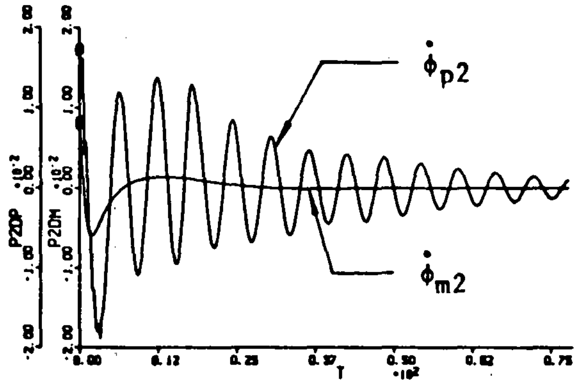

(m) $\dot{\phi}_{p2}$, $\dot{\phi}_{m2}$ (deg/sec)

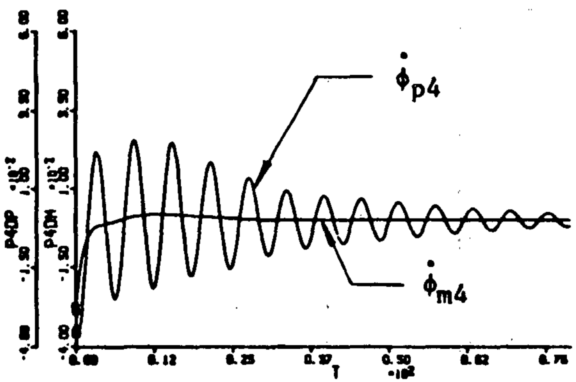

(n) $\dot{\phi}_{p4}$, $\dot{\phi}_{m4}$ (deg/sec)

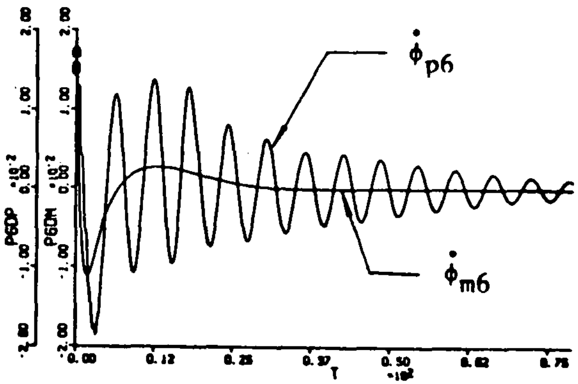

(o) $\dot{\phi}_{p6}$, $\dot{\phi}_{m6}$ (deg/sec)

Figure 69 Continued

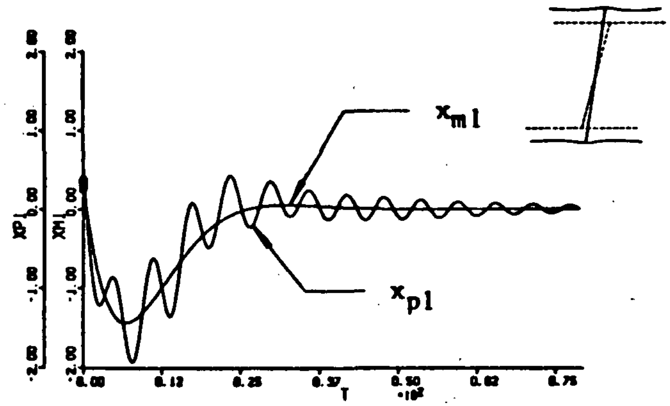

(a) Mode 1

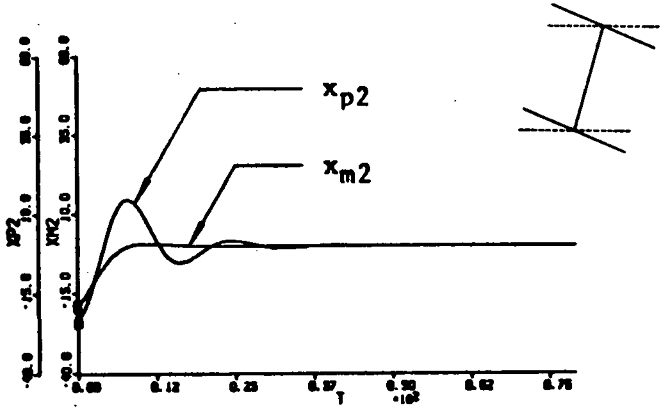

(b) Mode 2

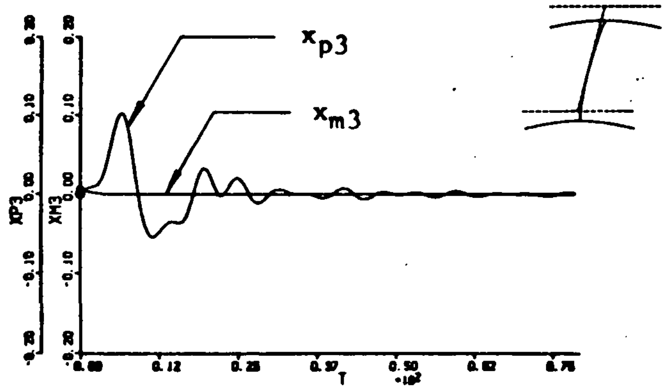

(c) Mode 3

Figure 70 Adaptive Regulator Control for Four-Panel Configuration

-- Plant and Model Rigid Body Modal Responses

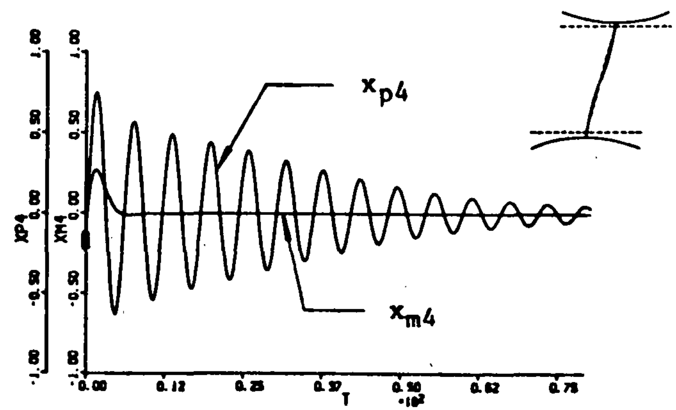

(a) Mode 4

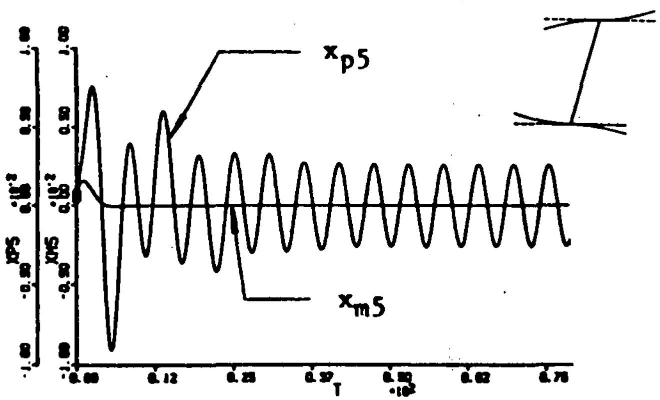

(b) Mode 5

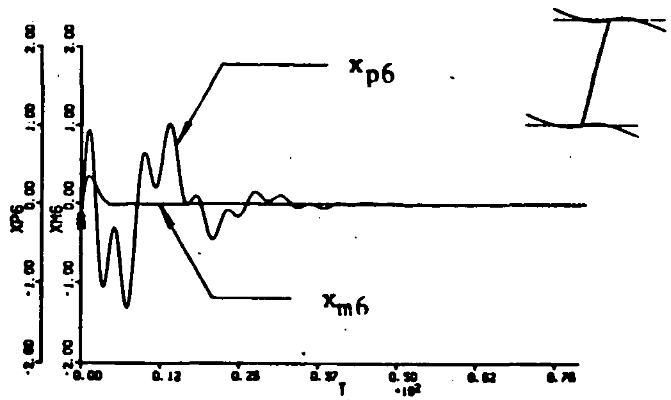

(c) Mode 6

Figure 71 Adaptive Regulator Control for Four-Panel Configuration

-- Plant and Model First Bending Group Modal Responses

ORIGINAL PAGE IS
OF POOR QUALITY

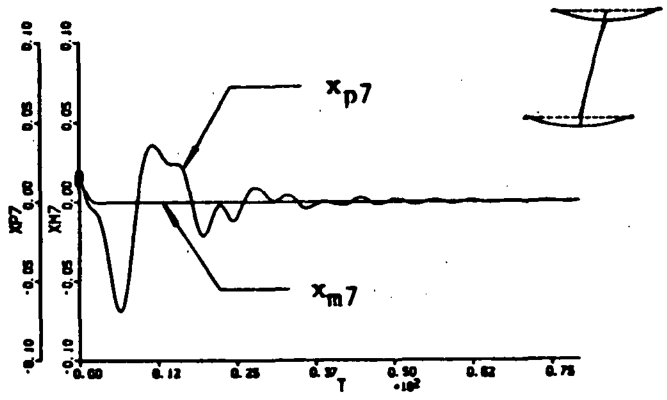

(d) Mode 7

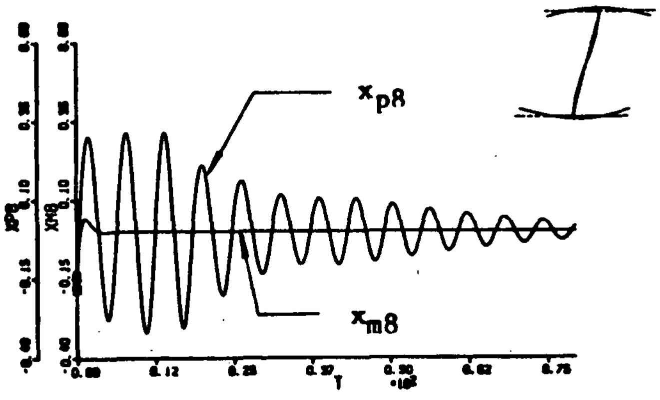

(e) Mode 8

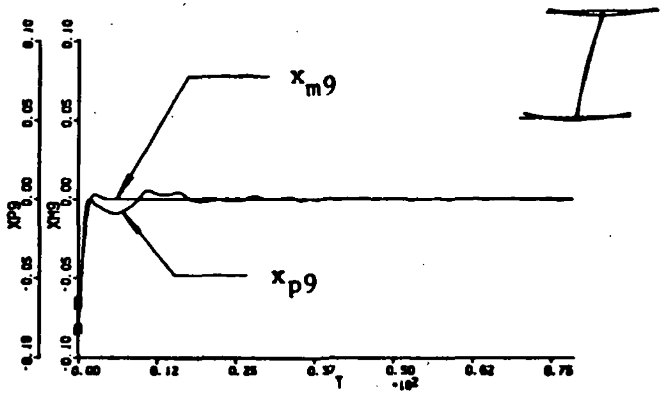

(f) Mode 9

Figure 71 Continued

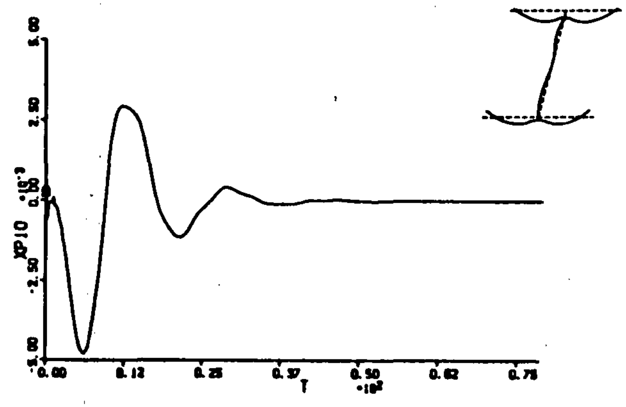

(a) Mode 10

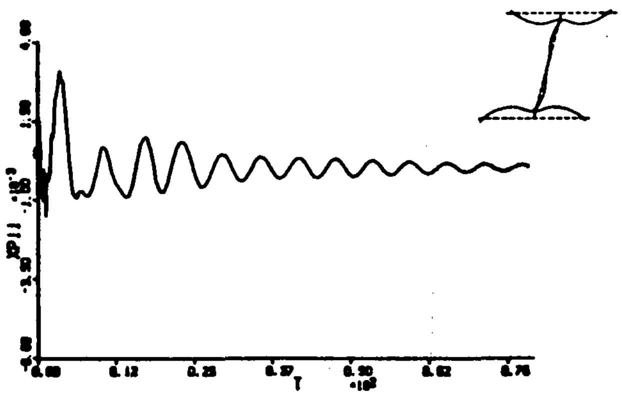

(b) Mode 11

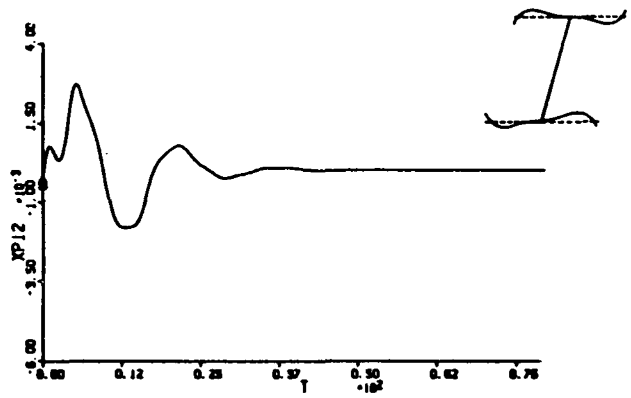

(c) Mode 12

Figure 72 Adaptive Regulator Control for Four-Panel Configuration

— Plant Second Bending Group Modal Responses

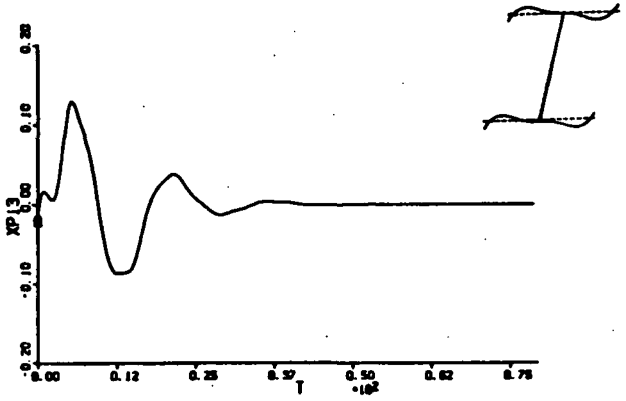

(d) Mode 13

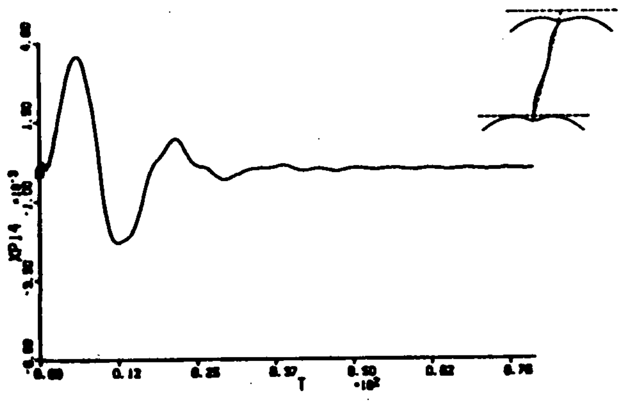

(e) Mode 14

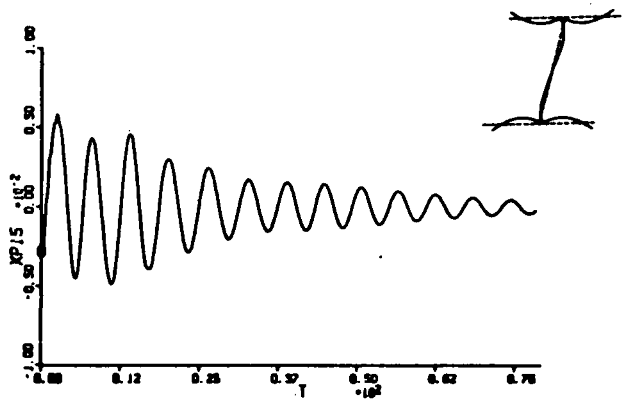

(f) Mode 15

Figure 72 Continued

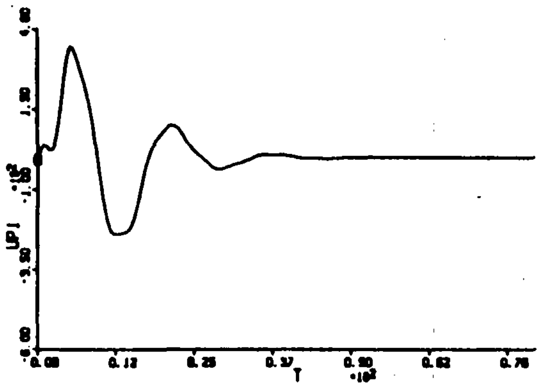

(a) u_{p1}: Control Torque at Left South Panel Tip (ft-lb)

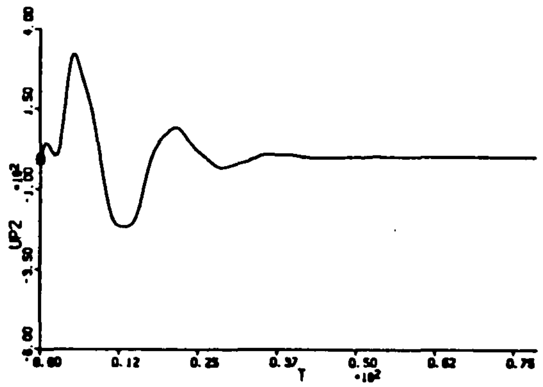

(b) u_{p2}: Control Torque at Right South Panel Tip (ft-lb)

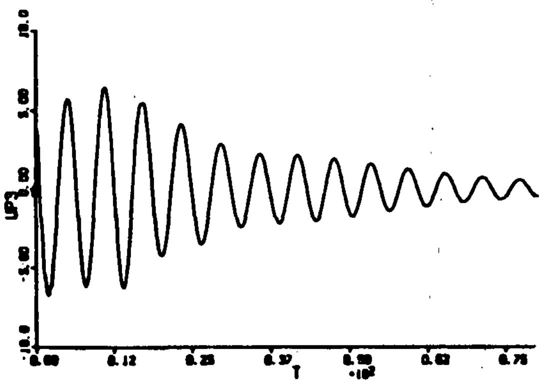

(c) u_{p3}: Control Force at the Root of South Panel (lb)

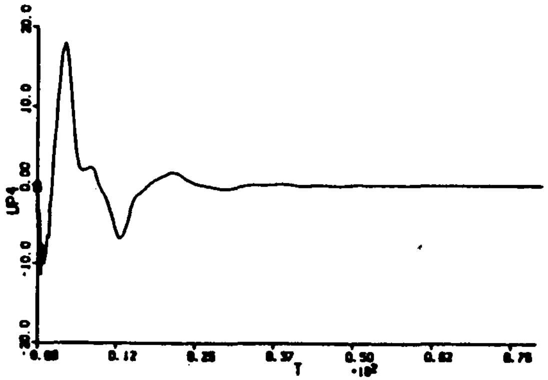

(d) u_{p4}: Control Torque (Bending) at the Root of South Panel (ft-lb)

Figure 73 Adaptive Regulator Control for Four-Panel Configuration

-- Adaptive Control Inputs

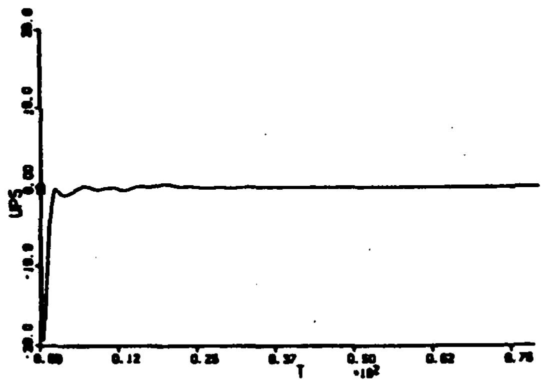

(e) u_{p5}: Control Force at Central Bus (lb)

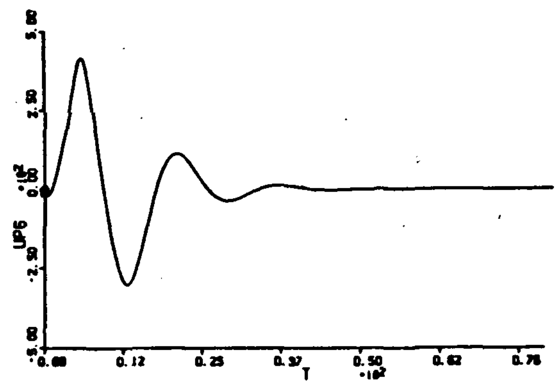

(f) u_{p6}: Control Torque (Twisting) at Central Bus (ft-lb)

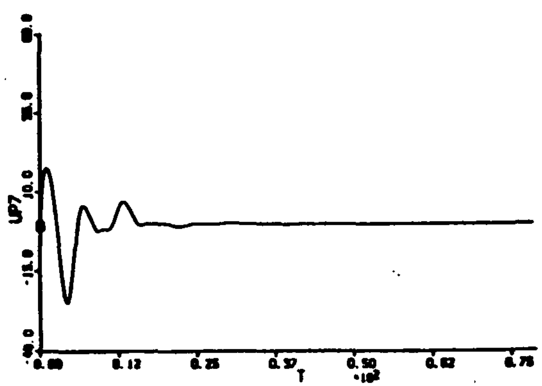

(g) u_{p7}: Control Torque (Bending) at Central Bus (ft-lb)

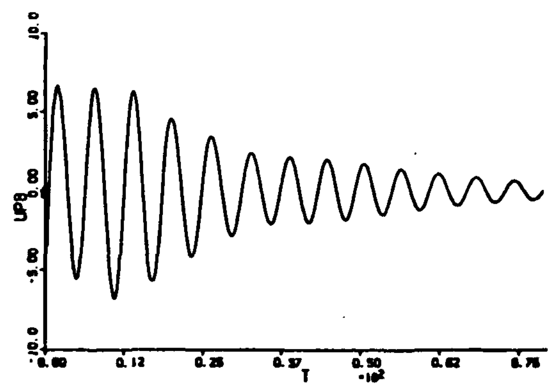

(h) u_{p8}: Control Force at the Root of North Panel (lb)

Figure 73 Continued

ORIGINAL PAGE IS
OF POOR QUALITY

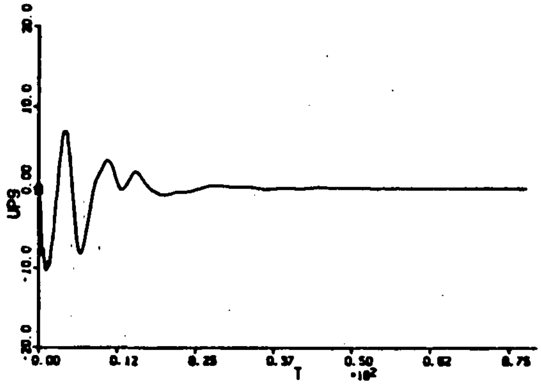

(i) u_{p9}: Control Torque (Bending) at the Root of North Panel (ft-lb)

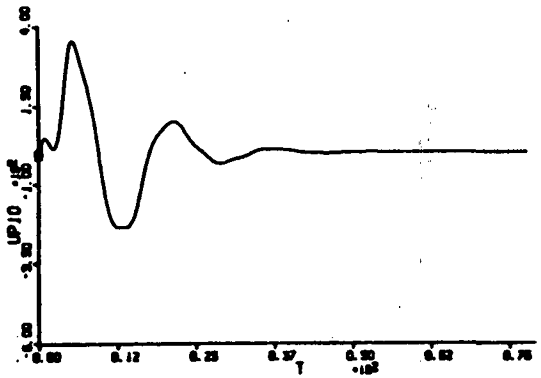

(j) u_{p10}: Control Torque at Left North Panel Tip (ft-lb)

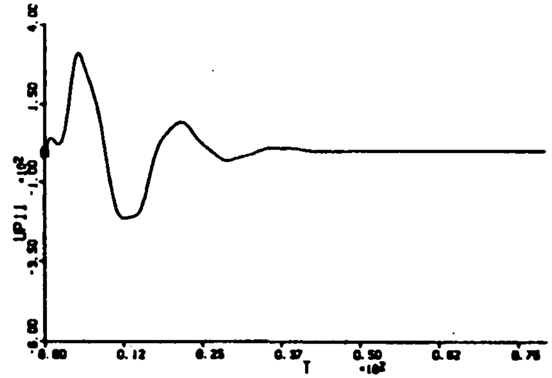

(k) u_{p11}: Control Torque at Right North Panel Tip (ft-lb)

Figure 73 Continued

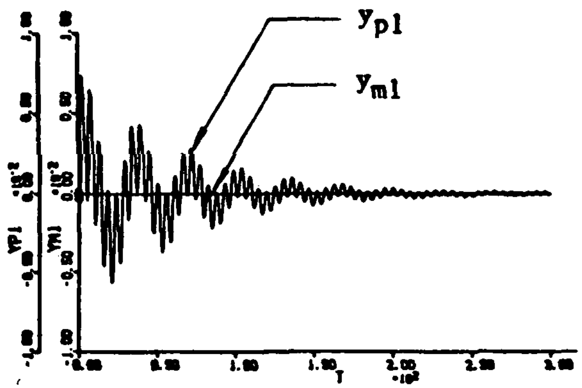

(a) $y_{p1} = \alpha\ \theta_{p1} + \dot{\theta}_{p1}$ (rad)

$y_{m1} = \alpha\ \theta_{m1} + \dot{\theta}_{m1}$ (rad)

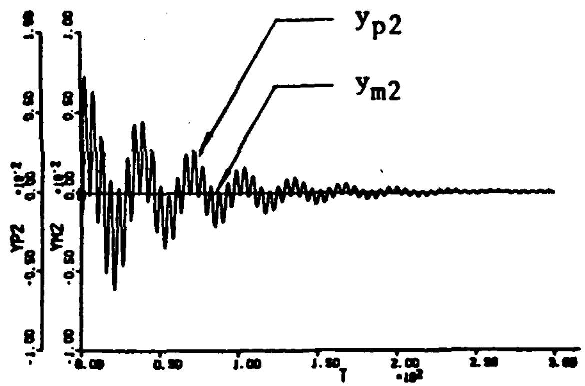

(b) $y_{p2} = \alpha\ \theta_{p3} + \dot{\theta}_{p3}$ (rad)

$y_{m2} = \alpha\ \theta_{m3} + \dot{\theta}_{m3}$ (rad)

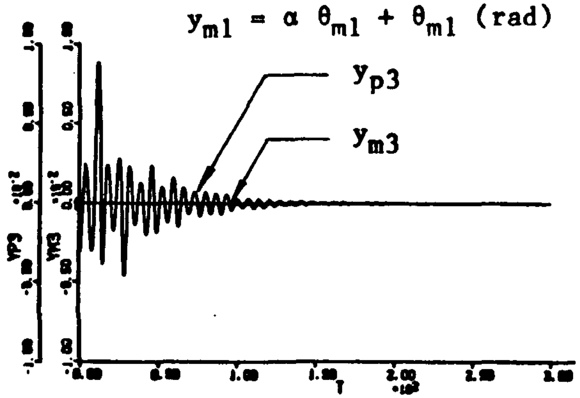

(c) $y_{p3} = \alpha\ Z_{p2} + \dot{Z}_{p2}$ (ft)

$y_{m3} = \alpha\ Z_{m2} + \dot{Z}_{m2}$ (ft)

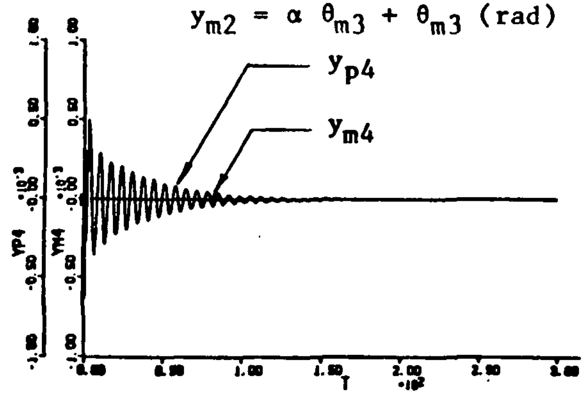

(d) $y_{p4} = \alpha\ \phi_{p2} + \dot{\phi}_{p2}$ (rad)

$y_{m4} = \alpha\ \phi_{m2} + \dot{\phi}_{m2}$ (rad)

Figure 74 Adaptive Control During Shuttle Hard Docking for Four-Panel Configuration

-- Plant and Model Outputs

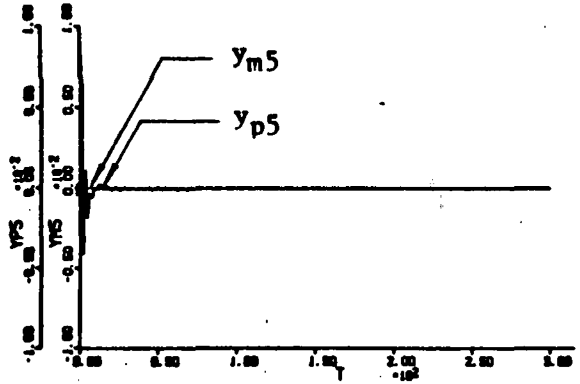

(e) $y_{p5} = \alpha\ Z_{p4} + \dot{Z}_{p4}$ (ft)

$y_{m5} = \alpha\ Z_{m4} + \dot{Z}_{m4}$ (ft)

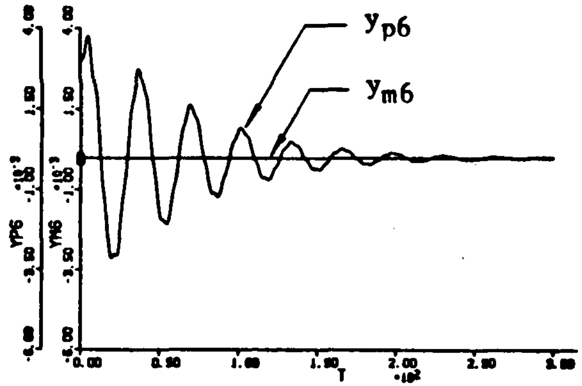

(f) $y_{p6} = \alpha\ \theta_{p4} + \dot{\theta}_{p4}$ (rad)

$y_{m6} = \alpha\ \theta_{m4} + \dot{\theta}_{m4}$ (rad)

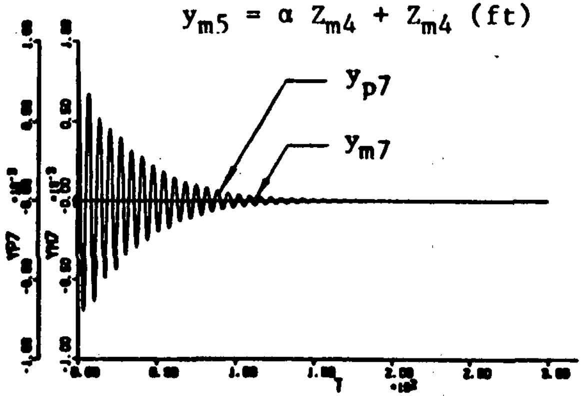

(g) $y_{p7} = \alpha\ \phi_{p4} + \dot{\phi}_{p4}$ (rad)

$y_{m7} = \alpha\ \phi_{m4} + \dot{\phi}_{m4}$ (rad)

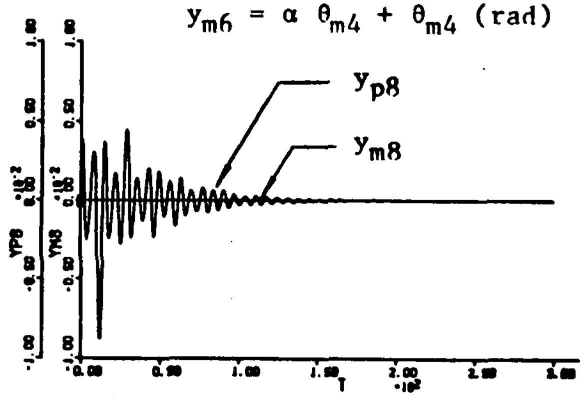

(h) $y_{p8} = \alpha\ Z_{p6} + \dot{Z}_{p6}$ (ft)

$y_{m8} = \alpha\ Z_{m6} + \dot{Z}_{m6}$ (ft)

Figure 74 Continued

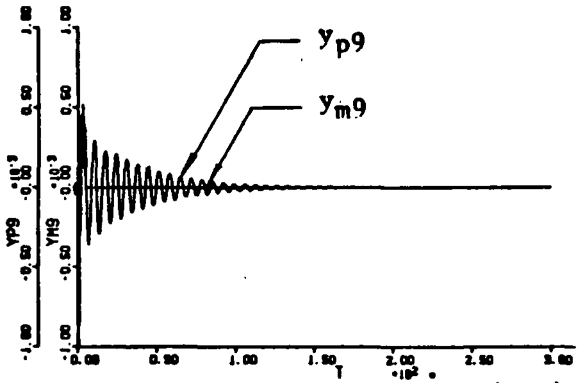

(i) $y_{p9} = \alpha\ \phi_{p6} + \dot{\phi}_{p6}$ (rad)

$y_{m9} = \alpha\ \phi_{m6} + \dot{\phi}_{m6}$ (rad)

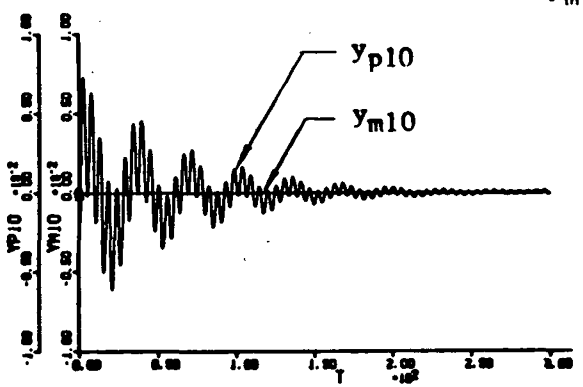

(j) $y_{p10} = \alpha\ \theta_{p5} + \dot{\theta}_{p5}$ (rad)

$y_{m10} = \alpha\ \theta_{m5} + \dot{\theta}_{m5}$ (rad)

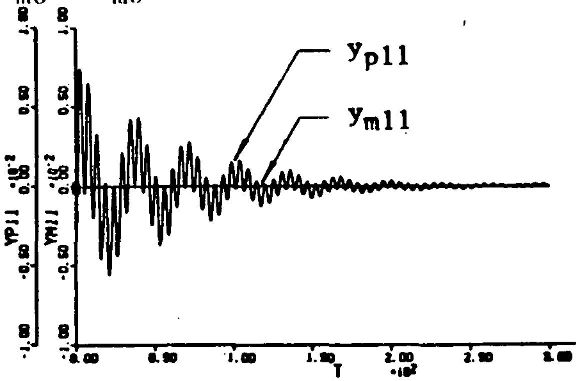

(k) $y_{p11} = \alpha\ \theta_{p7} + \dot{\theta}_{p7}$ (rad)

$y_{m11} = \alpha\ \theta_{m7} + \dot{\theta}_{m7}$ (rad)

Figure 74 Continued

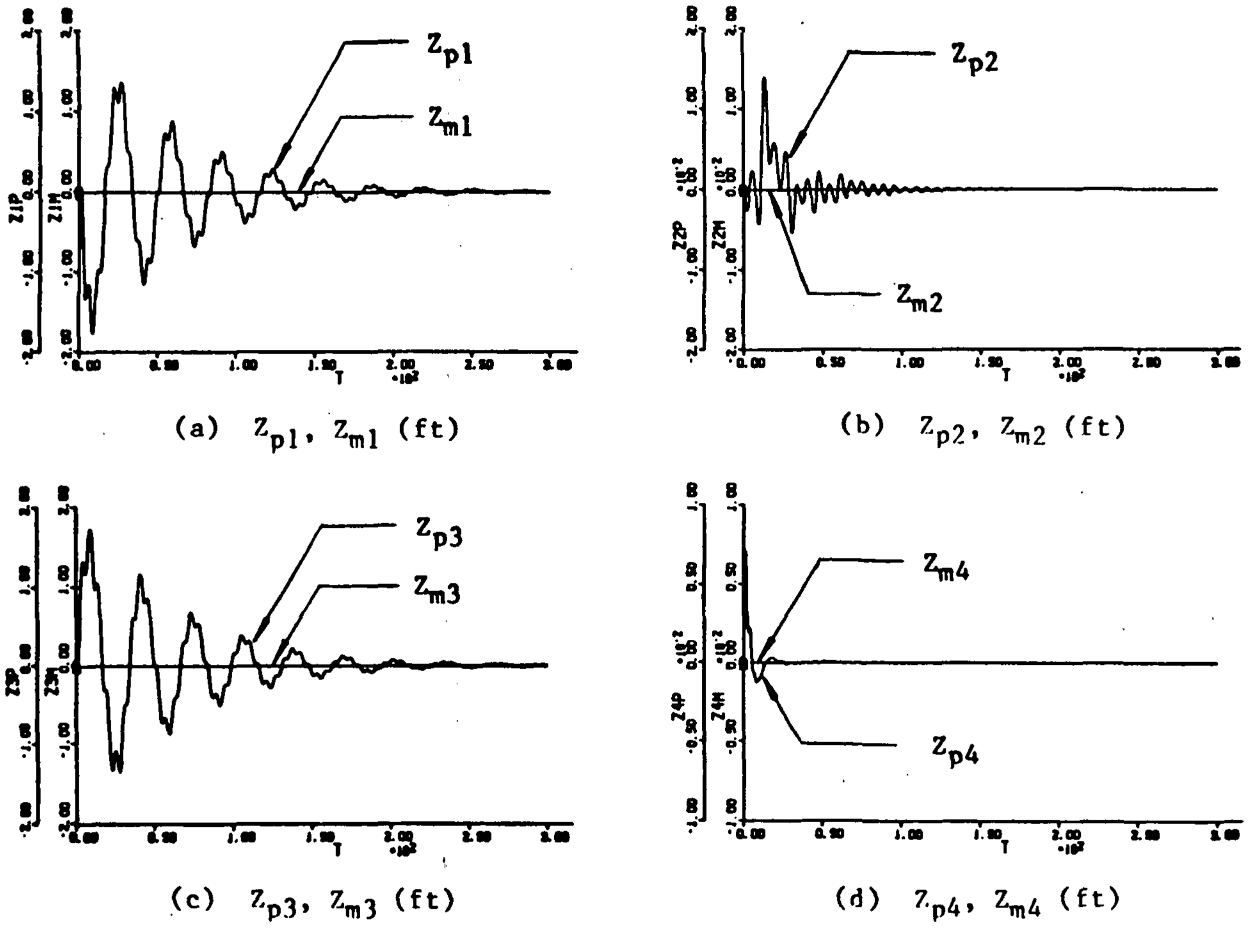

Figure 75 Adaptive Control During Shuttle Hard Docking for Four-Panel Configuration — Plant and Model Physical State Responses

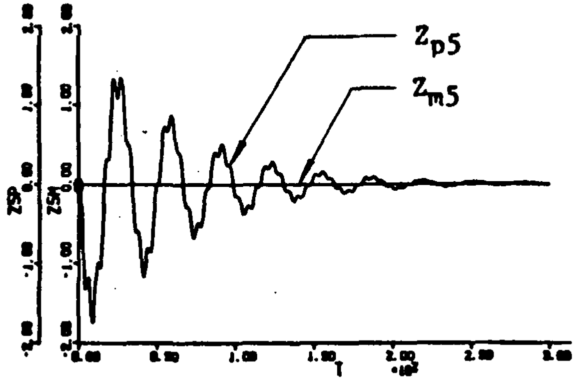

(e) Z_{p5}, Z_{m5} (ft)

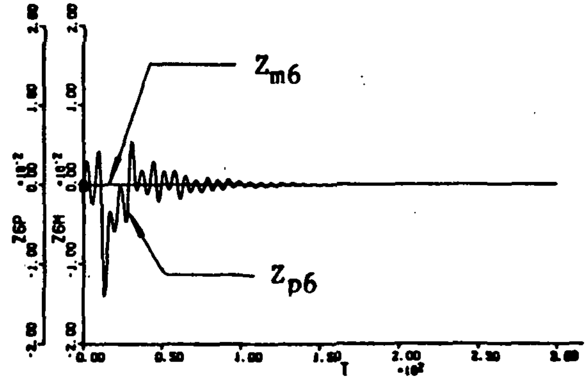

(f) Z_{p6}, Z_{m6} (ft)

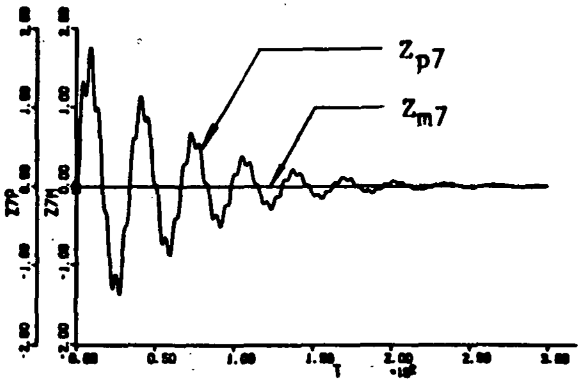

(g) Z_{p7}, Z_{m7} (ft)

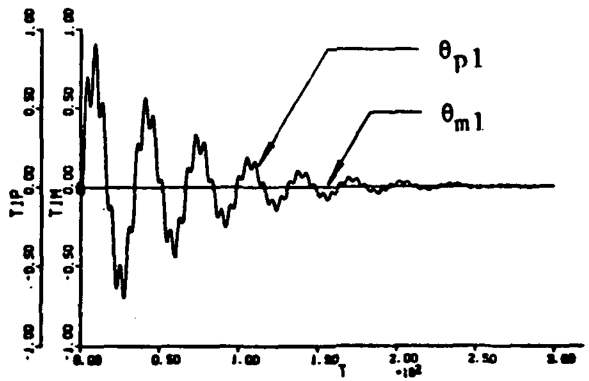

(h) θ_{p1}, θ_{m1} (deg)

Figure 75 Continued

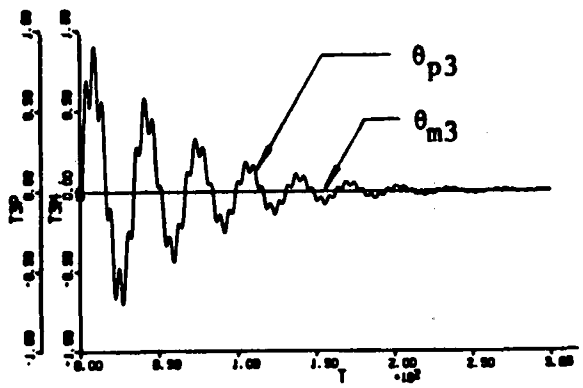

(i) θ_{p3}, θ_{m3} (deg)

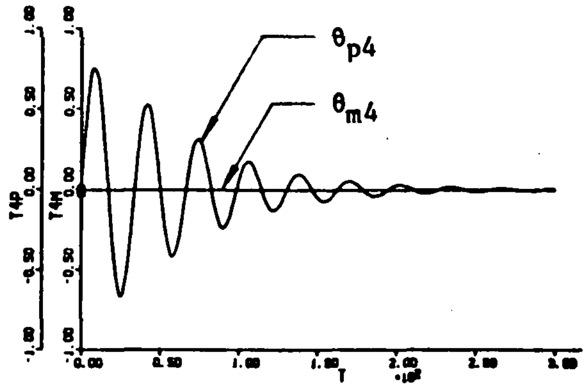

(j) θ_{p4}, θ_{m4} (deg)

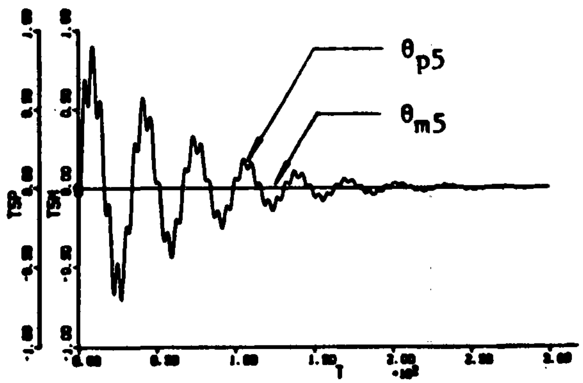

(k) θ_{p5}, θ_{m5} (deg)

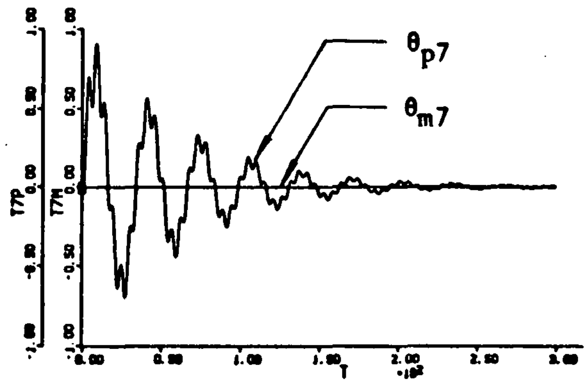

(l) θ_{p7}, θ_{m7} (deg)

Figure 75 Continued

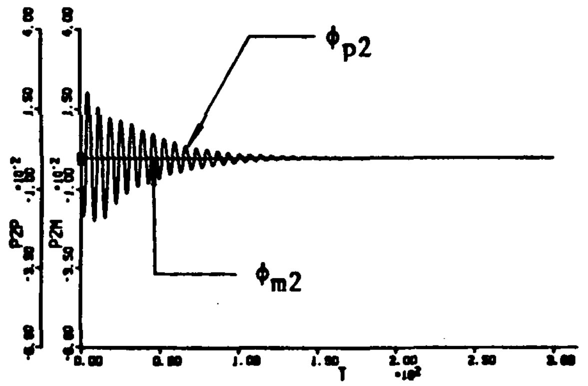

(m) ϕ_{p2}, ϕ_{m2} (deg)

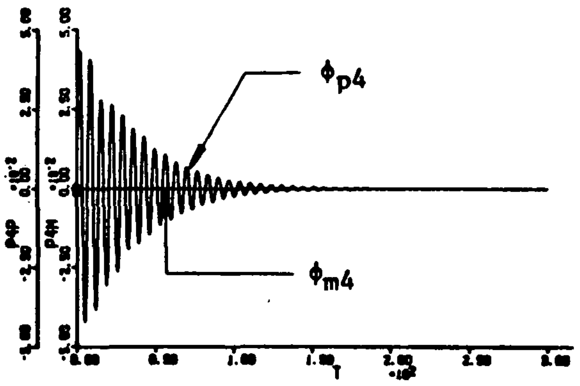

(n) ϕ_{p4}, ϕ_{m4} (deg)

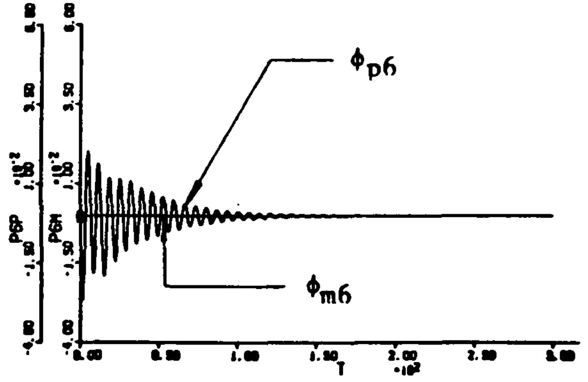

(o) ϕ_{p6}, ϕ_{m6} (deg)

Figure 75 Continued

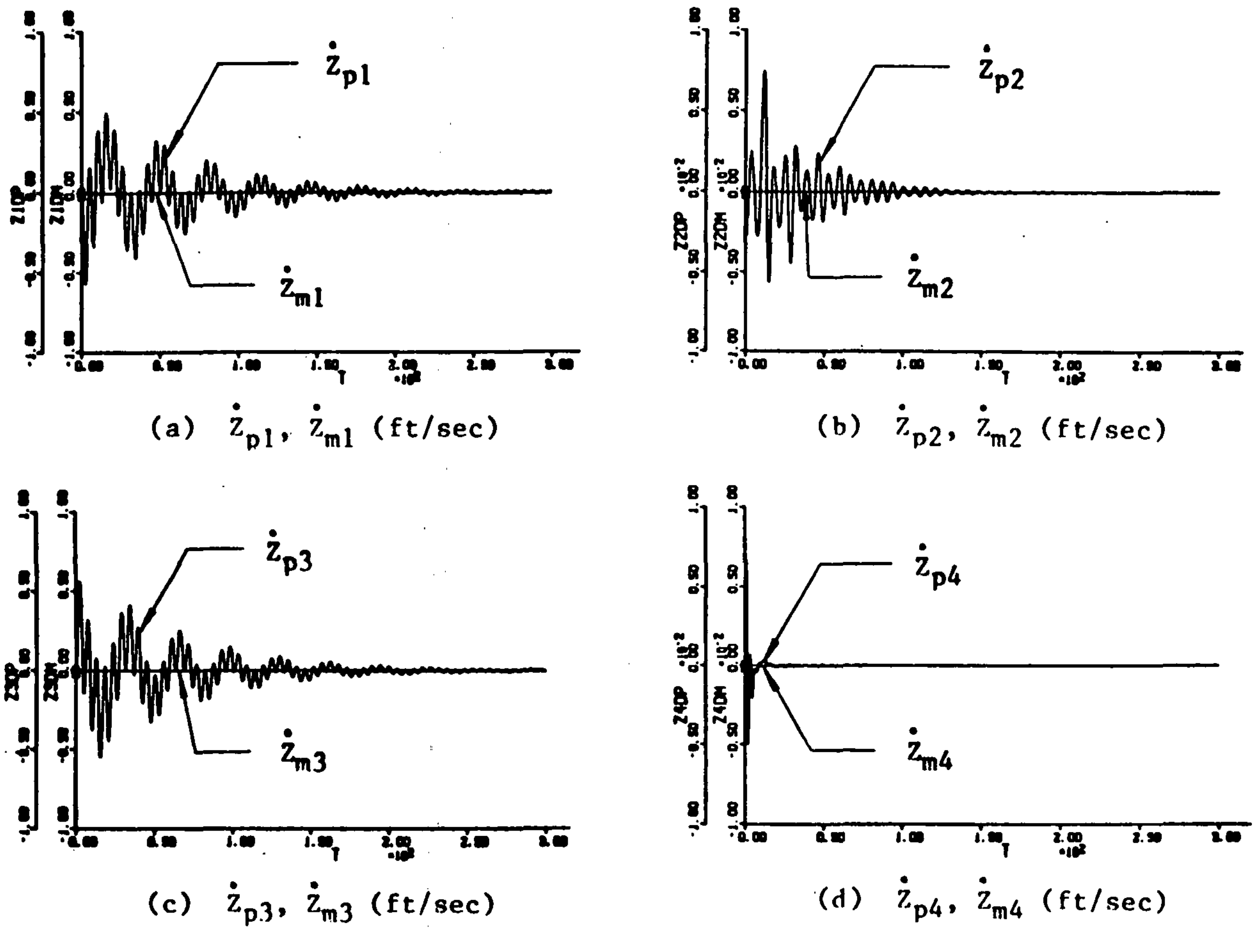

Figure 76 Adaptive Control During Shuttle Hard Docking for Four-Panel Configuration
-- Plant and Model Physical State Rate Responses

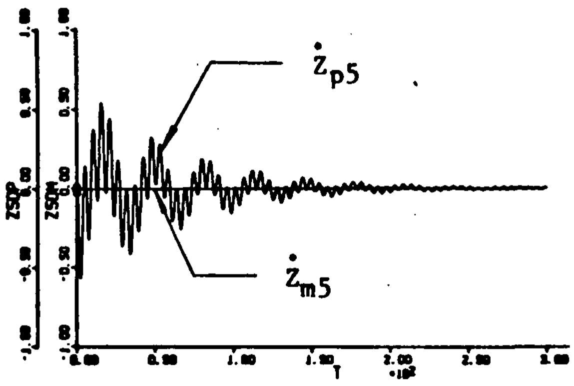

(e) $\dot{z}_{p5}$, $\dot{z}_{m5}$ (ft/sec)

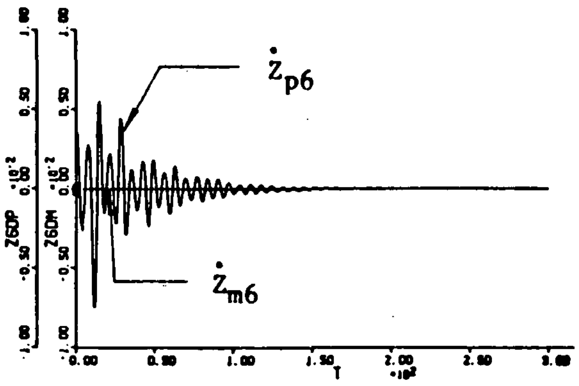

(f) $\dot{z}_{p6}$, $\dot{z}_{m6}$ (ft/sec)

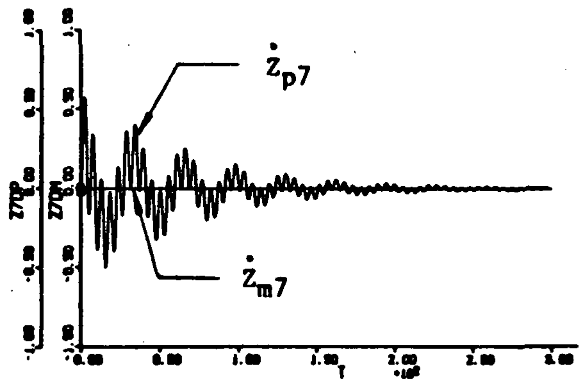

(g) $\dot{z}_{p7}$, $\dot{z}_{m7}$ (ft/sec)

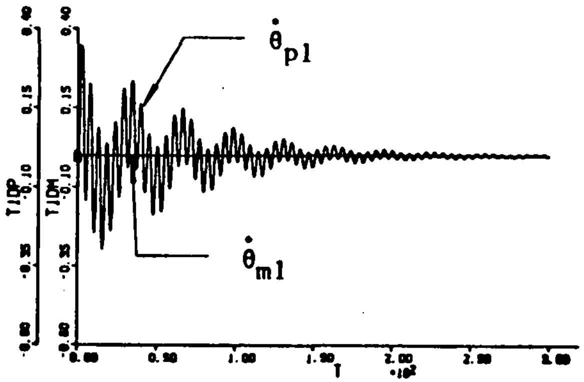

(h) $\dot{\theta}_{p1}$, $\dot{\theta}_{m1}$ (deg/sec)

Figure 76 Continued

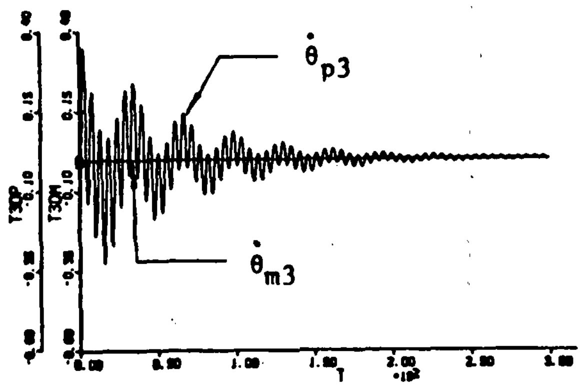

(i) $\dot{\theta}_{p3}$, $\dot{\theta}_{m3}$ (deg/sec)

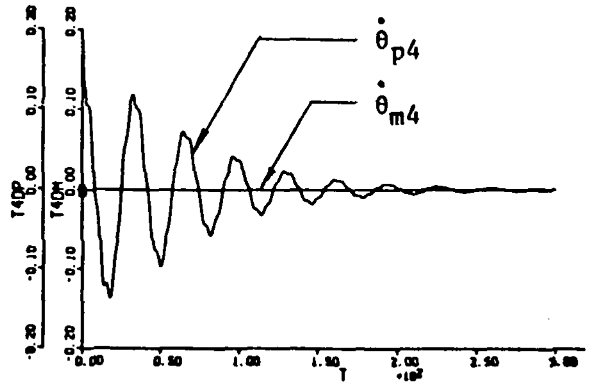

(j) $\dot{\theta}_{p4}$, $\dot{\theta}_{m4}$ (deg/sec)

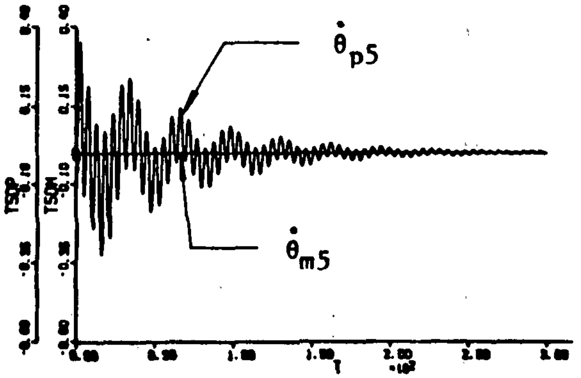

(k) $\dot{\theta}_{p5}$, $\dot{\theta}_{m5}$ (deg/sec)

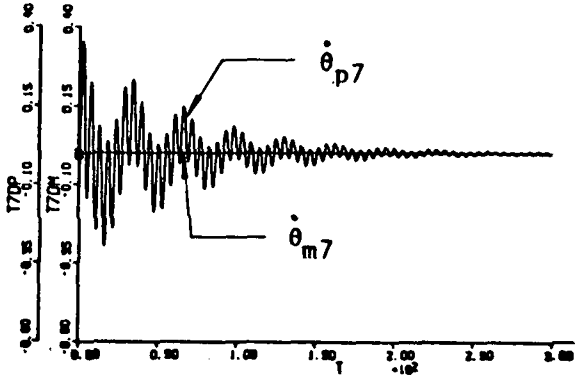

(l) $\dot{\theta}_{p7}$, $\dot{\theta}_{m7}$ (deg/sec)

Figure 76 Continued

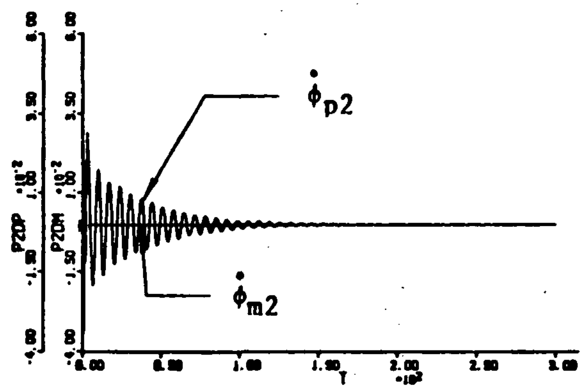

(m) $\dot{\phi}_{p2}$, $\dot{\phi}_{m2}$ (deg/sec)

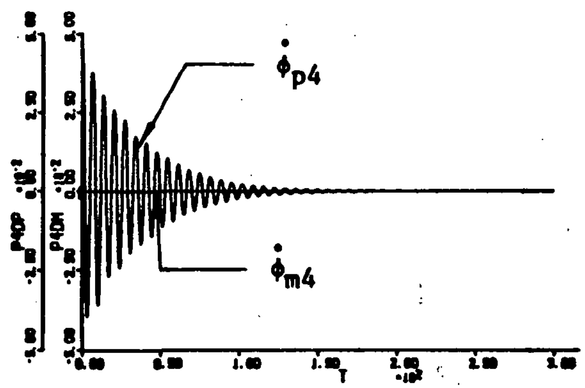

(n) $\dot{\phi}_{p4}$, $\dot{\phi}_{m4}$ (deg/sec)

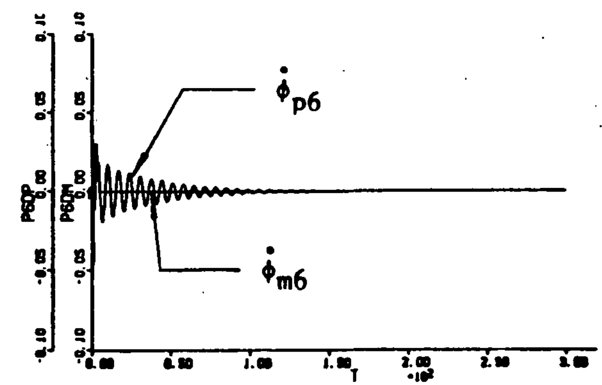

(o) $\dot{\phi}_{p6}$, $\dot{\phi}_{m6}$ (deg/sec)

Figure 76 Continued

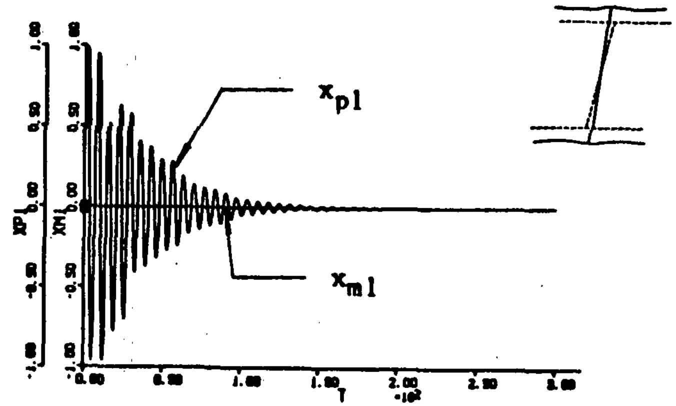

(a) Mode 1

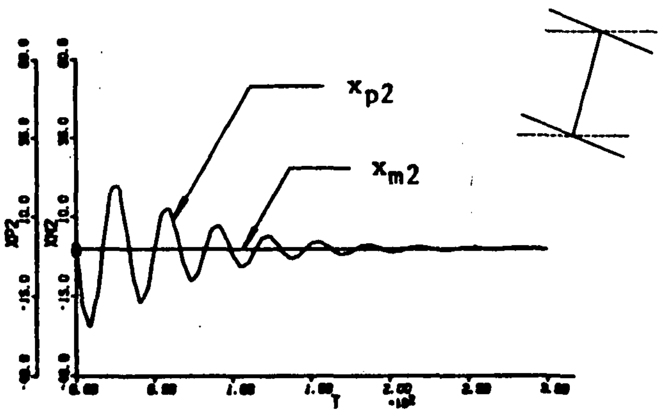

(b) Mode 2

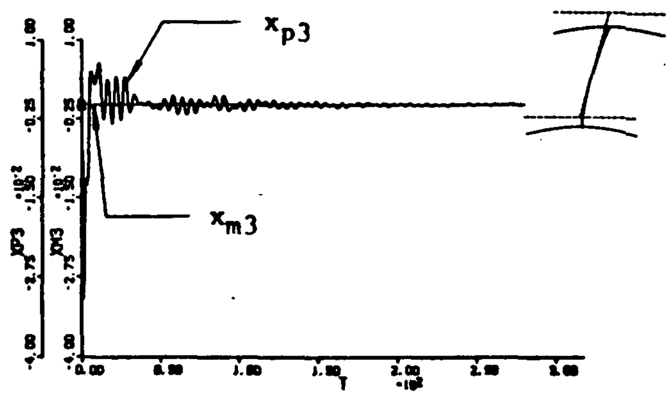

(c) Mode 3

Figure 77 Adaptive Control During Shuttle Hard Docking for Four-Panel Configuration -- Plant and Model Rigid Body Modal Responses

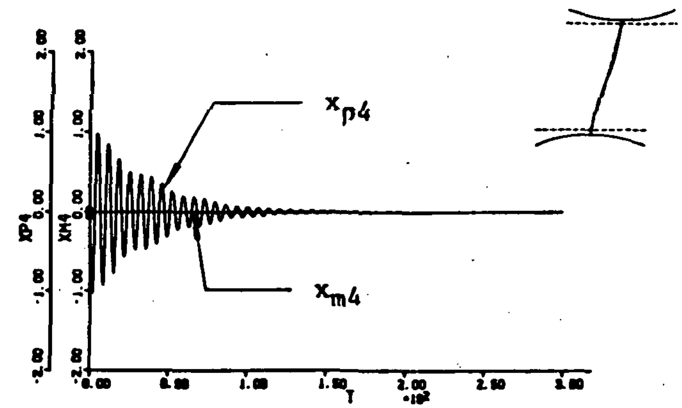

(a) Mode 4

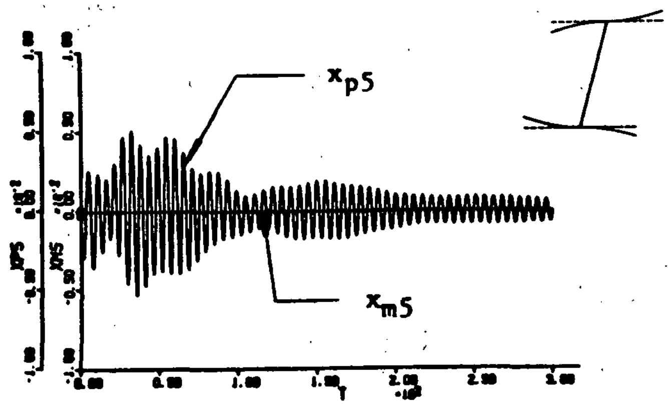

(b) Mode 5

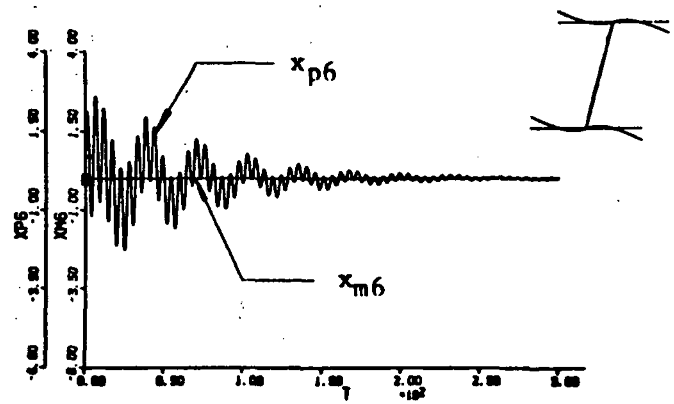

(c) Mode 6

Figure 78 Adaptive Control During Shuttle Hard Docking for Four-Panel Configuration

-- Plant and Model First Bending Group Modal Responses

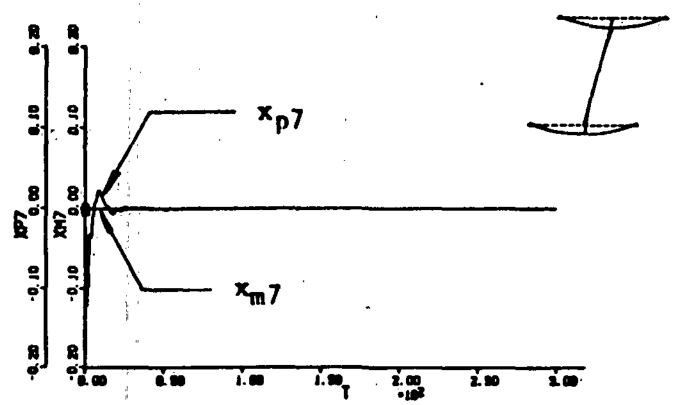

(d) Mode 7

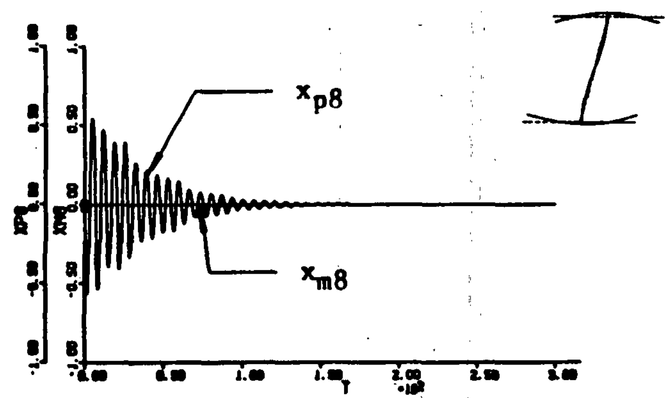

(e) Mode 8

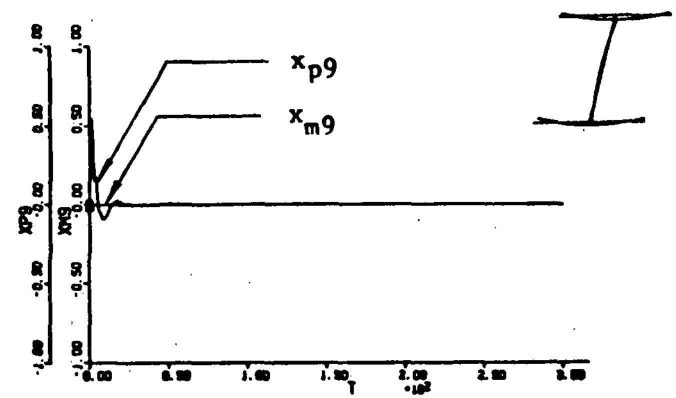

(f) Mode 9

Figure 78 Continued

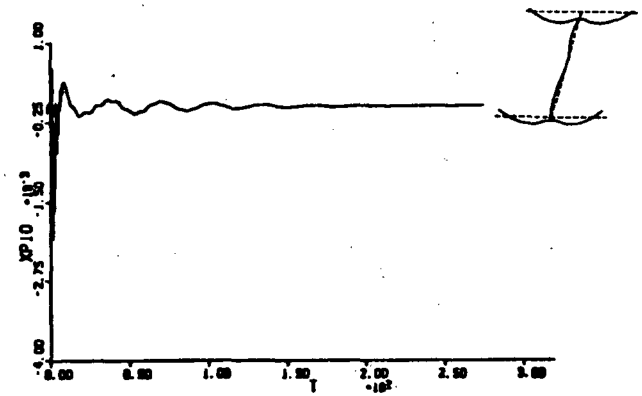

(a) Mode 10

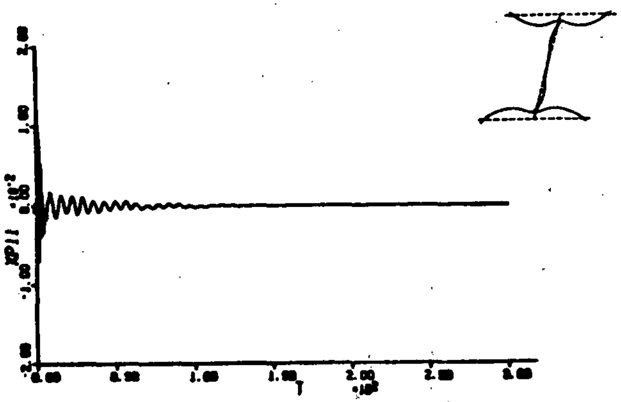

(b) Mode 11

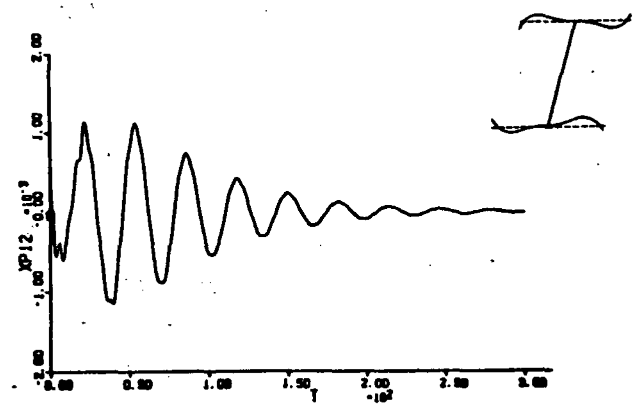

(c) Mode 12

Figure 79 Adaptive Control During Shuttle Hard Docking for Four-Panel Configuration

-- Plant Second Bending Group Modal Responses

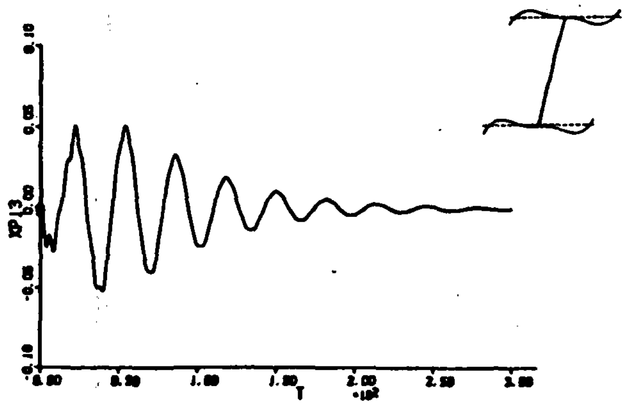

(d) Mode 13

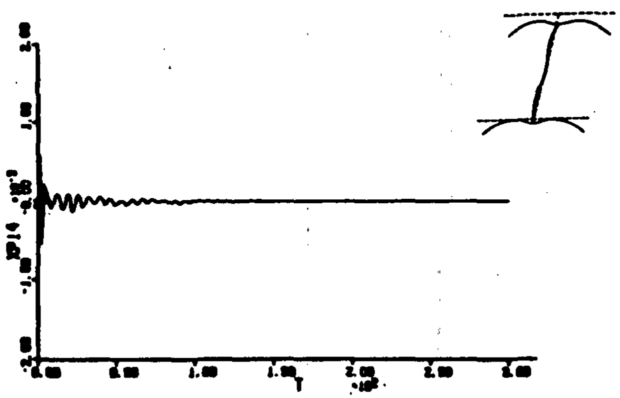

(e) Mode 14

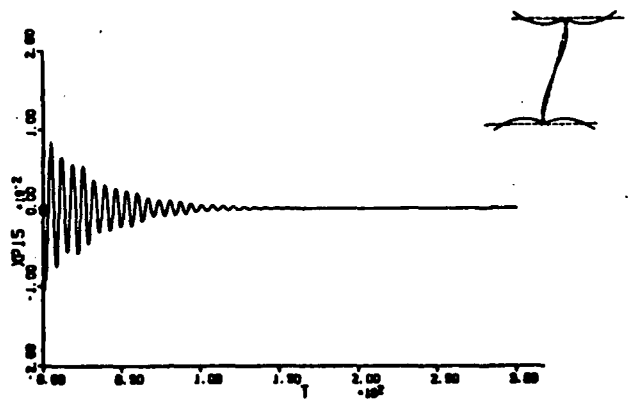

(f) Mode 15

Figure 79 Continued

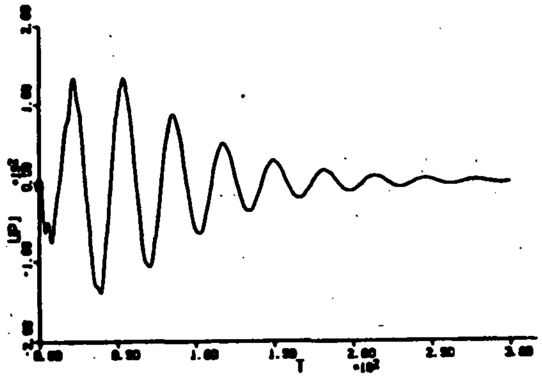

(a) u_{p1}: Control Torque at Left South Panel Tip (ft-lb)

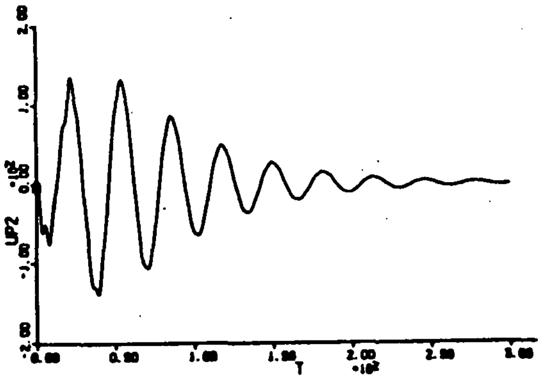

(b) u_{p2}: Control Torque at Right South Panel Tip (ft-lb)

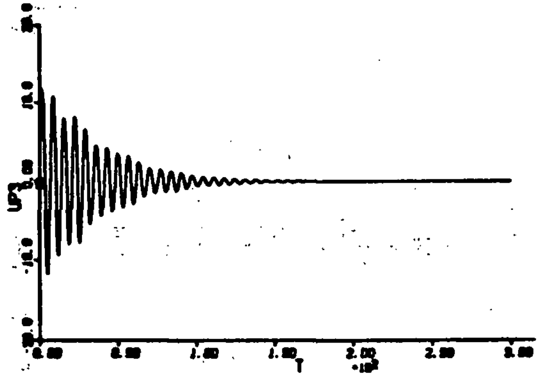

(c) u_{p3}: Control Force at the Root of South Panel (lb)

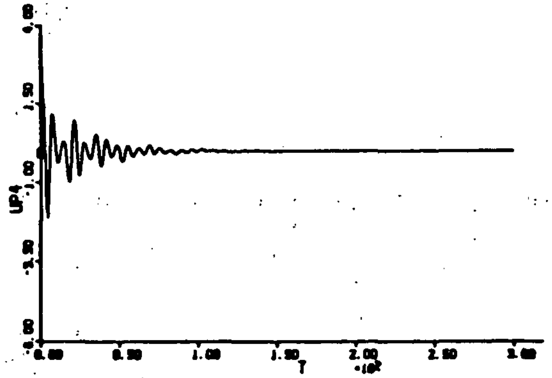

(d) u_{p4}: Control Torque (Bending) at the Root of South Panel (ft-lb)

Figure 80 Adaptive Control During Shuttle Hard Docking for Four-Panel Configuration

— Adaptive Control Inputs

(e) u_{p5}: Control Force at Central Bus (lb)

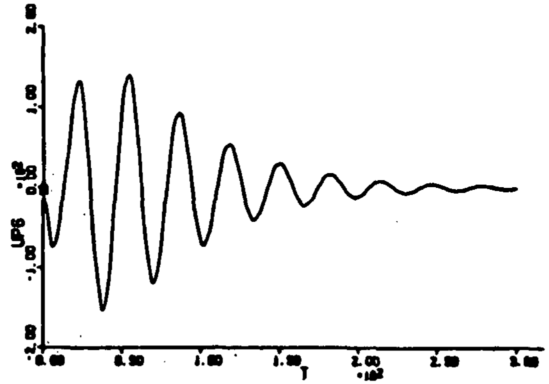

(f) u_{p6}: Control Torque (Twisting) at Central Bus (ft-lb)

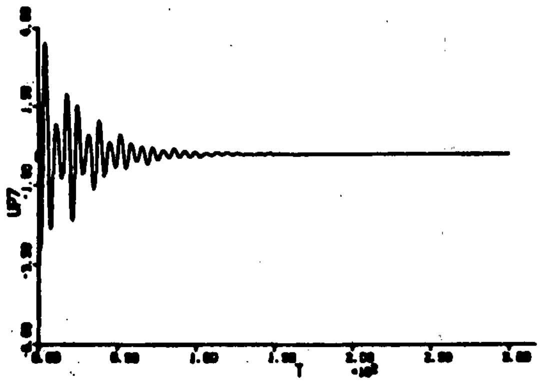

(g) u_{p7}: Control Torque (Bending) at Central Bus (ft-lb)

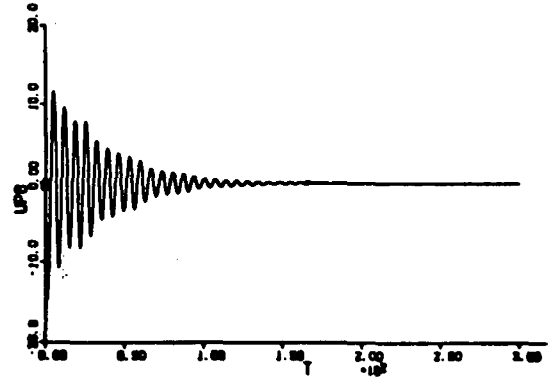

(h) u_{p8}: Control Force at the Root of North Panel (lb)

Figure 80 Continued

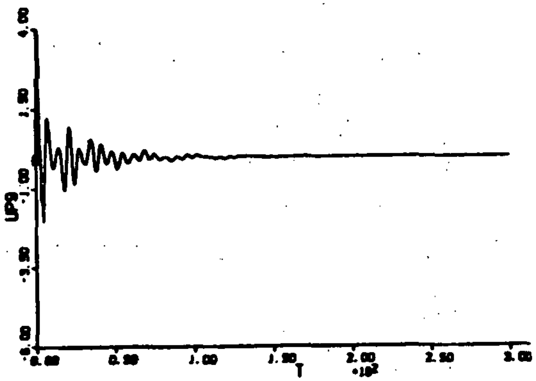

(i) u_{p9}: Control Torque (Bending) at the Root of North Panel (ft-lb)

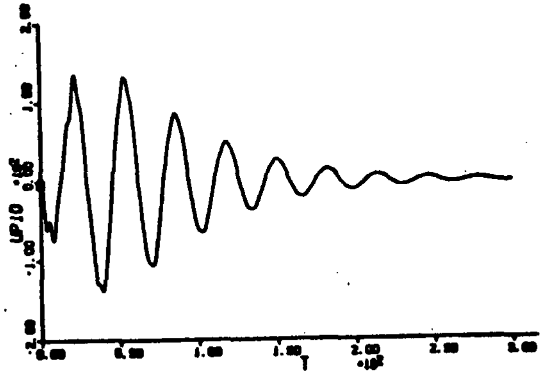

(j) u_{p10}: Control Torque at Left North Panel Tip (ft-lb)

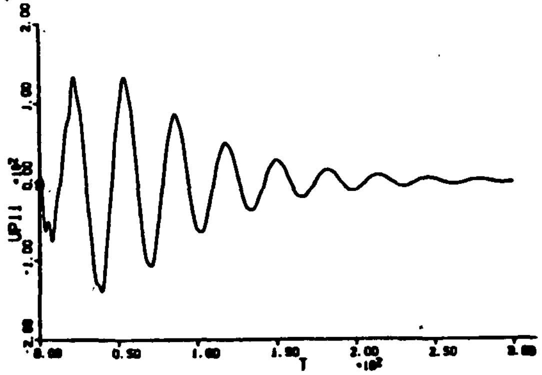

(k) u_{p11}: Control Torque at Right North Panel Tip (ft-lb)

Figure 80 Continued

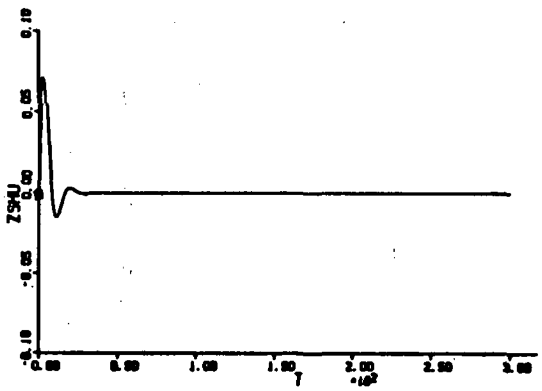

(a) $Z_{shuttle}$ (ft)

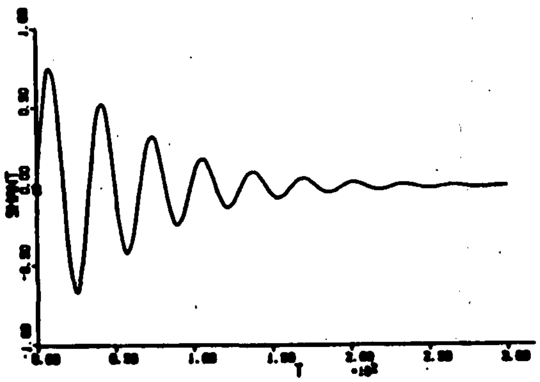

(b) $\theta_{shuttle}$ (deg)

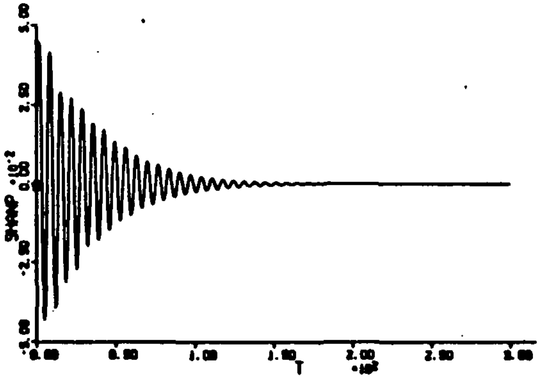

(c) $\phi_{shuttle}$ (deg)

Figure 81 Adaptive Control During Shuttle Hard Docking for Four-Panel Configuration

— Shuttle Linear and Angular Position

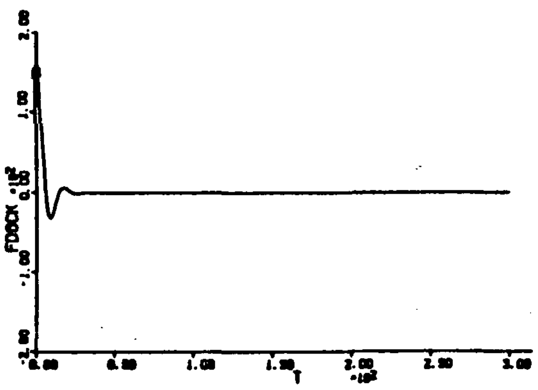

(a) Docking Force F_d (lb)

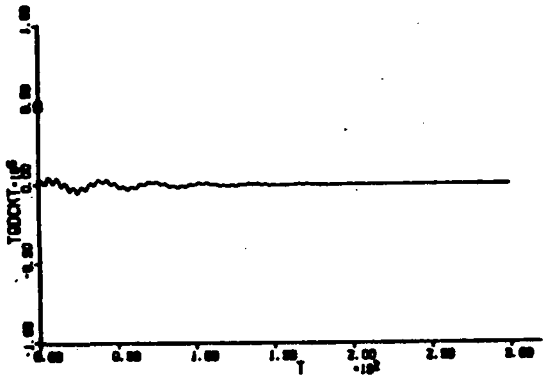

(b) Docking Torque T_d (ft-lb)

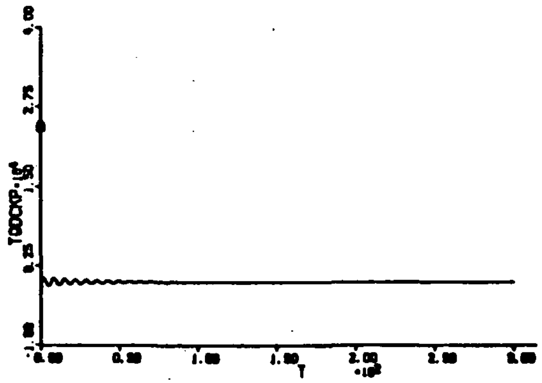

(c) Docking Torque P_d (ft-lb)

Figure 82 Adaptive Control During Shuttle Hard Docking for Four-Panel Configuration

— Docking Force and Torque

APPENDIX A

DEVELOPMENT OF HINGED PAYLOAD DYNAMICS USING LAGRANGIAN APPROACH FOR FOUR-PANEL CONFIGURATION

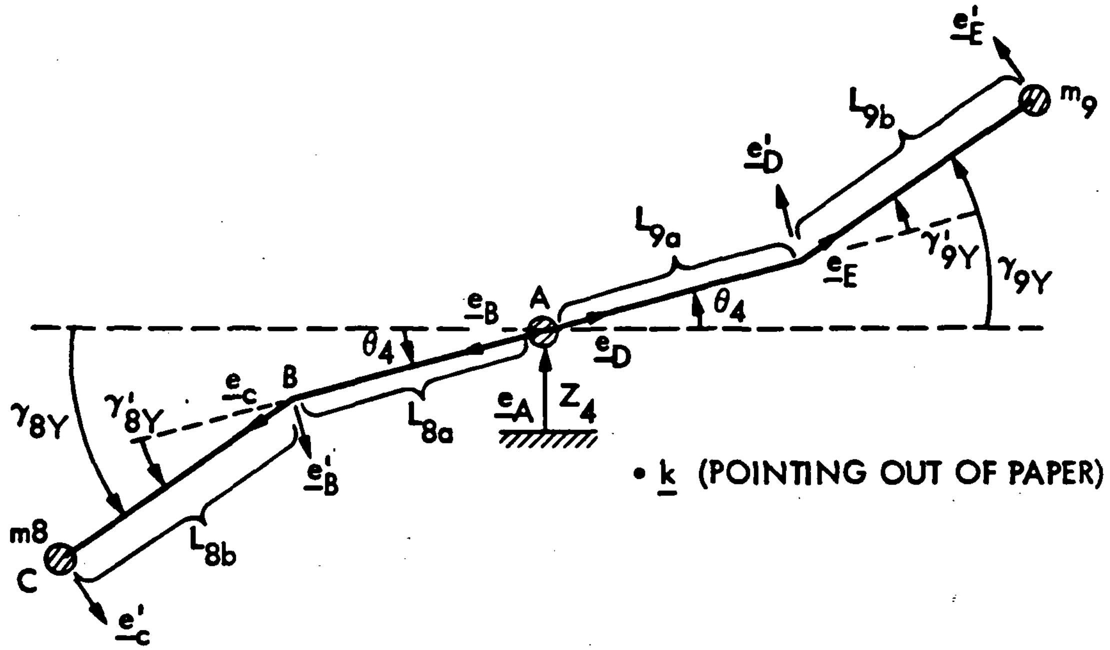

Lagrange's equation:

$$\frac{d}{dt}\left(\frac{\partial L}{\partial \dot{q}_i}\right) - \frac{\partial L}{\partial q_i} = Q_i \qquad \text{(A.1)}$$

Starting from taking position vectors for points A, B and C

$$\underline{P}_A = Z_4\,\underline{e}_A$$

$$\underline{P}_B = Z_4\,\underline{e}_A + L_{8a}\,\underline{e}_B$$

$$\underline{P}_C = Z_4\,\underline{e}_A + L_{8a}\,\underline{e}_B + L_{8b}\,\underline{e}_C$$

then

$$\underline{V}_A = \dot{Z}_4\,\underline{e}_A$$

$$\underline{V}_B = \dot{Z}_4\,\underline{e}_A + L_{8a}\,\dot{\underline{e}}_B$$

$$= \dot{Z}_4 \underline{e}_A + L_{8a} (\dot{\theta}_4 \underline{k} \times \underline{e}_B)$$

$$= \dot{Z}_4 \underline{e}_A + L_{8a} \dot{\theta}_4 \underline{e}_B'$$

$$\underline{V}_C = \dot{Z}_4 \underline{e}_A + L_{8a} \dot{\theta}_4 \underline{e}_B' + L_{8b} \overbrace{(\dot{\gamma}_{8Y} \underline{k} \times \underline{e}_C)}^{\dot{\underline{e}}_C}$$

$$= \dot{Z}_4 \underline{e}_A + L_{8a} \dot{\theta}_4 \underline{e}_B' + L_{8b} \dot{\gamma}_{8Y} \underline{e}_C'$$

Similarly,

$$\underline{V}_D = \dot{Z}_4 \underline{e}_A + L_{9a} \dot{\theta}_4 \underline{e}_D'$$

$$\underline{V}_E = \dot{Z}_4 \underline{e}_A + L_{9a} \dot{\theta}_4 \underline{e}_D' + L_{9b} \dot{\gamma}_{9Y} \underline{e}_E'$$

$$\therefore V_C^2 = \underline{V}_C \cdot \underline{V}_C$$

$$= \dot{Z}_4^2 + L_{8a}^2 \dot{\theta}_4^2 + L_{8b}^2 \dot{\gamma}_{8Y}^2 + 2 \dot{Z}_4 L_{8a} \dot{\theta}_4 (\underline{e}_A \cdot \underline{e}_B')$$

$$+ 2 \dot{Z}_4 L_{8b} \dot{\gamma}_{8Y} (\underline{e}_A \cdot \underline{e}_C') + 2 L_{8a} L_{8b} \dot{\theta}_4 \dot{\gamma}_{8Y} (\underline{e}_B' \cdot \underline{e}_C')$$

$$= \dot{Z}_4^2 + L_{8a}^2 \dot{\theta}_4^2 + L_{8b}^2 \dot{\gamma}_{8Y}^2 - 2 \dot{Z}_4 L_{8a} \dot{\theta}_4 \cos \theta_4$$

$$- 2 \dot{Z}_4 L_{8b} \dot{\gamma}_{8Y} \cos \gamma_{8Y} + 2 L_{8a} L_{8b} \dot{\theta}_4 \dot{\gamma}_{8Y} \cos \gamma_{8Y}'$$

Similarly,

$$V_E^2 = \underline{V}_E \cdot \underline{V}_E$$

$$= \dot{Z}_4^2 + L_{9a}^2 \dot{\theta}_4^2 + L_{9b}^2 \dot{\gamma}_{9Y}^2 + 2 \dot{Z}_4 L_{9a} \dot{\theta}_4 \cos \theta_4$$

$$+ 2 \dot{Z}_4 L_{9b} \dot{\gamma}_{9Y} \cos \gamma_{9Y} + 2 L_{9a} L_{9b} \dot{\theta}_4 \dot{\gamma}_{9Y} \cos \gamma_{9Y}'$$

Hence,

$$T = \frac{1}{2} m_4 \dot{Z}_4^2 + \frac{1}{2} m_8 V_C^2 + \frac{1}{2} m_9 V_E^2 + \frac{1}{2} I_{4YY} \dot{\theta}_4^2 + \frac{1}{2} I_{8YS} \dot{\gamma}_{8Y}^2$$

$$+ \frac{1}{2} I_{9YS} \dot{\gamma}_{9Y}^2 + \frac{1}{2} I_{4XX} \dot{\phi}_4^2 + \frac{1}{2} I_{8XS} \dot{\gamma}_{8X}^2 + \frac{1}{2} I_{9XS} \dot{\gamma}_{9X}^2$$

$$= \frac{1}{2} m_4 \dot{Z}_4^2 + \frac{1}{2} m_8 \Big[\dot{Z}_4^2 + L_{8a}^2 \dot{\theta}_4^2 + L_{8b}^2 (\dot{\theta}_4 + \dot{\gamma}'_{8Y})^2$$

$$- 2 \dot{Z}_4 L_{8a} \dot{\theta}_4 \cos \theta_4 - 2 \dot{Z}_4 L_{8b} (\dot{\gamma}'_{8Y} + \dot{\theta}_4) \cos (\theta_4 + \gamma'_{8Y})$$

$$+ 2 L_{8a} L_{8b} \dot{\theta}_4 (\dot{\gamma}'_{8Y} + \dot{\theta}_4) \cos \gamma'_{8Y} \Big] + \frac{1}{2} m_9 \Big[\dot{Z}_4^2 + L_{9a}^2 \dot{\theta}_4^2$$

$$+ L_{9b}^2 (\dot{\theta}_4 + \dot{\gamma}'_{9Y})^2 + 2 \dot{Z}_4 L_{9a} \dot{\theta}_4 \cos \theta_4$$

$$+ 2 \dot{Z}_4 L_{9b} (\dot{\gamma}'_{9Y} + \dot{\theta}_4) \cos (\theta_4 + \gamma'_{9Y})$$

$$+ 2 L_{9a} L_{9b} \dot{\theta}_4 (\dot{\gamma}'_{9Y} + \dot{\theta}_4) \cos \gamma'_{9Y} \Big] + \frac{1}{2} I_{4YY} \dot{\theta}_4^2$$

$$+ \frac{1}{2} I_{8YS} (\dot{\theta}_4 + \dot{\gamma}'_{8Y})^2 + \frac{1}{2} I_{9YS} (\dot{\theta}_4 + \dot{\gamma}'_{9Y})^2 + \frac{1}{2} I_{4XX} \dot{\phi}_4^2$$

$$+ \frac{1}{2} I_{8XS} (\dot{\phi}_4 + \dot{\gamma}'_{8X})^2 + \frac{1}{2} I_{9XS} (\dot{\phi}_4 + \dot{\gamma}'_{9X})^2$$

$\because V = 0$

$\therefore L = T - V = T$

There are 7 independent variables: Z_4, θ_4, γ'_{8Y}, γ'_{9Y}, ϕ_4, γ'_{8X}, γ'_{9X}, one equation for each of them. The generalized forces are:

$$Q_{Z_4} = \underline{F}_4 \cdot \frac{\partial \underline{P}_A}{\partial Z_4} = \underline{F}_4 \cdot \underline{e}_A = F_4$$

$$Q_{\theta_4} = \underline{T}_{4\theta} \cdot \frac{\partial \dot{\theta}_4 \underline{k}}{\partial \dot{\theta}_4} + \underline{T}_{8Y} \cdot \cancelto{0}{\frac{\partial \dot{\gamma}'_{8Y} \underline{k}}{\partial \dot{\theta}_4}} + \underline{T}_{9Y} \cdot \cancelto{0}{\frac{\partial \dot{\gamma}'_{9Y} \underline{k}}{\partial \dot{\theta}_4}} = T_{4\theta}$$

$$Q_{\gamma'_{8Y}} = \underline{T}_{4\theta} \cdot \cancelto{0}{\frac{\partial \dot{\theta}_4 \underline{k}}{\partial \dot{\gamma}'_{8Y}}} + \underline{T}_{8Y} \cdot \frac{\partial \dot{\gamma}'_{8Y} \underline{k}}{\partial \dot{\gamma}'_{8Y}} + \underline{T}_{9Y} \cdot \cancelto{0}{\frac{\partial \dot{\gamma}'_{9Y} \underline{k}}{\partial \dot{\gamma}'_{8Y}}} = T_{8Y}$$

$$Q_{\gamma'_{9Y}} = \underline{T}_{4\theta} \cdot \cancelto{0}{\frac{\partial \dot{\theta}_4 \underline{k}}{\partial \dot{\gamma}'_{9Y}}} + \underline{T}_{8Y} \cdot \cancelto{0}{\frac{\partial \dot{\gamma}'_{8Y} \underline{k}}{\partial \dot{\gamma}'_{9Y}}} + \underline{T}_{9Y} \cdot \frac{\partial \dot{\gamma}'_{9Y} \underline{k}}{\partial \dot{\gamma}'_{9Y}} = T_{9Y}$$

similarly

$$Q_{\phi_4} = T_{4\phi}$$

$$Q_{\gamma'_{8X}} = T_{8X}$$

$$Q_{\gamma'_{9X}} = T_{9X}$$

Equation for Z_4:

$$\frac{d}{dt}\left(\frac{\partial L}{\partial \dot{Z}_4}\right) - \left(\frac{\partial L}{\partial Z_4}\right) = F_4$$

i.e.,

$$\frac{d}{dt}\Big[m_4\dot{Z}_4 + m_8\dot{Z}_4 - m_8L_{8a}\dot{\theta}_4 \cos\theta_4 - m_8L_{8b}(\dot{\gamma}'_{8Y} + \dot{\theta}_4)\cos(\theta_4 + \gamma'_{8Y})$$

$$+ m_9\dot{Z}_4 + m_9L_{9a}\dot{\theta}_4 \cos\theta_4 + m_9L_{9b}(\dot{\gamma}'_{9Y} + \dot{\theta}_4)\cos(\theta_4 + \gamma'_{9Y})\Big] - 0 = F_4$$

Expand it, we have,

$$m_4\ddot{Z}_4 + m_8\ddot{Z}_4 - m_8L_{8a}\ddot{\theta}_4 \cos\theta_4 + m_8L_{8a}\dot{\theta}_4^2 \sin\theta_4$$

$$- m_8L_{8b}(\ddot{\gamma}'_{8Y} + \ddot{\theta}_4)\cos(\theta_4 + \gamma'_{8Y}) + m_8L_{8b}(\dot{\gamma}'_{8Y} + \dot{\theta}_4)^2 \sin(\gamma'_{8Y} + \theta_4)$$

$$+ m_9\ddot{Z}_4 + m_9L_{9a}\ddot{\theta}_4 \cos\theta_4 - m_9L_{9a}\dot{\theta}_4^2 \sin\theta_4$$

$$+ m_9L_{9b}(\ddot{\gamma}'_{9Y} + \ddot{\theta}_4)\cos(\gamma'_{9Y} + \theta_4)$$

$$- m_9L_{9b}(\dot{\gamma}'_{9Y} + \dot{\theta}_4)^2 \sin(\gamma'_{9Y} + \theta_4) = F_4 \qquad \text{(A.2)}$$

Equation for θ_4:

$$\frac{d}{dt}\left(\frac{\partial L}{\partial \dot{\theta}_4}\right) - \frac{\partial L}{\partial \theta_4} = T_{4\theta}$$

i.e.,

$$\frac{d}{dt}\Big[m_8 L_{8a}^2 \dot{\theta}_4 + m_8 L_{8b}^2 (\dot{\theta}_4 + \dot{\gamma}'_{8Y}) - m_8 \dot{Z}_4 L_{8a} \cos \theta_4$$

$$- m_8 \dot{Z}_4 L_{8b} \cos (\theta_4 + \gamma'_{8Y}) + m_8 L_{8a} L_{8b} \dot{\gamma}'_{8Y} \cos \gamma'_{8Y}$$

$$+ 2\, m_8 L_{8a} L_{8b} \dot{\theta}_4 \cos \gamma'_{8Y} + m_9 L_{9a}^2 \dot{\theta}_4 + m_9 L_{9b}^2 (\dot{\theta}_4 + \dot{\gamma}'_{9Y})$$

$$+ m_9 \dot{Z}_4 L_{9a} \cos \theta_4 + m_9 \dot{Z}_4 L_{9b} \cos (\theta_4 + \gamma'_{9Y})$$

$$+ m_9 L_{9a} L_{9b} \dot{\gamma}'_{9Y} \cos \gamma'_{9Y} + 2\, m_9 L_{9a} L_{9b} \dot{\theta}_4 \cos \gamma'_{9Y} + I_{4YY} \dot{\theta}_4$$

$$+ I_{8YS} (\dot{\theta}_4 + \dot{\gamma}'_{8Y}) + I_{9YS} (\dot{\theta}_4 + \dot{\gamma}'_{9Y})\Big]$$

$$- \Big[m_8 \dot{Z}_4 L_{8a} \dot{\theta}_4 \sin \theta_4 + m_8 \dot{Z}_4 L_{8b} (\dot{\gamma}'_{8Y} + \dot{\theta}_4) \sin (\theta_4 + \gamma'_{8Y})$$

$$- m_9 \dot{Z}_4 L_{9a} \dot{\theta}_4 \sin \theta_4 - m_9 \dot{Z}_4 L_{9b} (\dot{\gamma}'_{9Y} + \dot{\theta}_4) \sin (\theta_4 + \gamma'_{9Y})\Big] = T_{4\theta}$$

Expand it, we have,

$$m_8 L_{8a}^2 \ddot{\theta}_4 + m_8 L_{8b}^2 \ddot{\theta}_4 + m_8 L_{8b}^2 \ddot{\gamma}'_{8Y} - m_8 \ddot{Z}_4 L_{8a} \cos \theta_4$$

$$- m_8 \ddot{Z}_4 L_{8b} \cos (\theta_4 + \gamma'_{8Y}) + m_8 L_{8a} L_{8b} \ddot{\gamma}'_{8Y} \cos \gamma'_{8Y}$$

$$- m_8 L_{8a} L_{8b} \dot{\gamma}'^2_{8Y} \sin \gamma'_{8Y} + 2\, m_8 L_{8a} L_{8b} \ddot{\theta}_4 \cos \gamma'_{8Y}$$

$$- 2\, m_8 L_{8a} L_{8b} \dot{\theta}_4 \dot{\gamma}'_{8Y} \sin \gamma'_{8Y} + m_9 L_{9a}^2 \ddot{\theta}_4 + m_9 L_{9b}^2 \ddot{\theta}_4 + m_9 L_{9b}^2 \ddot{\gamma}'_{9Y}$$

$$+ m_9 \ddot{Z}_4 L_{9a} \cos \theta_4 + m_9 \ddot{Z}_4 L_{9b} \cos (\theta_4 + \gamma'_{9Y})$$

$$+ m_9 L_{9a} L_{9b} \ddot{\gamma}'_{9Y} \cos \gamma'_{9Y} - m_9 L_{9a} L_{9b} \dot{\gamma}'^2_{9Y} \sin \gamma'_{9Y}$$

$$+ 2\, m_9 L_{9a} L_{9b} \ddot{\theta}_4 \cos \gamma'_{9Y} - 2\, m_9 L_{9a} L_{9b} \dot{\theta}_4 \dot{\gamma}'_{9Y} \sin \gamma'_{9Y}$$

$$+ I_{4YY} \ddot{\theta}_4 + I_{8YS} \ddot{\theta}_4 + I_{8YS} \ddot{\gamma}'_{8Y} + I_{9YS} \ddot{\theta}_4 + I_{9YS} \ddot{\gamma}'_{9Y} = T_{4\theta} \qquad \text{(A.3)}$$

Equation for γ'_{8Y}:

$$\frac{d}{dt}\left(\frac{\partial L}{\partial \dot{\gamma}'_{8Y}}\right) - \frac{\partial L}{\partial \gamma'_{8Y}} = T_{8Y}$$

i.e.,

$$\frac{d}{dt}\Big[m_8 L_{8b}^2 (\dot{\theta}_4 + \dot{\gamma}'_{8Y}) - m_8 \dot{Z}_4 L_{8b} \cos (\theta_4 + \gamma'_{8Y}) + m_8 L_{8a} L_{8b} \dot{\theta}_4 \cos \gamma'_{8Y}$$

$$+ I_{8YS} (\dot{\theta}_4 + \dot{\gamma}'_{8Y}) \Big] - \Big[m_8 \dot{Z}_4 L_{8b} (\dot{\gamma}'_{8Y} + \dot{\theta}_4) \sin (\theta_4 + \gamma'_{8Y})$$

$$- m_8 L_{8a} L_{8b} \dot{\theta}_4 (\dot{\gamma}'_{8Y} + \dot{\theta}_4) \sin \gamma'_{8Y} \Big] = T_{8Y}$$

Expand it, we have,

$$m_8 L_{8b}^2 \ddot{\theta}_4 + m_8 L_{8b}^2 \ddot{\gamma}'_{8Y} - m_8 \ddot{Z}_4 L_{8b} \cos(\theta_4 + \gamma'_{8Y}) + m_8 L_{8a} L_{8b} \ddot{\theta}_4 \cos \gamma'_{8Y}$$

$$+ I_{8YS} \ddot{\theta}_4 + I_{8YS} \ddot{\gamma}'_{8Y} + m_8 L_{8a} L_{8b} \dot{\theta}_4^2 \sin \gamma'_{8Y} = T_{8Y} \qquad \text{(A.4)}$$

Equation for γ'_{9Y}:

$$\frac{d}{dt}\left(\frac{\partial L}{\partial \dot{\gamma}'_{9Y}}\right) - \frac{\partial L}{\partial \gamma'_{9Y}} = T_{9Y}$$

i.e.,

$$\frac{d}{dt}\Big[m_9 L_{9b}^2 (\dot{\theta}_4 + \dot{\gamma}'_{9Y}) + m_9 \dot{Z}_4 L_{9b} \cos(\theta_4 + \gamma'_{9Y})$$

$$+ m_9 L_{9a} L_{9b} \dot{\theta}_4 \cos \gamma'_{9Y} + I_{9YS} (\dot{\theta}_4 + \dot{\gamma}'_{9Y}) \Big]$$

$$- \Big[- m_9 \dot{Z}_4 L_{9b} (\dot{\gamma}'_{9Y} + \dot{\theta}_4) \sin(\theta_4 + \gamma'_{9Y})$$

$$- m_9 L_{9a} L_{9b} \dot{\theta}_4 (\dot{\gamma}'_{9Y} + \dot{\theta}_4) \sin \gamma'_{9Y} \Big] = T_{9Y}$$

Expand it, we have,

$$m_9 L_{9b}^2 \ddot{\theta}_4 + m_9 L_{9b}^2 \ddot{\gamma}'_{9Y} + m_9 \ddot{Z}_4 L_{9b} \cos(\theta_4 + \gamma'_{9Y}) + m_9 L_{9a} L_{9b} \ddot{\theta}_4 \cos \gamma'_{9Y}$$

$$+ I_{9YS} \ddot{\theta}_4 + I_{9YS} \ddot{\gamma}'_{9Y} + m_9 L_{9a} L_{9b} \dot{\theta}_4^2 \sin \gamma'_{9Y} = T_{9Y} \qquad \text{(A.5)}$$

After linearization, Eqs. (A.2), (A.3), (A.4), and (A.5) become:

Equation for Z_4:

$$\boxed{(m_4 + m_8 + m_9)\ddot{Z}_4 + (m_9 L_9 - m_8 L_8)\ddot{\theta}_4 - m_8 L_{8b}\ddot{\gamma}'_{8Y} + m_9 L_{9b}\ddot{\gamma}'_{9Y} = F_4}$$

Equation for θ_4:

$$\boxed{\begin{aligned}&(m_9 L_9 - m_8 L_8)\ddot{Z}_4 + \left(m_8 L_8^2 + m_9 L_9^2 + I_{4YY} + I_{8YS} + I_{9YS}\right)\ddot{\theta}_4\\&+ \left(m_8 L_{8b}^2 + m_8 L_{8a} L_{8b} + I_{8YS}\right)\ddot{\gamma}'_{8Y}\\&+ \left(m_9 L_{9b}^2 + m_9 L_{9a} L_{9b} + I_{9YS}\right)\ddot{\gamma}'_{9Y} = T_{4\theta}\end{aligned}}$$

Equation for γ'_{8Y}:

$$\boxed{- m_8 L_{8b}\ddot{Z}_4 + \left(m_8 L_{8b}^2 + m_8 L_{8a} L_{8b} + I_{8YS}\right)\ddot{\theta}_4 + \left(m_8 L_{8b}^2 + I_{8YS}\right)\ddot{\gamma}'_{8Y} = T_{8Y}}$$

Equation for γ'_{9Y}:

$$\boxed{m_9 L_{9b}\ddot{Z}_4 + \left(m_9 L_{9b}^2 + m_9 L_{9a} L_{9b} + I_{9YS}\right)\ddot{\theta}_4 + \left(m_9 L_{9b}^2 + I_{9YS}\right)\ddot{\gamma}'_{9Y} = T_{9Y}}$$

The equations for ϕ_4, γ'_{8X}, γ'_{9X} are:

Equation for ϕ_4:

$$\frac{d}{dt}\left(\frac{\partial L}{\partial \dot{\phi}_4}\right) - \frac{\partial L}{\partial \phi_4} = T_{4\phi}$$

i.e.,

$$\frac{d}{dt}\left[I_{4XX}\dot{\phi}_4 + I_{8XS}\left(\dot{\phi}_4 + \dot{\gamma}'_{8X}\right) + I_{9XS}\left(\dot{\phi}_4 + \dot{\gamma}'_{9X}\right) \right] = T_{4\phi}$$

i.e.,

$$\boxed{(I_{4XX} + I_{8XS} + I_{9XS})\,\ddot{\phi}_4 + I_{8XS}\ddot{\gamma}'_{8X} + I_{9YS}\ddot{\gamma}'_{9X} = T_{4\phi}}$$

Equation for γ'_{8X}:

$$\frac{d}{dt}\left(\frac{\partial L}{\partial \dot{\gamma}'_{8X}}\right) - \frac{\partial L}{\partial \gamma'_{8X}} = T_{8X}$$

i.e.,

$$\frac{d}{dt}\left[I_{8XS}\left(\dot{\phi}_4 + \dot{\gamma}'_{8X}\right)\right] = T_{8X}$$

i.e.,

$$\boxed{I_{8XS}\ddot{\phi}_4 + I_{8XS}\ddot{\gamma}'_{8X} = T_{8X}}$$

Equation for γ'_{9X}:

$$\frac{d}{dt}\left(\frac{\partial L}{\partial \dot{\gamma}'_{9X}}\right) - \frac{\partial L}{\partial \gamma'_{9X}} = T_{9X}$$

$$\frac{d}{dt}\left[I_{9XS}\left(\dot{\phi}_4 + \dot{\gamma}'_{9X}\right)\right] = T_{9X}$$

$$\boxed{I_{9XS}\ddot{\phi}_4 + I_{9XS}\ddot{\gamma}'_{9X} = T_{9X}}$$

APPENDIX B

DEFINITION OF POSITIVE REALNESS AND STRICTLY POSITIVE REALNESS OF MATRICES [55]

Definition B.1

An m x m matrix $H(s)$ of real rational functions is positive real if

(1) All elements of $H(s)$ are analytic in the open right half plane $Re[s] > 0$ (i.e., they do not have poles with positive real parts).

(2) The eventual poles of any element of $H(s)$ on the axis $Re[s] = 0$ are distinct, and the associated residual matrix of $H(s)$ is positive semidefinite Hermitian.

(3) The matrix $H(j\omega)+H^T(-j\omega)$ is a positive semidefinite Hermitian for all real values of ω which are not a pole of any element of $H(s)$.

Definition B.2

An m x m matrix $H(s)$ of real rational functions is strictly positive real if

(1) All elements of $H(s)$ are analytic in the closed right half plane $Re[s] \geq 0$ (i.e., they do not have poles with non-negative real parts).

(2) The matrix $H(j\omega)+H^T(-j\omega)$ is a positive definite Hermitian for all real ω.

APPENDIX C

DERIVATION OF FORMULAS FOR CALCULATING THE

SPRING CONSTANTS AND DAMPING FACTORS OF DOCKING DEVICE

Consider the angular springs and dampers first. Referring to the following figure, the moment of inertia I_2 of the core body of the space station is used to represent the space station and I_s represents the shuttle

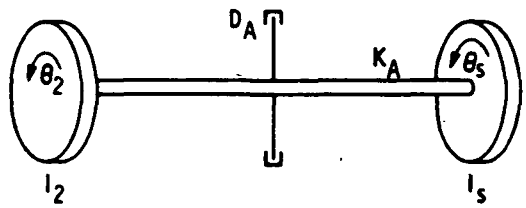

the equations of motion can be written as

$$I_2\ddot{\theta}_2 + D_A(\dot{\theta}_2-\dot{\theta}_s) + K_A(\theta_2-\theta_s) = T_2 \tag{C.1}$$

$$I_2\ddot{\theta}_s + D_A(\dot{\theta}_s-\dot{\theta}_2) + K_A(\theta_s-\theta_2) = T_s \tag{C.2}$$

Assume that docking occurs at time $t = 0$, and $\theta_2(0) = \theta_s(0) = 0$ (this will not affect the values of K_A and D_A). Take Laplace Transforms, Eqs. (C.1) and (C.2) become

$$(I_2s^2 + D_As + K_A)\theta_2(s) - (D_As+K_A)\theta_s(s) = T_2(s) \tag{C.3}$$

$$(I_ss^2 + D_As + K_A)\theta_s(s) - (D_As+K_A)\theta_2(s) = T_s(s) \tag{C.4}$$

From Eq. (C.4)

$$\theta_s(s) = \frac{(D_A s + K_A)\theta_2(s)}{I_s s^2 + D_A s + K_A} + \frac{T_s(s)}{I_s s^2 + D_A s + K_A} \quad \text{(C.5)}$$

Substituting Eq. (C.5) into Eq. (C.3), we have,

$$(I_2 s^2+D_A s+K_A)\theta_2(s) - \frac{(D_A s+K_A)^2}{(I_s s^2+D_A s+K_A)}\theta_2(s) = T_2(s) + \frac{(D_A s+K_A)}{(I_s s^2+D_A s+K_A)}T_s(s) \quad \text{(C.6)}$$

i.e.,

$$(I_2 s^2+D_A s+K_A)\ (I_s s^2+D_A s+K_A)\theta_2(s) - (D_A s+K_A)^2\theta_2(s)$$

$$= (I_s s^2+D_A s+K_A)\ T_2(s) + (D_A s+K_A)\ T_s(s) \quad \text{(C.7)}$$

For the purpose of obtaining the characteristics of the system, the right-hand side of Eq. (C.7) is set to zero. Then we have

$$[I_2 I_s s^2 + (I_2+I_s)D_A s + (I_2+I_s)K_A]s^2 = 0 \quad \text{(C.8)}$$

for $s \neq 0$ ($\because s^2 = 0$ implies two rigid modes at the origin)

$$I_2 I_s s^2 + (I_2+I_s)D_A s + (I_2+I_s)K_A = 0 \quad \text{(C.9)}$$

or

$$s^2 + \underbrace{\left(\frac{I_2+I_s}{I_2 I_s}\right) D_A}_{2\zeta_A \omega_A} s + \underbrace{\left(\frac{I_2+I_s}{I_2 I_s}\right) K_A}_{\omega_A^2} = 0 \tag{C.10}$$

Hence,

$$\omega_A = \sqrt{\left(\frac{I_2+I_s}{I_2 I_s}\right) K_A} \tag{C.11}$$

$$\zeta_A = \frac{1}{2\omega_A}\left(\frac{I_2+I_s}{I_2 I_s}\right) D_A = \frac{D_A}{2} \sqrt{\left(\frac{I_2+I_s}{I_2 I_s}\right)\frac{1}{K_A}} \tag{C.12}$$

and

$$K_A = \omega_A^2 \left(\frac{I_2 I_s}{I_2+I_s}\right) \tag{C.13}$$

$$D_A = 2\zeta_A \omega_A \left(\frac{I_2 I_s}{I_2+I_s}\right) \tag{C.14}$$

For the linear springs and dampers, K_L and D_L are obtained as follows by using the same approach

$$K_L = \omega_L^2 \left(\frac{M_2 M_s}{M_2+M_s}\right) \tag{C.15}$$

$$D_L = 2\zeta_L \omega_L \left(\frac{M_2 M_s}{M_2+M_s}\right) \tag{C.16}$$

where M_2 is the mass of the core body of the space station and M_s is the mass of the shuttle.

APPENDIX D

PROGRAM LISTING FOR THE SIMULATION OF ADAPTIVE CONTROL DURING SHUTTLE HARD DOCKING TO FOUR-PANEL SPACE STATION

```
PROGRAM  APPLICATION OF ADAPTIVE CONTROL ON SPACE STATION (15 DOF)
'             CREATED OCT 1984 --BY C.H.C.IH                          '
'====================== INITIAL ================================'
INITIAL
'          ****************************************************'
'          *             TYPE AND DIMENSION OF VARIABLES        *'
'          ****************************************************'
 INTEGER N,N2,M,L,L2,Q,II,J,K,NSTP1,NSTP2
   ARRAY ZP(15),ZPD(15),ZM(15),ZMD(15),ZP0(15),ZPD0(15),ZPDD(15)
   ARRAY AP(30,30),BP(30,11),CP(11,30)
   ARRAY AM(18,18),BM(18,11),CM(11,18)
   ARRAY XP(30),XPD(30),XP0(30),XM(18),XMD(18),XM0(18)
   ARRAY B(15,11),C(11,15),BPF(15,11),CPF(11,15),BMF(9,11),CMF(11,9)
   ARRAY YP(11),YM(11),UP(11),UM(11)
   ARRAY ETA(15),ETA0(15),ETAD(15),ETAD0(15),ETADD(15)
   ARRAY ETAS(9),ETASD(9),ETAS0(9),ETASD0(9)
   ARRAY EVAL(15),EVEC(15,15),EVECT(15,15),EVECI(15,15)
   ARRAY EVECS(15,9),EVECST(9,15),EVECSB(15,9)
   ARRAY TA(40,40),TB(40,40),TAS(40),TBS(40),R(40),RT(1,40)
   ARRAY DAMPFC(15),DAMP(15,15),ZETA(9),DAM(9,9),W2(15,15),W2M(9,9)
   ARRAY KI(11,40),KP(11,40),KID(11,40),KI0(11,40),MASS(15,15)
   ARRAY DUMY4(1,40),DUMY5(1,40),DUMY6(11),MT(15,15),MTT(15,15)
   ARRAY DUMY7(11),DUMY8(30),DUMY9(30),DUMY10(18),DUMY11(18)
   ARRAY EYS(11),EY(11,1),STIFF(15,15),K1(15,15)
   ARRAY FDDOCK(3),B1(15,3),BDF(15,3),BD(30,3)
   ARRAY DUMY12(30),DUMY13(30),SCR1(15),SCR2(15),FREQ(15)
CONSTANT  N=15            $'NUMBER OF PHYSICAL COORDINATES'
                           '(ALSO NUMBER OF MODAL COORDINATES)'
CONSTANT  N2=30           $'NUMBER OF PLANT STATES'
CONSTANT  M=11            $'NUMBER OF PLANT INPUTS AND MODEL INPUTS'
                           '(ALSO NUMBER OF PLANT OUTPUTS AND MODEL'
                           ' OUTPUTS)                               '
CONSTANT  L=9             $'NUMBER OF THE MODES RETAINED(TO FORM    '
                           'THE MODEL)                              '
CONSTANT  L2=18           $'NUMBER OF MODEL STATES'
CONSTANT  UM=11*0.        $'MODEL INPUT'
CONSTANT  TFINAL=100.0    $'TIME TO STOP'
CINTERVAL CINT=0.2        $'COMMUNICATION INTERVAL'
'          ****************************************************'
'          * DEFINE THE PHYSICAL PARAMETERS OF THE SPACE STATION *'
'          ****************************************************'
CONSTANT  G=32.174        $'GRAVITATIONAL ACCELERATION'
CONSTANT  ZETA=9*0.707    $'DAMPING RATIOS OF THE REFERENCE MODEL'
CONSTANT  EIS=9475776.
CONSTANT  LS=115.
CONSTANT  LE=140.
CONSTANT  RHOS=.541
CONSTANT  RHOE=1.048
CONSTANT  M4=4165.35
CONSTANT  M8=994.72
```

```
CONSTANT  M9=994.72
CONSTANT  I4XX=3.869E+6
CONSTANT  I4YY=1.343E+6
CONSTANT  I8XS=2.437E+4
CONSTANT  I9XS=2.437E+4
CONSTANT  I8YS=5.637E+4
CONSTANT  I9YS=5.637E+4
CONSTANT  L8A=7.
CONSTANT  L8B=11.
CONSTANT  L9A=7.
CONSTANT  L9B=11.
CONSTANT  FAC=10.
CONSTANT  PI=3.14159265
          L8=L8A+L8B
          L9=L9A+L9B
          EIE=FAC*EIS
CONSTANT  TAS=5*2.5E+6,2*2.5E+8,4*2.5E+6,18*1000.,11*400.
CONSTANT  TBS=5*2.5E+6,2*2.5E+8,4*2.5E+6,18*1000.,11*400.
CONSTANT  DAMPFC=15*0.005$'MODAL DAMPING RATIOS OF THE PLANT'
CONSTANT  ALPHA=0.2
CONSTANT  NSTP1=200
CONSTANT  NSTP2=50
CONSTANT  TSW=5.0
          DTRCC=PI/180.0
          Q=M+L2+M
          DO 40 II=1,N
          DO 30 J=1,N
          K1(II,J)=0.
      30..CONTINUE
      40..CONTINUE
          K1(7,7)=28184.
          K1(8,8)=339324.
          K1(9,9)=244388.
          DO 60 II=1,M
          DO 50 J=1,Q
          K10(II,J)=0.
      50..CONTINUE
      60..CONTINUE
          DO 62 II=1,N
          DO 61 J=1,3
          B1(II,J)=0.
      61..CONTINUE
      62..CONTINUE
          B1(7,1)=1.
          B1(8,2)=1.
          B1(9,3)=1.
          DO 65 II=1,N
          DO 63 J=1,M
          B(II,J)=0.
      63..CONTINUE
      65..CONTINUE
          B(2,1)=1.
          B(4,2)=1.
          B(5,3)=1.
          B(6,4)=1.
          B(7,5)=1.
          B(8,6)=1.
          B(9,7)=1
```

```
             B(10,8)=1.
             B(11,9)=1.
             B(13,10)=1.
             B(15,11)=1.
             DO 68 II=1,M
             DO 66 J=1,N
             C(II,J)=0.
         66..CONTINUE
         68..CONTINUE
             C(1,2)=1.
             C(2,4)=1.
             C(3,5)=1.
             C(4,6)=1.
             C(5,7)=1.
             C(6,8)=1.
             C(7,9)=1.
             C(8,10)=1.
             C(9,11)=1.
             C(10,13)=1.
             C(11,15)=1.

'            *********************************************************'
'            *        DEFINE THE DOCKING DISTURBANCE PARAMETERS      *'
'            *********************************************************'

CONSTANT     ZDAM=3.06E+3    $'SOFT DOCKING LINEAR DAMPING COEFF'
CONSTANT     ZSTI=1.3597E+3  $'SOFT DOCKING LINEAR SPRING CONST'
CONSTANT     RDAMT=1.4593E+7$'SOFT DOCKING ANGULAR DAMPING COEFF'
CONSTANT     RDAMP=7.078E+6
CONSTANT     RSTIT=6.4845E+7$'SOFT DOCKING ANGULAR SPRING CONST'
CONSTANT     RSTIP=3.145E+7
CONSTANT     MSHUT=251600.   $'MASS OF THE SHUTTLE'
CONSTANT     ISHUTT=7.54E+6  $'MOMENT OF INERTIA OF THE SHUTTLE'
CONSTANT     ISHUTP=1.0E+6

'            *******************************************************'
'            *   CALCULATES M AND K MATRICES,THE EIGENVALUES AND   *'
'            *   EIGENVECTORS OF THE OPEN LOOP SYSTEM,FORM THE     *'
'            *   DAMPING MATRIX IN MODAL COORDINATES,ASSEMBLE AP   *'
'            *   BP AND CP MATRICES OF THE PLANT                   *'
'            *******************************************************'

PROCEDURAL(MASS,STIFF,EVAL,EVEC,DAMP,FREQ,AP,BP,CP,BD=...
              EIS,EIE,RHOS,RHOE,LS,LE,M4,M8,M9,I4XX,I4YY,I8XS,I9XS,...
              I8YS,I9YS,L8A,L9A,L8B,L9B,L8,L9,DAMPFC,B1)
             CALL READMK(MASS,STIFF,EIS,EIE,RHOS,RHOE,LS,LE,M4,M8,...
                         M9,I4XX,I4YY,I8XS,I9XS,I8YS,I9YS,L8A,L9A,...
                         L8B,L9B,L8,L9)
             CALL MADD(STIFF,K1,STIFF,N,N)
             CALL OPLOOP(MASS,STIFF,EVAL,EVEC)
             DO 69 II=1,N
             SCR1(II)=ABS(EVAL(II))
             SCR2(II)=SQRT(SCR1(II))
             FREQ(II)=SCR2(II)/(2.*PI)
         69..CONTINUE
             CALL MPRINT(MASS,N,N,12,12H MASS MATRIX)
             CALL MPRINT(STIFF,N,N,17,17H STIFFNESS MATRIX)
             CALL MPRINT(EVAL,1,N,19,19H EIGENVALUES (W**2))
```

```
      CALL MPRINT(EVEC,N,N,20,20H MODAL MATRIX (EVEC))
      CALL MPRINT(FREQ,1,N,23,23H MODAL FREQUENCIES (HZ))
      DO 80 II=1,N
      DO 70 J=1,N
      W2(II,J)=0.0
   70..CONTINUE
      W2(II,II)=ABS(EVAL(II))
   80..CONTINUE
      CALL MPRINT(W2,N,N,43,...
                 43H GENERALIZED STIFFNESS MATRIX OF PLANT (W2))
      CALL MTRANS(EVEC,EVECT,N,N)
      CALL MMULT(EVECT,MASS,MT,N,N,N)
      CALL MMULT(MT,EVEC,MTT,N,N,N)
      CALL MPRINT(MTT,N,N,4,4H MTT)
      DO 90 II=1,N
      DO 90 J=1,N
      DAMP(II,J)=0.0
   90..CONTINUE
      DO 95 II=1,N
      DAMP(II,II)=2.0*DAMPFC(II)*SQRT(W2(II,II))
   95..CONTINUE
      CALL MCOPY(EVEC,EVECI,N,N)
      CALL INVERS(EVECI,N)
      CALL MPRINT(DAMP,N,N,5,5H DAMP)
      DO 110 II=1,N
      DO 110 J=1,N
      AP(II,J)=0.
  110..CONTINUE
      DO 120 II=1,N
      DO 120 J=1,N
      AP(II,N+J)=0.
      IF(II.EQ.J) AP(II,N+J)=1.
  120..CONTINUE
      DO 130 II=1,N
      DO 130 J=1,N
      AP(N+II,J)=-1.*W2(II,J)
  130..CONTINUE
      DO 140 II=1,N
      DO 140 J=1,N
      AP(N+II,N+J)=-1.*DAMP(II,J)
  140..CONTINUE
      CALL MMULT(EVECT,B1,BDF,N,N,3)
      CALL MMULT(EVECT,B,BPF,N,N,M)
      CALL MMULT(C,EVEC,CPF,M,N,N)
      DO 143 II=1,N
      DO 142 J=1,3
      BD(II,J)=0.
      BD(N+II,J)=BDF(II,J)
  142..CONTINUE
  143..CONTINUE
      DO 145 II=1,N
      DO 144 J=1,M
      BP(II,J)=0.0
      BP(N+II,J)=BPF(II,J)
  144..CONTINUE
  145..CONTINUE
      DO 148 II=1,M
```

```
          DO 147 J=1,N
          CP(II,J)=ALPHA*CPF(II,J)
          CP(II,N+J)=CPF(II,J)
    147..CONTINUE
    148..CONTINUE

END       $'END OF PROCEDURAL'

'         ****************************************************'
'         *  ASSEMBLE AM,BM,CM MATRICES OF THE REFERENCE MODEL *'
'         ****************************************************'

PROCEDURAL(AM,BM,CM,EVECS,EVECST,DAM,W2M=ZETA,EVEC,W2,B,C,ALPHA)
          DO 150 II=1,L
          DO 150 J=1,L
          W2M(II,J)=0.
    150..CONTINUE
          DO 152 II=1,6
          W2M(II,II)=W2(6+II,6+II)*0.6
    152..CONTINUE
          DO 153 II=1,3
          W2M(6+II,6+II)=W2(12+II,12+II)*1.4
    153..CONTINUE
          DO 160 II=1,L
          DO 155 J=1,L
          DAM(II,J)=0.0
    155..CONTINUE
          DAM(II,II)=2.0*ZETA(II)*SQRT(W2M(II,II))
    160..CONTINUE
          DO 170 II=1,L
          DO 170 J=1,L
          AM(II,J)=0.
    170..CONTINUE
          DO 180 II=1,L
          DO 180 J=1,L
          AM(II,L+J)=0.
          IF(II.EQ.J) AM(II,L+J)=1.
    180..CONTINUE
          DO 190 II=1,L
          DO 190 J=1,L
          AM(L+II,J)=-1.*W2M(II,J)
    190..CONTINUE
          DO 200 II=1,L
          DO 200 J=1,L
          AM(L+II,L+J)=-1.*DAM(II,J)
    200..CONTINUE
          DO 205 II=1,N
          DO 205 J=1,9
          EVECSB(II,J)=EVEC(II,6+J)
    205..CONTINUE
          DO 212 J=1,L
          EVECS(1,J)=EVECSB(1,J)*0.7
          EVECS(2,J)=EVECSB(2,J)*0.7
          EVECS(3,J)=EVECSB(3,J)*1.3
          EVECS(4,J)=EVECSB(4,J)*1.3
          EVECS(5,J)=EVECSB(5,J)*1.0
          EVECS(6,J)=EVECSB(6,J)*0.7
          EVECS(7,J)=EVECSB(7,J)*1.0
          EVECS(8,J)=EVECSB(8,J)*1.0
```

```
                 EVECS(9,J)=EVECSB(9,J)*1.0
                 EVECS(10,J)=EVECSB(10,J)*1.0
                 EVECS(11,J)=EVECSB(11,J)*1.3
                 EVECS(12,J)=EVECSB(12,J)*0.7
                 EVECS(13,J)=EVECSB(13,J)*0.7
                 EVECS(14,J)=EVECSB(14,J)*1.3
                 EVECS(15,J)=EVECSB(15,J)*1.3
          212..CONTINUE
                 CALL MTRANS(EVECS,EVECST,N,L)
                 CALL MMULT(EVECST,B,BMF,L,N,M)
                 CALL MMULT(C,EVECS,CMF,M,N,L)
                 DO 215 II=1,L
                 DO 215 J=1,M
                 BM(II,J)=0.
                 BM(L+II,J)=BMF(II,J)
          215..CONTINUE
                 DO 220 II=1,M
                 DO 220 J=1,L
                 CM(II,J)=ALPHA*CMF(II,J)
                 CM(II,L+J)=CMF(II,J)
          220..CONTINUE

END              $'END OF PROCEDURAL'

'                ***********************************************************'
'                *   SET THE INITIAL CONDITIONS IN PHYSICAL COORDINATES    *'
'                ***********************************************************'

CONSTANT         Z10=0.
CONSTANT         T10=0.
CONSTANT         Z30=0.
CONSTANT         T30=0.
CONSTANT         Z20=0.
CONSTANT         P20=0.
CONSTANT         Z40=0.
CONSTANT         T40=0.
CONSTANT         P40=0.
CONSTANT         Z60=0.
CONSTANT         P60=0.
CONSTANT         Z50=0.
CONSTANT         T50=0.
CONSTANT         Z70=0.
CONSTANT         T70=0.
CONSTANT         Z1D0=0.
CONSTANT         T1D0=0.
CONSTANT         Z3D0=0.
CONSTANT         T3D0=0.
CONSTANT         Z2D0=0.
CONSTANT         P2D0=0.
CONSTANT         Z4D0=0.
CONSTANT         T4D0=0.
CONSTANT         P4D0=0.
CONSTANT         Z6D0=0.
CONSTANT         P6D0=0.
CONSTANT         Z5D0=0.
CONSTANT         T5D0=0.
CONSTANT         Z7D0=0.
```

```
CONSTANT  T7D0=0.
          ZP0(1)=Z10
          ZP0(2)=T10*DTRCC
          ZP0(3)=Z30
          ZP0(4)=T30*DTRCC
          ZP0(5)=Z20
          ZP0(6)=P20*DTRCC
          ZP0(7)=Z40
          ZP0(8)=T40*DTRCC
          ZP0(9)=P40*DTRCC
          ZP0(10)=Z60
          ZP0(11)=P60*DTRCC
          ZP0(12)=Z50
          ZP0(13)=T50*DTRCC
          ZP0(14)=Z70
          ZP0(15)=T70*DTRCC
          ZPD0(1)=Z1D0
          ZPD0(2)=T1D0*DTRCC
          ZPD0(3)=Z3D0
          ZPD0(4)=T3D0*DTRCC
          ZPD0(5)=Z2D0
          ZPD0(6)=P2D0*DTRCC
          ZPD0(7)=Z4D0
          ZPD0(8)=T4D0*DTRCC
          ZPD0(9)=P4D0*DTRCC
          ZPD0(10)=Z6D0
          ZPD0(11)=P6D0*DTRCC
          ZPD0(12)=Z5D0
          ZPD0(13)=T5D0*DTRCC
          ZPD0(14)=Z7D0
          ZPD0(15)=T7D0*DTRCC
CONSTANT  DSHU1=0.2
CONSTANT  SHU1=0.
CONSTANT  DSHU2=0.2
CONSTANT  SHU2=0.
CONSTANT  ZDSHU0=0.05
CONSTANT  ZSHU0=0.
          DSHUT0=DSHU1*DTRCC
          SHUT0=SHU1*DTRCC
          DSHUP0=DSHU2*DTRCC
          SHUP0=SHU2*DTRCC

'         **********************************************************'
'         *  FIND THE INITIAL CONDITIONS IN MODAL COORDINATES      *'
'         **********************************************************'

PROCEDURAL(XP0,XM0=EVECI,ZP0,ZPD0)
          CALL MVMULT(EVECI,ZP0,ETA0,N,N)
          CALL MVMULT(EVECI,ZPD0,ETAD0,N,N)
          DO 250 II=1,N
          XP0(II)=ETA0(II)
          XP0(N+II)=ETAD0(II)
     250..CONTINUE
          DO 258 II=1,L
          ETAS0(II)=0.9*ETA0(6+II)
          ETASD0(II)=0.9*ETAD0(6+II)
     258..CONTINUE
          DO 280 II=1,L
```

```
            XM0(II)=ETAS0(II)
            XM0(L+II)=ETASD0(II)
      200..CONTINUE
            CALL MPRINT(XP0,1,N2,4,4H XP0)
            CALL MPRINT(XM0,1,L2,4,4H XM0)
END         $'END OF PROCEDURAL'
'           *****************************************************'
'           *        DEFINE THE SCALING MATRICES TA AND TB      *'
'           *****************************************************'
PROCEDURAL(TA,TB=TAS,TBS)
            DO 290 II=1,Q
            DO 290 J=1,Q
            TA(II,J)=0.0
      290..CONTINUE
            DO 300 II=1,Q
            TA(II,II)=TAS(II)
      300..CONTINUE
            DO 310 II=1,Q
            DO 310 J=1,Q
            TB(II,J)=0.0
      310..CONTINUE
            DO 320 II=1,Q
            TB(II,II)=TBS(II)
      320..CONTINUE
END         $'END OF PROCEDURAL'
END
'======================== END OF INITIAL ========================'
'========================== DYNAMIC =============================='
DYNAMIC
            TERMT(T.GT.TFINAL)
            TERMT(XP(1).GT.1.0E+10)
            TERMT(XP(2).GT.1.0E+10)
PROCEDURAL(NSTP=T,TSW,NSTP1,NSTP2)
            IF(T.GT.TSW) GO TO 325
            NSTP=NSTP1
            GO TO 327
      325..NSTP=NSTP2
      327..CONTINUE
END         $'END OF PROCEDURAL'
'======================== DERIVATIVE ============================'
DERIVATIVE
```

```
'              ***********************************************************'
'              * CALCULATE THE SOFT DOCKING DISTURBANCE FORCE & TORQUE *'
'              ***********************************************************'

PROCEDURAL(FDOCK,TQDCKT,TQDCKP,FDDOCK,DDSHUT,DDSHUP,ZDDSHU=...
               RDAMT,RDAMP,ZDAM,DSHUT,DSHUP,ZDSHU,ZPD,RSTIT,...
               RSTIP,ZSTI,SHUT,SHUP,ZSHU,ZP,ISHUTT,ISHUTP,MSHUT,G)
              TQDCKT=RDAMT*(DSHUT-ZPD(8))+RSTIT*(SHUT-ZP(8))
              TQDCKP=RDAMP*(DSHUP-ZPD(9))+RSTIP*(SHUP-ZP(9))
              FDOCK=ZDAM*(ZDSHU-ZPD(7))+ZSTI*(ZSHU-ZP(7))
              DDSHUT=-(TQDCKT/ISHUTT)
              DDSHUP=-(TQDCKP/ISHUTP)
              ZDDSHU=-(FDOCK/(MSHUT/G))
              FDDOCK(1)=FDOCK
              FDDOCK(2)=TQDCKT
              FDDOCK(3)=TQDCKP

END           $'END OF PROCEDURAL'

'              ******************************************************'
'              *DEFINE THE INTEGRAL GAIN KI AND PROPORTIONAL GAIN KP*'
'              ******************************************************'

PROCEDURAL(KI,KP=YM,YP,XM,UM,TA,TB,KI0)
              DO 330 II=1,M
              EYS(II)=YM(II)-YP(II)
        330..CONTINUE
              DO 340 II=1,M
              R(II)=EYS(II)
        340..CONTINUE
              DO 350 II=1,L2
              R(M+II)=XM(II)
        350..CONTINUE
              DO 360 II=1,M
              R(M+L2+II)=UM(II)
        360..CONTINUE
              DO 365 II=1,M
              EY(II,1)=EYS(II)
        365..CONTINUE
              CALL VTRANS(R,RT,Q)
              CALL MMULT(RT,TA,DUMY4,1,Q,Q)
              CALL MMULT(RT,TB,DUMY5,1,Q,Q)
              CALL MMULT(EY,DUMY4,KID,M,1,Q)
              CALL MMULT(EY,DUMY5,KP,M,1,Q)
              KI=INTVC(KID,KI0)

END           $'END OF PROCEDURAL'

'              ******************************************************'
'              *              FIND THE CONTROL UP FOR THE PLANT     *'
'              ******************************************************'

PROCEDURAL(UP=KI,KP,R)
              CALL MVMULT(KI,R,DUMY6,M,Q)
              CALL MVMULT(KP,R,DUMY7,M,Q)
              CALL VADD(DUMY6,DUMY7,UP,M)

END           $'END OF PROCEDURAL'
```

```
'          ****************************************************'
'          * INTEGRATE THE EQUATIONS OF THE PLANT AND THE MODEL *'
'          ****************************************************'

           CALL MVMULT(AP,XP,DUMY8,N2,N2)
           CALL MVMULT(BP,UP,DUMY9,N2,M)
           CALL MVMULT(BD,FDDOCK,DUMY12,N2,3)
           CALL VADD(DUMY8,DUMY9,DUMY13,N2)
           CALL VADD(DUMY13,DUMY12,XPD,N2)
           XP=INTVC(XPD,XP0)
           CALL MVMULT(CP,XP,YP,M,N2)
           CALL MVMULT(AM,XM,DUMY10,L2,L2)
           CALL MVMULT(BM,UM,DUMY11,L2,M)
           CALL VADD(DUMY10,DUMY11,XMD,L2)
           XM=INTVC(XMD,XM0)
           CALL MVMULT(CM,XM,YM,M,L2)
           DSHUT=INTEG(DDSHUT,DSHUT0)
           DSHUP=INTEG(DDSHUP,DSHUP0)
           SHUT=INTEG(DSHUT,SHUT0)
           SHUP=INTEG(DSHUP,SHUP0)
           ZDSHU=INTEG(ZDDSHU,ZDSHU0)
           ZSHU=INTEG(ZDSHU,ZSHU0)

'          ****************************************************'
'          *       OBTAIN RESULTS IN PHYSICAL COORDINATES      *'
'          ****************************************************'

PROCEDURAL(ZP,ZPD,ZPDD,ZM,ZMD=XP,XPD,XM,EVEC)
           DO 370 II=1,N
           ETA(II)=XP(II)
           ETAD(II)=XP(N+II)
           ETADD(II)=XPD(N+II)
      370..CONTINUE
           CALL MVMULT(EVEC,ETA,ZP,N,N)
           CALL MVMULT(EVEC,ETAD,ZPD,N,N)
           CALL MVMULT(EVEC,ETADD,ZPDD,N,N)
           DO 380 II=1,L
           ETAS(II)=XM(II)
           ETASD(II)=XM(L+II)
      380..CONTINUE
           CALL MVMULT(EVECS,ETAS,ZM,N,L)
           CALL MVMULT(EVECS,ETASD,ZMD,N,L)

END        $'END OF PROCEDURAL'


END


'==================== END OF DERIVATIVE ======================'

'          ****************************************************'
'          *             CHANGE RADIANS TO DEGREES             *'
'          ****************************************************'

           Z1P=ZP(1)
           T1P=ZP(2)/DTRCC
           Z3P=ZP(3)
```

```
      T3P=ZP(4)/DTRCC
      Z2P=ZP(5)
      P2P=ZP(6)/DTRCC
      Z4P=ZP(7)
      T4P=ZP(8)/DTRCC
      P4P=ZP(9)/DTRCC
      Z6P=ZP(10)
      P6P=ZP(11)/DTRCC
      Z5P=ZP(12)
      T5P=ZP(13)/DTRCC
      Z7P=ZP(14)
      T7P=ZP(15)/DTRCC
      Z1DP=ZPD(1)
      T1DP=ZPD(2)/DTRCC
      Z3DP=ZPD(3)
      T3DP=ZPD(4)/DTRCC
      Z2DP=ZPD(5)
      P2DP=ZPD(6)/DTRCC
      Z4DP=ZPD(7)
      T4DP=ZPD(8)/DTRCC
      P4DP=ZPD(9)/DTRCC
      Z6DP=ZPD(10)
      P6DP=ZPD(11)/DTRCC
      Z5DP=ZPD(12)
      T5DP=ZPD(13)/DTRCC
      Z7DP=ZPD(14)
      T7DP=ZPD(15)/DTRCC
      Z1M=ZM(1)
      T1M=ZM(2)/DTRCC
      Z3M=ZM(3)
      T3M=ZM(4)/DTRCC
      Z2M=ZM(5)
      P2M=ZM(6)/DTRCC
      Z4M=ZM(7)
      T4M=ZM(8)/DTRCC
      P4M=ZM(9)/DTRCC
      Z6M=ZM(10)
      P6M=ZM(11)/DTRCC
      Z5M=ZM(12)
      T5M=ZM(13)/DTRCC
      Z7M=ZM(14)
      T7M=ZM(15)/DTRCC
      Z1DM=ZMD(1)
      T1DM=ZMD(2)/DTRCC
      Z3DM=ZMD(3)
      T3DM=ZMD(4)/DTRCC
      Z2DM=ZMD(5)
      P2DM=ZMD(6)/DTRCC
      Z4DM=ZMD(7)
      T4DM=ZMD(8)/DTRCC
      P4DM=ZMD(9)/DTRCC
      Z6DM=ZMD(10)
      P6DM=ZMD(11)/DTRCC
      Z5DM=ZMD(12)
      T5DM=ZMD(13)/DTRCC
      Z7DM=ZMD(14)
      T7DM=ZMD(15)/DTRCC
```

```
      DSHANT=DSHUT/DTRCC
      SHANT=SHUT/DTRCC
      DSHANP=DSHUP/DTRCC
      SHANP=SHUP/DTRCC
      XP15=XP(1)
      XP14=XP(2)
      XP13=XP(3)
      XP12=XP(4)
      XP11=XP(5)
      XP10=XP(6)
      XP9=XP(7)
      XP8=XP(8)
      XP7=XP(9)
      XP6=XP(10)
      XP5=XP(11)
      XP4=XP(12)
      XP3=XP(13)
      XP2=XP(14)
      XP1=XP(15)
      XM9=XM(1)
      XM8=XM(2)
      XM7=XM(3)
      XM6=XM(4)
      XM5=XM(5)
      XM4=XM(6)
      XM3=XM(7)
      XM2=XM(8)
      XM1=XM(9)
      YP1=YP(1)
      YP2=YP(2)
      YP3=YP(3)
      YP4=YP(4)
      YP5=YP(5)
      YP6=YP(6)
      YP7=YP(7)
      YP8=YP(8)
      YP9=YP(9)
      YP10=YP(10)
      YP11=YP(11)
      YM1=YM(1)
      YM2=YM(2)
      YM3=YM(3)
      YM4=YM(4)
      YM5=YM(5)
      YM6=YM(6)
      YM7=YM(7)
      YM8=YM(8)
      YM9=YM(9)
      YM10=YM(10)
      YM11=YM(11)
      UP1=UP(1)
      UP2=UP(2)
      UP3=UP(3)
      UP4=UP(4)
      UP5=UP(5)
      UP6=UP(6)
```

```
          UP7=UP(7)
          UP8=UP(8)
          UP9=UP(9)
          UP10=UP(10)
          UP11=UP(11)

END

'=========================== END OF DYNAMIC ==========================='



'============================== TERMINAL =============================='

TERMINAL

'         ******************************************************'
'         *                PRINT SYSTEM PARAMETERS             *'
'         ******************************************************'

          CALL MPRINT(EVECT,N,N,34,...
                    34H TRANSPOSE OF MODAL MATRIX (EVECT))
          CALL MPRINT(EVECI,N,N,32,...
                    32H INVERSE OF MODAL MATRIX (EVECI))
          CALL MPRINT(EVECS,N,L,31,...
                    31H TRUNCATED MODAL MATRIX (EVECS))
          CALL MPRINT(DAMP,N,N,35,...
                    35H DAMPING MATRIX OF THE PLANT (DAMP))
          CALL MPRINT(DAM,L,L,34,...
                    34H DAMPING MATRIX OF THE MODEL (DAM))
          CALL MPRINT(W2,N,N,43,...
                    43H GENERALIZED STIFFNESS MATRIX OF PLANT (W2))

          CALL MPRINT(W2M,L,L,44,...
                   44H GENERALIZED STIFFNESS MATRIX OF MODEL (W2M))

          CALL MPRINT(AP,N2,N2,10,10H MATRIX AP)
          CALL MPRINT(BP,N2,M,10,10H MATRIX BP)
          CALL MPRINT(CP,M,N2,10,10H MATRIX CP)
          CALL MPRINT(AM,L2,L2,10,10H MATRIX AM)
          CALL MPRINT(BM,L2,M,10,10H MATRIX BM)
          CALL MPRINT(CM,M,L2,10,10H MATRIX CM)
          CALL MPRINT(TA,Q,Q,10,10H MATRIX TA)
          CALL MPRINT(TB,Q,Q,10,10H MATRIX TB)





END

'======================== END OF TERMINAL ========================'



END       $'END OF PROGRAM'
```

```
      SUBROUTINE READMK(MASS,STIFF,EIS,EIE,RHOS,RHOE,LS,LE,M4,
     $M8,M9,I4XX,I4YY,I8XS,I9XS,I8YS,I9YS,L8A,L9A,L8B,L9B,
     $L8,L9)
      REAL MASS(15,15),STIFF(15,15),MC(15,15),MD(15,15)
      REAL I4XX,I4YY,I8XS,I9XS,I8YS,I9YS,L8A,L8B,L9A,L9B,L8,L9
      REAL ALPHA,BETA,A,B,EIS,EIE,RHOS,RHOE,LS,LE,M4,M8,M9
      ALPHA=2.*EIS/(LS**3)
      BETA=2.*EIE/(LE**3)
      A=RHOS*LS/420.
      B=RHOE*LE/420.
      DO 10 I=1,15
      DO 10 J=1,15
      STIFF(I,J)=0.
   10 CONTINUE
      STIFF(1,1)=6.*ALPHA
      STIFF(1,2)=3.*LS*ALPHA
      STIFF(1,5)=-6.*ALPHA
      STIFF(1,8)=3.*LS*ALPHA
      STIFF(2,2)=2.*(LS**2)*ALPHA
      STIFF(2,5)=-3.*LS*ALPHA
      STIFF(2,8)=(LS**2)*ALPHA
      STIFF(3,3)=6.*ALPHA
      STIFF(3,4)=-3.*LS*ALPHA
      STIFF(3,5)=-6.*ALPHA
      STIFF(3,8)=-3.*LS*ALPHA
      STIFF(4,4)=2.*(LS**2)*ALPHA
      STIFF(4,5)=3.*LS*ALPHA
      STIFF(4,8)=(LS**2)*ALPHA
      STIFF(5,5)=12.*ALPHA+6.*BETA
      STIFF(5,6)=3.*LE*BETA
      STIFF(5,7)=-6.*BETA
      STIFF(5,9)=3.*LE*BETA
      STIFF(6,6)=2.*(LE**2)*BETA
      STIFF(6,7)=-3.*LE*BETA
      STIFF(6,9)=(LE**2)*BETA
      STIFF(7,7)=12.*BETA
      STIFF(7,10)=-6.*BETA
      STIFF(7,11)=3.*LE*BETA
      STIFF(8,8)=8.*(LS**2)*ALPHA
      STIFF(8,12)=3.*LS*ALPHA
      STIFF(8,13)=(LS**2)*ALPHA
      STIFF(8,14)=-3.*LS*ALPHA
      STIFF(8,15)=(LS**2)*ALPHA
      STIFF(9,9)=4.*(LE**2)*BETA
      STIFF(9,10)=-3.*LE*BETA
      STIFF(9,11)=(LE**2)*BETA
      STIFF(10,10)=12.*ALPHA+6.*BETA
      STIFF(10,11)=-3.*LE*BETA
      STIFF(10,12)=-6.*ALPHA
      STIFF(10,13)=-3.*LS*ALPHA
      STIFF(10,14)=-6.*ALPHA
      STIFF(10,15)=3.*LS*ALPHA
      STIFF(11,11)=2.*(LE**2)*BETA
      STIFF(12,12)=6.*ALPHA
      STIFF(12,13)=3.*LS*ALPHA
      STIFF(13,13)=2.*(LS**2)*ALPHA
      STIFF(14,14)=6.*ALPHA
      STIFF(14,15)=-3.*LS*ALPHA
      STIFF(15,15)=2.*(LS**2)*ALPHA
```

```
      DO 20 I=1,14
      K=I+1
      DO 20 J=K,15
      STIFF(J,I)=STIFF(I,J)
   20 CONTINUE

      DO 30 I=1,15
      DO 30 J=1,15
      MC(I,J)=0.
   30 CONTINUE
      MC(1,1)=156.*A
      MC(1,2)=22.*LS*A
      MC(1,5)=54.*A
      MC(1,8)=-13.*LS*A
      MC(2,2)=4.*(LS**2)*A
      MC(2,5)=13.*LS*A
      MC(2,8)=-3.*(LS**2)*A
      MC(3,3)=156.*A
      MC(3,4)=-22.*LS*A
      MC(3,5)=54.*A
      MC(3,8)=13.*LS*A
      MC(4,4)=4.*(LS**2)*A
      MC(4,5)=-13.*LS*A
      MC(4,8)=-3.*(LS**2)*A
      MC(5,5)=312.*A+156*B
      MC(5,6)=22.*LE*B
      MC(5,7)=54.*B
      MC(5,9)=-13.*LE*B
      MC(6,6)=4.*(LE**2)*B
      MC(6,7)=13.*LE*B
      MC(6,9)=-3.*(LE**2)*B
      MC(7,7)=312.*B
      MC(7,10)=54.*B
      MC(7,11)=-13.*LE*B
      MC(8,8)=16.*(LS**2)*A
      MC(8,12)=-13.*LS*A
      MC(8,13)=-3.*(LS**2)*A
      MC(8,14)=13.*LS*A
      MC(8,15)=-3.*(LS**2)*A
      MC(9,9)=8.*(LE**2)*B
      MC(9,10)=13.*LE*B
      MC(9,11)=-3.*(LE**2)*B
      MC(10,10)=156.*B+312.*A
      MC(10,11)=-22.*LE*B
      MC(10,12)=54.*A
      MC(10,13)=13.*LS*A
      MC(10,14)=54.*A
      MC(10,15)=-13.*LS*A
      MC(11,11)=4.*(LE**2)*B
      MC(12,12)=156.*A
      MC(12,13)=22.*LS*A
      MC(13,13)=4.*(LS**2)*A
      MC(14,14)=156.*A
      MC(14,15)=-22.*LS*A
      MC(15,15)=4.*(LS**2)*A
      DO 40 I=1,14
      K=I+1
      DO 40 J=K,15
      MC(J,I)=MC(I,J)
```

```
   40 CONTINUE
      DO 50 I=1,15
      DO 50 J=1,15
      MD(I,J)=0.
   50 CONTINUE
      MD(7,7)=M4+M8+M9
      MD(7,8)=M9*L9-M8*L8
      MD(8,8)=I4YY+M8*(L8**2)+M9*(L9**2)+I8YS+I9YS
      MD(9,9)=I4XX+I8XS+I9XS
      DO 60 I=1,14
      K=I+1
      DO 60 J=K,15
      MD(J,I)=MD(I,J)
   60 CONTINUE
      DO 70 I=1,15
      DO 70 J=1,15
      MASS(I,J)=MC(I,J)+MD(I,J)
   70 CONTINUE
      RETURN
      END
```

```
      SUBROUTINE OPLOOP(MASS,STIFF,EVAL,EVEC)

C ***********************************************************************
C *                                                                     *
C *  MASS AND STIFF ARE THE INPUT M AND K MATRICES.                     *
C *  SUBROUTINE FIRST FINDS SIMILARITY TRANSFORMATION PHI1 SUCH         *
C *  THAT THE COLUMNS OF PHI1 ARE EIGENVECTORS OF MASS NORMALIZED       *
C *  SUCH THAT                                                          *
C *                                                                     *
C *      (PHI1)'(MASS)(PHI1)=(IDENTITY)      (' DENOTES TRANSPOSE)      *
C *                                                                     *
C *  THEN FINDS ANOTHER SIMILARITY TRANSFORMATION PHI2 NORMALIZED       *
C *  SUCH THAT                                                          *
C *                                                                     *
C *     (PHI2)'(PHI1)'(STIFF)(PHI1)(PHI2)=DIAG(EVAL)                    *
C *                                                                     *
C *  WHERE EVAL ARE THE EIGENVALUES OF THE OPEN-LOOP SYSTEM,            *
C *  I.E., THE SQUARES OF THE EIGENFREQUENCIES.                         *
C *                                                                     *
C *  FINALLY, THE PRODUCT                                               *
C *                                                                     *
C *       EVEC=(PHI1)(PHI2)                                             *
C *                                                                     *
C *  IS RETURNED - THE J COLUMN IS EIGENVECTOR OF OPEN-LOOP             *
C *  SYSTEM CORRESPONDING TO J EIGENVALUE.                              *
C *                                                                     *
C *  (UNTIL THE SECOND CALL TO SYMQRR, PHI2 IS USED FOR                 *
C *     INTERMEDIARY CALCULATIONS)                                      *
C *                                                                     *
C ***********************************************************************

      PARAMETER N=15

      REAL MASS(N,N)
      DIMENSION STIFF(N,N)
      DIMENSION EVEC(N,N),EVAL(N)
      DIMENSION PHI1(N,N),PHI2(N,N),PHI1T(N,N),WORK(500)


      CALL MCOPY(MASS,PHI1,N,N)
      CALL SYMQRR($601,PHI1,N,N,EVAL,WORK)
C
C     RENORMALIZE FIRST SIMILARITY TRANSFORMATION
C
      DO 100 I=1,N
      DO 100 J=1,N
      PHI1(I,J)=PHI1(I,J)/SQRT(EVAL(J))
  100 CONTINUE
C
      CALL MTRANS(PHI1,PHI1T,N,N)
      CALL MMULT(STIFF,PHI1,PHI2,N,N,N)
      CALL MMULT(PHI1T,PHI2,EVEC,N,N,N)
      CALL MCOPY(EVEC,PHI2,N,N)
      CALL SYMQRR($701,PHI2,N,N,EVAL,WORK)

C     EVAL NOW CONTAINS THE SQUARES OF THE EIGENFREQUENCIES

      CALL MMULT(PHI1,PHI2,EVEC,N,N,N)

C     EVEC NOW CONTAINS THE CORRESPONDING EIGENVECTORS AS
C     COLUMNS

      GO TO 900
```

```
  601 CONTINUE
      WRITE(6,602)
  602 FORMAT(1X,'CLUTCHED ON FIRST CALL TO SYMQRR')
      GO TO 900
  701 CONTINUE
      WRITE(6,702)
  702 FORMAT(1X,'CLUTCHED ON SECOND CALL TO SYMQRR')
  900 CONTINUE
      RETURN
      END
```

```
      SUBROUTINE INVERS(A,N)

      DIMENSION A(N,N),WORK(1000)

C     THIS SUBROUTINE WILL CALL AINV FOR AN ACSL PROGRAM
C     AND IT WILL HANDLE THE ERROR TRAPPING

      CALL AINVR(A,N,N,$100,WORK)

      RETURN


C     HANDLE  ERROR BOMB OUTS
  100 CONTINUE
      WRITE(6,1000)
 1000 FORMAT(1X,'  ************* INVERSION PROBLEM *****************')

      RETURN 0
      END
```

```
      SUBROUTINE MADD(A,B,C,L,N)
C  THIS SUBROUTINE CALCULATES THE SUM A+B AND STORES THE RESULT IN C
C  L = ROWS OF A AND B ,  N = COLS OF A AND B
      DIMENSION A(L,N),B(L,N),C(L,N)
      DO 100 I=1,L
      DO 100 J=1,N
      C(I,J) = A(I,J)+B(I,J)
100   CONTINUE
      RETURN
      END
```

```
      SUBROUTINE MMULT(A,B,C,L,M,N)
C  THIS SUBROUTINE CALCULATES THE PRODUCT AB AND STORES THE RESULT IN C

C  L = ROWS OF A ,  M = COLS OF A AND ROWS OF B,  N = COLS OF B
      DIMENSION A(L,M),B(M,N),C(L,N)
      DO 100 I=1,L
      DO 100 J=1,N
      C(I,J) = 0.0
      DO 100 K=1,M
      CC = A(I,K)*B(K,J)
      C(I,J) = C(I,J) + CC
100   CONTINUE
      RETURN
      END
```

```
      SUBROUTINE MVMULT(A,B,C,M,N)
C  THIS SUBROUTINE CALCULATES THE PRODUCT OF MATRIX A AND
C  VECTOR B AND STORES THE RESULT IN VECTOR C
      DIMENSION A(M,N),B(N),C(M)
      DO 100 I=1,M
      C(I)=0.0
      DO 100 J=1,N
      CC=A(I,J)*B(J)
      C(I)=C(I)+CC
  100 CONTINUE
      RETURN
      END
```

```
      SUBROUTINE MTRANS(A,AT,M,N)
C  THIS SUBROUTINE CALCULATES A TRANSPOSE AND STORES RESULT IN AT
C  M = ROWS OF A ,  N = COLUMNS OF A
      DIMENSION A(M,N),AT(N,M)
      DO 100 J=1,M
      DO 100 I=1,N
      AT(I,J) = A(J,I)
100   CONTINUE
      RETURN
      END
```

```
      SUBROUTINE VADD(A,B,C,M)
C  THIS SUBROUTINE CALCULATES THE SUM OF VECTORS A AND B AND
C  STORES THE RESULT IN VECTOR C
      DIMENSION A(M),B(M),C(M)
      DO 100 I=1,M
      C(I)=A(I)+B(I)
  100 CONTINUE
      RETURN
      END
```

```
      SUBROUTINE VTRANS(A,AT,M)
C  THIS SUBROUTINE CALCULATES THE TRANSPOSE OF VECTOR A AND
C  STORES THE RESULT IN MATRIX AT
      DIMENSION A(M),AT(1,M)
      DO 100 I=1,M
      AT(1,I)=A(I)
  100 CONTINUE
      RETURN
      END
```

```
      SUBROUTINE MCOPY(A1,B1,M,N)
C  THIS SUBROUTINE COPIES A INTO B
C   (BOTH ARE M ROWS BY N COLUMNS)
      DIMENSION A1(M,N),B1(M,N)
      DO 500 I=1,M
         DO 200 J=1,N
            B1(I,J)=A1(I,J)
  200    CONTINUE
  500 CONTINUE
      RETURN
      END
```

```
      SUBROUTINE MPRINT(A,M,N,NCHAR,TEXT)
C  THIS SUBROUTINE PRINTS A MATRIX WITH TEXT AS A HEADING
C  M = ROWS OF A  ,  N = COLUMNS OF A
      DIMENSION A(M,N),TEXT(50)
      IREM=MOD(NCHAR,6)
      IF(IREM.EQ.0) NWORDS=NCHAR/6
      IF(IREM.NE.0) NWORDS=NCHAR/6 + 1
      WRITE(6,10)(TEXT(I),I=1,NWORDS)
10    FORMAT(//1X,50A6//)
      DO 100 I=1,M
      WRITE(6,20)(A(I,J),J=1,N)
100   CONTINUE
20    FORMAT(5X,11G11.5)
      WRITE (6,30)
30    FORMAT (//)
      RETURN
      END
```

ORIGINAL PAGE IS
OF POOR QUALITY

APPENDIX E

NUMERICAL OUTPUTS FOR THE SIMULATION OF ADAPTIVE CONTROL DURING SHUTTLE HARD DOCKING TO FOUR-PANEL SPACE STATION

```
' ******* ACSL RUN PARAMETERS *******'
SET CALPLT=.TRUE.
SET XINCPL=8.0
SET YINCPL=4.0
SET NPYPPL=60,NGYPPL=15,NPXPPL=50,NGXPPL=10
SET DIS=99
SET MALPRN=36
' '
' ******* VARIABLE DEFINITIONS ******* '
SET TFINAL=300.
SET ALPHA=0.2
SET CINT=0.25
' '
' ******* PREPARE VARIABLES ******* '
PREPAR T,YP1,YM1,YP2,YM2,YP3,YM3,YP4,YM4,YP5,YM5,YP6,YM6,YP7,YM7,...
         YP8,YM8,YP9,YM9,YP10,YM10,YP11,YM11,XP1,XM1,XP2,XM2,XP3,...
         XM3,XP4,XM4,XP5,XM5,XP6,XM6,XP7,XM7,XP8,XM8,XP9,XM9,...
         XP10,XP11,XP12,XP13,XP14,XP15,UP1,UP2,UP3,UP4,UP5,...
         UP6,UP7,UP8,UP9,UP10,UP11,Z1P,Z1M,T1P,T1M,Z3P,Z3M,...
         T3P,T3M,Z2P,Z2M,P2P,P2M,Z4P,Z4M,T4P,T4M,P4P,P4M,Z6P,...
         Z6M,P6P,P6M,Z5P,Z5M,T5P,T5M,Z7P,Z7M,T7P,T7M,Z10P,...
         Z10M,T1DP,T1DM,Z3DP,Z3DM,T3DP,T3DM,ZEDP,Z2DM,P2DP,...
         P2DM,Z4DP,Z4DM,T4DP,T4DM,P4DP,P4DM,Z6DP,Z6DM,P6DP,...
         P6DM,Z5DP,Z5DM,T5DP,T5DM,Z7DP,Z7DM,T7DP,T7DM,Z8M,...
         ZDSMU,SHANP,DSHANP,SHANT,DSHANT,FDOCK,TODCKT,TODCKP
OUTPUT T,YP1,YM1,YP2,YM2,YP3,YM3,YP4,YM4,YP5,YM5,YP6,YM6,YP7,YM7,...
         YP8,YM8,YP9,YM9,YP10,YM10,YP11,YM11,XP1,XM1,XP2,XM2,...
         XP3,XM3,XP4,XM4,XP5,XM5,XP6,XM6,XP7,XM7,XP8,XM8,...
         XP9,XM9,XP10,XP11,XP12,XP13,XP14,XP15,UP1,UP2,UP3,...
         UP4,UP5,UP6,UP7,UP8,UP9,UP10,UP11,Z1P,Z1M,T1P,T1M,...
         Z3P,Z3M,T3P,T3M,Z2P,Z2M,P2P,P2M,Z4P,Z4M,T4P,T4M,P4P,...
         P4M,Z6P,Z6M,P6P,P6M,Z5P,Z5M,T5P,T5M,Z7P,Z7M,T7P,T7M,...
         Z10P,Z10M,T1DP,T1DM,Z3DP,Z3DM,T3DP,T3DM,Z2DP,Z2DM,...
         P2DP,P2DM,Z4DP,Z4DM,T4DP,T4DM,P4DP,P4DM,Z6DP,Z6DM,...
         P6DP,P6DM,Z5DP,Z5DM,T5DP,T5DM,Z7DP,Z7DM,T7DP,T7DM,...
         Z5MU,ZDSMU,SHANP,DSHANP,SHANT,DSHANT,FDUCK,...
         TODCKT,TODCKP,'NCIOUT'=40
' '
START

 MASS MATRIX
      23.108     374.77     .00000     .00000     7.9991     .00000     .00000    -221.46     .00000     .00000     .00000
      .00000     .00000     .00000     .00000
      374.77     7836.1     .00000     .00000     221.46     .00000     .00000    -5877.1     .00000     .00000     .00000
      .00000     .00000     .00000     .00000
      .00000     .00000     23.108    -374.77     7.9991     .00000     .00000     221.46     .00000     .00000     .00000
      .00000     .00000     .00000     .00000
      .00000     .00000    -374.77     7836.1    -221.46     .00000     .00000    -5877.1     .00000     .00000     .00000
      .00000     .00000     .00000     .00000
      7.9991     221.46     7.9991    -221.46     100.71     1075.9     10.864     .00000    -635.79     .00000     .00000
      .00000     .00000     .00000     .00000
      .00000     .00000     .00000     .00000     1075.9     27388.     635.79     .00000    -20541.     .00000     .00000
      .00000     .00000     .00000     .00000
```

.00000	.00000	.00000	.00000	18.864	635.79	6863.8	.00000	.00000	18.864	-635.79
.00000	.00000	.00000	.00000							
-221.46	-5877.1	221.46	-5877.1	.00000	.00000	.00000	.21317+07	.00000	.00000	.00000
-221.46	-5877.1	221.46	-5877.1							
.00000	.00000	.00000	.00000	-635.79	-20541.	.00000	.00000	.39725+07	635.79	-20541.
.00000	.00000	.00000	.00000							
.00000	.00000	.00000	.00000	.00000	.00000	18.864	.00000	635.79	100.71	-1075.9
7.9991	221.46	7.9991	-221.46							
.00000	.00000	.00000	.00000	.00000	.00000	-635.79	.00000	-20541.	-1075.9	27388.
.00000	.00000	.00000	.00000							
.00000	.00000	.00000	.00000	.00000	.00000	.00000	-221.46	.00000	7.9991	.00000
23.108	374.77	.00000	.00000							
.00000	.00000	.00000	.00000	.00000	.00000	.00000	-5877.1	.00000	221.46	.00000
374.77	7836.1	.00000	.00000							
.00000	.00000	.00000	.00000	.00000	.00000	.00000	221.46	.00000	7.9991	.00000
.00000	.00000	23.108	-374.77							
.00000	.00000	.00000	.00000	.00000	.00000	.00000	-5877.1	.00000	-221.46	.00000
.00000	.00000	-374.77	7836.1							

STIFFNESS MATRIX

74.766	4299.0	.00000	.00000	-74.766	.00000	.00000	4299.0	.00000	.00000	.00000
.00000	.00000	.00000	.00000							
4299.0	.32959+06	.00000	.00000	-4299.0	.00000	.00000	.16480+06	.00000	.00000	.00000
.00000	.00000	.00000	.00000							
.00000	.00000	74.766	-4299.0	-74.766	.00000	.00000	-4299.0	.00000	.00000	.00000
.00000	.00000	.00000	.00000							
.00000	.00000	-4299.0	.32959+06	4299.0	.00000	.00000	.16480+06	.00000	.00000	.00000
.00000	.00000	.00000	.00000							
-74.766	-4299.0	-74.766	4299.0	563.92	29007.	-414.39	.00000	29007.	.00000	.00000
.00000	.00000	.00000	.00000							
.00000	.00000	.00000	.00000	29007.	.27074+07	-29007.	.00000	.13537+07	.00000	.00000
.00000	.00000	.00000	.00000							
.00000	.00000	.00000	.00000	-414.39	-29007.	29013.	.00000	.00000	-414.39	29007.
.00000	.00000	.00000	.00000							
4299.0	.16480+06	-4299.0	.16480+06	.00000	.00000	.00000	.16577+07	.00000	.00000	.00000
4299.0	.16480+06	-4299.0	.16480+06							
.00000	.00000	.00000	.00000	29007.	.13537+07	.00000	.00000	.56591+07	-29007.	.13537+07
.00000	.00000	.00000	.00000							
.00000	.00000	.00000	.00000	.00000	.00000	-414.39	.00000	-29007.	563.92	-29007.
-74.766	-4299.0	-74.766	4299.0							
.00000	.00000	.00000	.00000	.00000	.00000	29007.	.00000	.13537+07	-29007.	.27074+07
.00000	.00000	.00000	.00000							
.00000	.00000	.00000	.00000	.00000	.00000	.00000	4299.0	.00000	-74.766	.00000
74.766	4299.0	.00000	.00000							
.00000	.00000	.00000	.00000	.00000	.00000	.00000	.16480+06	.00000	-4299.0	.00000
4299.0	.32959+06	.00000	.00000							
.00000	.00000	.00000	.00000	.00000	.00000	.00000	-4299.0	.00000	-74.766	.00000
.00000	.00000	74.766	-4299.0							
.00000	.00000	.00000	.00000	.00000	.00000	.00000	.16480+06	.00000	4299.0	.00000
.00000	.00000	-4299.0	.32959+06							

```
EIGENVALUES (W**2)

     815.97     815.51     122.82     121.35    110.29     109.64     4.9885     3.6131     3.0340     1.9268     1.8500
     1.1632     .69267     .10306     .22203-01

MODAL MATRIX (EVEC)
   -.13679    -.14168    -.18162     .17400    -.11874     .11143     .18978-01  .90609-01  .10586     .10881     .12785
   -.91971-01 -.83796-01  .68815-01 -.44574-01
    .10500-01  .10869-01  .12084-01 -.11535-01  .76595-02 -.71756-02 -.85267-03 -.19545-02 -.21073-02 -.14714-02 -.15317-02
    .10494-02  .49641-03 -.61874-03  .10138-04
   -.13726    -.14216     .18260    -.17504    -.11728     .11016     .18998-01  .90719-01  .10602    -.10880    -.12816
   -.91531-01 -.83782-01 -.68814-01 -.44371-01
   -.10525-01 -.10895-01  .12141-01 -.11593-01 -.75576-02  .70870-02  .85285-03  .19557-02  .21090-02 -.14704-02 -.15347-02
   -.10440-02 -.49620-03 -.61870-03 -.14112-04
   -.73357-01 -.75707-01 -.11311-03  .11011-03  .10531-01 -.10496-01 -.15798-01 -.63155-01 -.62310-01 -.30675-04 -.27623-04
   -.81719-02 -.81532-01 -.15653-05 -.43153-01
    .47154-02  .48442-02  .18911-04 -.19361-04 -.36561-02  .34739-02  .30061-03  .72661-03  .58464-03  .35986-06  .58846-06
    .21730-03  .43498-03  .92326-08  .31337-03
    .11120-04 -.69359-03 -.22144-05  .23421-05  .88959-04 -.99187-03  .12399-01  .19132-05 -.22580-02 -.35667-06 -.18137-06
   -.12829-06 -.37357-03  .31755-08 -.19190-08
   -.30478-07 -.29572-07  .75290-08  .16672-05  .16708-06 -.14210-06 -.90847-08 -.59343-07 -.10623-06  .41659-03 -.16960-06
   -.10132-06 -.51629-07 -.54261-03  .97482-08
    .36010-04  .54736-06  .13308-06 -.13475-06 -.54757-04 -.15750-05  .22248-07 -.21626-03 -.43173-07 -.10023-06 -.59032-06
   -.33814-03 -.58933-08  .14920-07  .29728-03
    .75758-01 -.73447-01  .23213-05  .80384-06 -.98613-02 -.11041-01 -.15815-01  .63215-01 -.62290-01 -.92432-05  .12906-06
    .41310-02 -.41533-01  .24226-05  .43198-01
    .48687-02 -.46986-02  .82597-06 -.31913-06 -.38458-02 -.36767-02 -.30079-03  .72715-03 -.58440-03 -.37016-07  .30777-06
    .21717-03 -.43498-03  .18476-07  .31337-03
    .14120    -.13737    -.17414    -.18229     .11142     .11739     .18997-01 -.90701-01  .10582     .10873    -.12790
    .91945-01 -.83800-01  .68819-01  .44371-01
   -.10839-01  .10540-01  .11568-01  .12084-01 -.71880-02 -.75608-02 -.49314-03  .19565-02 -.21065-02 -.14702-02  .15320-02
   -.10492-02  .49645-03 -.61876-03 -.14118-04
    .14119    -.13738     .17408     .18232     .11136     .11749     .18999-01 -.90691-01  .10585    -.10867     .12820
    .91552-01 -.83820-01 -.68814-01  .44373-01
    .10838-01 -.10540-01  .11585-01  .12086-01  .71842-02  .75663-02  .45318-03 -.19564-02  .21069-02 -.14692-02  .15357-02
    .10446-02 -.49666-03 -.61875-03  .14137-04

MODAL FREQUENCIES (HZ)
     8.3389     8.3365     1.7638     1.7533    1.6714     1.6665     .34002     .30253     .27728     .22089     .17798
     .17165     .11171     .51093-01  .83715-01

GENERALIZED STIFFNESS MATRIX OF PLANT (HZ)
     815.97     .00000     .00000     .00000    .00000     .00000     .00000     .00000     .00000     .00000     .00000
     .00000     .00000     .00000     .00000
     .00000     815.51     .00000     .00000    .00000     .00000     .00000     .00000     .00000     .00000     .00000
     .00000     .00000     .00000     .00000
     .00000     .00000     122.82     .00000    .00000     .00000     .00000     .00000     .00000     .00000     .00000
     .00000     .00000     .00000     .00000
     .00000     .00000     .00000     121.35    .00000     .00000     .00000     .00000     .00000     .00000     .00000
     .00000     .00000     .00000     .00000
```

ORIGINAL PAGE IS
OF POOR QUALITY

.00000	.00000	.00000	.00000	110.29	.00000	.00000	.00000	.00000	.00000	.00000
.00000	.00000	.00000	.00000							
.00000	.00000	.00000	.00000	.00000	109.64	.00000	.00000	.00000	.00000	.00000
.00000	.00000	.00000	.00000							
.00000	.00000	.00000	.00000	.00000	.00000	4.3885	.00000	.00000	.00000	.00000
.00000	.00000	.00000	.00000							
.00000	.00000	.00000	.00000	.00000	.00000	.00000	3.6131	.00000	.00000	.00000
.00000	.00000	.00000	.00000							
.00000	.00000	.00000	.00000	.00000	.00000	.00000	.00000	3.0340	.00000	.00000
.00000	.00000	.00000	.00000							
.00000	.00000	.00000	.00000	.00000	.00000	.00000	.00000	.00000	1.9262	.00000
.00000	.00000	.00000	.00000							
.00000	.00000	.00000	.00000	.00000	.00000	.00000	.00000	.00000	.00000	1.2500
.00000	.00000	.00000	.00000							
.00000	.00000	.00000	.00000	.00000	.00000	.00000	.00000	.00000	.00000	.00000
1.1632	.00000	.00000	.00000							
.00000	.00000	.00000	.00000	.00000	.00000	.00000	.00000	.00000	.00000	.00000
.00000	.49267	.00000	.00000							
.00000	.00000	.00000	.00000	.00000	.00000	.00000	.00000	.00000	.00000	.00000
.00000	.00000	.10706	.00000							
.00000	.00000	.00000	.00000	.00000	.00000	.00000	.00000	.00000	.00000	.00000
.00000	.00000	.00000	.22203-01							

MTT

.99996	-.32097-04	-.23515-03	.21385-03	.23229-03	-.23046-03	-.90734-04	-.37075-03	-.40573-03	.15623-03	.19683-03
.12406-03	-.19372-04	.10347-03	-.89284-04							
-.32098-04	.99995	-.23330-03	.22297-03	.24748-03	-.22183-03	-.89388-04	-.39870-03	-.40792-03	.17065-03	.20055-03
.14246-03	-.23369-04	.11344-03	-.90655-04							
-.23516-03	-.23332-03	1.0002	-.26589-03	-.24300-03	.21750-03	.48776-04	.20658-03	.22378-03	-.16482-03	-.22356-03
-.16112-03	-.11428-03	-.11129-03	-.49589-04							
.21387-03	.22294-03	-.26585-03	1.0002	.22159-03	-.21130-03	-.43553-04	-.18959-03	-.21943-03	.17700-03	.18553-03
.14725-03	.11048-03	.11867-03	.44202-04							
.23229-03	.24747-03	-.24299-03	.22158-03	1.0002	-.17128-03	-.25549-04	-.10480-03	-.13687-03	.14451-03	.17491-03
.12505-03	.13076-03	.95414-04	.73840-04							
-.23047-03	-.22184-03	.21749-03	-.21130-03	-.17129-03	1.0001	.20199-04	.11274-03	.11511-03	-.14336-03	-.16570-03
-.13358-03	-.12035-03	-.95285-04	-.74513-04							
-.90735-04	-.89390-04	.48776-04	-.43554-04	-.25551-04	.20200-04	.99998	-.22449-04	-.20479-04	-.25871-04	-.26844-04
-.25334-04	-.47572-04	-.17171-04	-.40870-04							
-.37074-03	-.39871-03	.20658-03	-.18959-03	-.10479-03	.11274-03	-.22449-04	.99991	-.55060-04	-.11194-03	-.13426-03
-.10185-03	-.21168-03	-.73552-04	-.16894-03							
-.40573-03	-.40794-03	.22377-03	-.21944-03	-.13688-03	.11511-03	-.20479-04	-.55055-04	.99995	-.13853-03	-.15406-03
-.13360-03	-.21938-03	-.92337-04	-.17781-03							
.15623-03	.17068-03	-.16481-03	.17700-03	.14451-03	-.14336-03	-.25870-04	-.11193-03	-.13853-03	1.0001	.14591-03
.98634-04	.66576-04	.71139-04	.38731-04							
.19684-03	.20055-03	-.22353-03	.18553-03	.17492-03	-.16570-03	-.26844-04	-.13427-03	-.15406-03	.14592-03	1.0001
.12095-03	.10241-03	.97278-04	.49492-04							
.12406-03	.14246-03	-.16112-03	.14723-03	.12504-03	-.13359-03	-.25335-04	-.10185-03	-.13361-03	.98632-04	.12095-03
1.0001	.72153-04	.65423-04	.27847-04							
-.19390-04	-.23369-04	-.11427-03	.11048-03	.13078-03	-.12036-03	-.47575-04	-.21168-03	-.21939-03	.66576-04	.10241-03
.72149-04	.99998	.57948-04	-.52465-04							
.10348-03	.11345-03	-.11128-03	.11866-03	.95414-04	-.95287-04	-.17171-04	-.73551-04	-.92340-04	.71156-04	.97285-04
.63424-04	.57955-04	1.0000	.26080-04							
-.49291-04	-.40863-04	-.49549-04	.44201-04	.73857-04	-.74519-04	-.40871-04	-.16896-03	-.17782-03	.38735-04	.49898-04
.27849-04	-.52462-04	.26081-04	.99993							

DAMP

.14696	.00000	.00000	.00000	.00000	.00000	.00000	.00000	.00000	.00000	.00000
.00000	.00000	.00000	.00000							
.00000	.14680	.00000	.00000	.00000	.00000	.00000	.00000	.00000	.00000	.00000
.00000	.00000	.00000	.00000							
.00000	.00000	.11082	.00000	.00000	.00000	.00000	.00000	.00000	.00000	.00000
.00000	.00000	.00000	.00000							
.00000	.00000	.00000	.11016	.00000	.00000	.00000	.00000	.00000	.00000	.00000
.00000	.00000	.00000	.00000							
.00000	.00000	.00000	.00000	.10502	.00000	.00000	.00000	.00000	.00000	.00000
.00000	.00000	.00000	.00000							
.00000	.00000	.00000	.00000	.00000	.10471	.00000	.00000	.00000	.00000	.00000
.00000	.00000	.00000	.00000							
.00000	.00000	.00000	.00000	.00000	.00000	.21421-01	.00000	.00000	.00000	.00000
.00000	.00000	.00000	.00000							
.00000	.00000	.00000	.00000	.00000	.00000	.00000	.19008-01	.00000	.00000	.00000
.00000	.00000	.00000	.00000							
.00000	.00000	.00000	.00000	.00000	.00000	.00000	.00000	.17418-01	.00000	.00000
.00000	.00000	.00000	.00000							
.00000	.00000	.00000	.00000	.00000	.00000	.00000	.00000	.00000	.13879-01	.00000
.00000	.00000	.00000	.00000							
.00000	.00000	.00000	.00000	.00000	.00000	.00000	.00000	.00000	.00000	.11180-01
.00000	.00000	.00000	.00000							
.00000	.00000	.00000	.00000	.00000	.00000	.00000	.00000	.00000	.00000	.00000
.10785-01	.00000	.00000	.00000							
.00000	.00000	.00000	.00000	.00000	.00000	.00000	.00000	.00000	.00000	.00000
.00000	.70191-02	.00000	.00000							
.00000	.00000	.00000	.00000	.00000	.00000	.00000	.00000	.00000	.00000	.00000
.00000	.00000	.32103-02	.00000							
.00000	.00000	.00000	.00000	.00000	.00000	.00000	.00000	.00000	.00000	.00000
.00000	.00000	.00000	.14901-02							

XPO

.00000	.00000	.00000	.00000	.00000	.00000	.00000	.00000	.00000	.00000	.00000
.00000	.00000	.00000	.00000	.00000	.00000	.00000	.00000	.00000	.00000	.00000
.00000	.00000	.00000	.00000	.00000	.00000	.00000	.00000			

XMO

.00000	.00000	.00000	.00000	.00000	.00000	.00000	.00000	.00000	.00000	.00000
.00000	.00000	.00000	.00000	.00000	.00000	.00000				

T	0.00000	YP1	0.00000	YM1	0.00000
YP2	0.00000	YM2	0.00000	YP3	0.00000
YM3	0.00000	YP4	0.00000	YM4	0.00000
YP5	0.00000	YM5	0.00000	YP6	0.00000
YM6	0.00000	YP7	0.00000	YM7	0.00000
YP8	0.00000	YM8	0.00000	YP9	0.00000

YM9	0.00000	YP10	0.00000	YM10	0,00000
YP11	0.00000	YM11	0.00000	XP1	0,00000
XM1	0.00000	XP2	0.00000	XM2	0,00000
XP3	0.00000	XM3	0.00000	XP4	0,00000
XM4	0.00000	XP5	0.00000	XM5	0,00000
XP6	0.00000	XM6	0.00000	XP7	0,00000
XM7	0.00000	XP8	0.00000	XM8	0,00000
XP9	0.00000	XM9	0.00000	XP10	0,00000
XP11	0.00000	XP12	0.00000	XP13	0,00000
XP14	0.00000	XP15	0.00000	UP1	0,00000
UP2	0.00000	UP3	0.00000	UP4	0,00000
UP5	0.00000	UP6	0.00000	UP7	0,00000
UP8	0.00000	UP9	0.00000	UP10	0,00000
UP11	0.00000	Z1P	0.00000	Z1M	0,00000
T1P	0.00000	T1M	0.00000	Z3P	0,00000
Z3M	0.00000	T3P	0.00000	T3M	0,00000
Z2P	0.00000	Z2M	0.00000	P2P	0,00000
P2M	0.00000	Z4P	0.00000	Z4M	0,00000
T4P	0.00000	T4M	0.00000	P4P	0,00000
P4M	0.00000	Z6P	0.00000	Z6M	0,00000
P6P	0.00000	P6M	0.00000	Z5P	0,00000
Z5M	0.00000	T5P	0.00000	T5M	0,00000
Z7P	0.00000	Z7M	0.00000	T7P	0,00000
T7M	0.00000	Z10P	0.00000	Z10M	0,00000
T10P	0.00000	T10M	0.00000	Z30P	0,00000
Z30M	0.00000	T30P	0.00000	T30M	0,00000
Z20P	0.00000	Z20M	0.00000	P20P	0,00000
P20M	0.00000	Z40P	0.00000	Z40M	0,00000
T40P	0.00000	T40M	0.00000	P40P	0,00000
P40M	0.00000	Z60P	0.00000	Z60M	0,00000
P60P	0.00000	P60M	0.00000	Z50P	0,00000
Z50M	0.00000	T50P	0.00000	T50M	0,00000
Z70P	0.00000	Z70M	0.00000	T70P	0,00000
T70M	0.00000	Z8HU	0.00000	Z0SHU	5,00000-02
SHANP	0.00000	DSHANP	2.00000-01	SHANT	0,00000
DSHANT	2.00000-01	FDOCK	1.53000+08	TDOCKT	5,09392+04
TDOCKP	2.47069+04				

T	8.00000+01	YP1	1.97513-04	YM1	0,00000
YP2	-4.13676-05	YM2	0.00000	YP3	-1,73033-03
YM3	0.00000	YP4	2.43198-05	YM4	0,00000
YP5	9.44583-05	YM5	0.00000	YP6	-1,55337-03
YM6	0.00000	YP7	-1.07286-05	YM7	0,00000
YP8	1.72205-03	YM8	0.00000	YP9	2,30106-05
YM9	0.00000	YP10	-5.47427-05	YM10	0,00000
YP11	1.85295-04	YM11	0.00000	XP1	2,96514-01
XM1	0.00000	XP2	-8.96223-01	XM2	0,00000
XP3	-8.66484-04	XM3	0.00000	XP4	-2,69190-01
XM4	0.00000	XP5	1.82798-03	XM5	0,00000
XP6	3.11463-01	XM6	0.00000	XP7	-3,83474-04
XM7	0.00000	XP8	-1.72393-01	XM8	0,00000
XP9	8.61140-03	XM9	0.00000	XP10	-5,76809-05
XP11	6.26142-04	XP12	7.47187+04	XP13	3,33205-02
XP14	-4.22562-05	XP15	-2.40589-03	UP1	8,51966+01
UP2	8.52443+01	UP3	3.48259+00	UP4	2,53712-02

ORIGINAL PAGE IS
OF POOR QUALITY

UP5	9.66771-01	UP6	9.62704+01	UP7	-1.79800-01
UP8	-3.49723+00	UP9	-6.91027-03	UP10	8.52756+01
UP11	8.51975+01	Z1P	-3.71505-02	Z1M	0.00000
T1P	3.00709-02	T1M	0.00000	Z3P	2.96891-02
Z3M	0.00000	T3P	8.58303-02	T3M	0.00000
Z2P	-5.94348-04	Z2M	0.00000	P2P	-5.95720-03
P2M	0.00000	Z4P	3.30745-05	Z4M	0.00000
T4P	3.58432-02	T4M	0.00000	P4P	1.23927-02
P4M	0.00000	Z6P	6.07013-04	Z6M	0.00000
P6P	-5.99120-03	P6M	0.00000	Z5P	-3.01269-02
Z5M	0.00000	T5P	2.61414-02	T5M	0.00000
Z7P	3.79577-02	Z7M	0.00000	T7P	3.06169-02
T7M	0.00000	Z1DP	4.81417-02	Z1DM	0.00000
T1DP	5.30259-03	T1DM	0.00000	Z3DP	-7.01276-02
Z3DM	0.00000	T3DP	-7.53625-03	T3DM	0.00000
Z2DP	-1.61146-03	Z2DM	0.00000	P2DP	8.58486-03
P2DM	0.00000	Z4DP	6.78834-05	Z4DM	0.00000
T4DP	-9.60901-02	T4DM	0.00000	P4DP	-3.09324-03
P4DM	0.00000	Z6DP	1.60065-03	Z6DM	0.00000
P6DP	2.51665-03	P6DM	0.00000	Z5DP	7.13844-02
Z5DM	0.00000	T5DP	-8.36480-03	T5DM	0.00000
Z7DP	-4.93367-02	Z7DM	0.00000	T7DP	4.49325-03
T7DM	0.00000	Z8HU	8.30330-06	ZDSHU	1.42033-05
SHANP	1.27369-02	DSHANP	-3.13412-03	SHANT	3.62126-02
DSHANT	-9.71619-02	FDOCK	-1.36620-01	TQDCKT	5.98110+02
TQDCKP	1.85016+02				

T	1.00000+02	YP1	8.93516-04	YM1	0.00000
YP2	8.75736-04	YM2	0.00000	YP3	2.16519-04
YM3	0.00000	YP4	1.53915-05	YM4	0.00000
YP5	-1.80940-05	YM5	0.00000	YP6	7.97573-04
YM6	0.00000	YP7	-3.49628-05	YM7	0.00000
YP8	-2.02605-04	YM8	0.00000	YP9	1.59428-05
YM9	0.00000	YP10	8.74804-04	YM10	0.00000
YP11	8.87699-04	YM11	0.00000	XP1	-3.35916-02
XM1	0.00000	XP2	-1.56366+00	XM2	0.00000
XP3	-1.96926-04	XM3	0.00000	XP4	4.94334-02
XM4	0.00000	XP5	8.85766-04	XM5	0.00000
XP6	-1.77618-01	XM6	0.00000	XP7	-7.04157-06
XM7	0.00000	XP8	2.32743-02	XM8	0.00000
XP9	-1.81401-04	XM9	0.00000	XP10	4.42052-05
XP11	-1.23022-04	XP12	-5.14978-04	XP13	-2.31116-02
XP14	1.04740-05	XP15	3.17888-04	UP1	-5.94888+01
UP2	-5.94849+01	UP3	-4.54382-01	UP4	-1.47934-02
UP5	-1.87236-01	UP6	-6.44074+01	UP7	6.04428-02
UP8	4.58673-01	UP9	-5.93629-03	UP10	-5.94910+01
UP11	-5.94891+01	Z1P	-1.23672-01	Z1M	0.00000
T1P	5.51322-02	T1M	0.00000	Z3P	1.21744-01
Z3M	0.00000	T3P	5.41314-02	T3M	0.00000
Z2P	-2.32118-04	Z2M	0.00000	P2P	1.06869-03
P2M	0.00000	Z4P	-2.07956-06	Z4M	0.00000
T4P	4.42731-02	T4M	0.00000	P4P	-1.81777-03
P4M	0.00000	Z6P	2.58510-04	Z6M	0.00000

P6P	1.08739-03	P6M	0.00000	Z5P	-1.21930-01
Z5M	0.00000	T5P	5.42789-02	T5M	0.00000
Z7P	1.23868-01	Z7M	0.00000	T7P	5.52483-02
T7M	0.00000	Z10P	-7.98536-02	Z10M	0.00000
T10P	4.01683-02	T10M	0.00000	Z30P	7.91793-02
Z30M	0.00000	T30P	3.93497-02	T30M	0.00000
Z20P	2.62939-04	Z20M	0.00000	P20P	6.68130-04
P20M	0.00000	Z40P	-1.76780-05	Z40M	0.00000
T40P	3.68430-02	T40M	0.00000	P40P	-1.63967-03
P40M	0.00000	Z60P	-2.54307-04	Z60M	0.00000
P60P	6.95961-04	P60M	0.00000	Z50P	-7.90537-02
Z50M	0.00000	T50P	3.92668-02	T50M	0.00000
Z70P	7.93609-02	Z70M	0.00000	T70P	3.98232-02
T70M	0.00000	Z8MU	-8.65069-06	ZD6MU	3.23426-06
BHANP	-1.85978-03	DBHANP	-1.69071-03	BHANT	4.41381-02
DBHANT	3.68072-02	PDDCK	5.50569-02	TDDCKT	-1.66385+02
TDDCKP	-2.93656+01				

T	1.50000+02	YP1	-7.66489-04	YM1	0.00000
YP2	-7.58794-04	YM2	0.00000	YP3	1.36179-05
YM3	0.00000	YP4	-3.93910-06	YM4	0.00000
YP5	1.57121-07	YM5	0.00000	YP6	-3.36021-04
YM6	0.00000	YP7	7.42556-06	YM7	0.00000
YP8	-1.84311-05	YM8	0.00000	YP9	-3.99263-06
YM9	0.00000	YP10	-7.56201-04	YM10	0.00000
YP11	-7.62909-04	YM11	0.00000	XP1	-4.11058-03
XM1	0.00000	XP2	1.40566+00	XM2	0.00000
XP3	5.96302-04	XM3	0.00000	XP4	-3.87345-03
XM4	0.00000	XP5	1.82938-03	XM5	0.00000
XP6	-3.85906-02	XM6	0.00000	XP7	-1.66786-04
XM7	0.00000	XP8	1.83686-03	XM8	0.00000
XP9	-2.72884-04	XM9	0.00000	XP10	-2.15636-05
XP11	1.47757-05	XP12	2.38322-04	XP13	1.07379-02
XP14	-5.49834-06	XP15	2.03590-05	UP1	2.79864+01
UP2	2.80089+01	UP3	-3.39775-02	UP4	-1.23141-03
UP5	-2.02075-02	UP6	2.91269+01	UP7	-5.00508-03
UP8	4.05854-02	UP9	-1.05697-03	UP10	2.80058+01
UP11	2.79853+01	Z1P	9.14826-02	Z1M	0.00000
T1P	-3.98360-02	T1M	0.00000	Z3P	-9.02211-02
Z3M	0.00000	T3P	-3.90553-02	T3M	0.00000
Z2P	6.45315-05	Z2M	0.00000	P2P	-3.30360-05
P2M	0.00000	Z4P	-3.20510-06	Z4M	0.00000
T4P	-4.45756-02	T4M	0.00000	P4P	-1.62918-05
P4M	0.00000	Z6P	-8.15803-05	Z6M	0.00000
P6P	-3.91556-05	P6M	0.00000	Z5P	8.96182-02
Z5M	0.00000	T5P	-3.86548-02	T5M	0.00000
Z7P	-9.11615-02	Z7M	0.00000	T7P	-3.96040-02
T7M	0.00000	Z10P	5.80724-02	Z10M	0.00000
T10P	-3.59494-02	T10M	0.00000	Z30P	-5.76559-02
Z30M	0.00000	T30P	-3.56646-02	T30M	0.00000
Z20P	7.11603-07	Z20M	0.00000	P20P	-2.19067-04
P20M	0.00000	Z40P	7.98157-07	Z40M	0.00000

T4DP	-1.03374-02	T4DM	0.00000	P4DP	4.28711-04
P4DM	0.00000	Z6DP	-2.11388-06	Z6DM	0.00000
P6DP	-2.20930-04	P6DM	0.00000	Z5DP	5.79531-02
Z5DM	0.00000	T5DP	-3.55962-02	T5DM	0.00000
Z7DP	-5.78431-02	Z7DM	0.00000	T7DP	-3.57907-02
T7DM	0.00000	Z8HU	5.97550-06	ZD8HU	-3.68129-06
8HANP	-1.84937-05	D8HANP	4.40362-04	8HANT	-4.47625-02
D8HANT	-1.00968-02	FDOCK	-1.22413-03	TQDCKT	-1.50840+02
TQDCKP	2.30599-01				

T	2.00000+02	YP1	3.12860-04	YM1	0.00000
YP2	3.11714-04	YM2	0.00000	YP3	-1.66010-07
YM3	0.00000	YP4	3.63351-07	YM4	0.00000
YP5	3.86439-06	YM5	0.00000	YP6	1.26498-04
YM6	0.00000	YP7	-6.20679-07	YM7	0.00000
YP8	-3.26147-06	YM8	0.00000	YP9	2.39623-07
YM9	0.00000	YP10	3.13628-04	YM10	0.00000
YP11	3.15860-04	YM11	0.00000	XP1	1.12597-03
XM1	0.00000	XP2	-7.50858-01	XM2	0.00000
XP3	-1.17370-04	XM3	0.00000	XP4	-1.52944-03
XM4	0.00000	XP5	9.10320-04	XM5	0.00000
XP6	1.15981-01	XM6	0.00000	XP7	7.96028-05
XM7	0.00000	XPA	-4.61675-04	XM8	0.00000
XP9	6.87533-05	XM9	0.00000	XP10	4.13608-06
XP11	-6.44929-06	XP12	-8.91507-05	XP13	-4.01865-03
XP14	2.30239-06	XP15	-4.27894-06	UP1	-1.07284+01
UP2	-1.07395+01	UP3	4.26711-03	UP4	1.29761-03
UP5	1.23083-02	UP6	-1.10911+01	UP7	-8.09352-04
UP8	-1.12962-02	UP9	1.55187-03	UP10	-1.07381+01
UP11	-1.07280+01	Z1P	-3.81491-02	Z1M	0.00000
T1P	1.39765-02	T1M	0.00000	Z3P	3.82852-02
Z3M	0.00000	T3P	1.40909-02	T3M	0.00000
Z2P	-1.61888-05	Z2M	0.00000	P2P	-1.69131-05
P2M	0.00000	Z4P	6.70782-07	Z4M	0.00000
T4P	2.60945-02	T4M	0.00000	P4P	5.31792-05
P4M	0.00000	Z6P	8.45326-06	Z6M	0.00000
P6P	-2.24498-05	P6M	0.00000	Z5P	-3.84931-02
Z5M	0.00000	T5P	1.42280-02	T5M	0.00000
Z7P	3.84370-02	Z7M	0.00000	T7P	1.41798-02
T7M	0.00000	Z10P	-2.30079-02	Z10M	0.00000
T10P	1.51303-02	T10M	0.00000	Z3DP	2.28925-02
Z3DM	0.00000	T3DP	1.50417-02	T3DM	0.00000
Z2DP	3.07175-06	Z2DM	0.00000	P2DP	2.42011-05
P2DM	0.00000	Z4DP	3.73023-06	Z4DM	0.00000
T4DP	2.02890-03	T4DM	0.00000	P4DP	-4.61973-05
P4DM	0.00000	Z6DP	-4.95212-06	Z6DM	0.00000
P6DP	1.82193-05	P6DM	0.00000	Z5DP	-2.30118-02
Z5DM	0.00000	T5DP	1.51239-02	T5DM	0.00000
Z7DP	2.31971-02	Z7DM	0.00000	T7DP	1.52615-02
T7DM	0.00000	Z8HU	-3.49217-06	ZD8HU	1.27707-06
8HANP	5.67273-05	D8HANP	-4.71730-05	8HANT	2.63083-02
D8HANT	1.92880-03	FDOCK	-1.31126-02	TQDCKT	2.16431+02
TQDCKP	7.31406-01				

T	2.90000+02	YP1	-3.48680-05	YM1	0.00000
YP2	-3.47851-05	YM2	0.00000	YP3	1.22339-06
YM3	0.00000	YP4	-1.27689-08	YM4	0.00000
YP5	-2.06248-06	YM5	0.00000	YP6	-4.48214-05
YM6	0.00000	YP7	-4.44044-08	YM7	0.00000
YP8	1.54335-06	YM8	0.00000	YP9	6.26413-08
YM9	0.00000	YP10	-3.12778-05	YM10	0.00000
YP11	-3.19728-05	YM11	0.00000	XP1	-6.31685-05
XM1	0.00000	XP2	3.27930-01	XM2	0.00000
XP3	-6.76422-05	XM3	0.00000	XP4	5.76370-04
XM4	0.00000	XP5	8.29276-05	XM5	0.00000
XP6	-7.84022-02	XM6	0.00000	XP7	-6.27752-06
XM7	0.00000	XP8	-5.20423-05	XM8	0.00000
XP9	8.80630-05	XM9	0.00000	XP10	-2.56110-06
XP11	3.32839-06	XP12	2.70977-05	XP13	1.21626-03
XP14	-2.97979-07	XP15	-6.12676-07	UP1	3.36014+00
UP2	3.35792+00	UP3	2.49340-04	UP4	-1.26122-03
UP5	1.88559-02	UP6	3.71169+00	UP7	1.15562-03
UP8	-6.55778-04	UP9	-1.97446-03	UP10	3.35849+00
UP11	3.36021+00	Z1P	1.37810-02	Z1M	0.00000
T1P	-4.16010-03	T1M	0.00000	Z3P	-1.38775-02
Z3M	0.00000	T3P	-4.23771-03	T3M	0.00000
Z2P	7.30169-06	Z2M	0.00000	P2P	1.89095-06
P2M	0.00000	Z4P	1.16039-06	Z4M	0.00000
T4P	-1.20612-02	T4M	0.00000	P4P	-1.08723-05
P4M	0.00000	Z6P	-3.22779-07	Z6M	0.00000
P6P	4.61131-06	P6M	0.00000	Z5P	1.38774-02
Z5M	0.00000	T5P	-4.23219-03	T5M	0.00000
Z7P	-1.37572-02	Z7M	0.00000	T7P	-4.14873-03
T7M	0.00000	Z10P	1.64690-05	Z10M	0.00000
T10P	-1.14858-03	T10M	0.00000	Z30P	-1.64703-03
Z30M	0.00000	T30P	-1.14550-03	T30M	0.00000
Z20P	-2.36950-07	Z20M	0.00000	P20P	-1.10979-06
P20M	0.00000	Z40P	-2.29456-06	Z40M	0.00000
T40P	-1.55639-04	T40M	0.00000	P40P	-3.69729-07
P40M	0.00000	Z60P	1.60790-06	Z60M	0.00000
P60P	2.66682-06	P60M	0.00000	Z50P	1.35651-03
Z50M	0.00000	T50P	-9.45631-04	T50M	0.00000
Z70P	-1.43198-03	Z70M	0.00000	T70P	-1.00216-03
T70M	0.00000	ZSHU	1.41415-06	ZDSHU	1.53396-07
SHANP	-1.11162-05	DSHANP	-4.21585-07	SHANT	-1.21774-02
DSHANT	-1.67676-04	FDDCK	7.83579-03	TUDCKT	-1.34494+02
TODCKP	-1.41377-01				

T	3.00000+02	YP1	-4.06713-05	YM1	0.00000
YP2	-3.98891-05	YM2	0.00000	YP3	-1.90413-06
YM3	0.00000	YP4	1.91551-08	YM4	0.00000
YP5	1.77570-07	YM5	0.00000	YP6	1.40656-05
YM6	0.00000	YP7	4.51552-09	YM7	0.00000
YP8	1.76254-06	YM8	0.00000	YP9	1.41846-08
YM9	0.00000	YP10	-3.79090-05	YM10	0.00000
YP11	-3.84385-05	YM11	0.00000	XP1	-1.56608-05
XM1	0.00000	XP2	-1.30678-01	XM2	0.00000
XP3	7.94691-05	XM3	0.00000	XP4	-7.16862-05
XM4	0.00000	XP5	-2.43378-04	XM5	0.00000
XP6	2.42532-02	XM6	0.00000	XP7	-1.52388-05
XM7	0.00000	XP8	4.21552-05	XM8	0.00000
XP9	-6.51242-05	XM9	0.00000	XP10	6.18535-07
XP11	-1.37721-06	XP12	-6.10919-06	XP13	-2.70229-04
XP14	-2.70638-07	XP15	6.27234-08	UP1	-7.72170-01
UP2	-7.67469-01	UP3	3.21333-05	UP4	8.01116-04
UP5	-2.03768-02	UP6	-1.02444+00	UP7	-7.53680-04
UP8	1.05403-03	UP9	1.41470+03	UP10	-7.68343-01
UP11	-7.72339-01	Z1P	-6.33518-03	Z1M	0.00000
T1P	2.42269-03	T1M	0.00000	Z3P	6.33801-03
Z3M	0.00000	T3P	2.43036-03	T3M	0.00000
Z2P	-3.20147-06	Z2M	0.00000	P2P	1.07503-06
P2M	0.00000	Z4P	-1.05997-06	Z4M	0.00000
T4P	8.64040-03	T4M	0.00000	P4P	3.59271-07
P4M	0.00000	Z6P	1.76321-07	Z6M	0.00000
P6P	6.05058-07	P6M	0.00000	Z5P	-6.29783-03
Z5M	0.00000	T5P	2.40037-03	T5M	0.00000
Z7P	6.25641-03	Z7M	0.00000	T7P	2.37072-03
T7M	0.00000	Z10P	4.24271-03	Z10M	0.00000
T10P	-2.81483-03	T10M	0.00000	Z30P	-4.18164-03
Z30M	0.00000	T30P	-2.77155-03	T30M	0.00000
Z20P	-1.26384-06	Z20M	0.00000	P20P	8.82499-07
P20M	0.00000	Z40P	3.89484-07	Z40M	0.00000
T40P	-1.22179-04	T40M	0.00000	P40P	1.86866-07
P40M	0.00000	Z60P	1.74727-06	Z60M	0.00000
P60P	6.91704-07	P60M	0.00000	Z50P	4.00795-03
T50M	0.00000	T50P	-2.65210-03	T50M	0.00000
Z70P	-4.04078-03	Z70M	0.00000	T70P	-2.67651-03
T70M	0.00000	Z8HU	-2.71766-07	ZUSHU	-3.58079-07
BHANP	3.54313-07	DBHANP	1.67024-07	SHANT	4.67275-03
DBHANT	-9.03920-05	FDOCK	-1.21636-03	TUDCKT	4.47054+01
TQDCKP	-5.17244-03				

TRANSPOSE OF MODAL MATRIX (EVECT)

-.13679	.10500-01	-.13726	-.10595-01	-.73357-01	.47159-02	.11120-04	-.30478-07	.36010-09	.75798-01	.88687-02
.14120	-.10839-01	.14119	.10838-01							
-.14168	.10869-01	-.14216	-.10895-01	-.75707-01	.48448-02	-.69359-03	-.29572-07	.54736-06	-.73447-01	-.46986-02
-.13737	.10540-01	-.13738	-.10580-01							
-.18162	.12086-01	.18260	.12141-01	-.11311-03	.18911-04	-.22144-05	.75290-08	.13308-06	.23213-05	.82597-06
-.17414	.11588-01	.17408	.11585-01							
.17400	-.11535-01	-.17504	-.11593-01	.11011-03	-.19361-04	.23421-05	.16672-05	-.13475-06	.80384-06	-.31913-06
-.18829	.12084-01	.18232	.12086-01							
-.11874	.76595-02	-.11728	-.75576-02	.10931-01	-.36561-02	.28959-04	.16708-06	-.54757-04	-.98613-02	-.34458-02
.11142	-.71880-02	.11136	.71842-02							
.11143	-.71756-02	.11016	.70870-02	-.10496-01	.34739-02	-.99187-03	-.14210-06	-.15750-05	-.11041-01	-.36767-02
.11739	-.75604-02	.11749	.75663-02							
.18978-01	-.45267-03	.18998-01	.45285-03	-.15798-01	.30061-03	.12399-01	-.90847-08	.22248-07	-.15815-01	-.30079-03
.18997-01	-.45314-03	.18999-01	.45318-03							
.90609-01	-.19545-02	.90719-01	.19557-02	-.63155-01	.72661-03	.19132-05	-.59343-07	-.81626-03	.63215-01	.72715-03
-.90701-01	.19565-02	-.90691-01	-.19564-02							
.10586	-.21073-02	.10402	.21090-02	-.62310-01	.58469-03	-.22580-02	-.10623-06	-.43173-07	-.62290-01	-.58440-03
.10582	-.21065-02	.10585	.21049-02							
.10881	-.14718-02	-.10880	-.14704-02	-.30675-04	.35986-06	-.35667-06	.41659-03	-.10023-06	-.92432-05	-.37016-07
.10873	-.14702-02	-.10867	-.14692-02							
.12785	-.15317-02	-.12816	-.15387-02	-.27623-04	.58846-06	-.18137-06	-.16960-06	-.59032-06	.12906-06	.30777-06
-.12790	.15320-02	.12820	.15397-02							
-.91971-01	.10494-02	-.91931-01	-.10440-02	-.41719-02	.21738-03	-.12829-06	-.10132-06	-.33814-03	.41510-02	.21717-03
.91949-01	-.10492-02	.91952-01	.10446-02							
-.83796-01	.49641-03	-.83782-01	-.49620-03	-.41532-01	.43498-03	-.37357-03	-.51680-07	-.58933-08	-.41533-01	-.43498-03
-.83800-01	.49645-03	-.83820-01	-.49666-03							
.68819-01	-.61876-03	-.68814-01	-.61870-03	-.19659-05	.92326-08	.31759-08	-.54261-03	.14924-07	.24226-05	.18476-07
.68819-01	-.61876-03	-.68814-01	-.61875-03							
-.44374-01	.14138-04	-.44371-01	-.14112-04	-.43185-01	.31337-03	-.19150-08	.97482-08	.29728-03	.43154-01	.31337-03
.44371-01	-.14118-04	.44373-01	.14137-04							

INVERSE OF MODAL MATRIX (EVECI)

.18704	14.761	.18739	-14.790	.12297	49.483	.17486-01	-.10941-01	40.988	-.12725	51.086
-.19310	-15.239	-.19309	15.237							
.19393	15.307	.19429	-15.337	.11963	50.762	-1.0910	-.10780-01	.68431	.11631	-49.830
.18807	14.848	.18808	-14.844							
.31521	26.183	-.31638	26.287	.52908-02	.39218	-.44199-02	39.681	.19680	-.29524-03	.18606-01
.30226	25.108	-.30218	25.097							
-.30143	-25.165	.30273	-25.280	-.55891-02	-.40768	.47328-02	.88592	-.19969	.15574-03	-.82598-02
.31503	26.364	-.31588	26.368							
.21093	17.851	.20798	-17.603	-1.3558	-87.657	.60390-01	.94486-01	-84.612	1.2793	-82.657
-.19796	-16.753	-.19786	16.798							
-.19823	-16.791	-.19561	16.578	1.2766	83.252	-2.0730	-.80558-01	-2.4410	1.3331	-88.153
-.20888	-17.693	-.20904	17.706							
.14253	.66657-01	.14270	-.73001-01	-.93126	-.08229	77.453	-.16577-01	.80791-01	-.93205	.89483
.14267	.66611-01	.14269	-.66565-01							
.85619	8.6565	.85722	-8.6896	-8.8596	-83.609	.18754-01	-.11159	-808.60	8.8624	-43.661
-.85707	-8.6610	-.85692	8.6588							
1.1981	9.3625	1.1598	-9.4066	-8.9509	-52.465	-15.751	-.80339	-.16536	-4.9273	52.452
1.1976	9.3570	1.1580	-9.3619							
1.8709	26.792	-1.8701	26.813	-.50098-02	-.21410-01	-.27848-02	826.27	-.39065	-.72508-03	.11360-01
1.8694	26.779	-1.8685	26.769							
2.3801	35.903	-2.3958	36.013	-.38149-02	-.16289-02	-.16179-02	-.34490	-2.3458	.94933-03	.20239-01
-2.3813	-35.926	2.3470	-36.012							
-1.7654	-27.170	-1.7563	27.048	-.97986	8.4108	-.10934-02	-.20669	-1346.9	.97348	8.4273
1.7447	27.156	1.7579	-27.049							

-2.0825	-36.714	-2.0819	36.708	-4.8446	-39.911	-5.3539	-.10906	-.21814-01	-4.8428	39.012
-2.0826	-36.713	-2.0831	36.719							
1.4785	24.128	-1.4778	24.131	-.29828-03	-.17817-02	.19198-04	-1203.1	.62157-01	.25999-03	-.22890-02
1.4786	24.132	-1.4788	24.129							
-1.3653	-26.078	-1.3648	26.075	-4.9038	-47.956	-.82363-04	.22926-01	1223.0	4.9016	-43.956
1.3653	26.075	1.3653	-26.076							

TRUNCATED MODAL MATRIX (EVECR)

.13284-01	.63426-01	.74101-01	.76168-01	.89493-01	-.64379-01	-.58657-01	.48170-01	-.31062-01
-.31687-03	-.13684-02	-.14751-02	-.10300-02	-.10722-02	.73495-03	.34749-03	-.43313-03	.98963-05
.24697-01	.11794	.13782	-.14144	-.16661	-.11499	-.10892	-.89458-01	-.57682-01
.58871-03	.25424-02	.27417-02	-.19115-02	-.19930-02	-.13571-02	-.64506-03	-.80432-03	-.18346-04
-.15798-01	-.63155-01	-.62310-01	-.30675-04	-.27623-04	-.41719-02	-.41532-01	-.15653-05	-.43155-01
.21043-03	.50863-03	.40925-03	.25190-06	.41192-06	.15217-03	.30448-03	.64628-08	.21936-03
.12399-01	.19132-05	-.22580-02	-.35667-06	-.18137-06	-.12829-06	-.37357-03	.31755-08	-.19150-08
-.90847-08	-.59343-07	-.10623-06	.41659-03	-.16960-06	-.10132-06	-.51629-07	-.54261-03	.97482-08
.22248-07	-.21626-03	-.43173-07	-.10023-06	-.59032-06	-.33814-03	-.58933-08	.14924-07	.29728-03
-.15815-01	.63215-01	-.62290-01	-.92432-05	.12906-06	.41510-02	-.41533-01	.24226-05	.43154-01
-.39103-03	.94529-03	-.75972-03	-.48121-07	.40010-06	.28232-03	-.56548-03	.24019-07	.40738-03
.13298-01	-.63491-01	.74072-01	.76112-01	-.89527-01	.64361-01	-.58660-01	.48174-01	.31060-01
-.31720-03	.13696-02	-.14744-02	-.10291-02	.10728-02	-.73487-03	.38752-03	-.43313-03	-.98826-05
.24699-01	-.11790	.13760	-.14128	.16666	.11902	-.10897	-.89458-01	.57685-01
.58914-03	-.25433-02	.27390-02	-.19100-02	.19964-02	.13580-02	-.64566-03	-.80438-03	.18378-04

DAMPING MATRIX OF THE PLANT (DAMP)

.14696	.00000	.00000	.00000	.00000	.00000	.00000	.00000	.00000	.00000	.00000
.00000	.00000	.00000	.00000							
.00000	.14680	.00000	.00000	.00000	.00000	.00000	.00000	.00000	.00000	.00000
.00000	.00000	.00000	.00000							
.00000	.00000	.11082	.00000	.00000	.00000	.00000	.00000	.00000	.00000	.00000
.00000	.00000	.00000	.00000							
.00000	.00000	.00000	.11016	.00000	.00000	.00000	.00000	.00000	.00000	.00000
.00000	.00000	.00000	.00000							
.00000	.00000	.00000	.00000	.10502	.00000	.00000	.00000	.00000	.00000	.00000
.00000	.00000	.00000	.00000							
.00000	.00000	.00000	.00000	.00000	.10471	.00000	.00000	.00000	.00000	.00000
.00000	.00000	.00000	.00000							
.00000	.00000	.00000	.00000	.00000	.00000	.21421-01	.00000	.00000	.00000	.00000
.00000	.00000	.00000	.00000							
.00000	.00000	.00000	.00000	.00000	.00000	.00000	.19008-01	.00000	.00000	.00000
.00000	.00000	.00000	.00000							
.00000	.00000	.00000	.00000	.00000	.00000	.00000	.00000	.17418-01	.00000	.00000
.00000	.00000	.00000	.00000							
.00000	.00000	.00000	.00000	.00000	.00000	.00000	.00000	.00000	.13879-01	.00000
.00000	.00000	.00000	.00000							
.00000	.00000	.00000	.00000	.00000	.00000	.00000	.00000	.00000	.00000	.11180-01
.00000	.00000	.00000	.00000							
.00000	.00000	.00000	.00000	.00000	.00000	.00000	.00000	.00000	.00000	.00000
.10785-01	.00000	.00000	.00000							
.00000	.00000	.00000	.00000	.00000	.00000	.00000	.00000	.00000	.00000	.00000
.00000	.70191-02	.00000	.00000							
.00000	.00000	.00000	.00000	.00000	.00000	.00000	.00000	.00000	.00000	.00000

ORIGINAL PAGE IS
OF POOR QUALITY

```
   .00000     .00000     .32103-02  .00000
   .00000     .00000     .00000     .00000     .00000     .00000     .00000     .00000     .00000     .00000     .00000
   .00000     .00000     .00000     .14901-02
```

DAMPING MATRIX OF THE MODEL (DAM)

```
   2.3462     .00000     .00000     .00000     .00000     .00000     .00000     .00000     .00000
   .00000     2.0819     .00000     .00000     .00000     .00000     .00000     .00000     .00000
   .00000     .00000     1.9078     .00000     .00000     .00000     .00000     .00000     .00000
   .00000     .00000     .00000     1.5201     .00000     .00000     .00000     .00000     .00000
   .00000     .00000     .00000     .00000     1.2246     .00000     .00000     .00000     .00000
   .00000     .00000     .00000     .00000     .00000     1.1813     .00000     .00000     .00000
   .00000     .00000     .00000     .00000     .00000     .00000     1.1743     .00000     .00000
   .00000     .00000     .00000     .00000     .00000     .00000     .00000     .53710     .00000
   .00000     .00000     .00000     .00000     .00000     .00000     .00000     .00000     .24930
```

GENERALIZED STIFFNESS MATRIX OF PLANT (N2)

```
   215.97     .00000     .00000     .00000     .00000     .00000     .00000     .00000     .00000     .00000     .00000
   .00000     .00000     .00000     .00000
   .00000     215.51     .00000     .00000     .00000     .00000     .00000     .00000     .00000     .00000     .00000
   .00000     .00000     .00000     .00000
   .00000     .00000     122.82     .00000     .00000     .00000     .00000     .00000     .00000     .00000     .00000
   .00000     .00000     .00000     .00000
   .00000     .00000     .00000     121.35     .00000     .00000     .00000     .00000     .00000     .00000     .00000
   .00000     .00000     .00000     .00000
   .00000     .00000     .00000     .00000     110.29     .00000     .00000     .00000     .00000     .00000     .00000
   .00000     .00000     .00000     .00000
   .00000     .00000     .00000     .00000     .00000     109.64     .00000     .00000     .00000     .00000     .00000
   .00000     .00000     .00000     .00000
   .00000     .00000     .00000     .00000     .00000     .00000     4.5885     .00000     .00000     .00000     .00000
   .00000     .00000     .00000     .00000
   .00000     .00000     .00000     .00000     .00000     .00000     .00000     3.6131     .00000     .00000     .00000
   .00000     .00000     .00000     .00000
   .00000     .00000     .00000     .00000     .00000     .00000     .00000     .00000     3.0340     .00000     .00000
   .00000     .00000     .00000     .00000
   .00000     .00000     .00000     .00000     .00000     .00000     .00000     .00000     .00000     1.9262     .00000
   .00000     .00000     .00000     .00000
   .00000     .00000     .00000     .00000     .00000     .00000     .00000     .00000     .00000     .00000     1.2500
   .00000     .00000     .00000     .00000
   .00000     .00000     .00000     .00000     .00000     .00000     .00000     .00000     .00000     .00000     .00000
   1.1632     .00000     .00000     .00000
   .00000     .00000     .00000     .00000     .00000     .00000     .00000     .00000     .00000     .00000     .00000
   .00000     .49267     .00000     .00000
   .00000     .00000     .00000     .00000     .00000     .00000     .00000     .00000     .00000     .00000     .00000
   .00000     .00000     .10306     .00000
   .00000     .00000     .00000     .00000     .00000     .00000     .00000     .00000     .00000     .00000     .00000
   .00000     .00000     .00000     .22203-01
```

GENERALIZED STIFFNESS MATRIX OF MODEL (W2M)

2.7531	.00000	.00000	.00000	.00000	.00000	.00000	.00000	.00000
.00000	2.1679	.00000	.00000	.00000	.00000	.00000	.00000	.00000
.00000	.00000	1.6204	.00000	.00000	.00000	.00000	.00000	.00000
.00000	.00000	.00000	1.1557	.00000	.00000	.00000	.00000	.00000
.00000	.00000	.00000	.00000	.75001	.00000	.00000	.00000	.00000
.00000	.00000	.00000	.00000	.00000	.69794	.00000	.00000	.00000
.00000	.00000	.00000	.00000	.00000	.00000	.68974	.00000	.00000
.00000	.00000	.00000	.00000	.00000	.00000	.00000	.14428	.00000
.00000	.00000	.00000	.00000	.00000	.00000	.00000	.00000	.31084-01

MATRIX AP

.00000	.00000	.00000	.00000	.00000	.00000	.00000	.00000	.00000	.00000	.00000
.00000	.00000	.00000	.00000	1.0000	.00000	.00000	.00000	.00000	.00000	.00000
.00000	.00000	.00000	.00000	.00000	.00000	.00000	.00000			
.00000	.00000	.00000	.00000	.00000	.00000	.00000	.00000	.00000	.00000	.00000
.00000	.00000	.00000	.00000	.00000	1.0000	.00000	.00000	.00000	.00000	.00000
.00000	.00000	.00000	.00000	.00000	.00000	.00000	.00000			
.00000	.00000	.00000	.00000	.00000	.00000	.00000	.00000	.00000	.00000	.00000
.00000	.00000	.00000	.00000	.00000	.00000	1.0000	.00000	.00000	.00000	.00000
.00000	.00000	.00000	.00000	.00000	.00000	.00000	.00000			
.00000	.00000	.00000	.00000	.00000	.00000	.00000	.00000	.00000	.00000	.00000
.00000	.00000	.00000	.00000	.00000	.00000	.00000	1.0000	.00000	.00000	.00000
.00000	.00000	.00000	.00000	.00000	.00000	.00000	.00000			
.00000	.00000	.00000	.00000	.00000	.00000	.00000	.00000	.00000	.00000	.00000
.00000	.00000	.00000	.00000	.00000	.00000	.00000	.00000	1.0000	.00000	.00000
.00000	.00000	.00000	.00000	.00000	.00000	.00000	.00000			
.00000	.00000	.00000	.00000	.00000	.00000	.00000	.00000	.00000	.00000	.00000
.00000	.00000	.00000	.00000	.00000	.00000	.00000	.00000	.00000	1.0000	.00000
.00000	.00000	.00000	.00000	.00000	.00000	.00000	.00000			
.00000	.00000	.00000	.00000	.00000	.00000	.00000	.00000	.00000	.00000	.00000
.00000	.00000	.00000	.00000	.00000	.00000	.00000	.00000	.00000	.00000	1.0000
.00000	.00000	.00000	.00000	.00000	.00000	.00000	.00000			
.00000	.00000	.00000	.00000	.00000	.00000	.00000	.00000	.00000	.00000	.00000
.00000	.00000	.00000	.00000	.00000	.00000	.00000	.00000	.00000	.00000	.00000
1.0000	.00000	.00000	.00000	.00000	.00000	.00000	.00000			
.00000	.00000	.00000	.00000	.00000	.00000	.00000	.00000	.00000	.00000	.00000
.00000	.00000	.00000	.00000	.00000	.00000	.00000	.00000	.00000	.00000	.00000
.00000	1.0000	.00000	.00000	.00000	.00000	.00000	.00000			
.00000	.00000	.00000	.00000	.00000	.00000	.00000	.00000	.00000	.00000	.00000
.00000	.00000	.00000	.00000	.00000	.00000	.00000	.00000	.00000	.00000	.00000
.00000	.00000	1.0000	.00000	.00000	.00000	.00000	.00000			
.00000	.00000	.00000	.00000	.00000	.00000	.00000	.00000	.00000	.00000	.00000
.00000	.00000	.00000	.00000	.00000	.00000	.00000	.00000	.00000	.00000	.00000
.00000	.00000	.00000	1.0000	.00000	.00000	.00000	.00000			
.00000	.00000	.00000	.00000	.00000	.00000	.00000	.00000	.00000	.00000	.00000
.00000	.00000	.00000	.00000	.00000	.00000	.00000	.00000	.00000	.00000	.00000
.00000	.00000	.00000	.00000	1.0000	.00000	.00000	.00000			
.00000	.00000	.00000	.00000	.00000	.00000	.00000	.00000	.00000	.00000	.00000
.00000	.00000	.00000	.00000	.00000	.00000	.00000	.00000	.00000	.00000	.00000
.00000	.00000	.00000	.00000	.00000	1.0000	.00000	.00000			
.00000	.00000	.00000	.00000	.00000	.00000	.00000	.00000	.00000	.00000	.00000
.00000	.00000	.00000	.00000	.00000	.00000	.00000	.00000	.00000	.00000	.00000
.00000	.00000	.00000	.00000	.00000	.00000	1.0000	.00000			
.00000	.00000	.00000	.00000	.00000	.00000	.00000	.00000	.00000	.00000	.00000
.00000	.00000	.00000	.00000	.00000	.00000	.00000	.00000	.00000	.00000	.00000
.00000	.00000	.00000	.00000	.00000	.00000	.00000	1.0000			

-215.97	.00000	.00000	.00000	.00000	.00000	.00000	.00000	.00000	.00000	.00000
.00000	.00000	.00000	.00000	-.14696	.00000	.00000	.00000	.00000	.00000	.00000
.00000	.00000	.00000	.00000	.00000	.00000	.00000	.00000			
.00000	-215.51	.00000	.00000	.00000	.00000	.00000	.00000	.00000	.00000	.00000
.00000	.00000	.00000	.00000	.00000	-.14680	.00000	.00000	.00000	.00000	.00000
.00000	.00000	.00000	.00000	.00000	.00000	.00000	.00000			
.00000	.00000	-122.82	.00000	.00000	.00000	.00000	.00000	.00000	.00000	.00000
.00000	.00000	.00000	.00000	.00000	.00000	-.11082	.00000	.00000	.00000	.00000
.00000	.00000	.00000	.00000	.00000	.00000	.00000	.00000			
.00000	.00000	.00000	-121.35	.00000	.00000	.00000	.00000	.00000	.00000	.00000
.00000	.00000	.00000	.00000	.00000	.00000	.00000	-.11016	.00000	.00000	.00000
.00000	.00000	.00000	.00000	.00000	.00000	.00000	.00000			
.00000	.00000	.00000	.00000	-110.29	.00000	.00000	.00000	.00000	.00000	.00000
.00000	.00000	.00000	.00000	.00000	.00000	.00000	.00000	-.10502	.00000	.00000
.00000	.00000	.00000	.00000	.00000	.00000	.00000	.00000			
.00000	.00000	.00000	.00000	.00000	-109.64	.00000	.00000	.00000	.00000	.00000
.00000	.00000	.00000	.00000	.00000	.00000	.00000	.00000	.00000	-.10471	.00000
.00000	.00000	.00000	.00000	.00000	.00000	.00000	.00000			
.00000	.00000	.00000	.00000	.00000	.00000	-4.5865	.00000	.00000	.00000	.00000
.00000	.00000	.00000	.00000	.00000	.00000	.00000	.00000	.00000	.00000	-.21421-01
.00000	.00000	.00000	.00000	.00000	.00000	.00000	.00000			
.00000	.00000	.00000	.00000	.00000	.00000	.00000	-3.4131	.00000	.00000	.00000
.00000	.00000	.00000	.00000	.00000	.00000	.00000	.00000	.00000	.00000	.00000
-.19008-01	.00000	.00000	.00000	.00000	.00000	.00000	.00000			
.00000	.00000	.00000	.00000	.00000	.00000	.00000	.00000	-3.0340	.00000	.00000
.00000	.00000	.00000	.00000	.00000	.00000	.00000	.00000	.00000	.00000	.00000
.00000	-.17418-01	.00000	.00000	.00000	.00000	.00000	.00000			
.00000	.00000	.00000	.00000	.00000	.00000	.00000	.00000	.00000	-1.9262	.00000
.00000	.00000	.00000	.00000	.00000	.00000	.00000	.00000	.00000	.00000	.00000
.00000	.00000	-.13879-01	.00000	.00000	.00000	.00000	.00000			
.00000	.00000	.00000	.00000	.00000	.00000	.00000	.00000	.00000	.00000	-1.2500
.00000	.00000	.00000	.00000	.00000	.00000	.00000	.00000	.00000	.00000	.00000
.00000	.00000	.00000	-.11180-01	.00000	.00000	.00000	.00000			
.00000	.00000	.00000	.00000	.00000	.00000	.00000	.00000	.00000	.00000	.00000
-1.1652	.00000	.00000	.00000	.00000	.00000	.00000	.00000	.00000	.00000	.00000
.00000	.00000	.00000	.00000	-.10785-01	.00000	.00000	.00000			
.00000	.00000	.00000	.00000	.00000	.00000	.00000	.00000	.00000	.00000	.00000
.00000	-.49267	.00000	.00000	.00000	.00000	.00000	.00000	.00000	.00000	.00000
.00000	.00000	.00000	.00000	.00000	-.70191-02	.00000	.00000			
.00000	.00000	.00000	.00000	.00000	.00000	.00000	.00000	.00000	.00000	.00000
.00000	.00000	-.10306	.00000	.00000	.00000	.00000	.00000	.00000	.00000	.00000
.00000	.00000	.00000	.00000	.00000	.00000	-.32103-02	.00000			
.00000	.00000	.00000	.00000	.00000	.00000	.00000	.00000	.00000	.00000	.00000
.00000	.00000	.00000	-.22203-01	.00000	.00000	.00000	.00000	.00000	.00000	.00000
.00000	.00000	.00000	.00000	.00000	.00000	.00000	-.14901-02			

MATRIX BP

.00000	.00000	.00000	.00000	.00000	.00000	.00000	.00000	.00000	.00000	.00000
.00000	.00000	.00000	.00000	.00000	.00000	.00000	.00000	.00000	.00000	.00000
.00000	.00000	.00000	.00000	.00000	.00000	.00000	.00000	.00000	.00000	.00000
.00000	.00000	.00000	.00000	.00000	.00000	.00000	.00000	.00000	.00000	.00000
.00000	.00000	.00000	.00000	.00000	.00000	.00000	.00000	.00000	.00000	.00000
.00000	.00000	.00000	.00000	.00000	.00000	.00000	.00000	.00000	.00000	.00000
.00000	.00000	.00000	.00000	.00000	.00000	.00000	.00000	.00000	.00000	.00000
.00000	.00000	.00000	.00000	.00000	.00000	.00000	.00000	.00000	.00000	.00000
.00000	.00000	.00000	.00000	.00000	.00000	.00000	.00000	.00000	.00000	.00000

ORIGINAL PAGE IS
OF POOR QUALITY

.00000	.00000	.00000	.00000	.00000	.00000	.00000	.00000	.00000	.00000	.00000
.00000	.00000	.00000	.00000	.00000	.00000	.00000	.00000	.00000	.00000	.00000
.00000	.00000	.00000	.00000	.00000	.00000	.00000	.00000	.00000	.00000	.00000
.00000	.00000	.00000	.00000	.00000	.00000	.00000	.00000	.00000	.00000	.00000
.00000	.00000	.00000	.00000	.00000	.00000	.00000	.00000	.00000	.00000	.00000
.00000	.00000	.00000	.00000	.00000	.00000	.00000	.00000	.00000	.00000	.00000
.10500-01	-.10525-01	-.73357-01	.47154-02	.11120-04	-.30078-07	.36010-04	.75758-01	.48687-02	-.10839-01	.10838-01
.10869-01	-.10895-01	-.75707-01	.48442-02	-.69359-03	-.29572-07	.54734-06	-.73447-01	-.46986-02	.10540-01	-.10540-01
.12086-01	.17141-01	-.11311-03	.18911-04	-.22144-05	.75290-04	.13308-06	.23213-05	.82597-06	.11588-01	.11585-01
-.11535-01	-.11593-01	.11011-03	-.19361-04	.23421-05	.16672-05	-.13475-06	.80384-06	-.31913-06	.12084-01	.12086-01
.76595-02	-.75576-02	.10531-01	-.36561-02	.28959-04	.16708-06	-.54757-04	-.98613-02	-.34458-02	-.71880-02	.71882-02
-.71756-02	.70870-02	-.10496-01	.34739-02	-.99187-03	-.14210-06	-.15750-05	-.11041-01	-.36767-02	-.75604-02	.75663-02
-.45267-03	.45285-03	-.15798-01	.30041-03	.12399-01	-.90887-08	.22248-07	-.15815-01	-.30079-03	-.45314-03	.45318-03
-.19545-02	.19557-02	-.63155-01	.72661-03	.19132-05	-.59343-07	-.21626-03	.63215-01	.72715-03	.19565-02	-.19564-02
-.21073-02	.21090-02	-.62310-01	.58464-03	-.22580-02	-.10423-06	-.43173-07	-.62290-01	-.58440-03	-.21065-02	.21069-02
-.14714-02	-.14704-02	-.30675-04	.35986-06	-.35667-06	.81459-03	-.10023-06	-.92432-05	-.37016-07	-.14702-02	-.14692-02
-.15317-02	-.15347-02	-.27623-04	.58846-06	-.18137-06	-.16960-06	-.59038-06	.12906-06	.30777-06	.15320-02	.15357-02
.10494-02	-.10440-02	-.41719-02	.21738-03	-.12829-06	-.10132-06	-.33814-03	.81510-02	.21717-03	-.10492-02	.10446-02
.49641-03	-.49620-03	-.41532-01	.83498-03	-.37357-03	-.51629-07	-.58933-08	-.41535-01	-.83498-03	.49645-03	-.49666-03
-.61876-03	-.61870-03	-.15653-05	.92326-08	.31755-08	-.54261-03	.14924-07	.24226-05	.18476-07	-.61876-03	-.61875-03
.14138-04	-.14112-04	-.43155-01	.31337-03	-.19150-08	.97482-08	.29728-03	.43154-01	.31337-03	-.14118-04	.14137-04

MATRIX CP

.20999-02	.21739-02	.24173-02	-.23069-02	.15319-02	-.18351-02	-.90534-04	-.39091-05	-.42145-03	-.29428-03	-.30634-03
.20987-03	.99282-04	-.12379-03	.28275-05	.10500-01	.10869-01	.12086-01	-.11535-01	.76595-02	-.71756-02	-.45267-03
-.19545-02	-.21073-02	-.14714-02	-.15317-02	.10494-02	.49641-03	-.61876-03	.14138-04			
-.21050-02	-.21791-02	.24282-02	-.23186-02	-.15115-02	.14174-02	.90571-04	.39114-05	.42181-03	-.29407-03	-.30693-03
-.20879-03	-.99239-04	-.12374-03	-.28274-05	-.10525-01	-.10895-01	.12141-01	-.11593-01	-.75576-02	.70870-02	.45285-03
.19557-02	.21090-02	-.14704-02	-.15347-02	-.10440-02	-.49620-03	-.61870-03	-.14112-04			
-.14671-01	-.15141-01	-.22622-04	.22023-04	.21065-02	-.20992-02	-.31597-02	-.12631-01	-.12462-01	-.61351-05	-.55249-05
-.83438-03	-.87064-02	-.31305-06	-.86310-02	-.73357-01	-.75707-01	-.11311-03	.11011-03	.10531-01	-.10496-01	-.15798-01
-.63155-01	-.62310-01	-.30675-04	-.27623-04	-.41719-02	-.41532-01	-.15653-05	-.43155-01			
.94308-03	.96884-03	.37822-05	-.38722-05	-.73121-03	.69478-03	.60128-04	.14532-03	.11693-03	.71973-07	.11769-06
.43477-04	.86996-04	.18465-08	.62674-04	.47154-02	.48442-02	.18911-04	-.19361-04	-.36561-02	.34739-02	.30061-03
.72661-03	.58464-03	.35986-06	.58846-06	.21738-03	.83498-03	.92326-08	.31337-03			
.22240-05	-.13872-03	-.88288-06	.46842-06	.57919-05	-.19837-03	.24799-02	.38265-06	-.45159-03	-.71338-07	-.36275-07
-.25658-07	-.74715-04	.63510-09	-.38300-09	.11120-04	-.69359-03	-.22144-05	.23421-05	.28959-04	-.99187-03	.12399-01
.19132-05	-.22580-02	-.35667-06	-.18137-06	-.12829-06	-.37357-03	.31755-08	-.19150-08			
-.60956-08	-.59143-08	.15058-04	.33363-06	.33417-07	-.28420-07	-.18169-08	-.11869-07	-.21245-07	.83319-04	-.33919-07
-.20263-07	-.10326-07	-.10852-03	.19496-08	-.30478-07	-.29572-07	.75290-04	.16672-05	.16708-06	-.14210-06	-.90847-08
-.59343-07	-.10623-06	.81659-03	-.16960-06	-.10132-06	-.51629-07	-.54261-03	.97482-08			
.72020-05	.10947-06	.26616-07	-.26950-07	-.10951-04	-.31499-06	.44496-08	-.43251-06	-.86346-08	-.20046-07	-.11806-06
-.67629-04	-.11787-08	.29848-08	.59457-04	.36010-04	.94736-06	.13308-06	-.13475-06	-.54757-04	-.15750-05	.22248-07
-.21626-03	-.43173-07	-.10023-06	-.59032-06	-.33814-03	-.58933-08	.14924-07	.29728-03			
.15152-01	-.14689-01	.46425-06	.16077-06	-.19723-02	-.22082-02	-.31631-02	.12643-01	-.12458-01	-.18486-05	.25811-07
.83021-03	-.83066-02	.88451-06	.86309-02	.75758-01	-.73447-01	.23213-05	.80384-06	-.98613-02	-.11041-01	-.15815-01
.63215-01	-.62290-01	-.92432-05	.12906-06	.81510-02	-.41533-01	.24226-05	.43154-01			
.97375-03	-.93972-03	.16519-06	-.63825-07	-.68917-03	-.73533-03	-.60159-04	.14543-03	-.11688-03	-.74033-08	.61550-07
.43434-04	-.86997-04	.36952-08	.62673-04	.48687-02	-.46986-02	.82597-06	-.31913-06	-.34458-02	-.36767-02	-.30079-03
.72715-03	-.58440-03	-.37016-07	.30777-06	.21717-03	-.43498-03	.18476-07	.31337-03			
-.21678-02	.21080-02	.23177-02	.24167-02	-.18376-02	-.15121-02	-.90624-04	.39131-03	-.42130-03	-.29403-03	.30641-03
-.20985-03	.99290-04	-.12375-03	-.28236-05	-.10839-01	.10540-01	.11588-01	.12084-01	-.71880-02	-.75604-02	-.45314-03
.19565-02	-.21065-02	-.14702-02	.15320-02	-.10492-02	.49645-03	-.61876-03	-.14118-04			
.21676-02	-.21080-02	.23170-02	.24171-02	.14368-02	.15133-02	.90637-04	-.39127-03	.42139-03	-.29384-03	.30714-03
.20892-03	-.99332-04	-.12375-03	.28274-05	.10838-01	-.10540-01	.11585-01	.12086-01	.71882-02	.75663-02	.45318-03
-.19564-02	.21069-02	-.14692-02	.15357-02	.10446-02	-.49666-03	-.61875-03	.14137-04			

C-4

MATRIX AM

.00000	.00000	.00000	.00000	.00000	.00000	.00000	.00000	.00000	1.0000	.00000
.00000	.00000	.00000	.00000	.00000	.00000	.00000				
.00000	.00000	.00000	.00000	.00000	.00000	.00000	.00000	.00000	.00000	1.0000
.00000	.00000	.00000	.00000	.00000	.00000	.00000				
.00000	.00000	.00000	.00000	.00000	.00000	.00000	.00000	.00000	.00000	.00000
1.0000	.00000	.00000	.00000	.00000	.00000	.00000				
.00000	.00000	.00000	.00000	.00000	.00000	.00000	.00000	.00000	.00000	.00000
.00000	1.0000	.00000	.00000	.00000	.00000	.00000				
.00000	.00000	.00000	.00000	.00000	.00000	.00000	.00000	.00000	.00000	.00000
.00000	.00000	1.0000	.00000	.00000	.00000	.00000				
.00000	.00000	.00000	.00000	.00000	.00000	.00000	.00000	.00000	.00000	.00000
.00000	.00000	.00000	1.0000	.00000	.00000	.00000				
.00000	.00000	.00000	.00000	.00000	.00000	.00000	.00000	.00000	.00000	.00000
.00000	.00000	.00000	.00000	1.0000	.00000	.00000				
.00000	.00000	.00000	.00000	.00000	.00000	.00000	.00000	.00000	.00000	.00000
.00000	.00000	.00000	.00000	.00000	1.0000	.00000				
.00000	.00000	.00000	.00000	.00000	.00000	.00000	.00000	.00000	.00000	.00000
.00000	.00000	.00000	.00000	.00000	.00000	1.0000				
-2.7531	.00000	.00000	.00000	.00000	.00000	.00000	.00000	.00000	-2.3462	.00000
.00000	.00000	.00000	.00000	.00000	.00000	.00000				
.00000	-2.1678	.00000	.00000	.00000	.00000	.00000	.00000	.00000	.00000	-2.0819
.00000	.00000	.00000	.00000	.00000	.00000	.00000				
.00000	.00000	-1.8204	.00000	.00000	.00000	.00000	.00000	.00000	.00000	.00000
-1.9078	.00000	.00000	.00000	.00000	.00000	.00000				
.00000	.00000	.00000	-1.1557	.00000	.00000	.00000	.00000	.00000	.00000	.00000
.00000	-1.5201	.00000	.00000	.00000	.00000	.00000				
.00000	.00000	.00000	.00000	-.75001	.00000	.00000	.00000	.00000	.00000	.00000
.00000	.00000	-1.2246	.00000	.00000	.00000	.00000				
.00000	.00000	.00000	.00000	.00000	-.69794	.00000	.00000	.00000	.00000	.00000
.00000	.00000	.00000	-1.1813	.00000	.00000	.00000				
.00000	.00000	.00000	.00000	.00000	.00000	-.68974	.00000	.00000	.00000	.00000
.00000	.00000	.00000	.00000	-1.1743	.00000	.00000				
.00000	.00000	.00000	.00000	.00000	.00000	.00000	-.14428	.00000	.00000	.00000
.00000	.00000	.00000	.00000	.00000	-.53710	.00000				
.00000	.00000	.00000	.00000	.00000	.00000	.00000	.00000	-.31084-01	.00000	.00000
.00000	.00000	.00000	.00000	.00000	.00000	-.24930				

MATRIX BM

.00000	.00000	.00000	.00000	.00000	.00000	.00000	.00000	.00000	.00000	.00000
.00000	.00000	.00000	.00000	.00000	.00000	.00000	.00000	.00000	.00000	.00000
.00000	.00000	.00000	.00000	.00000	.00000	.00000	.00000	.00000	.00000	.00000
.00000	.00000	.00000	.00000	.00000	.00000	.00000	.00000	.00000	.00000	.00000
.00000	.00000	.00000	.00000	.00000	.00000	.00000	.00000	.00000	.00000	.00000
.00000	.00000	.00000	.00000	.00000	.00000	.00000	.00000	.00000	.00000	.00000
.00000	.00000	.00000	.00000	.00000	.00000	.00000	.00000	.00000	.00000	.00000
.00000	.00000	.00000	.00000	.00000	.00000	.00000	.00000	.00000	.00000	.00000
.00000	.00000	.00000	.00000	.00000	.00000	.00000	.00000	.00000	.00000	.00000
-.31687-03	.58671-03	-.15798-01	.21063-03	.12399-01	-.90847-08	.22248-07	-.15015-01	-.39103-03	-.31720-03	.56914-03
-.13662-02	.25424-02	-.63155-01	.50663-03	.19132-05	-.59545-07	-.21626-03	.63215-01	.94529-03	.13696-02	-.25433-02
-.14751-02	.27417-02	-.62310-01	.40925-03	-.22580-02	-.10623-06	-.43173-07	-.62290-01	-.75972-03	-.14746-02	.27390-02

ORIGINAL PAGE IS
OF POOR QUALITY

-.10300-02	-.19115-02	-.30675-04	.25190-06	-.35667-06	.41659-03	-.10023-06	-.92432-05	-.48121-07	-.10291-02	-.19100-02
-.10722-02	-.19950-02	-.27623-04	.41192-06	-.18137-06	-.16960-06	-.59032-06	.12906-06	.40010-06	.10724-02	.19964-02
.73455-03	-.13571-02	-.41719-02	.15217-03	-.12829-06	-.10132-06	-.33814-03	.41510-02	.28232-03	-.73447-03	.13580-02
.34749-03	-.64506-03	-.41532-01	.30448-03	-.37357-03	-.51629-07	-.58933-08	-.41533-01	-.56548-03	.34752-03	-.64566-03
-.43313-03	-.80432-03	-.15653-05	.64628-08	.31755-08	-.54261-03	.14924-07	.24226-05	.24019-07	-.43313-03	-.80438-03
.98963-05	-.18346-04	-.43155-01	.21936-03	-.19150-08	.97482-08	.29728-03	.43154-01	.40738-03	-.98826-05	.18378-04

MATRIX CM

-.63374-04	-.27363-03	-.29502-03	-.20600-03	-.21443-03	.14691-03	.69498-04	-.86626-04	.19793-05	-.31687-03	-.13682-02
-.14751-02	-.10300-02	-.10722-02	.73455-03	.34749-03	-.43313-03	.98963-05				
.11774-03	.50848-03	.54835-03	-.38230-03	-.39901-03	-.27143-03	-.12901-03	-.16086-03	-.36691-05	.58871-03	.25424-02
.27417-02	-.19115-02	-.19950-02	-.13571-02	-.64506-03	-.80432-03	-.18346-04				
-.33597-02	-.12631-01	-.12462-01	-.61351-05	-.55245-05	-.83438-03	-.83064-02	-.31305-06	-.86310-02	-.15798-01	-.63155-01
-.62310-01	-.30675-04	-.27623-04	-.41719-02	-.41532-01	-.15653-05	-.43155-01				
.42086-04	.10173-03	.81850-04	.50381-07	.82385-07	.30434-04	.60897-04	.12926-08	.43872-04	.21043-03	.50863-03
.40925-03	.25190-06	.41192-06	.15217-03	.30448-03	.64628-08	.21936-03				
.24799-02	.38265-06	-.45159-03	-.71334-07	-.36275-07	-.25650-07	-.74715-04	.63510-09	-.38300-09	.12399-01	.19132-05
-.22580-02	-.35667-06	-.18137-06	-.12829-06	-.37357-03	.31755-08	-.19150-08				
-.16169-08	-.11869-07	-.21245-07	.83319-04	-.33919-07	-.20263-07	-.10326-07	-.10852-03	.19496-08	-.90847-08	-.59343-07
-.10623-06	.41659-03	-.16960-06	-.10132-06	-.51629-07	-.54261-03	.97482-08				
.44496-08	-.43251-04	-.86346-08	-.20046-07	-.11806-06	-.67629-04	-.11787-08	.29848-08	.59457-04	.22248-07	-.21626-03
-.43173-07	-.10023-06	-.59032-06	-.33814-03	-.58933-08	.14924-07	.29728-03				
-.31631-02	.12643-01	-.12458-01	-.18486-05	.25811-07	.83021-03	-.83066-02	.48451-06	.86309-02	-.15815-01	.63215-01
-.62290-01	-.92432-05	.12906-06	.41510-02	-.41533-01	.24226-05	.43154-01				
-.78207-04	.18906-03	-.15194-03	-.96242-08	.80020-07	.56469-04	-.11310-03	.48037-08	.81475-04	-.39103-03	.94529-03
-.75972-03	-.48121-07	.40010-06	.28232-03	-.56548-03	.24019-07	.40738-03				
-.63440-04	.27391-03	-.29491-03	-.20582-03	.21449-03	-.14689-03	.69503-04	-.86627-04	-.19765-05	-.31720-03	.13696-02
-.14746-02	-.10291-02	.10724-02	-.73447-03	.34752-03	-.43313-03	-.98826-05				
.11783-03	-.50866-03	.54781-03	-.38200-03	.39929-03	.27160-03	-.12913-03	-.16088-03	.36757-05	.58914-03	-.25433-02
.27390-02	-.19100-02	.19964-02	.13580-02	-.64566-03	-.80438-03	.18378-04				

BIBLIOGRAPHY

1. Wang, S.J. and J.M. Cameron, "Dynamics and control of a large space antenna," Journal of Guidance, Control and Dynamics, Vol. 7, No. 1, Jan.-Feb. 1984, pp. 69-76.

2. Cameron, J.M., M. Hamidi, Y.H. Lin, and S.J. Wang, "Distributed control of large space antennas," paper presented at the Workshop on Applications of Distributed System Theory to the Control of Large Space Structures, July 14-16, 1982, Pasadena, Ca., pp. 225-247.

3. Landau, I.D., Adaptive Control: The Model Reference Approach, Marcel Dekker, Inc., New York, 1979.

4. Kalman, R.E., "Design of self-optimizing control," Trans. ASME, Vol. 80, No. 2, 1958, pp. 468-478.

5. Feldbaum, A.A., "Dual control theory," collected in Optimal and Self-Optimizing, R. Oldenburger, Ed., MIT Press, Cambridge, Mass., 1966, pp. 458-496.

6. Iserman, R., U. Baur, W. Bamberger, P. Kneppo, and H. Sibert, "Comparison of six on-line identification and parameter estimation methods," Automatica, Vol. 10, 1974, pp. 81-103.

7. Ljung, L., "Analysis of recursive stochastic algorithms," IEEE Trans. on Automatic Control, Vol. AC-22, 1977, pp. 551-575.

8. Ljung, L., "On positive real transfer functions and the convergence of some recursive schemes," IEEE Trans. on Automatic Control, Vol. AC-22, 1977, pp. 539-551.

9. Landau, I.D., "Elimination of the real positivity condition in the design of parallel MRAS," IEEE Trans. on Automatic Control, Vol. AC-23, No. 6, Dec. 1978, pp. 1015-1020.

10. Martin-Sanchez, J.M., "A new solution to adaptive control," Proc. IEEE, Vol. 64, 1976, pp. 1209-1218.

11. Johnstone, R.M., D.G. Fisher, and S.L. Shah, "Hyperstable adaptive control -- an indirect, input-output approach with explicit model identification," Joint Automatic Control Conference, 1979, pp. 487-494.

12. Narendra, K.S., and L.S. Valavani, "Direct and indirect adaptive control," Automatica, Vol. 15, No. 6, Nov. 1979, pp. 653-654.

13. Goodwin, G.C., P.J. Ramadge and P.E. Caines, "Discrete time multivariable adaptive control," IEEE Trans. on Automatic Control, Vol. AC-25, No. 3, June 1980, pp. 449-456.

14. Goodwin, G.C., P.J. Ramadge, and P.E. Caines, "Discrete time stochastic adaptive control," SIAM Journal of Control and Optimization, Vol. 19, 1981, pp. 282-285.

15. Whitaker, H.P., P.V. Osburn, and A. Keezer, "New developments in the design of adaptive control systems," Institute of Aeronautical Sciences, Paper 61-39, 1961.

16. Donalson, D.D., and C.T. Leondes, "A model referenced parameter tracking technique for adaptive control systems," IEEE Trans. Appl. Ind., Sept. 1963, pp. 241-262.

17. Winsor, C.A., "Model reference adaptive design," NASA-CR-98453, Nov. 1968.

18. Butchart, R.L. and B. Shackcloth, "Synthesis of model reference adaptive control systems by Lyapunov's second method," Proc. 1965 IFAC Symp. Adaptive Control (Teddington, England), ISA, 1966, pp. 145-152.

19. Parks, P.C. "Lyapunov redesign of model reference adaptive control systems," IEEE Trans. on Automatic Control., Vol. AC-11, July 1966, pp. 362-367.

20. Phillipson, P.H., "Design methods for model reference adaptive systems," Proc. Inst. Mechanical Engineers, Vol. 183, Part I, 1968-1969, pp. 695-706.

21. Gilbart, J.W., R.V. Monopoli and C.F. Price, "Improved convergence and increased flexibility in the design of model reference adaptive control systems," Proc. 9th IEEE Symp. Adaptive Processes Design and Control, Dec. 1970, pp. IV.3.1-3.10.

22. Landau, I.D. and B. Courtiol, "Adaptive model following systems for flight control and simulation," AIAA 10th Aerospace Sciences Meeting, No. 72-95, January 1972.

23. Popov, V.M., "The solution of a new stability problem for controlled systems," Automation and Remote Control, 24, 1963, pp. 1-23.

24. Landau, I.D., "Synthesis of discrete model reference adaptive control," IEEE Trans. on Automatic Control, Vol. AC-16, 1971, pp. 507-508.

25. Landau, I.D. and H.M. Silveira, "A stability theorem with applications to adaptive control system," Proc. 3rd IFAC Symp. on Sensitivity, Adaptivity, and Optimality, Ischia, Italy, June 1973, pp. 282-286.

26. Bethoux, B. and B. Courtiol, "A hyperstable discrete model reference adaptive control system," Proc. 3rd IFAC Symp. on Sensitivity, Adaptivity, and Optimality, Ischia, Italy, June 1973, pp. 287-289.

27. Anderson, B.D.O., "A simplified view of hyperstability," IEEE Trans. on Automatic Control, Vol. AC-13, 1968, pp. 292-294.

28. Monopoli, R.V., "Model reference adaptive control with an augmented error signal," IEEE Trans. on Automatic Control, Vol. AC-19, Oct. 1974, pp. 474-485.

29. Morse, A.S., A. Feuer, and B.R. Barmish, "An unstable dynamical system associated with model reference adaptive control," IEEE Trans. on Automatic Control, Vol. AC-23, June 1978, pp. 499-500.

30. Narendra, K.S. and L.S. Valavani, "Stable adaptive controller design - direct control," IEEE Trans. on Automatic Control, Vol. AC-23, Aug. 1978, pp. 570-583.

31. Narendra, K.S., Y.H. Lin and L.S. Valavani, "Stable adaptive controller design - part II: proof of stability," IEEE Trans. on Automatic Control, Vol. AC-25, No. 3, June 1980, pp. 440-448.

32. Morse, S. and A. Feuer, "Adaptive control of single-input single-output linear systems," IEEE Trans. on Automatic Control, Vol. AC-23, August 1978, pp. 557-570.

33. Morse, A.S., "Global stability of parameter-adaptive control systems," IEEE Trans. on Automatic Control, Vol. AC-25, No. 3, June 1980, pp. 433-439.

34. Ionescu, T. and R.V. Monopoli, "Discrete model reference adaptive control with an augmented error signal," Automatica, Vol. 13, 1977, pp. 507-517.

35. Narendra, K.S. and Y.H. Lin, "Stable discrete adaptive control," IEEE Trans. on Automatic Control, Vol. AC-25, No. 3, June 1980, pp. 456-461.

36. Suzuki, T. and S. Takashima, "A hyperstable scheme for discrete model reference adaptive control system," International Journal of Control, Vol. 28, 1978, pp. 245-252.

37. Johnstone, R.M., S.L. Shah, and D.G. Fisher, "An extension of hyperstable adaptive control to nonminimum phase systems," International Journal of Control, Vol. 31, 1980, pp. 539-545.

38. Narendra, K.S. and L.S. Valavani, "Direct and indirect model reference adaptive control," Automatica, Vol. 15, 1979, pp. 653-664.

39. Narendra, K.S. and L.S. Valavani, "A comparison of Lyapunov and hyperstability approaches to adaptive control of continuous systems," IEEE Trans. on Automatic Control, Vol. AC-25, No. 2, April 1980, pp. 243-247.

40. Monopoli, R.V. and C.C. Hsing, "Parameter adaptive control of multivariable systems," International Journal of Control, 22, No. 3, 1975, pp. 313-327.

41. Sobel, K., H. Kaufman, and L. Mabius, "Model reference output adaptive control systems without parameter identification," 18th IEEE Conference on Decision and Control, Ft. Lauderdale, FL, Dec. 1979, pp. 347-351.

42. Sobel, K., H. Kaufman, and L. Mabius, "Implicit adaptive control systems for a class of multi-input multi-output systems," IEEE Trans. on Aerospace and Electronics Systems, Sept. 1982, pp. 576-590.

43. Broussard, J.R. and M.J. O'Brien, "Feedforward control to track the output of a forced model," Proc. 17th IEEE Conference on Decision and Control, Jan. 1979, pp. 1149-1154.

44. Balas, M.J. and C.R. Johnson, "Toward adaptive control of large structures in space," Applications of Adaptive Control, Academic Press, 1980, pp. 313-344.

45. Johnson, C.R., "Adaptive modal control of large flexible spacecraft," AIAA Journal of Guidance and Control, Vol. 3, No. 4, July-August 1980, pp. 369-375.

46. Rohrs, C.E., L. Valavani, M. Athans, and G. Stein, "Robustness of adaptive control algorithms in the presence of unmodeled dynamics," Proc. 21st IEEE Conference on Decision and Control, Dec. 1982, pp. 3-11.

47. Bar-Kana, I., H. Kaufman, and M. Balas, "Model reference adaptive control of large structural systems," AIAA Journal of Guidance and Control, Vol. 6, No. 2, March-April 1983, pp. 112-118.

48. Workshop Briefing Charts, Study Task No. 9 - Berthing, NASA Space Station Task Force Concept Development Group, Dec. 5-9, 1983.

49. Craig, M., Study Task No. 11 - Configuration and Controllability Studies, NASA Space Station Task Force Concept Development Group, Dec. 16, 1983.

50. Clough, R.W. and J. Penzien, Dynamics of Structures, McGraw-Hill, N.Y., N.Y., 1975.

51. Juang, J.N. and S.J. Wang, "An investigation of quasi-inertial attitude control for a solar power satellite," Space Solar Power Review, Vol. 3, 1982, pp. 337-352.

52. Hahn, W., Theory and Application of Lyapunov's Direct Method, Prentice-Hall, Inc., New Jersey, 1963.

53. Lyapunov, M.A., "Investigation of a singular case of the problem of stability of motion," Mat. Sbornik 17, 1893, pp. 252-333

54. Bar-Kana, I., "Direct multivariable model reference adaptive control with application to large structural systems," Ph.D. Dissertation, Rensselaer Polytechnic Institute, Troy, New York, May, 1983.

55. Landau, I.D., "Design of discrete model reference adaptive systems using the positivity concepts," in Proc. 3rd Symp. on Sensitivity, Adaptivity and Optimality, Ischia, Italy, 1973, pp. 307-314.

NASA—JPL—Coml., L.A., Calif.

TECHNICAL REPORT STANDARD TITLE PAGE

1. Report No. JPL 85-57	2. Government Accession No.	3. Recipient's Catalog No.
4. Title and Subtitle Dynamic Modeling and Adaptive Control for Space Stations		5. Report Date July 15, 1985
		6. Performing Organization Code
7. Author(s) Che-Hang Charles Ih and Shyh John Wang		8. Performing Organization Report No.
9. Performing Organization Name and Address JET PROPULSION LABORATORY California Institute of Technology 4800 Oak Grove Drive Pasadena, California 91109		10. Work Unit No.
		11. Contract or Grant No. NAS7-918
12. Sponsoring Agency Name and Address NATIONAL AERONAUTICS AND SPACE ADMINISTRATION Washington, D.C. 20546		13. Type of Report and Period Covered JPL Publication
		14. Sponsoring Agency Code

15. Supplementary Notes

16. Abstract Of all large space structural systems, space stations present a unique challenge and requirement to advanced control technology. Their operations require control system stability over an extremely broad range of parameter changes and high level of disturbances. During shuttle docking the system mass may suddenly increase by more than 100% and during station assembly the mass may vary even more drastically. These coupled with the inherent dynamic model uncertainties associated with large space structural systems require highly sophisticated control systems that can grow as the stations evolve and cope with the uncertainties and time-varying elements to maintain the stability and pointing of the space stations.

This report first deals with the aspects of space station operational properties including configurations, dynamic models, shuttle docking contact dynamics, solar panel interaction and load reduction to yield a set of system models and conditions. A model reference adaptive control algorithm along with the inner-loop plant augmentation design for controlling the space stations under severe operational conditions of shuttle docking, excessive model parameter errors, and model truncation are then investigated. The instability problem caused by the zero-frequency rigid body modes and a proposed solution using plant augmentation are addressed. Two sets of sufficient conditions which guarantee the globablly asymptotic stability for the space station systems are obtained.

The performance of this adaptive control system on space stations is analyzed through extensive simulations. Asymptotic stability, high rate of convergence, and robustness of the system are observed under the above-mentioned severe conditions and constraints induced by control hardware saturation.

17. Key Words (Selected by Author(s)) Astronautics (General) Engineering (General) Computer Programming and Software Systems Analysis	18. Distribution Statement Unlimited/Unclassified

19. Security Classif. (of this report)	20. Security Classif. (of this page)	21. No. of Pages	22. Price
Unclassified	Unclassified		